The University of Nottingham
Department of Civil Engineering
Resilience Engineering Research Group

RAILWAY BRIDGE CONDITION MONITORING AND FAULT DIAGNOSTICS

Matteo Vagnoli

A Doctoral Thesis

Thesis submitted to the University of Nottingham for the degree of Doctor of Philosophy

November 2018

Abstract

The European transportation network is ageing continuously due to environmental threats, such as traffic, wind and temperature changes. Bridges are vital assets of the transportation network, and consequently their safety and availability need to be guaranteed to provide a safe transportation network to passenger and freights traffic. The main objective of this thesis is to develop a bridge condition monitoring and damage diagnostics method. The main element of the proposed Structural Health Monitoring (SHM) method is to monitor and assess the health state of a bridge continuously, by taking account of the health state of each element of the bridge. In this way, an early detection of the ongoing degradation of the bridge can be achieved, and a fast and cost-effective recovery of the optimal health state of the infrastructure can be achieved.

A BBN-based approach for bridge condition monitoring and damage diagnostics is proposed and developed to assess and update the health state of the bridge continuously, by taking account of the health state of each element of the bridge. At the same time, the proposed BBN approach allows to detect and diagnose damage of the bridge infrastructure.

Firstly, the BBN method is developed for monitoring the condition of two bridges, which are modelled via two Finite Element Models (FEMs). The Conditional Probability Tables (CPTs) of the BBN are defined by using an expert knowledge elicitation process. Results shows that the BBN allows to detect and diagnose damage of the bridges, however the performance of the BBN can be improved by pre-processing the data of the bridge behaviour and improving the definition of the CPTs.

A data analysis methodology is then proposed to pre-process the data of the bridge behaviour, and to use the results of the analysis as an input to the BBN. The proposed data analysis methodology relies on a five-step process: *i)* remove of the outlier of the bridge data; *ii)* identify of the free-vibration of the bridge; *iii)* extract statistical, frequency-based and vibration -based features from the free-vibration behaviour of the bridge; *iv)* assess the features trend over time, by using the extracted features as an input to an Empirical Mode Decomposition (EMD) algorithm; *v)* evaluate of the Health Indicator (HI) of the bridge element. The proposed data analysis methodology is tested on two in-field bridges, a steel truss bridge and a post-tensioned concrete bridge, which are subject to a progressive damage test.

A machine learning method is also developed in order to assess the health state of the bridge automatically. A Neuro Fuzzy Classifier (NFC) is adopted for this purpose. The results of the NFC can potentially be used as an input to the BBN nodes, to select the states of the BBN nodes, and improve the BBN performance. In fact, the NFC shows high accuracy in assessing the health state of bridge elements. An optimal set of HIs, which allows to maximize the accuracy of the NFC, is identified by adopting an iterative Modified Binary Differential Evolution (MBDE) method. The NFC is applied to the post-tensioned concrete in-field bridge that is subject to a progressive damage test.

Hence, the performance of the BBN is improved significantly by pre-processing the bridge data, but also by developing a novel method to continuously update the CPTs of the BBN. The CPTs update process relies on the actual health state of the bridge element, and the knowledge of bridge engineers. Indeed, the CPT updating method aims to merge the expert knowledge with the analysis of the bridge behaviour. In this way, the diagnostic ability of the BBN is improved by merging the expertise of bridge engineer, who can analyse hypothetical damage scenarios of the bridge, and the analysis of a database of known bridge behaviour in different health states. The method is verified on the post-tensioned concrete in-field bridge, by developing a BBN to monitor the health state of the bridge continuously. The damages of the bridge are diagnosed by the proposed BBN.

Finally, a method to analyse database of unknown infrastructure behaviour is finally proposed. An ensemble-based change-point detection method is presented to analyse a database of past unknown infrastructure behaviour. The method aims to identify the most critical change of the health state of the infrastructure, by providing the characteristics of such a change, in terms of time duration and possible causes. The method is applied to a database of tunnel behaviour, which is subject to renewal activities that influence the health state of the infrastructure.

To my Family…

"…Laugh as we always laughed at the little jokes that we enjoyed together…
...Play, smile, think of me…It is the same as it ever was...
…How we shall laugh at the trouble of parting when we meet again!"

Acknowledgements

The acknowledgement section is usually the most boring and most important part of a thesis. It is boring because it's merely a list of thank-you's, yet it's important because most of the people that will read a thesis would never go beyond this section. For this reason, I will try to be as boring as possible, to sincerely thank all the people that I have met throughout my PhD. To any readers that are scrolling this thesis casually, please consider this as your final warning.

I will start my acknowledgments by thanking the European Union, which allows thousands of students to experience a fantastic journey of personal and technical growth through the Marie-Curie Fellowship. If such an experience would have been available for more people, who would have had the possibility of experiencing different cultures and make new friends from all over the word, we would be more united, and we would probably have less brexiters-style of people.

I sincerely thank Prof. John Andrews, for giving me this opportunity after a short, fun and constructive skype interview. At the same time, I have really appreciated his wise managing style of the Research Engineering Research Group (RERG).

It is difficult to find enough words to thank Dr. Rasa Remenyte-Prescott adequately. I am grateful to have had such a great, smart and patient supervisor, who gave me precious and intelligent technical suggestions continuously, while also helping me in growing as a Man. Thank you Rasa. I recognise I was not the easiest PhD student of your career, and I am sorry for all the unrequested comments, ideas, actions, etc. I have learnt a lot as a person thanks to your guidance. I would like also to thank you for being part of my kidnap during February 2017, when I left home for going to the grocery shop, and I ended up in Iceland.

Obviously, I need to thank the whole TRUSS crew, from the project coordinator Prof. Arturo Gonzalez (who also shared some data to validate the method developed in this thesis) to Loreto and Parisa, who magnificently organized each TRUSS event. Similarly, all the Professors (with a special mention for Prof. Juan Ramon Casas) and people of the TRUSS consortium need my warmest acknowledgment.

I'll skip the acknowledgments to the TRUSS ESRs, they already know that they rock, all of them. Similarly, the RERG and NTEC PhD students and researchers are among the smartest and funniest people that I have ever met.

AECOM needs to be warmly recognized for allowing me to experience the consulting world, for having hosted me for four months during my PhD and having provided data and case studies. Particularly, I would thank Matt Brough, Paul Clarke, Neil Atkinson (even if I am still waiting his reply to my emails) and Daniel Thompson. I hope you are doing a great job with the codes that we developed together.

Last but not least (a classic closing remark in any well-respected acknowledgement section), for the PhD-related appreciation, I would like to thank Network Rail, for giving me the opportunity to take part in some visual inspections of railway bridges along with the engineering team.

All my dear friends in Nottingham are worth to be mentioned, for their continuous support, time and friendship: thank you Federico and Kamila for Michelin star home cooked dinners, thanks to Francesco for (almost) continuously loosing squash matches against me, and to his awesome girlfriend Roberta, who bakes the best mascarpone and the best parigina of the world. Thanks also to Alberto and Francesca for lovely feeding the ducks of the Nottingham Canal, we will conquer them one day. The Brazilian couple Gustavo and Emily is one of the best couples that I ever seen, and I would like to thank them for their delicious mayonnaise with potatoes. Andrea, thank you for your pesto-, risotto-, lasagna-, whatever-nights, you are great. Francesco Cannarile, Silvia Marino and Claudia Picoco are worth mentioning for hours of chatting and ideas sharing.

Finally, I must thank my whole family, Sonja and Mario, Filippo and Monica. We have spent hours face-timing each other to minimize the distance between us, and to talk and support each other for any decision we were facing. We are a great Team, which is able to face and solve everything, without losing our smiles. I am grateful to have a family like ours. Similarly, Fabio, Nicoletta, Francesco, Lorenzo, Elvira and Rossano have been a strong column that kept me motivated and happy.

The very last person to acknowledge is the one that is sitting right next to me during this Rome to Liverpool Sunday morning flight. I have sincerely lost the count of how many flights we have caught together during these three years. We should be co-owners of EasyJet, for having flown with them from Luton to Paris CDG every single weekend from September 2015 to February 2017. All that travelling was hard, exhausting and a great moment of excitement (on Friday) and solitude (on Sunday), but it was worth every second. It is just thank to you if I am here writing this thesis, as you have been supporting me since the application phase. You have challenged me

every single second throughout the journey, even going against me in order to allow me to see the bigger picture. Thank you for this, it allowed me to grow and view different unknown prospective. Thank you, Allegra, let’s keep exploring the world with last minute unpredictable and unscheduled journeys, together.

Table of Contents

List of Figures

List of Tables

Publication based on the thesis work

Journal papers:

1. Vagnoli, M., Remenyte-Prescott, R., Andrews, J., "*Railway bridge structural health monitoring and fault detection: state-of-the-art methods and future challenges*", Structural Health Monitoring, 17 (4), pp. 971-1007, 2018.
2. Vagnoli, M., Remenyte-Prescott, R., "*An ensemble-based change-point detection method for identifying unexpected behaviour of railway tunnel infrastructures*", Tunnelling and Underground Space Technology Journal, 81, pp. 68-82, 2018.
3. Vagnoli, M., Remenyte-Prescott, R., Andrews, J., "*Condition monitoring and deterioration diagnostics of bridges: a Bayesian belief network approach*", under review, Structural Control and Health Monitoring Journal.
4. Vagnoli, M., Remenyte -Prescott, R., Andrews, J., "*A data-driven methodology for bridge condition monitoring and damage diagnostics*", under review, Structural control and health monitoring journal, since 26/07/2018.
5. Vagnoli, M., Remenyte -Prescott, R., Andrews, J., "*A Bayesian Network method for real-time bridge structural health monitoring*", being drafted and going to be submitted to Reliability Engineering & System Safety Technology Journal.

Conference papers:

1. Vagnoli, M., Remenyte-Prescott, R., Andrews, J., "*Railway bridge fault detection using Bayesian belief network*", the Stephenson conference (London, 25-27 April 2017).
2. Vagnoli, M., Remenyte-Prescott, R., Andrews, J., "*Towards a continuous Structural Health Monitoring of railway bridges*", the 52nd European Safety, Reliability & Data Association (ESReDA) seminar (Kaunas, 30-31 May 2017).
3. Vagnoli, M., Remenyte-Prescott, R., Andrews, J., "*A fuzzy-based Bayesian Belief Network approach for railway bridge condition monitoring and fault detection*", the European Safety and RELiability (ESREL) conference (Portoroz, 18-22 June, 2017).
4. Vagnoli, M., Remenyte-Prescott, R, Thompson, D., Andrews, J., Clarke, P., Atkinson, N., "*A data mining tool for detecting and predicting abnormal behaviour of railway tunnels*", 11th International Workshop of Structural Health Monitoring (IWSHM) (Stanford, 12-14 September, 2017).
5. A. González, F. Huseynov, B. Heitner, M. Vagnoli, J.J. Moughty, A. Barrias, D. Martinez, S. Chen, E. OBrien, D. Laefer, J.R. Casas, R. Remenyte-Prescott, T. Yalamas, J. Brownjohn, "*Structural Health Monitoring Developments in TRUSS Marie Skłodowska-Curie Innovative Training Network*", The 8th

International Conference on Structural Health Monitoring of Intelligent Infrastructure (Brisbane, Australia, 5-8 December 2017).

6. Vagnoli, M., Remenyte -Prescott, R., Andrews, J., "*Structural health monitoring of bridges: a Bayesian approach*", the Sixth International Symposium on Life-Cycle Civil Engineering (IALCCE 2018) (Gent, 28-31 October 2018).
7. Vagnoli, M., R. Remenyte-Prescott, J. Andrews, "*A machine learning classifier for condition monitoring and damage detection of bridge infrastructure*", Civil Engineering Research in Ireland conference (CERI2018), Dublin, 29-30 August 2018.

Funding

This project has received funding from the European Union's Horizon 2020 research and innovation programme under the Marie Skłodowska-Curie grant agreement No. 642453.

List of Abbreviations

ABNN - Acceleration-Based Neural Networks

AIC - Akaike Information Criterion

AICc - Akaike Information Criterion corrected

ANNs - Artificial Neural Networks

BBN - Bayesian Belief Network

CPTs - Conditional Probability Tables

CI - Consistency Index

CR - Consistency Ratio

CAV - Cumulative Absolute Velocity

CDF - Cumulative Distribution Function

CUSUM - Cumulative Sum

DI - Damage Indexes

DPI - Damage Potential Indicator

DBN - Dynamic Bayesian Network

EMD - Empirical Mode Composition

EEMD - Ensemble Empirical Mode Composition

FFT - Fast Fourier Transform

FT - Fault Tree

FEM - Finite Element Model

FAHP - Fuzzy Analytic Hierarchy Process

GA - Genetic Algorithm

GI - Goodness Index

GVW - Gross Vehicle Weights

HI - Health Indicators

IMF- Intrinsic Mode Functions

MAC - Modal Assurance Criterion

MBNN - Modal feature-Based Neural Network

MBDE - Modified Binary Differential Evolution

MPCA - Moving Principal Component Analysis

MEMD - Multivariate Empirical Mode Composition

NFC - Neuro-Fuzzy Classifier

OOBN - Objected Oriented Bayesian Network

OLE - Overhead Line Equipment

PD - Partially Degraded

PCA - Principal Component Analysis

PELT - Pruned Exact Linear Time

RI - Random Index

RuLSIF - Relative Unconstrained Least-Squares Importance Fitting

RMS - Root Mean Square

SD - Severely Degraded

SAA - Shape Accel Array

SHM - Structural Health Monitoring

SVD - Singular-Value Decomposition

Chapter 1 Introduction

1.1 Introduction

This thesis investigates methods for bridge condition monitoring and damage (degradation) diagnostics, in order to propose a methodology that can be used to monitor and assess the health state of an infrastructure continuously. Degradation detection and diagnostics strategies are needed to guarantee the safety, reliability and availability of the infrastructure during the life-cycle of the asset. Structural Health Monitoring (SHM) strategies rely on the analysis of the infrastructure behaviour, which is measured by sensors installed on the infrastructure. A large amount of data is usually generated by sensors, and as a consequence, SHM methods are required in order to transform the recorded data into valuable information for decision-makers.

1.1.1 Introduction to Structural Health Monitoring

The size of the European railway network is expected to continuously increase in order to transport most of the long-distance passengers and freight by 2030 [IRA, 2015]. Railways are, indeed, among the most emission-efficient transportation systems, and electric trains can offer a carbon-free journey (if they are powered using nuclear or renewable power sources). More than one million of bridges are present on the European transportation network, which is composed of highways and railways [European Commission, 2012]. These assets are continuously deteriorating due to aging, traffic load (which nowadays exceeds original design criteria of bridges), and environmental effects [Moughty et al., 2017]. Time-consuming and expensive visual inspection techniques are widely adopted to assess the health state of bridges, at fixed time intervals, ranging from one to six years [Wellalage et al., 2015]. Furthermore, visual inspections are based on expert knowledge, and consequently the outcomes can be significantly variable in terms of structural condition assessment, due to subjectivity of the assessor [Phares et al., 2004; Stajano et al., 2010]. In order to overcome the limitations of visual inspections, SHM methods are used to assess the health state of civil infrastructure (including bridges) accurately, remotely and continuously, by

relying on the analysis of static and dynamic responses of the infrastructure [Lynch et al., 2006]. In fact, SHM methods allows to define a damage detection strategy for assessing the health state of structures, by analysing the structure response that is monitored via sensors installed on the structures. Therefore, a SHM strategy consist of a measurement system, which measures the behaviour of the structure, and a data analysis method, that allows to analyse the structure behaviour to assess the health state of the structure and point out damage of the structure promptly. In this way, maintenance costs can be reduced dramatically when the degradation of the infrastructure is identified at an early stage. Conversely, visual inspections might identify the degradation years after its first occurrence, and therefore maintenance costs can increase accordingly.

SHM methods can monitor the health state of the infrastructure continuously, and thus the ongoing degradation can be detected promptly. As a result, information about the health state of the bridge can help in finding an optimal maintenance schedule, which would result in minimizing the whole life cycle cost of the asset [Frangopol et al., 2012; Webb et al., 2015; Zhao et al., 2015]. At the same time, SHM methods, which are able to detect and diagnose sudden and unexpected changes of the infrastructure health state (i.e. damage of the infrastructure), are needed to guarantee the safety and reliability of the asset [Moughty et al., 2017]. Therefore, SHM methods for analysing bridge behaviour data are presented in this thesis in order to assess the health state of bridges.

1.1.2 **Structural Health Monitoring desiderata**

According to the definition of SHM given by [Andersen et al., 2006], *"Structural Health Monitoring (SHM) aims to give, at every moment during the life of a structure, a diagnosis of the "state" of the constituent materials, of the different parts, and of the full assembly of these parts constituting the structure as a whole"*, different individual elements of the infrastructure influence the health state of the whole asset. Therefore, the health state of each element of the system should be assessed simultaneously. Following this definition, the desiderata of the SHM can be given as follows:

- **Real-time monitoring of the structure**. In order to achieve a continuous SHM (i.e. "*at every moment during the life of a structure, a diagnosis of the "state"*" [Andersen et al., 2006]), a continuous flow of data, which measures changes in the behaviour of the monitored asset, is needed [Yeung et al., 2005; Nair et al.,

2010]. Indeed, continuous SHM methods can allow an early identification of a degradation process, and as a result a reduction of the direct life cost of the asset can be achieved by performing maintenance activities when early signs of degradation are identified [Adey et al., 2004; Sekuła et al., 2012; Yi et al., 2013; Chang et al., 2014].

- **A cost-effective monitoring system**. Sensors need to be installed on the most informative position, i.e. the location that provides the least uncertainty in the evaluations of the bridge parameters, in order to optimize the cost and quality of the retrieve information [Liu et al., 2008]. The sensor position is usually determined using expert knowledge; however, for a structure that has not been monitored before, it may be difficult to determine the optimal sensor location, based on the expert knowledge [Li et al., 2004]. Some studies have been proposed in order to find the best configuration of the measurement system, in terms of the appropriate number of sensors and the most informative locations [Meo & Zumpano, 2005; Liu et al., 2008; Laory et al., 2012].
- **Mathematical methods for exhaustive SHM process**. Once sensor data is transmitted through the communications network, it has to be then analysed by a mathematical method in order to automatically, remotely and rapidly assess the level of degradation of the asset [Soyoz et al., 2009]. The main objective of the SHM method is to detect and diagnose a degradation mechanism during its early stage, so that the maintenance crew can go to the site, knowing the required level of maintenance or repair to be carried out [Katipamula et al., 2005]. Furthermore, the assessment of possible future damage of the infrastructure elements can be desired by an SHM method, in order to prevent undesired and unscheduled bridge closure. Basically, an SHM method is required to meet all the four requirements of the damage detection process: *i)* identification of the damage (degradation) existence; *ii)* identification of the damage (degradation) location; *iii)* identification of the damage (degradation) magnitude and causes; *iv)* assessment of the residual useful life (RUL) of the structure, i.e. the period of time during which the reliability of the asset is guaranteed [Wang et al., 2009]. However, it should be noted that the fourth requirement, *iv)*, of the damage detection process is usually used by prognostics strategies, such as Prognostics and Health Management (PHM) strategies, which aim to predict the future health state of the infrastructure,

based on its current state (SHM). Finally, an optimal SHM method is required to be adaptive to environmental changes in order to detect only actual changes to the infrastructure health state, without activating false alarms due to changes in environmental conditions [Cao et al., 2011; Zhou & Yi, 2014].

Graphically, the desiderata of a comprehensive SHM procedure for a bridge infrastructure can be depicted as proposed in Figure 1-1. The bridge performance is influenced by environmental conditions, such as weather condition and traffic load, which influence the vibration properties of the bridge. The climate change can also influence the future performance of the bridge, e.g. more than 3,000 hours of delays have been experienced during two particularly hot summers in 2003 and 2004 in the UK railway network [Hooper et al., 2012; Santillán et al., 2015]. Therefore, the variability of environmental conditions under current and future scenarios, e.g. climate and traffic scenarios, has to be considered in the SHM analysis. Once the bridge is excited by an external disturbance (such as passing train, wind, etc.), the response of the bridge is recorded by sensors, which are installed in the optimal position. Sensor data is then pre-processed in order to remove noise and any influence of changing environmental condition. Then, processed data is used as input data to the SHM method, such as a Finite Element Model (FEM) updating (where, for example, the initial FEM is based on the blueprint of the bridge and on the historical visual inspection reports) or a data-driven (non-model-based) SHM method. If the bridge is in a good condition, damages do not occur, and the next set of measurements can be analysed. At the same time, the prognostic analysis of the bridge can be carried out, i.e. the degradation mechanism and the bridge behaviour can be predicted and simulated, by relying on both environmental and bridge behaviour data. In this way, the future expected health state of the bridge can be assessed. It should be noted, however, that SHM mainly aims to assess the current health state of the infrastructure, whereas similar disciplines, such as Prognostics and Health Management (PHM), aim to predict the residual useful life of the infrastructure. Therefore, a comprehensive analysis of the infrastructure health state would require both the assessment of the current and future condition of the infrastructure.

If degradation is detected (level *i)* [Wang et al., 2009]), a diagnostic analysis has to be performed. During the degradation diagnostic step, level *ii)* and level *iii)* of the degradation analysis evaluation are investigated, through the assessment of the

degradation location and severity, respectively [Wang et al., 2009]. In the case when the degradation on the bridge is particularly severe and, thus, the safety and reliability of the bridge is compromised, an alarm is raised. On the other hand, if the safety of the bridge is still within an acceptable level of risk, the expected residual time, during which the bridge can be safely used, has to be assessed (level *iv)* [Wang et al., 2009]). In this way, a condition-based maintenance strategy can be evaluated by optimizing the time-intervention of the maintenance, based on the future health state of the element of the structure and on the cost of the maintenance activities.

Finally, it is worth mentioning that the desirable characteristics of a comprehensive SHM depicted in Figure 1-1 can lead to the assessment of the degradation existence, location and severity, and to determining the system RUL, which means that the degradation analysis evaluation can performed at all four levels [Venkatasubramanian et al., 2003; Wang et al., 2009; Zio, 2012].

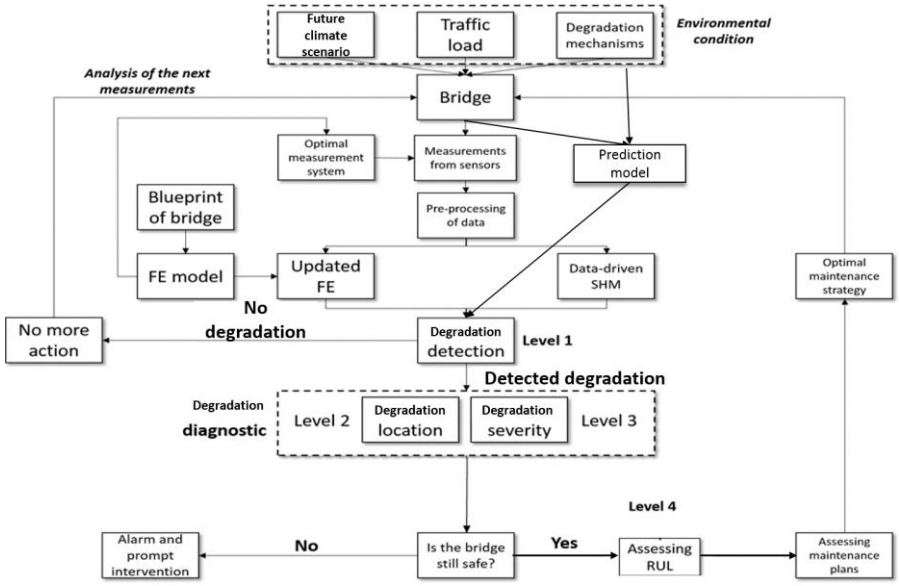

Figure 1-1 . *Flowchart of a comprehensive SHM analysis*

1.1.3 **The need of a Bayesian Belief Network (BBN) approach**

A Bayesian Belief Network (BBN) method for condition monitoring and deterioration diagnostics of bridges is proposed in this thesis, to overcome the criticalities of both model-based and non-model-based methods. For example, model-based methods, such as FEM updating methods [Sanayei et al., 2015; Shabbir et al., 2016], require a complex and time-consuming procedure to develop an accurate FEM, i.e. an FEM that is able to represent the behaviour of a real structure with good

accuracy [Vagnoli et al., 2018]. In contrast, non-model-based methods, such as Artificial Neural Networks (ANNs) [Hakim et al., 2013], Principal Component Analysis (PCA) [Hsu et al., 2010; Cavadas et al., 2013], supervised and unsupervised clustering techniques [Alves et al., 2016; Santos et al., 2016], show promising results for continuous condition monitoring of bridges. However, the performance of non-model-based methods strongly depends on the quality of available data [Kim et al., 2007; Casas et al., 2017; Moughty et al., 2017]. At the same time, non-model-based methods do not take into account the knowledge of structural engineers that design and maintain bridges, and the influence of degradation of individual elements on the health state of the whole bridge.

Hence, bridge managers are in need of SHM methods that are able to: *i)* assess the health state of the bridge by taking account of influences between different elements of the bridge; *ii)* take account of the expertise of bridge engineers without requiring time-consuming process to develop the SHM method; *iii)* manage different sources of data, such as evidence of the bridge behaviour provided by sensors and visual inspection reports; *iv)* update the assessment of the bridge health state every time when new evidence of the behaviour becomes available; *v)* detect and diagnose slow degradation mechanism and sudden changes of the bridge condition (damage), in order to provide rapid information about the health state of the bridge to bridge managers. A BBN approach can satisfy these requirements, by providing a graphical interface to bridge managers, who can interact with the BBN model to assess the health state of the bridge and the influence between different elements of the bridge [Fenton et al., 2013; Rafiq et al., 2015; Kabir et al., 2016].

1.1.4 Data analysis methodology, machine learning methods and BBN

The BBN method is able to assess the health state of a railway infrastructure, and of its elements, at the same time. However, pre-processing of data of the infrastructure behaviour is needed to remove the data noise, which is usually present in the measurement of the infrastructure behaviour. In this way, crisp information about the behaviour of the bridge elements is provided to the BBN. In fact, when the behaviour of an in-field bridge is monitored, it is difficult to clearly point out changes in the bridge health states, due to the statistical variability of the measurements and changing environmental conditions [Kim et al., 2007; Santos et al., 2016]. For these reasons, in this thesis a data analysis methodology is proposed, in order to analyse vibration

behaviour of the bridge and monitor the health state of bridge. The main novelty of the proposed methodology lies in the use of the Empirical Mode Composition (EMD), which is adopted to assess the trend of time and frequency-domain features of the bridge behaviour. The trend of the extracted features is then lumped into Health Indicators (HIs) of the bridge.

The EMD is generally adopted in the SHM framework to identify structural changes by analysing the bridge dynamic behaviour directly, i.e. the dynamic behaviour of the bridge is used as an input to the EMD process, rather than the extracted features [Cahill et al., 2018; Han et al., 2014]. Eventually, HIs can be used as an input to a Neuro-Fuzzy Classifier (NFC), which is able to automatically assess the health state of bridge elements [Cetişli & Barkana, 2010]. This information is finally used as an input to the BBN, which assess the health state of the whole bridge by taking account of influences between different bridge elements.

1.1.5 **A method to update the CPTs of the BBN by taking account of expert judgment and bridge behaviour data**

The Conditional Probability Tables (CPTs) represent the quantitative part of the BBN and allow to define the dependencies between connected nodes of the BBN. An expert knowledge elicitation process is usually adopted to define the CPTs, if no data about the bridge behaviour are available [Loughney & Wang, 2017]. Therefore, experts are interviewed to retrieve the values of conditional probabilities. However, such an approach can be subjective. On the contrary, when data of the bridge behaviour are available, the CPTs can be defined by using learning methods [Sun et al., 2006]. This latter approach requires a large amount of data.

For these reasons, in this thesis, a method to merge the expert judgments with the analysis of a small amount of bridge behaviour data is proposed. The method aims to define the CPTs by the means of the expert knowledge elicitation process, and then to update the CPTs every time when a new measurement of the bridge behaviour is available. The updating process requires the knowledge of Cumulative Distribution Function (CDF) of an optimal HI, which is used to monitor the evolution of the bridge health state. The CDF is retrieved by analysing a database of bridge behaviour, when the bridge behaviour in different health states of the bridge is known.

1.1.6 A method to analyse a database of infrastructure behaviour

The analysis of a database of unknown infrastructure behaviour requires a robust data mining technique to analyse the data automatically, accurately and rapidly [Duan and Zhang, 2006]. In this way, the data of the infrastructure behaviour can be transformed into valuable information for decision makers, by pointing out past abnormal behaviour of the infrastructure.

In this thesis, an ensemble-based change-point detection method is proposed in order to identify changes of the condition of railway infrastructure. This information can be used to: *i)* help the construction of the quantitative part of the BBN, by providing insights about interdependencies between different elements of the asset and (or) changes of environmental condition; *ii)* identify the time when the most severe change of the asset health state occurred, and consequently diagnose the causes of such changes.

An ensemble of change-point detection method is needed due to the fact that individual change-point methods, such as Cumulative Sum (CUSUM)-based [Carslaw et al., 2006] or probability distributions-based [Liu et al., 2013] methods, are able to detect only abrupt changes in the data, without pointing out the most severe changes. As a result, the most severe changes in the data can be lost among all the change-points [Killick et al., 2012]. Furthermore, individual change-point methods are also usually unable to identify the duration of the most critical system behaviour, as their objective is to point out the moment when the data deviates from the average behaviour.

1.2 Research aims and objectives

1.2.1 Research aims

The main goal of this thesis is to a bridge condition monitoring and damage diagnostics method of a critical infrastructure continuously. The focus is on the continuous monitoring, by taking account of the interdependencies between different elements of the infrastructure and diagnosing the damage of the structure. At the same time, methods to analyse database of infrastructure behaviour are investigated, and a method to analyse database of unknown infrastructure behaviour is proposed.

The goals of the thesis are to:

- Propose a method for bridge condition monitoring and damage diagnostics, to assess the health state of a bridge and its elements simultaneously.

- Analyse the performance of the proposed method, by assessing the health state of both in-field bridges and FEM of bridges.
- Achieve a robust assessment of the bridge health state by pre-processing data of bridge behaviour to remove the noise.
- Assess the health state of a bridge in an automatic manner, by taking account of the past behaviour of the bridge.
- Merge the expertise of bridge engineer with the analysis of the bridge behaviour during the assessment of the bridge health state.
- Analyse a database of unknown infrastructure behaviour, with the aim of pointing out changes of the health state of the infrastructure.

1.2.2 **Research objectives**

The following objectives have been fulfilled in this thesis:

- A BBN-based approach is developed for monitoring the condition of a bridge and diagnosing its damage. The main element of the proposed method is to monitor and assess the health state of a bridge continuously, by taking account of the health state of each element of the bridge and without requiring a time-consuming process for its development. The BBN method is verified by monitoring and diagnosing the health state of two bridges, which are modelled via FEMs, and of an in-field bridge.
- A data analysis methodology is proposed to pre-process the bridge behaviour data. The proposed data analysis methodology allows to assess HIs of the bridge. The HIs are identified by extracting statistical, frequency-based and vibration-based features from the vibration behaviour of the bridge, and using the extracted features as an input to an EMD method to assess the trend of the features over time. In this way, the noise of the data is removed, and HIs of the bridge are provided to allow a robust assessment of the bridge health state.
- A machine learning method, which relies on an NFC, is introduced to assess the health state of a bridge element automatically. The method is trained on past behaviour of the bridge and allows to assess the health state of the bridge in an automatic manner.
- A method to update the CPTs of the BBN nodes, by merging the expert knowledge elicitation process and the analysis of a database of bridge

behaviour is proposed. This method allows to update the CPTs of the BBN nodes by taking account of the current health state of the bridge elements.

- A method to analyse database of unknown infrastructure behaviour is proposed. This method relies on an ensemble-based change-point detection algorithm, which is developed to identify the most critical change of the health state of an infrastructure.

1.3 Thesis Outline

The thesis is organized as follows:

- Chapter 2 provides a detailed literature review analysis. Previous researches on SHM are reviewed, by describing model-based methods and non-model-based methods. The advantages and disadvantages of each method are discussed.
- Chapter 3 introduces the proposed BBN method for bridge condition monitoring and damage diagnostics. The theoretical background of the BBN is presented. A step-by-step process is introduced in order to develop the BBN structure and define its CPTs. The BBN is applied using information from the FEMs of two bridges.
- Chapter 4 discusses the data analysis methodology and the machine learning method. The data analysis methodology is applied to two in-fields bridges to assess their health states. Similarly, the machine learning method is applied to an in-field bridge to assess the health state of the bridge automatically.
- Chapter 5 presents the method for defining and updating the CPTs of the BBN by merging the expert judgment with the analysis of the bridge behaviour. The method is applied to an in-field bridge.
- Chapter 6 presents the application of the proposed methods to an in-field bridge. The bridge is monitored by the means of a BBN, whose CPTs are updated by using the proposed method. The results of the data analysis methodology are used as an input to the BBN, to achieve the robust assessment of the bridge health state.
- Chapter 7 discusses the conclusion of the thesis, by highlighting the contributions and the future work.

Chapter 2 **Structural Health Monitoring of bridges**

2.1 Introduction to literature review

An extensive literature review was carried out in this study and is presented in this section, in order to identify the methods used for condition monitoring and damage detection of railway infrastructure, by pointing out the advantages and disadvantages of each method. The literature review focuses on the first three steps of the degradation (damage) analysis process, i.e. degradation identification, diagnostics of degradation location and severity. This is due to the fact that the aim of the thesis is to develop a SHM methodology that fulfils these first three requirements. The fourth point of the degradation (damage) analysis process, i.e. the prediction of the residual life of the bridge, is out of the scope of this thesis. However, the BBN method, which has been scarcely adopted in literature, has been used in few cases as Dynamic BBN (DBN), to predict the future condition of bridges. Although many SHM methods have been developed and applied for bridge condition monitoring, the research is still ongoing to fulfil the four requirements of the fault detection methods.

In the next sections, SHM methods are discussed by grouping them into two categories: model-based and non-model-based methods. A description of each category is provided, and furthermore, several methods for each category are presented individually by emphasizing: *i)* the infrastructure that is monitored; *ii)* how the method works; *iii)* the monitored variables of the infrastructure; *iv)* the results obtained with the considered method.

The requirements for a new condition monitoring and fault detection method are then discussed, with the aim of highlighting the need of an SHM method that has the advantages of both categories.

The content of this chapter has been published in the "*Structural health monitoring journal*", with the aim of discussing and analysing a comprehensive review of SHM methods [Vagnoli et al., 2018]. The tables of this chapters have been extracted from [Vagnoli et al., 2018].

2.2 Model-based condition monitoring and damage detection methods

A model-based condition monitoring and damage detection method aims to assess the condition of a bridge, by comparing the bridge behaviour that is simulated by a FEM of the bridge, with the behaviour of the real structure. FEMs are adopted usually to simulate the bridge behaviour under different environmental conditions, due to their computational and modelling capacity. However, during the development of the FEM, many model parameters (such as material properties, geometric properties and boundary conditions) are unknown and, thus, several assumptions and simplifications need to be made [Mottershead & Friswell, 1993]. An updating process of the bridge FEM parameters is then carried out, in order to obtain the FEM responses to be as similar as possible to the real measured responses of the bridge, and to increase the FEM accuracy by reducing the model uncertainties [Schlune et al., 2009]. This process of developing and updating the FEM can be complex and time-consuming. However, many authors have developed techniques to update FEM for damage detection analysis. In what follows, a description of FEM updating strategies is provided in section 2.2.1, and a discussion of the model-based methods is presented in section 2.2.1.1.

2.2.1 FEM updating methods

In this section FEM updating methods are described by highlighting the type of bridge that was analysed, the choice of the updating parameters and by describing the updating strategy. Finally, the results of each work are presented. Table 2-1 shows the information of the works presented in this section.

Table 2-1. *FE model updating literature examples*

Reference	Type of bridge	Updating parameter(s)	Updating strategy	Results
Sanayei et al., 2015	Bridge model that was designed as a grid system.	Bending rigidity, area mass and boundary link stiffness	To minimize the error function	High correlation between the empirical and analytical data
Teughels et al., 2002	Reinforced concrete beam	Young module	Global damage function	High correlation between the empirical and analytical data
Jaishi & Ren, 2005		Young module and moment of inertia	Frequency residuals	MAC and modal flexibility residuals

	Simple supported bridge		MAC related function Modal flexibility residual Combination of the above three options	result in the best methods to fault detection
He et al., 2008	Three-span-continuous steel truss	Elastic modulus of steel, equivalent node mass of deck and equivalent node mass of steel sleeper	To minimize the error function	Good agreement between the measured and theoretical modal data.
Feng et al., 2015	Steel short span bridge	Dynamic displacement	To minimize the error function	Good agreement between the measured and simulated displacements.
Xia et al., 2014	Box girder bridge	Springs stiffness and elastic modulus of ballast and girders	To minimize the error function	Modal parameters predicted by the FE agree with the real ones.

[Sanayei et al., 2015] analysed a laboratory model of a bridge. The objective error function, which has to be minimized, was defined as the difference between analytical and measured displacements of the bridge. Bridge stiffness and mass parameters were chosen as updating parameters. The results of experiments with static loads and vibrational measurements showed a good match between the updated FEM and measured modal characteristics. Therefore, the authors claimed that if the measured data is quite different from those predicted by the FEM, a damage might have occurred, i.e. the proposed updating strategy could be suitable for a fault detection process. However, the method was not tested in such damaged scenarios.

[Teughels et al., 2002] have studied a simply supported bridge, which was represented by a concrete simple beam. Authors developed a two-step FEM updating procedure by using the Young modulus as updating parameters. In the first step, the initial FEM was updated to a reference state, using measured vibrational data of the healthy bridge structure, and then in the second step, the reference model was updated in order to reproduce the measured vibrational data of the damaged bridge structure. Therefore, a damage could be identified by comparing the output of the reference (healthy) and the damaged FEM. The results showed that the simulated damages have

been correctly identified through an asymmetrical distribution of the updating parameter at the damaged location. The magnitude of the damage was not analysed.

[Jaishi & Ren, 2005] analysed a simply supported bridge. They proposed a sensitivity-based updating strategy using four different objective functions: *i)* frequency residuals, i.e. the residuals between the natural frequencies provided by the FEM and those measured; *ii)* a Modal Assurance Criterion (MAC) related function; *iii)* modal flexibility residual; *iv)* combination of the first three options.
The MAC related function has been defined as follows:

$$f(i) = \frac{(1-\sqrt{MAC_i})^2}{MAC_i} \tag{2-1}$$

where $f(i)$ is the MAC related function at step i. The method has been tested on a laboratory bridge model. The results showed that in each case of the four objective functions, an accurate damage detection becomes more difficult, as the number of updating parameters increases. Furthermore, the objective function based on the combination of frequency residuals, MAC and modal flexibility residuals, improves the performance of damage detection. Therefore, the results of the FEM updating strategy depends on the choice of the number and type of updating parameters. In fact, both physical (such as boundary and material properties) and numerical (such as mathematical modelling and numerical solution) parameters of the FEM are uncertain, and such uncertainty needs to be reduced, by choosing optimal updating parameters that allow a fast and reliable updating process [Başaĝa et al., 2011].

[He et al., 2008] studied a three-span continuous steel truss bridge. Authors proposed to optimize an objective function based on the difference between analytical and measured natural frequency of the bridge. A simple method of model updating was adopted by using the elastic modulus of steel, the equivalent node mass of deck and the equivalent node mass of steel sleeper as updating parameters. Results showed that there is a good agreement between the data provided by the FEM and those retrieved by the sensors, i.e. a maximum error of frequency is 4.09% and the minimum value of MAC is 85.92%. Hence, the method proposed by the authors can be adopted to monitor the evolution of the bridge condition over time, and point out unexpected behaviour of the bridge accordingly. However, the authors did not test the method in any damaged scenario of the bridge.

[Feng et al., 2015] have analysed a single-span railway steel bridge. They proposed an updating strategy of the FE model by optimizing an objective function, which was based on the difference between simulated and measured dynamic displacements of the bridge. The results showed that the displacements of the real bridge and those predicted using the updated FE model were in good agreement. However, the authors pointed out that in order to simulate the behaviour of the real bridge with good accuracy, the interaction between the bridge and the train needs to be modelled and updated accurately. As a result, a set of new variables is introduced in the updating process by resulting in an increase of computational time and uncertainty of the process.

[Xia et al., 2014] monitored a box-girder railway bridge. The authors proposed an FEM updating strategy based on the optimization of an objective function that aimed to minimize the differences between the real and simulated modal properties of a railway bridge. Results showed a good match between the predicted and measured modal parameters of the railway bridge. The optimization problem proposed by the authors showed good results when high modal parameters of the bridge were used to update the FEM characteristics, e.g. from the 6^{th} to the 11^{th} mode shapes. However, high modal parameters of the bridge, which are more sensitive to damage, are difficult to extract from the data measured in an in-field bridge in a reliable manner. As a consequence, the reliability of the condition monitoring process can be threatened [Casas et al., 2017].

2.2.1.1 **Summary of the FEM updating strategy**

FEM updating strategies are one of the most common techniques adopted for monitoring and assessing the health state of a bridge. In fact, an FEM method allows to simulate the behaviour of the bridge under changing environmental conditions. Furthermore, as soon as new information regarding the health state of the bridge, such as visual inspection reports of the bridge, or new measurement of the bridge behaviour, is available, the FEM can be updated accordingly. However, the development of an FE model can be complex and time-consuming. The choice of the updating parameters is a challenge, due to the fact that different updating parameters lead to different accuracy and computational time of the updating process. For example, it has been shown that the higher the complexity of the structure, the larger the number of updating

parameters: [Teughels et al., 2002; Jaishi & Ren, 2005] have studied a simple supported span bridge and beams, and consequently, only one or two updating parameter(s) have been selected; [He et al., 2008; Sanayei et al., 2015] have studied a more complex bridge structure, such as a three-span continuous bridge, and the number of updating parameter was consequently increased. The increase of the number of the updating parameters can lead to a reduction of the performance of the condition monitoring method, due to an increase of uncertainty and computational time of the updating process [Jaishi & Ren, 2005]. It is worth noting that, even if the initial FEM may not represent the real structural behaviour accurately due to modelling uncertainties, the responses provided by the initial FEM before the updating procedure need to be relatively similar to those provided by the real measured bridge responses, in order to avoid a long updating process, which might have no optimal solutions. The size and complexity of the FEM and its updating strategy can be a challenge for achieving a continuous SHM. Finally, the magnitude of the damage and the effect of environmental condition on the modal parameters of the bridge are not considered generally. Consequently, only the first two requirements of the damage detection process (identification of the damage existence and damage location) are satisfied.

2.3 Non-Model-based methods

Non-model-based methods can provide information about the health state of the bridge rapidly, by analysing the bridge behaviour directly, without requiring a development of an FEM of the structure. In literature, non-model-based methods have demonstrated to be suitable for real-time monitoring of complex systems, such as nuclear systems [Zio et al., 2010], industrial processes (including chemicals, microelectronics manufacturing, iron and steel, pharmaceutical processes, and power distribution networks) [Qin, 2012; Yin et al., 2014], petroleum and natural gas systems [Galotto et al., 2015] and electric vehicles [Rigamonti et al., 2016]. For these reasons, in what follows a survey of non-model-based methods for bridge condition monitoring and damage detection is provided. Particularly, ANN methods have been intensively used as a condition monitoring and damage detection method in the structural engineering framework, and as a result section 2.3.1 presents the analysis of these ANN-based methods. At the same time, other non-model-based methods have been presented in literature, such as unsupervised clustering methods or statistical approaches. These latter methods are presented and discussed in section 2.3.2. Finally,

section 2.3.3 shows some works based on BBNs, which can evaluate the condition of individual elements on the bridge as well as considering the structure as a whole.

2.3.1 Artificial Neural Network based methods

In this section ANN-based methods applied to monitor the condition of bridges are described. Table 2-2 shows the main characteristics of the works discussed in this section, by highlighting the type of the bridge under analysis, the nature of the ANN, the monitored behaviours of the bridge and the results of the considered method.

Table 2-2. *Examples of condition monitoring methods based on the ANN*

Reference	Type of bridge	Type of NN	Number of input nodes	Number of hidden nodes	Number of output nodes	Type of input data	Results
Shu et al., 2013	FE model of Banafjäl bridge, Sweden	Back propagation single layer	Not explained	19 for fault detection 23 for fault diagnostic	Not explained	Displacements and acceleration	Results strongly depend on the position of the fault and on the load and velocity of the train
Lee et al., 2005	FE model of a beam	Back propagation multi layers	20	20 first layer 20 second layer	8	Mode shape, mode shape difference before and after failure and mode shape ratio for the first four modes	Generally, the method shows good accuracy with some false alarms in the laboratory and Hannam bridge case study
	FE model of single span bridge		98	60 first layer 40 second layer	40		
	Laboratory model of bridge		24	24 first layer 8 second layer	8		
	Hannam Grand bridge, South Korea		80	60 first layer 60 second layer	40		
			6	19	5		
Park et al., 2009	FE and laboratory model of simply supported beam	Back propagation	50	50	Depending on the case study	Acceleration	Good accuracy as sequential FD method: acceleration-based NN monitors the bridge in real
			Depending on the	Depending on the case study	Depending on the case study	Modal data	

			case study				time, modal-based NN assesses the location and severity of the failure.
Mehrjoo et al., 2008	FE model of a truss	Feed forward	32	50	5	Natural frequencies and mode shape	98% of correct classification
	FE model of Louisville bridge, UK		Varying the number of the inputs	Depending on the number of the inputs	6		From 90 to 98% of correct classification
Cremona et al., 2012	Steel railway bridge	Feed forward	Not explained	Not explained	Not explained	Symbolic data of acceleration, natural frequencies and mode shapes	The method provides good accuracy by using the different input data.

[Shu et al., 2013] analysed an FEM of a simply supported bridge. An ANN damage detection method was proposed by monitoring acceleration and displacements of the bridge. Authors have demonstrated that the performance of the ANN decreases, as the signal noise increases and the load of the train that was passing over the bridge decreases. Furthermore, the damage location has been demonstrated to be an issue; indeed, a damage that has occurred in the middle of the bridge was easier to detect than at the end of the bridge due to different impact of the damage on the bridge behaviour.

[Lee et al., 2005] have presented an ANN-based damage detection method by studying four different bridge case studies (FEM of a beam, FEM of single span bridge, laboratory model of bridge and the Hannam Grand bridge, South Korea) with three different ANN input strategies: *i)* mode shapes; *ii)* mode shape differences between before and after damage; *iii)* mode shape ratios for the first four modes. Results showed that for all case studies, even when some false alarms have been raised, the proposed method was able to identify the damages, using the differences or the ratios of the mode shape between before and after the damage, as the data input. However, mode shape can be difficult to be obtained from the measured bridge behaviour. Indeed, false alarms were raised during the analysis of the real in-field bridge in all considered damaged scenarios.

[Park et al., 2009] have studied an FEM and laboratory model of simply supported bridge. The authors proposed a sequential damage detection method based on an acceleration-based ANN (ABNN) and on a modal feature-based ANN (MBNN). The ABNN was used to monitor the behaviour of the bridge and to detect the occurrence of a damage by using acceleration data as input; whilst the MBNN was used to estimate the location and the severity of the occurred damage by using modal parameters, such as mode shapes, as input. Results showed that the occurrence, the location and magnitude of damage is correctly identified by firstly adopting the ABNN and, sequentially, the MBNN. Although, the method shows good performance, it should be mentioned that the identification of modal parameters can be difficult for an in-field bridge [Casas et al., 2017].

[Mehrjoo et al., 2008] have analysed two FEMs of two steel truss bridges. They proposed an ANN-based method to detect damage of the bridge, by using natural frequencies and mode shape as input to the ANN. The accuracy detection of the proposed method was higher than 90%. However, the accuracy of the results and the architecture of the ANN strongly depended on the number of vibration modes, i.e. natural frequencies and mode shapes that have been considered as input of the ANN. At the same time, the accuracy of the ANN depended on the numbers of input and hidden neurons, i.e. the performance of the method depended on the structure of the ANN.

[Cremona et al., 2012] discussed a NN-based classification method in order to assess the condition of a steel railway bridge over time. Particularly, strengthening works were carried out on the bridge, and the authors aimed to assess the health state of the strengthened bridge. Therefore, symbolic data of the measured acceleration, natural frequencies and mode shapes were used as the input to an ANN, which has been trained using historical measurements. Results showed that when a new and unknown measurement was available, the proposed method was able to correctly assess the condition of the bridge up to 93% of the tested scenarios. It should be noted that due to the availability of a vast database of recorded behaviour of a real bridge, good results in terms of assessment of the condition of the bridge were achieved.

2.3.1.1 **Summary of ANN-based methods**

One of the most important issues of the ANN strategy is the selection of the model structure, i.e. the number of hidden layers and neurons. The number of the input neurons is, generally, taken to be equal to the number of the monitored variables of the system, e.g. [Mehrjoo et al., 2008] changed the number of input neurons based on the number of input variables. A general rule to select the optimal number of input nodes is not available, and thus, the optimal number of input nodes is defined by trial and error procedure usually. The number of hidden neurons is usually kept to as low as possible, in order to reach the best solution in terms of computational time cost and residual error. This procedure is one of the most critical aspects of the use the ANN, and it is generally addressed by using a trial and error procedure [Lee et al., 2005; Mehrjoo et al., 2008; Park et al., 2009]. Although a methodological criterion to choose the optimal ANN structure has not been proposed yet, Bayesian processes can be adopted to investigate how a different number of hidden layers and nodes influences the accuracy of the ANN-based method [Arangio et al., 2014]. Generally speaking, the accuracy increases as the number of hidden layer and neurons increases, however, an over-parameterization may be achieved. Indeed, if the ANN is over-parameterized, i.e. the number of hidden neurons is too high, the ANN is optimal to mimic the training set, but it is unable to manage new and unknown patterns. Furthermore, the best ANN structure is chosen for a particular case study usually, and as a consequence, it has to be changed if the case study changes (i.e. the bridge model under study or the number of the modal properties is changed), as demonstrated by [Lee et al., 2005; Mehrjoo et al., 2008; Park et al., 2009].

The performance of the ANN in terms of accuracy depends on the data used in the training set. For example, [Mehrjoo et al., 2008] have demonstrated that the ANN damage detection accuracy decreases and, thus, the number of false alarms increases, as the number of the considered modal characteristics (e.g., the number of considered natural frequencies or mode shapes) decreases and the noise of the data increases. Moreover, [Shu et al., 2013] have shown that the accuracy of the ANN is affected by the damage location: a failure close to the end of the bridge is more difficult to be detected than a failure in the middle of the bridge.

Finally, although the ANN method has been applied in a number of studies, it has three main limitations:

i) the ANN methods are able to approximate any function, but they are not directly correlated to the bridge model, and thus they do not represent the physical structure of the bridge. A model with the properties showed by the ANN is also called black-box model usually. Thus, the expertise of the structural engineers that have developed the FEM of the bridges is lost, as the damage detection methods based on the ANN rely only on the data retrieved by the bridge.

ii) there is no standard method to choose the optimal structure of the ANN. At the same time, a criterion to rigorously define how much and what type of training data are required, has to be defined in order to achieve a fast and reliable training process [Lee et al., 2014; Kan et al., 2015].

iii) there is a need of a large amount of data, which contains the behaviour of the bridge under changing environmental scenarios, in order to correctly assess the health state of the bridge.

2.3.2 **Other non-model-based methods**

Non-model-based methods can be based on a variety of different mathematical models, such as regression model, machine learning methods, genetic algorithm methods, clustering methods, etc. In what follows, a survey of non-model-based methods for bridge SHM is provided by describing unsupervised clustering methods or statistical approaches, such as regression and PCA methods. The unsupervised clustering methods are thoroughly described due to the fact that they are able to monitor the health state of the bridge in an unsupervised way by aiming to group different bridge behaviours in separate, well distanced and compact clusters. In this way, the distance between different clusters (between-cluster variance) is maximized, whilst the distance between behaviours of the bridge that have similar properties (within-cluster variance) is minimized. *Table 2-3* shows the methods described in this section.

Table 2-3. *Condition monitoring analysis using data-driven methods*

Reference	Type of bridge	Monitoring method	Type of input data	Results
Kim et al., 2015	Seven-span plate bridge	Bayesian regression	Acceleration of the bridge	Depends on the environmental conditions, such as traffic load

Laory et al., 2013	Steel truss railway bridge Five spans box girder bridge	Moving Principal component analysis coupled with regression methods	Quasi-static measurement	The coupling of MPCA and regression methods shows better results than the singular methods.
Cury et al., 2012	Steel bridge	Hierarchy-divisive and a dynamic clouds clustering method	Symbolic acceleration, natural frequencies and mode shapes	Good assessment of the health state of the bridge with very low false alarms raised.
Guo et al., 2012	Steel bridge	K-means clustering	Sorted acceleration data	Good performance in the analysis of the FE model. However, false alarms are raised in the analysis of the real bridge.
Langone et al., 2017	Concrete bridge	adaptive kernel spectral clustering	Natural frequencies	Good detection ability of the method, that decrease as the environmental condition changes.
Alves et al., 2016	Steel railway bridge and concrete highway bridge	K-means, hierarchy-agglomerative and fuzzy c-means clustering methods	Acceleration data	Good results for the railway bridge. Many misclassifications for the highway bridge due to changing environmental condition.

[Kim et al., 2015] studied a seven-span plate bridge. The authors used coefficients of an autoregressive model of the bridge acceleration as Damage Indexes (DI). The behaviour of the bridge is monitored by an online Bayesian updating process of the DIs, and consequently, if the value of the DIs changes suddenly, the health state of the bridge experienced a change. Acceleration data over one year have been used as input to the method. Three different data strategies have been considered: a) complete environmental change scenario, where acceleration, temperature and vehicle weight data have been used; b) temperature change scenario, where acceleration and temperature data have been used; c) no environmental change scenario, where only acceleration data without considering environmental changes have been used. Results showed that the analysis, considering both temperature and vehicle weight as environmental effects (case a), led to more accurate results than case b) and c). Therefore, a more accurate and reliable assessment of the bridge health state is achieved when changes of environmental condition are considered into the analysis, and not only the behaviour of the bridge (e.g. acceleration).

[Laory et al., 2013] analysed an FEM of a steel truss bridge. Authors developed a damage detection method by coupling a Moving PCA (MPCA) and regression methods. The performance of the proposed method was compared with those of the individual methods, i.e. MPCA and regression method alone. The results showed that the proposed method had better performance in terms of damage identification. The method was also tested on a real five-span box girder bridge, and it provide better results of each individual method. Although the method showed good performance, the data used for the analysis are quasi-static measurement, i.e. the excitation of the bridge was so small that the dynamical effects of the bridge were negligible.

[Cury et al., 2012] analysed a steel bridge by comparing the performance of a hierarchy-divisive and a dynamic clouds clustering method. Acceleration and natural frequencies of the bridge were used as the input to the analysis. During a pre-processing analysis, the acceleration and natural frequencies data were transformed into symbolic data by the means of a frequentist analysis. The condition monitoring of the bridge was carried out by assigning each new measurement to the cluster with the minimum distance. Results showed a very low rate of misclassification by using the acceleration data as the input to both clustering methods, i.e. the condition of the bridge were assessed correctly. However, when the analysis was performed by using the natural frequencies as the input to the clustering methods, misclassifications were identified due to noisy data.

[Guo et al., 2012] presented a K-means-based clustering method in order to assess the condition of a steel railway bridge (FEM and real in-field bridge). Acceleration data are used as input to the clustering method. The K-means algorithm was used in order to group the measured data into different groups. The method showed good performance in identifying damages when the FEM was analysed, however, when the real steel railway bridge was analysed, several false alarms were raised, due to the impact of environmental condition, which led to a noisy measurement of the bridge behaviour.

[Langone et al., 2017] analysed a concrete bridge. An unsupervised adaptive kernel spectral clustering method was proposed to monitor the health state of bridge infrastructure. Natural frequencies of the bridge were used as input to the proposed method. Results showed that damages of the bridge were identified correctly. However, when the environmental conditions changed, such as variation of the air temperature, the accuracy of the proposed method decreased.

[Alves et al., 2016] presented a study in order to compare the performance of three clustering algorithms, K-means, hierarchy-agglomerative and fuzzy c-means clustering methods, in two different case studies: a steel railway bridge and a concrete highway bridge. The symbolic values of the acceleration data were used for the analysis, i.e. the acceleration data were transformed into symbolic variable by the means of a frequentist analysis. The three methods showed good results when the steel railway bridge was analysed, where the K-means algorithm outperformed the other methods in identifying the changes of the stiffness of the bridge. On the other hand, the analysis of the highway bridge showed that the fuzzy c-means method was able to provide the best classification results. However, the changing environmental conditions led to a high number of misclassification (over 40%).

2.3.2.1 **Discussion of other non-model-based methods**

The presented non-model-based methods have demonstrated the ability to detect failures in the considered case study efficiently. However, false alarms and misclassification were obtained mainly due to changing environmental condition that led to the presence of noise in the data, particularly in the modal parameters of the bridge. [Kim et al., 2015] have pointed out that the understanding of how ambient temperature and traffic effects influence the behaviour of the bridge is of vital importance for bridge SHM. In fact, the impact of environmental variations on the bridge modal properties can lead the developed condition monitoring algorithms to raise many false alarms. The non-model-based methods are usually optimized for a specified structure that is subject to known environmental and operational conditions. Therefore, good performance for new and previously unknown environmental and operational conditions, which have been not included in the database used, cannot be guaranteed [Zio, 2012]. The methods presented in this section are mainly focused on the first two requirements of the damage detection process, i.e. failure existence and failure location. The magnitude of the damage is not assessed usually due to a lack of adequate dataset to develop the methods. Hence, a vast database that contains both healthy and degraded behaviours of the bridge is needed, in order to develop a reliable non-model-based condition monitoring and damage detection method.

Finally, the results provided by these methods need to be evaluated by an expert, in order to assess the actual health state of the bridge. In fact, these methods are only able

to point out a change of the bridge behaviour without diagnosing its causes, and without considering interdependencies between different elements of the infrastructure.

2.3.3 **Bayesian Belief Network methods**

In structural engineering framework, the BBN method has been mainly used in reliability assessment studies, e.g. probability of failure due to the scour phenomena [Salamatian et al., 2013], fragility of the reinforced concrete bridges [Franchin et al., 2016] and assessment of technical causes of that can lead to a catastrophic bridge downfall [Holický et al., 2013], and for prediction of future residual life of the bridge. Although the use of the BBN methods for condition monitoring and damage diagnostics of bridge is limited, BBN-based methods can be a great candidate for the real time SHM, due to the fact that BBN gives the opportunity to assess the health state of the whole bridge and its elements at the same time, by managing complex information from different sources, such as sensors and visual inspection reports. Furthermore, the extension of the BBN, called DBN, can be used to analyse problems with time varying domains. Table 2-4 shows the papers that have adopted a BBN-based strategy for SHM, by highlighting the strategy adopted to define the CPT of the network.

Table 2-4. *Condition monitoring strategies based on BBN*

Reference	Type of bridge	Proposed method	Definition of CPTs	Type of input data	Results
Rafiq et al., 2015	50 Masonry arch bridges	Condition modelling of the bridge based on BBN and DBN methods	Expert judgment	Bridge visual inspection results (SCMI)	Condition of the bridge over time
Attoh-Okine & Bowers, 2006	Single span steel girder, reinforced concrete deck bridge	Deterioration modelling of the bridge based on BBN	Expert judgment	Expert judgment	Probability of the bridge health state
Wang et al., 2012	Girder steel bridge	Condition modelling of the bridge based on DBN	Expert judgment	Simulated observations of the bridge	Condition of the bridge over time
Kosgodagan-Dalla Torre et al., 2017	4 steel bridges	Deterioration modelling of the bridge based on DBN	Expert judgment	Traffic and load data from a weigh-in-motion (WIM) system	The predicted useful life of the bridge strongly relies on the available information

[Rafiq et al., 2015] showed how a BBN method could be used as a condition-based deterioration modelling methodology for a bridge management system. The data used as the input to the BBN model were visual inspection reports of 50 masonry arch railway bridges. The condition of the whole bridge was obtained by considering the health state of each element of the bridge, i.e. the minor elements influences the major elements of the bridge, which influence the health state of the whole bridge. A DBN was developed to model and predict the future degradation level of the masonry bridges. CPTs of the network were defined by the means of the information provided by the visual inspection reports. Results showed that the BBN is able to assess how the health state of the whole bridge is influenced by the degradation of its elements, whereas the DBN was able to predict the health state of the bridge over time by highlighting the ability of the DBN in updating the bridge health state when new evidence of the bridge health state are available.

[Attoh-Okine & Bowers, 2006] built a BBN using a Fault Tree (FT) for a railway bridge [LeBeau et al., 2000]. The authors presented a qualitative case study in order to investigate the feasibility of SHM by using a BBN method. Consequently, the behaviour of a bridge was not considered in the analysis. The CPTs for the overall bridge deterioration process were described by using engineering judgment. The input data to the BBN were obtained by interviewing seven bridge engineers and inspectors in order to analyse three 'what if' scenarios, e.g. the authors analysed a scenario where the bridge joints are all in the acceptable condition state with the aim of analysing how the health state of the bridge is influenced by this information.

[Wang et al., 2012] studied the main girder of a steel railway bridge. Authors proposed a DBN to predict the condition of bridge elements. The deterioration process of bridge elements was modelled using maintenance actions, environmental effects (i.e. traffic volumes and loads, temperature, humidity). Evidence of the bridge behaviour were used as DBN input at each time step. The CPTs were estimated using the expertise knowledge. Results showed how the evolution of the bridge future condition changes significantly, when new bridge condition information, i.e. the visual inspection records, became available.

[Kosgodagan-Dalla Torre et al., 2017] presented a DBN to model and predict the degradation of a bridge network when limited data about the bridge behaviour are available. The authors considered a network of four steel bridges. The transaction

probabilities of the DBN, i.e. the probability that a bridge of the network improves or decreases its health state, are defined by using an expert knowledge elicitation process. Results showed that the accuracy of the prediction of the future degradation level of the bridge increases, when more information about environmental condition of the bridges are available.

2.3.3.1 **Discussion on Bayesian Belief Network**

Generally, the BBN method describes the deterioration process of the bridge by considering the effects of each individual bridge element on the health state of the whole bridge. Expert knowledge and bridge response data are merged in a BBN, and consequently the results of the BBN rely on the strength of the expert knowledge, and the comprehensive information regarding the behaviour of the bridge. However, the structural behaviour of the bridge is usually not considered as the input to the presented BBN-based methods. Instead, visual inspection reports are used as evidence of the bridge behaviour. The definition of the CPTs is one the major issues for the BBN application. The usual practice is to define CPTs by using an expert knowledge elicitation process. However, this process can be time-consuming and subjective. Furthermore, the size of the CPT can increase considerably with the number of parents, which can make the process of populating the CPTs intractable. This problem can be avoided using fewer states for each node and the divorcing node technique [Chen & Pollino, 2012].

2.4 Requirements for a new detection and diagnostics of bridge deterioration method

The literature review of model-based and non-model-based methods shows that several methods have been proposed to fulfil the requirements of the first three steps of the degradation (damage) analysis [Wang et al., 2009]. However, model-based and non-model-based methods show criticalities in monitoring the health state of a bridge continuously, by taking account of the influences between different elements of the bridge, managing different source of data (such as bridge behaviour and expert knowledge) and diagnosing the location and level of severity of the bridge degradation. Therefore, taking account of the criticalities of the reviewed approaches, the requirements for a new condition monitoring and damage detection method for bridge infrastructure can be defined as follows:

- Able to consider the knowledge of bridge engineers;
- Do not require time-consuming process to be developed;
- Able to update the health state of the bridge by taking account of the health state of each element of the bridge;
- Able to consider influences between different bridge elements;
- Able to monitor the health state of the bridge continuously;
- Able to use different source of information about the health state of the bridge, such as data provided by a measurement system installed on the bridge and visual inspection reports;
- Able to identify unexpected behaviour of the bridge (Level *i)* of the damage detection process [Wang et al., 2009]);
- Able to diagnose the unexpected behaviour of the bridge (Level *ii)* and *iii)* of the damage detection process [Wang et al., 2009]);
- Able to provide rapid information about the health state of the bridge to bridge managers;
- Able to assess the health state of the bridge under unknown environmental condition.

Chapter 3 The proposed Bayesian Belief Network approach

3.1 Introduction

A Bayesian Belief Network (BBN) methodology for bridge condition monitoring and damage diagnostics is developed in this thesis, with the aim of overcoming the criticalities of both model-based and non-model-based methods. The few applications of the BBN for SHM of bridges have demonstrated that a BBN can update the condition state of the bridge and its elements, every time when new evidence of the bridge behaviour becomes available. At the same time, a BBN is able to merge expert knowledge and bridge behaviour information and manage complex interactions between bridge elements and complex information from different sources (e.g. sensor data, visual inspection reports, etc.). For these reasons, a BBN methodology is proposed in this thesis, in order to monitor the condition state of a bridge continuously, by detecting unexpected behaviour and diagnosing the causes.

A similar approach has been studied by using FTs. In fact, FTs can analyse the health state of bridges by taking account of the interdependencies between different bridge elements [Attoh-Okine & Bowers, 2006; Lebeau et al., 2010]. FTs and BBNs agree in the development of the qualitative part of the model, i.e. both graphical interfaces can be developed by performing a step-by-step process that aims to identify the bridge elements that influence the health state of the bridge. However, FTs allow a binary analysis, e.g. each element of the bridge can be either degraded or not, and the severity of the degradation can be assessed only by introducing a node for each severity level into the graphical interface of the FT, i.e. each FT node represents a specific degradation state of the system. Therefore, the larger the number of health state level of the bridge, the larger the size of the FT [Noroozian et al., 2018]. As a result, BBNs can provide a compact representation of the bridge infrastructure by allowing a reliable detection and diagnostics process of the bridge degradation.

The proposed BBN methodology is presented in Figure 3-1: a BBN is composed of a graphical structure and a quantitative part, known as Conditional Probability Table (CPT), also discussed in the theoretical introduction to the BBN (Section 3.2). The steps to develop a BBN for bridge condition monitoring process are presented in

section 3.3, by discussing how the graphical structure of the BBN is developed by analysing the bridge structure (3.3.1), and how the CPTs are then defined through an expert knowledge elicitation process (section 3.3.2). When the BBN is developed, the condition of the bridge can be monitored, by using information about the health state of the bridge as an input to the BBN, such as the data provided by a measurement system installed on the bridge or visual inspection reports. The bridge behaviour is analysed by the nodes of the BBN, and the health state of the bridge elements is evaluated. At the same time, the condition of the whole bridge is updated accordingly. The causes of a change of the bridge condition can be analysed by using the diagnostic property of the BBN, which allows to diagnose the causes of a change in the bridge health state. The proposed method is applied to a steel truss railway bridge (section 3.4.1) and a beam-and-slab bridge (section 3.5.1), in order to investigate the performance of the BBN in terms of condition monitoring and damage diagnostics accuracy. The results of the bridge condition monitoring and damage diagnostics process are discussed in section 3.4.3 for the steel truss railway bridge, and section 3.5.3 for the beam-and-slab bridge, respectively. The drawbacks of the proposed method for each application are presented in section 3.4.5 and section 3.5.4, respectively. Finally, the results of the BBN-based SHM and the future developments of the method are summarised in section 3.6.

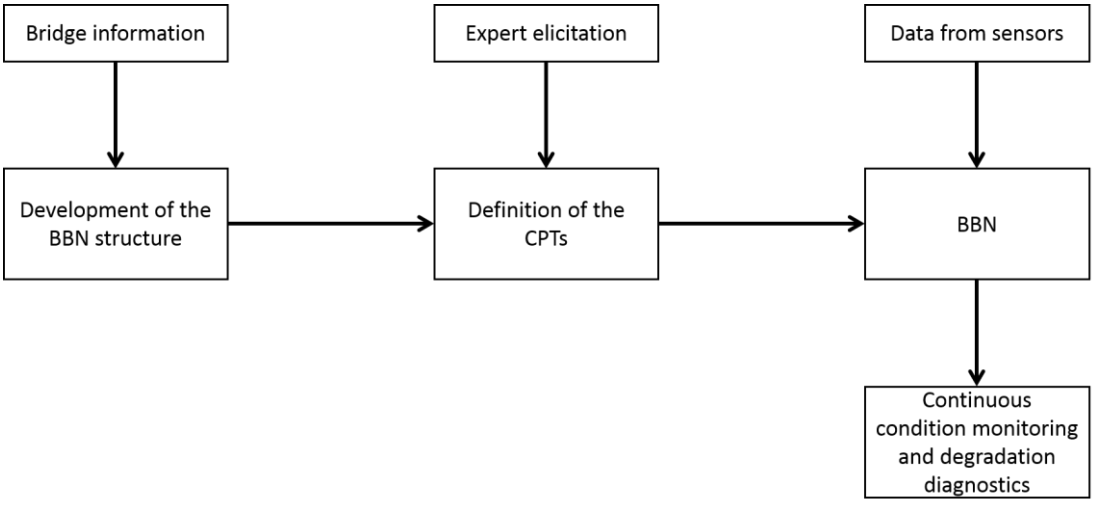

Figure 3-1. *Proposed methodology for BBN-based condition monitoring and degradation diagnostics of bridges*

3.2 Background of the Bayesian Belief Network method

BBNs have been developed in the 80s, when a novel approach to represent the expert knowledge within a computational architecture has been proposed by [Pearl, 1986]. In that work, Pearl developed a graphical interface between expert knowledge, statistics and computers, by linking nodes, which represent the object under study and its properties. Given a system that needs to be analysed, Pearl proposed to firstly identify the relevant system variables and the (causal) relations among them. In this way, the qualitative part of the BBN is developed by the means of a graphical interface. The quantitative part of the network is defined by assessing a set of conditional probability distributions in order to quantify the interdependencies between different connected nodes.

3.2.1 The structure of the BBN

The graphical interface of a BBN is made of a set of variables (called nodes) and a set of directed links (called arcs) between system variables of interest. The arcs represent a causal relationship between variables of interest of the system. For example, Figure 3-2 shows a directed graph from variables *A* and *B* to *C*, i.e. the directed arcs start from nodes *A* and *B* and end with node *C*, and as a consequence *A* and *B* are parent nodes of *C*, and *C* is a child node of *A* and *B*. BBNs are acyclic graphs, i.e. connections between nodes $A_1, A_2, A_3, ..., A_n$, such as $A_n = A_1$, are not permitted [Jensen & Nielsen, 2007].

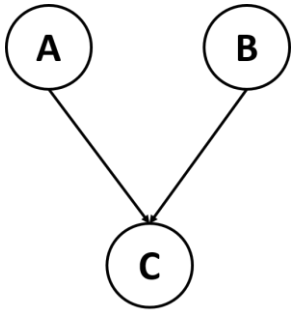

Figure 3-2. *Example of relationship between parent and child node*

3.2.2 Bayes theorem and CPTs

Generally speaking, the conditional probability of a variable *X* that is conditioned on the occurrence of another variable *Y* is defined as follows:

$$P(X \mid Y) = z \tag{3-1}$$

Eq. (3-1) shows that if *Y* has occurred and other known events are irrelevant for *X*, then the probability that *X* occurs is *z*.

Generally, the probability that the two events *X* and *Y* occur is:

$$P(X,Y) = P(Y \mid X)P(X) = P(X \mid Y)P(X) \tag{3-2}$$

where $P(X,Y)$ is called the joint probability of *X* and *Y*.

A BBN is able to update the probability about a certain variable *X*, given information about another variable *Y*, by adopting the Bayes' rule, which can be derived by rewriting Eq. (3-2) as follows:

$$P(X \mid Y) = \frac{P(Y \mid X)P(X)}{P(Y)} \tag{3-3}$$

The probabilities $P(X)$ and $P(Y)$ can be found by marginalising *Y* and *X* out, respectively, from the joint probability $P(X,Y)$:

$$P(X) = \sum_{Y} P(X,Y) \tag{3-4}$$

$$P(Y) = \sum_{X} P(Y,X) \tag{3-5}$$

The marginalization of *Y* and *X* in Eq. (3-4) and Eq. (3-5), respectively, is assessed by applying the rule of the total probability. For example, assuming that the two variables *X* and *Y* are defined by exhaustive and mutually exclusive states $X = (x_1, x_2, \ldots, x_n)$ and $Y = (y_1, y_2, \ldots, y_m)$, the rule of the total probability allows to assess $P(X)$ as follows:

$$\forall i \qquad P(x_i) = P(x_i, y_1) + P(x_i, y_2) + \ldots + P(x_i, y_m) = \sum_{j=1}^{m} P(x_i, y_j) \tag{3-6}$$

Eqs. from (3-1) to (3-6) allow to evaluate the conditional probability of each variable of the BBN, when the CPT of the variables are defined.

The quantitative part is represented by conditional probabilities associated with each node. The state of a node, from which the arc connection departs, influences the state of the node where the arc connection ends via a conditional probabilistic

relationship [Lampis et al., 2009]. Continuous or discrete conditional probability distributions can be used to describe the conditional probabilistic relationship between two connected nodes [Morales-Nápoles et al., 2014]. A set of exhaustive and mutually exclusive possible states has to be adopted when the nodes of the BBN are described through discrete conditional probability distributions [Vileiniskis et al., 2016]. The CPTs can be described by considering the network in Figure 3-2.

Assume that each node is described by two mutually exclusive states, such as $A = a_1, a_2$, $B = b_1, b_2$ and $C = c_1, c_2$. The parent nodes are not conditioned, and thus their CPTs coincide with the probability of each individual state: a_1, a_2 and b_1, b_2. The child node *C* is conditioned by the known state of its parent nodes, *A* and *B*, and therefore its CPT is as shown in Table 3-1. The sum of the conditional probabilities $P(C = c_i \mid A = a_j, B = b_k)$, where *j* and *k* are fixed, for all states of *i* has to be equal to 1, i.e. each column of the CPT must sum to 1.

Table 3-1 shows an important property of the CPTs: the size of the CPT increases with the number of parent nodes and the number of the states of both parent and child nodes. Indeed, a child node with *K* states and *N* parents with *H* states is described by a CPT with $K \cdot H^N$ entries. In fact, node *C*, which is described by 2 states and has 2 parent nodes with 2 states each, is described by a CPT that requires $2 \cdot 2^2 = 8$ entries.

Table 3-1. *CPT for the node C of Figure 3-2*

	$B = b_1$		$B = b_2$	
	$A = a_1$	$A = a_2$	$A = a_1$	$A = a_2$
$C = c_1$	$P(C = c_1 \mid A = a_1, B = b_1)$	$P(C = c_1 \mid A = a_2, B = b_1)$	$P(C = c_1 \mid A = a_1, B = b_2)$	$P(C = c_1 \mid A = a_2, B = b_2)$
$C = c_2$	$P(C = c_2 \mid A = a_1, B = b_1)$	$P(C = c_2 \mid A = a_2, B = b_1)$	$P(C = c_2 \mid A = a_1, B = b_2)$	$P(C = c_2 \mid A = a_2, B = b_2)$

3.2.3 **Chain rule and update of the conditional probabilities**

In the BBN framework, each node X_i is conditioned on its parent nodes, pa(X_i), and thus the probability $P(X)$ can be decomposed into a product of conditional probability distributions by using Eq.(3-2) repetitively:

$$P(X) = \prod_{i=1}^{n} P(X_i \mid X_{i+1}, \ldots, X_n) = \prod_{i=1}^{n} P(X_i \mid pa(X_i)) \tag{3-7}$$

where *n* is the number of nodes of the BBN. Eq. (3-7) is known as the probability chain rule and allows to assess the joint distribution of each set of BBN variables by using only conditional probabilities. Therefore, given a set of nodes $U = A_1, A_2, A_3, ..., A_n$ within the BBN, every time when new evidence e_m, with $m = 1, 2, ..., M$, about the state of the nodes of the BBN become available, the BBN is able to update the degree of belief of the node states by computing the posterior probability distribution of each node as follows:

$$P(A \mid e) = \frac{\sum_{A \in U} P(U, e)}{P(e)} \tag{3-8}$$

where $P(U, e)$ is the updated joint probability:

$$P(U, e) = \prod_{i=1}^{n} P(A_i \mid pa(A_i)) \prod_{m=1}^{M} e_m \tag{3-9}$$

Eq. (3-8) shows that the probability of each node, *A*, is updated given the evidence *e*, by applying the Bayes' rule (Eq. (3-3)), whereas Eq. (3-9) shows that the joint probability of the each BBN node is updated by applying the chain rule (Eq. (3-7)). Finally, it is worth noting that the evidence e_m is introduced into the BBN as a vector of zeros and ones, where the zeros represent the fact that the state of the node has not occurred, whilst the ones represent the fact that the state has occurred.

3.2.4 **BBN used to decompose systems into smaller parts**

The BBN also allows to decompose a complex system into smaller parts. In fact, the BBN of a complex and large system, such as a bridge, can result in a large and complex BBN structure. Consequently, the graphical representation of the BBN can become ineffective due to a large number of nodes of the BBN. Furthermore, some systems can consist of a number of similar elements installed next to each other, e.g. multiple similar beams of a bridge. In these cases, the BBN allows to decompose the system into Objected Oriented Bayesian Network (OOBN). From the graphical point of view, the OOBN allows to define a new separate BBN in order to represent all the elements of a part of the complex BBN system. Subsequently, the part of the BBN of the system is replaced by a single evidence node, which represents each element of the

considered part. For example, Figure 3-3 shows a BBN of a system that is composed of three components, A, B and C. Each component is made of five elements. The dependencies between different elements of the system can be difficult to be identified due to the high number of connections between different nodes. The OOBN allows to simplify the BBN, as shown in Figure 3-4.

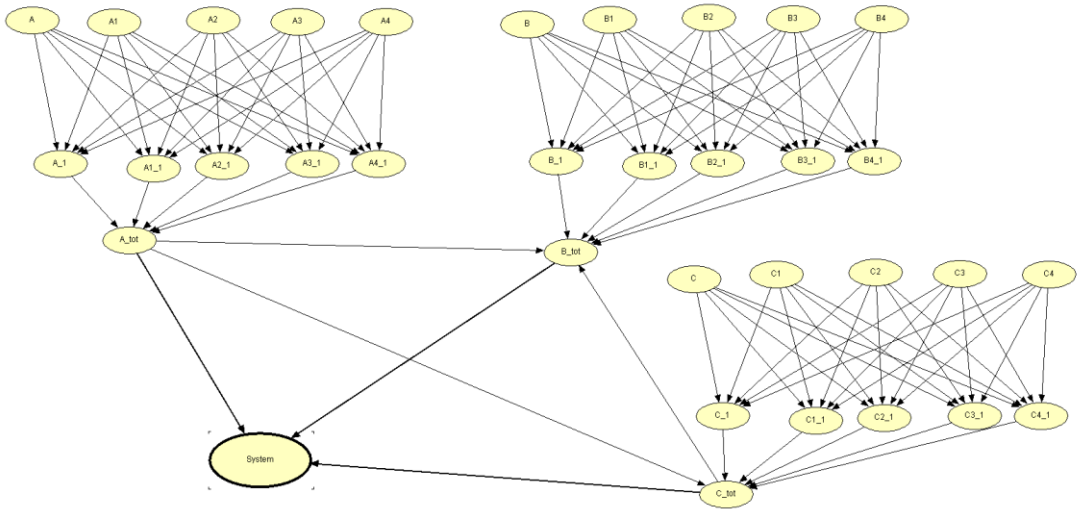

Figure 3-3. *Example of complex system for OOBN*

Figure 3-4 shows the OOBN of the system. The graphical view of the network is clearer than the one in Figure 3-3. In fact, the connections between the different components of the system are pointed out more clearly. Each node within a rectangular node represents evidence introduced to the BBN. For example, Figure 3-5 shows the BBN for the components A and C. It should be noted that the BBN of each component in Figure 3-5 is made of the same connections as in Figure 3-3. However, Figure 3-5b shows that the BBN of component C has an additional node, which is depicted by a dashed node and represents the evidence of the BBN about component A, i.e. the BBN of Figure 3-5a. In this way, the graphical view of the BBN can be simplified, and each component of the system can be analysed separately.

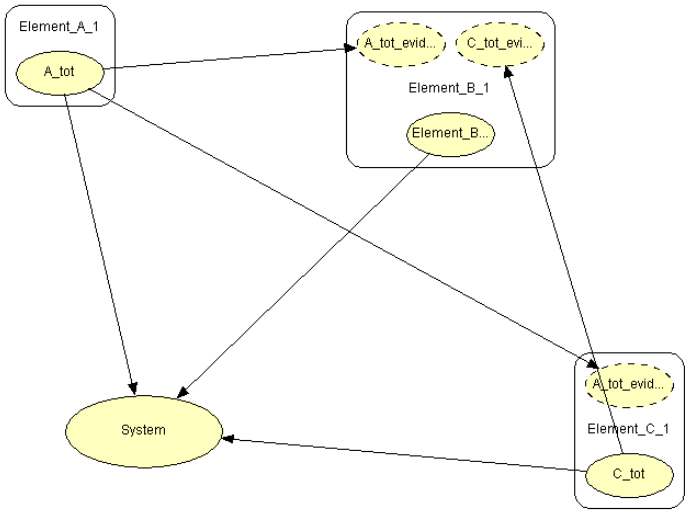

Figure 3-4. *Example of OOBN*

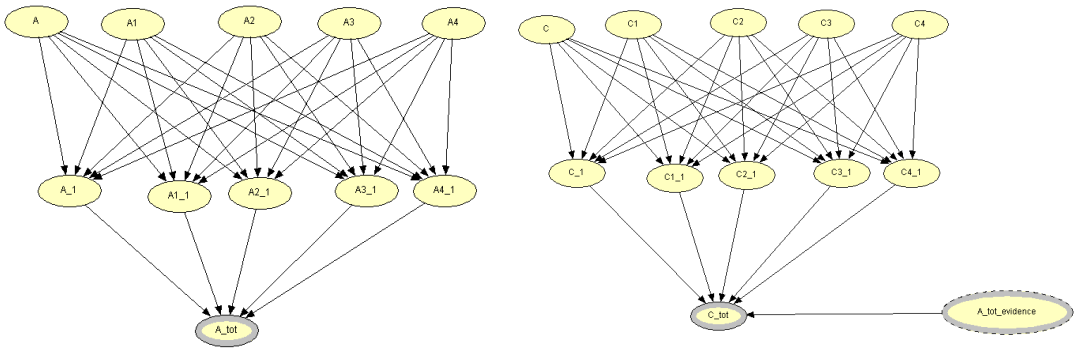

(a) (b)

Figure 3-5*. Evidence nodes of the OOBN*

Finally, the OOBN allows to simulate the evolution over time of the health state of a system. Indeed, the dynamic OOBN allows to assess the condition of a node of the BBN by taking account of the health state using evidence nodes of the BBN. Particularly, the whole system can be represented by the means of evidence nodes, and thus connecting consecutive evidence nodes of the system, the evolution of the condition of the system over time can be assessed.

3.3 The proposed methodology for building a Bayesian Belief Network for detection and diagnostics of bridge deterioration

In what follows, a step-by-step process is proposed with the aim of guiding the reader through the development of a BBN for bridge condition monitoring. Section

3.3.1 describes the steps to develop the graphical interface of the BBN, whereas section 3.3.2 describes the steps necessary to define the CPT.

3.3.1 The method of building the BBN

A step by step process to develop the structure of the BBN for condition monitoring and degradation diagnostics of a bridge infrastructure is hereafter described. The following steps are proposed:

1. **Identify the type of the bridge and its major and minor elements of interest**. Several types of bridge structure, such as box-girder, cable stayed, truss, arch, suspension, etc., are usually found within the transportation network [Catbas et al., 2008; Arangio et al., 2014; Xia et al., 2014; Ni, 2014; Gentile et al., 2015]. The analysis of the bridge structure helps to identify the bridge components (major elements) and sub-components (minor elements) of which a bridge manager needs to monitor the condition [LeBeau et al., 2000]. The identification of the elements of the bridge can be as detailed as the bridge manager requires. Indeed, each minor element is made of relatively small elements, such as smaller beams, joints, etc. However, a balance between the number of elements of interest and the size of the BBN needs to be reached, due to the fact that the size of the BBN increases as the number of the bridge elements of interest increases. Finally, it should be noted that sometimes guidelines that describe the bridge structure, i.e. major and minor elements of the bridge, can be provided by the bridge owner [Gangone et al., 2011].
2. **Define the BBN structure**. When the bridge elements of interest are identified, the structure of the BBN can be developed, i.e. the set of nodes and arcs can be defined. The nodes of the BBN represent the major and minor elements, whereas the arcs represent the interdependencies between the nodes of the BBN. The construction of the BBN should follow the same order as for the construction of the real bridge, i.e. from minor to major elements. In fact, the condition of a major element of the bridge is influenced by the condition of its minor elements, and thus each major element is child node of its minor element nodes. The health state of the whole bridge can be then evaluated by introducing a child node to the major elements of the bridge [Attoh-Okine & Bowers, 2006].

3. **Upgrade the BBN model to take account of the interdependencies among major/minor elements**. The health state of a major (minor) element depends also on the condition of the other major bridge (minor) elements. Thus, the BBN structure can be further developed in order to take into account the interdependencies between major (minor) elements of the bridge. As the BBN is an acyclic graph, additional nodes are introduced in order to evaluate interdependencies between different elements of the bridge that belong to the same class, i.e. major or minor elements.
4. **Choose the number of health states of each node.** An element of the bridge experiences different health states during its life time, such as good and degraded conditions. Therefore, each BBN node should be described by a set of mutually exclusive discrete states to describe these conditions. The number of states can be as large as the bridge manager would require. However, the size of the CPTs increases as the number of states increase. Bridge owners can usually provide information about the possible conditions of a bridge. For example, Network Rail, which is the owner of the UK railway network, assesses the condition of bridges by considering three classes: *i)* good condition, if the element is in good condition and maintenance actions are not required; *ii)* partially degraded, if maintenance action are required, but they can be postponed due to budgeting reasons, without compromising the safety of the asset; *iii)* severely degraded, if essential maintenance actions, i.e. that cannot be postponed, are required [Rafiq et al., 2015].
5. **Define nodes to represent the measurement system of the bridge**. If a measurement system is installed on the bridge, sensors, such as accelerometers, strain gauges, tiltmeters, etc., are used to monitor the bridge behaviour under changing environmental conditions [Roberts et al., 2004]. The data provided by the sensors is evidence of the bridge behaviour, and, as a consequence, a node for each sensor can be added to the BBN. The nodes representing the sensors are introduced as parent nodes of the bridge element(s) on which the sensors are installed. If a measurement system is not installed on the bridge, the BBN approach can be still adopted, by relying on different sources of information on the bridge behaviour, such as visual inspection reports.
6. **Review the BBN structure by analysing the bridge behaviour.** When the BBN is developed, its structure can be updated by analysing the behaviour of

the bridge elements. In fact, the BBN structure is developed by considering the expert knowledge, however, some connections between elements of the bridge can be redundant because such elements do not influence each other (or their influence is negligible) on the real bridge. A database of bridge behaviour is needed in order to assess the influences between elements of the bridge, and as a consequence to update the structure of the BBN.

7. **Obtain the final BBN structure.** When the sensor nodes are introduced, the structure of the BBN is completed.

In order to use the BBN in monitoring the bridge health state, the CPTs need to be defined in order to describe the relationship between the nodes. The steps to define the CPTs are presented in the next section 3.3.2.

3.3.2 The method of CPT definition

CPTs are used to define the dependencies between connected nodes of the BBN in a probabilistic manner, i.e. using conditional probabilities. The CPTs can be defined by adopting several techniques, depending on the nature of the available information about the system of interest: *i)* if a database of information about the past behaviour of the system is available, the CPTs can be defined by adopting a learning technique, e.g. expectation maximization [Sun et al., 2006]; *ii)* if such database is not available, the CPTs can be defined by using an expert knowledge elicitation process [Loughney & Wang, 2017]. In this part of the thesis, the CPTs of the BBN are defined by the means of an expert knowledge elicitation process. The expert elicitation process, which is usually adopted to define the CPTs of a BBN method, is going to be then merged with the analysis of the bridge behaviour in Chapter 5 . The chosen approach is to select a set of scenarios where minor or/and major element(s) of the bridge have reached a certain level of degradation, and ask bridge engineers to analyse these scenarios [Das, 2004]. The following process is proposed:

a) **Identify the experts**. This step is important as the accuracy of the elicitation process strongly depends on the knowledge and the level of expertise of experts. Selecting several experts with different level of expertise can lead to a more complex analysis of their answers. Conversely, a heterogenic group of experts, for example, practicing engineers and academics, can lead to a more reliable and accurate analysis. Indeed, a result that is retrieved by aggregating

the analysis from a group of experts is usually more reliable than each individual analysis [Surowiecki, 2004; Kabir et al., 2016].

b) **Identify the degraded scenarios.** The definition of the CPTs can be an extremely time-consuming process, due to the number of scenarios that the experts need to analyse. As a result, the uniformity and consistency of the expert knowledge elicitation process might not be achieved [Elmasry et al., 2017]. A smaller number of scenarios can be presented to the expert by considering scenarios that are physically consistent. For instance, if a minor element of a bridge is degraded in a specified health state, the major element, which contains that minor element, is expected to be in a similar health state [Das, 2004; Rafiq et al., 2015].

c) **Present the scenarios to the experts.** The set of degraded scenarios is presented to experts through interviews and online surveys [Perkusich et al., 2013]. Each scenario needs to be described accurately, by explaining the health state of the element of interest and its possible influence on the health state of the connected nodes.

d) **Provide a scale for answers.** A linguistic scale can be provided to the experts in order to answer the questions. In fact, experts can be more comfortable in providing a linguistic answer rather than a precise numerical value of the probability, due to the fact that the linguistic answer allows to take account of some uncertainty [Torfi et al., 2010]. An example of a linguistic scale is shown in Table 3-2.

Table 3-2. *Linguistic scale for assessing the interdependencies between different bridge elements*

Linguistic scale	**Meaning**
very unlikely	it is highly unlikely that the health state of the considered element would be influenced by the described critical scenario of the bridge element
unlikely	it is unlikely but possible that the health state of the considered element would be influenced by the described critical scenario of the bridge element
even chance	the likelihood that the health state of the considered element would be influenced by the described critical scenario of the bridge element is even chance

likely	it is likely that the health state of the considered element would be influenced by the described critical scenario of the bridge element
very likely	it is highly likely that the health state of the considered element would be influenced by the described critical scenario of the bridge element

e) **Merge the individual analyses.** The linguistic answers from the experts can be described numerically by using a fuzzy membership function (such as a triangular, Gaussian or trapezoidal function). In this way, the vagueness and subjectivity of the expert judgment is addressed mathematically [Ferdous et al., 2011]. All the individual membership functions are merged together, by weighing the experience of the experts. In this thesis, a weighing factor (W_l) is used to weigh the expert analysis with respect to the level of experience of the expert. Hence, the more experience the expert has, the greater weight is assigned to his judgment [Kabir et al., 2016]:

$$W_l = \frac{E_l^{\beta}}{\max_{l=1}^{N}(E_i^{\beta})} \tag{3-10}$$

where E_l is the number of years of experience of the expert l; β is a parameter employed to adequately weigh the analysis of each expert. β should be defined by guaranteeing a group judgment, which is based on the information retrieved by the whole group of experts [Tesfamariam et al., 2010].

f) **Assess the influence of each parent node on its child**. The influence of a parent node on its child nodes is evaluated by using a Fuzzy Analytic Hierarchy Process (FAHP) of the experts analyses. In what follows only the main steps of a FAHP are described [Wang et al., 2006; Torfi et al., 2010; Loughney & Wang, 2017]. The damaged scenarios presented to the experts can be seen as fuzzy pairwise comparison matrices [Loughney & Wang, 2017]. Assume that a triangular fuzzy membership function, which is characterized by $\mu = (a, b, c)$, Figure 3-6, where $a<b<c$, is adopted to describe the analysis of the experts. Consider that P_{hk} is the 1-pairwise comparison between the bridge element h and k. The first step of the FAHP is to compute a fuzzy synthetic extent value, S_h:

$$S_h = \sum_{k=1}^{C} P_{hk} \otimes \left[\sum_{h=1}^{D} \sum_{k=1}^{C} P_{hk} \right]^{-1} \tag{3-11}$$

where D is the number of rows of the pairwise comparison matrix, i.e. the number of bridge elements that influence the health state of other bridge elements, and C is the number of columns of the pairwise comparison, i.e. the number of bridge elements that are influenced by a selected bridge element. The sum of the pairwise comparison of each child node (the first term of Eq. (3-11)) can be easily computed as:

$$\sum_{k=1}^{C} P_{hk} = \left(\sum_{k=1}^{C} a_k, \sum_{k=1}^{C} b_k, \sum_{k=1}^{C} c_k \right) \tag{3-12}$$

whereas the second term of Eq. (3-11) is computed following the modified Chang extend analysis, which has been demonstrated to perform better than the original Chang extend analysis [Wang et al., 2006]. An integral value of each synthetic extend value is then evaluated as follows:

$$I_h = \frac{1}{2}\left(\alpha c_h + b_h + (1-\alpha) a_h\right) \tag{3-13}$$

where $\alpha \in [0,1]$ is the optimism of the expert on the results of his analysis, and (a_h, b_h, c_h) are the fuzzy membership of the *h-th* fuzzy synthetic extent [Kabir et al., 2016]. Finally, the importance weight vector (w_h) of each parent node on its child nodes can be assessed as:

$$w_h = \frac{I_h}{\sum_{h=1}^{D} I_h} \tag{3-14}$$

where $h = 1, 2, \ldots, D$.

g) **Assess the consistency of the expert analysis.** The expert knowledge elicitation process can be a long task for the experts. Consequently, the consistency of the expert analysis needs to be verified by assessing a Consistency Ratio (*CR*). Therefore, the fuzzy pairwise comparison matrix is defuzzified, and then a Consistency Index (*CI*) is computed as follows:

$$CI = \frac{\lambda_{\max} - D}{D - 1} \tag{3-15}$$

where $\lambda_{\max}$ is the maximum eigenvalue of the defuzzified pairwise comparison matrix. *CR* is evaluated by dividing *CI* by a Random Index (*RI*), which is provided in literature and depends on the size *D* of the pairwise comparison matrix [Saaty et al., 2007]:

$$CR = \frac{CI}{RI} \tag{3-16}$$

Generally, a FAHP is considered consistent, i.e. the analysis of the experts is consistent, if the *CR* is lower than 0.1 [Kabir et al., 2016].

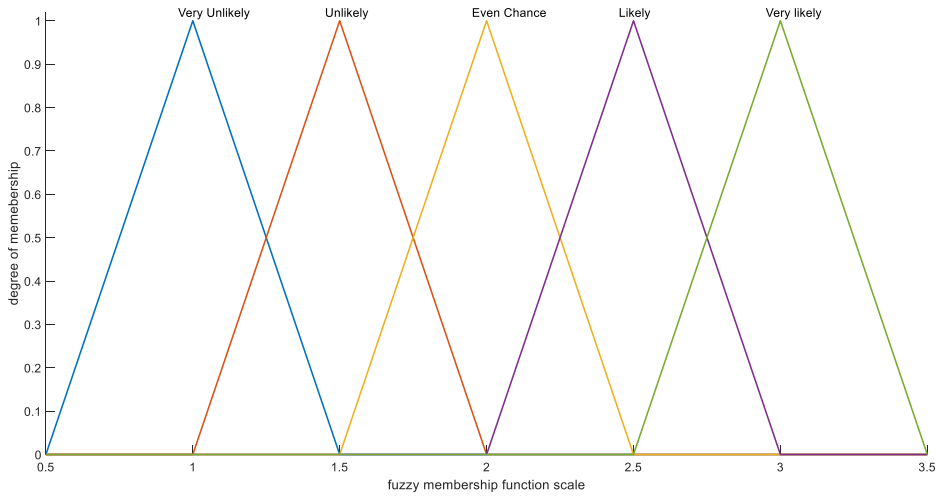

Figure 3-6. *Triangular fuzzy membership function to represent the linguistic scale*

h) **Compute the conditional probabilities for the bridge element nodes**. Consecutive inspections of in-field bridges have pointed out that the degradation of a bridge (such as cracks formation, paint degradation and corrosion of materials) can be modelled by adopting a linear model [Enright & Frangopol, 1998; Kreislova et al., 2012; Attema et al., 2017; Rao et al., 2017]. Hence, a linear model is used in the proposed method to define the probabilities in the CPTs. Assume that a bridge element, described by node *X*, is in state x_i. There are *N* parent nodes of this element, denoted as a set Y^k. The conditional probability is calculated using a linear function shown in Eq. (3-17):

$$P(x_i \mid \bigcap_{k=1}^{N} Y^k = y_k) = P(x_i \mid \bigcap_{k=1}^{N} Y^k = y_k = 1) + \sum_{m=1}^{M} P(x_i \mid \bigcap_{k=1}^{N} Y^k = y_k = 1) \cdot w_{h_m} \cdot f_{p_m} \cdot p_i \cdot \delta \quad (3\text{-}17)$$

where $P(x_i \mid \bigcap_{k=1}^{N} Y^k = y_k)$ is the probability of the child node in state x_i, with a condition that the health states of the parent nodes are known, denoted as y_k; $P(x_i \mid \bigcap_{k=1}^{N} Y^k = y_k = 1)$ is the probability of the child node X in state x_i, with a condition that all parent nodes are in the healthy state, y_k=1, i.e. the parent nodes show no degradation; M is the number of degraded parent nodes; w_{h_m} is the importance weight vector used to assess the influence of each degraded parent node on the state of the child node, note that w_{h_m} is calculated using Eq. (3-14); f_{p_m} is a penalty factor that increases as the condition of the bridge element(s) deteriorates; $\delta = -1$ if the child node is in the healthy state, x_i=1, and $\delta = 1$ if the child node is in the degraded state; p_i is a vector used to normalise the respective column of probabilities in the CPT and it depends on the state of the child node.

Overall, Eq. (3-17) shows that the probability of the child node being in state x_i, with a condition that M parent nodes are degraded, is computed as the total $\sum_{m=1}^{M} w_{h_m} f_{p_m}$ decrease or increase of $P(x_i \mid \bigcap_{k=1}^{N} Y^k = y_k = 1)$, caused by the influence of M degraded parent nodes. M can be between 0 to N, i.e. if M=0 (there are no degraded parent nodes), then $P(x_i \mid \bigcap_{k=1}^{N} Y^k = y_k = 1)$ does not change; if M=N (all parent nodes are degraded), then $P(x_i \mid \bigcap_{k=1}^{N} Y^k = y_k = 1)$ experiences its maximum variation.

Finally, when the CPTs are defined, the BBN is ready to be used to monitor the health state of the bridge and diagnose its unexpected behaviour.

In the next section, an FEM of a steel truss railway bridges is introduced, with the aim of simulating the beahviour of the bridge under changing condition, and to test the

proposed BBN method in monitoring the behaviour of the bridge in detecting and diagnosing its unexpected behaviour.

3.4 BBN model for a steel truss bridge and its application in detection and diagnostics of bridge deterioration

In this section, the proposed BBN methodology is applied to monitor the health state of a steel truss bridge, which is subject to a gradual degradation mechanism of its element(s). The aim of this case study is the testing of the updating capability of the BBN with respect to the bridge condition monitoring and damage diagnostics process. An FEM of a steel truss bridge is developed with the aim of simulating the behaviour of the bridge under an ongoing degradation mechanism, which leads to a gradual decrease of the bridge health state. The BBN is required to monitor the health state of the steel truss bridge continuously, by pointing out changes of the bridge condition and diagnosing the causes of such changes. The FEM is presented in section 3.4.1. The step by step process to develop the BBN is discussed in section 3.4.2, whereas its performance in monitoring the bridge condition is presented in section 3.4.3. Section 3.4.4 evaluates the performance of the proposed BBN method. The results of the proposed method are discussed in section 3.4.5.

3.4.1 FEM of a steel truss railway bridge

An FEM of a steel truss bridge is developed in order to test the proposed BBN methodology in monitoring the condition of the bridge over time, using a model. An FEM is required due to the fact that data from an in-field bridge are difficult to retrieve, because a bridge is a critical infrastructure of the transportation network, and thus usually bridge owners are not willing to share the data. Moreover, a laboratory model of a bridge is not available, and it would be more expensive and time-consuming to develop a laboratory model of a bridge, rather than an FEM.

The FEM model that is described in this section is developed by assuming that the boundary conditions are fixed, i.e. air temperature is fixed, wind is not present, and no traffic is passing over the bridge, and only a static uniform load is applied to the bridge. Although many bridge of the transportation network are more than 50 years old, and therefore they are built using old materials (such as iron), the materials of the developed FEM are defined by following the "*Innovative Bridge Design Handbook*" [Pipinato & Patton, 2016]. The aim of the FEM is not to simulate the behaviour of a real in-field bridge accurately, but rather to simulate the bridge behaviour under

changing condition of the bridge, i.e. the behaviour of the bridge when a degradation mechanism is present, in order to test the monitoring and damage detection and diagnostics ability of the proposed BBN method. The FEM is developed by using SAP2000, which is a structural software that allows to perform finite element analysis. Section 3.4.1.1 describes the developed steel truss railway bridge, whilst section 3.4.1.2 discusses the considered and modelled degradation mechanism of the bridge.

3.4.1.1 **FEM development**

A warren steel truss bridge is modelled, as shown in Figure 3-7 (a). A steel railway truss bridge is selected for the analysis since the degradation mechanisms of steel, such as corrosion and cracks, can develop rapidly after they are initiated. An early detection and management of such degraded condition can be of great importance to bridge owners, who can improve the safety and availability of the bridge, by decreasing its whole-life cycle cost [Katipamula et al., 2005]. Figure 3-7 (b) shows the elements on the top of the bridge: the top chords, which are 24 m long, are composed of 4 horizontal beams, each one long 6m; the cross beams, which are the vertical elements in Figure 3-7 (b), are 7m long; the top bracings, i.e. the diagonal components, are 9.2 m long. Figure 3-7 (c) shows the side view of the bridge, where the diagonals elements are 8.55m long. Figure 3-7 (d) shows the bottom part of the bridge: the external horizontal beams of Figure 3-7 (d) represent the bottom chords, which are composed of 5 beams, which all are 6m long. Furthermore, two stringers are modelled on the deck, i.e. the horizontal beams between the two bottom chords, and the connection between bottom chords and stringers is modelled through diagonal stringers. The elements of the bridge are modelled by considering the S355 steel, as this steel is commonly used in Europe to build steel railway bridges [Pipinato & Patton, 2016].

The reference system, which is depicted in Figure 3-7 and used throughout the body of the text, is defined as follows: the right-hand side of the bridge is considered as the side of the bridge at y = 0 m, the left-hand side is considered to be at y = 7 m.

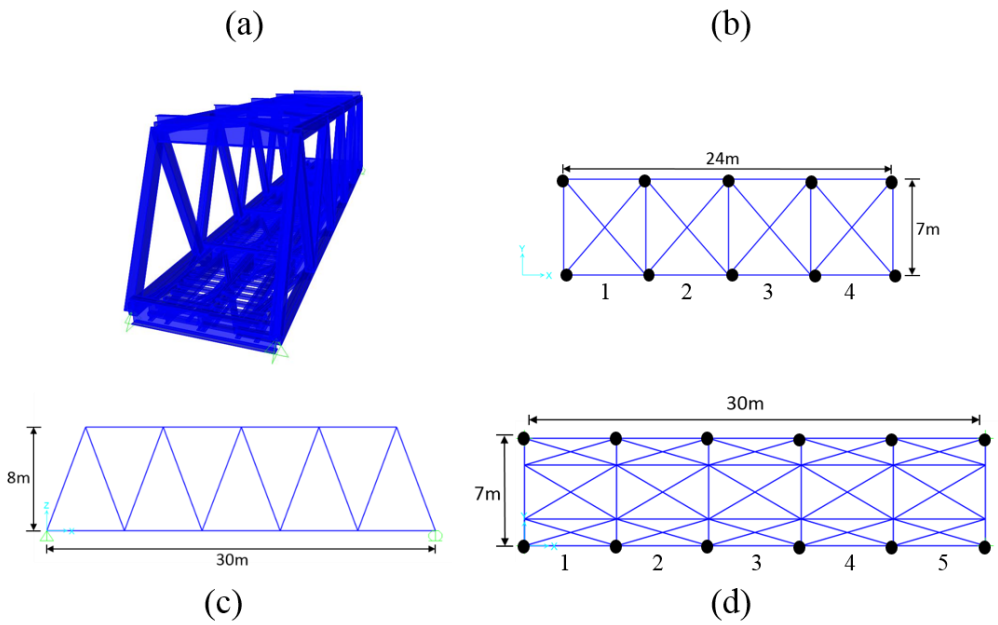

Figure 3-7. *The FEM of the steel truss bridge. Overview, top, lateral and bottom view of the steel truss bridge, in figure (a), (b), (c) and (d) respectively*

3.4.1.2 **Modelling the degradation mechanism**

A degradation mechanism of the bridge element(s) is simulated to investigate the bridge behaviour under different states of deterioration. The formation and propagation of micro-cracks at the joint location is analysed, due to the fact that micro-cracks are difficult to spot during a visual inspection. Therefore, monitoring techniques are very useful. More than 40% of the steel truss bridges are affected by the formation of micro-cracks at the joint location [Mehrjoo et al., 2008]. When the micro-cracks are initiated, their size can increase due to the effect of environmental factors (e.g. trains are continuously passing over the bridge), and thus the bridge can suffer with fatigue. The cross-sectional area of the degraded bridge element(s) at the joint location is gradually reduced with the aim of simulating this degradation mechanism. The displacement of the bridge elements at the joint location is recorded at 5 locations on each top chord and 6 locations on each bottom chord, as shown by dark circles in Figure 3-7. Displacements are chosen, due to the static load (40 kN/m) applied to the bridge.

The values of the FEM do not include any noise. However, measurement noise is unavoidable in in-field applications [Dowling et al., 2012]. For this reason, a Gaussian noise is added to the simulated displacements:

$$y_{pol} = y_{FE} + q_p N\sigma(y_{FE}) \quad (3\text{-}18)$$

where y_{pol} is the displacement of a bridge element when the noise is added, y_{FE} is the displacement value provided by the FEM, q_p is the ratio of standard deviation between the noise and the FEM displacement y_{FE} and is equal to 5%. *N* is a standard normal distribution of mean 0 and standard deviation 1, and $\sigma(y_{FE})$ is the standard deviation of the results of the FEM [Shu et al., 2013].

The deterioration mechanisms of the bridge element(s) is studied by developing 28 deterioration scenarios:

- 22 individual deterioration mechanism scenarios, where each joint of the top chords (10 scenarios) and bottom chords (12 scenarios) is individually degraded. The cross-sectional area of the corresponding minor elements at the joint location is gradually decreased down to the 70% of its initial value. The minor elements of the top and bottom chords are chosen due to the fact that they have shown the highest stresses during the service of a steel truss bridge [Ni et al., 2012].
- 6 multiple deterioration mechanism scenarios, where two or three joints of the top/bottom chords are degraded, by decreasing the cross-sectional area of the corresponding minor elements at the joint location.

For example, Figure 3-8 shows the evolution of the displacement of the third and fourth joints of the top chord on the right-hand side of the bridge, when the fourth joint is degraded over time, i.e. a gradual degradation of the joint is simulated by the means of consecutive simulations. The displacements provided by the FEM for the two joints, when a static uniform load of 40kN/m is applied to the bridge, are depicted by the solid lines in Figure 3-8 (a) and (b) for the third and fourth joint, respectively. The dotted lines of Figure 3-8 represent the displacement of the two elements of the bridge when the Gaussian noise is added. Figure 3-8 shows that with the same static load that is applied to the bridge, the higher the loss of cross-sectional area (i.e. the more degradation has occurred), the higher (in terms of absolute value) the displacement of the bridge elements. In a similar way, Figure 3-8(c) and (d) show that the displacement of the two joints increase as the joint degradation increases over time (i.e. consecutive

simulations time). Therefore, the displacements can be used as an indicator of the health condition of the bridge over time.

In what follows, the proposed BBN method is developed in order to test its performance in monitoring the condition of the presented FEM, by diagnosing the degraded element(s) of the bridge.

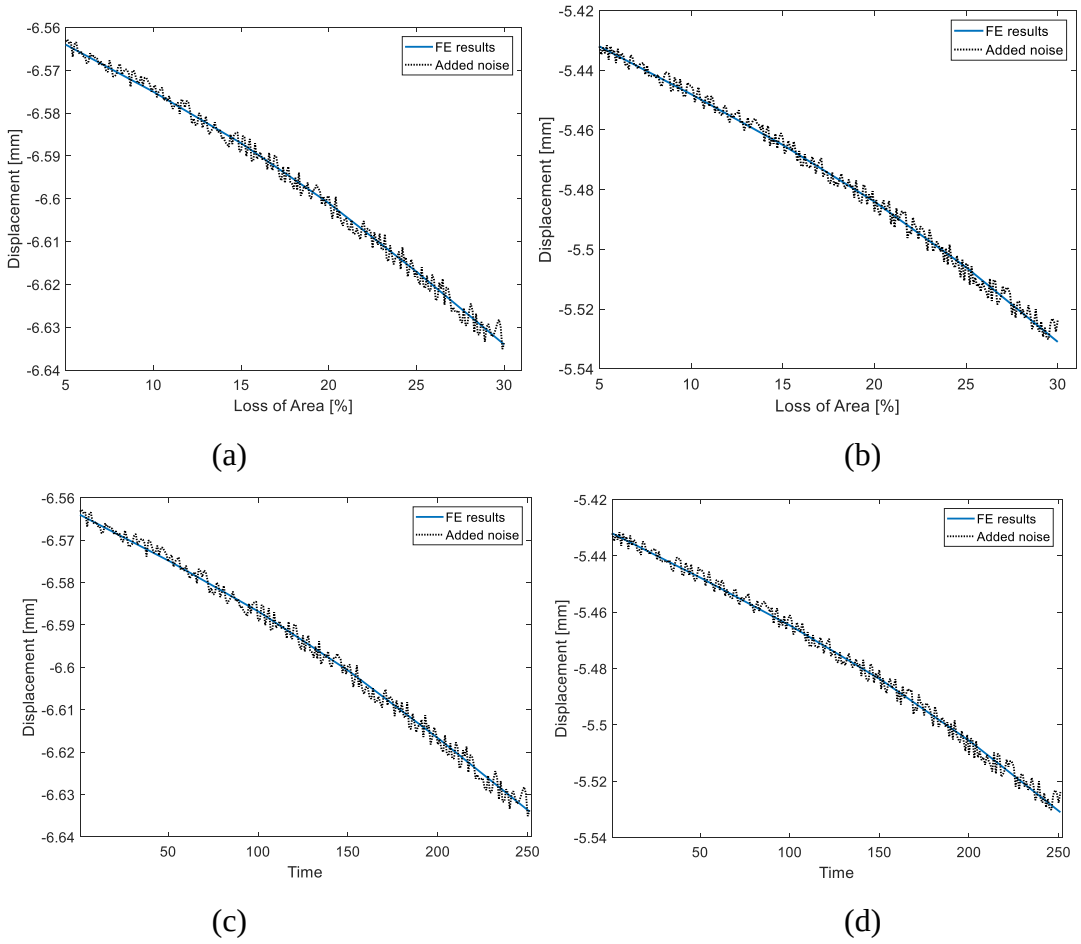

Figure 3-8. *Displacement of the third and fourth joints of the top chord at y=0m as the loss of area increase figures (a) and (b), respectively; effect of the degradation over time on the third (c) and fourth (d) joints, respectively*

3.4.2 **Development of the BBN model**

The proposed BBN-based condition monitoring and fault detection method is evaluated by analysing the developed FEM of the steel truss bridge. Particularly, the condition of the bridge is monitored during the 28 degradation scenarios, in order to point out the ongoing degradation of the bridge, by detecting and diagnosing the ongoing degradation of the bridge.

In what follows, the process to define the BBN structure is presented in section 3.4.2.1, whilst section 3.4.2.2 presents the process to define the CPTs of the BBN.

Section 3.4.3 presents a detailed analysis of the bridge condition monitoring during a degradation scenario, with the aim of illustrating how a bridge manager can adopt, and interact with, the BBN in order to monitor the bridge health state and diagnose its unexpected condition. The analysis of the BBN performance is then discussed in section 3.4.4 in order to point out the accuracy of the proposed method in analysing the 28 degraded scenarios, by highlighting its advantages and disadvantages. Finally, the proposed method is discussed in section 3.4.5 by pointing out the drawbacks of the proposed method, which are then managed in the following chapters of the thesis.

3.4.2.1 **The BBN model building**

The development of the structure of the BBN is carried out by following the 7 steps proposed in Section 3.3:

1. **Identify the type of the bridge and its major and minor elements of interest.** The bridge is a warren steel truss, and its major elements are identified as the deck, the top and bottom chords, the diagonals and the stringers. The minor elements of the bridge are represented by each individual beam that belongs to a major element and by the joints that connect each minor beam. Hereafter, only the condition of the top and bottom chords of the bridge are considered. Therefore, we assume that the health state of the whole bridge depends only on the health state of these two major elements. This assumption is due to the fact that the chords of the bridge show the highest stresses during the service of a steel truss bridge usually [Ni et al., 2012].
2. **Define the BBN structure.** Each top chord is made of 4 beams, as shown in Figure 3-7(a). Therefore, 4 nodes are used in the BBN framework to characterize these four elements: each *E_j_TCR* node in Figure 3-9 represents the condition of the minor elements *j*, where *j*=1, 2, 3, 4, of the top chord on the right hand side of the bridge (parent nodes of TCR node in Figure 3-9). Similarly, each bottom chord is made of 5 beams, as shown in Figure 3-7(c). Thus, 5 nodes representing the minor elements of the bottom chords are introduced in the BBN: each *E_i_BCR* represents the minor element *i*, where *i* =1, 2, 3, 4, 5, of the bottom chord on the right hand side of the bridge (parent nodes of BCR in Figure 3-9). The same definition is true for the left-hand side of the bridge, as shown in Figure 3-9 by the nodes ending with "*L*". Each minor

beam of both top and bottom chords is connected to its neighbour minor beam by the means of a joint. Therefore, a node for each joint is introduced in the BBN. For example, the node *TRC_J1* represents the first joint of the TCR. The same notation is adopted to describe each joint of each major element of the bridge. The nodes TCR, TCL, BCR and BCL are introduced to describe the health state of the major elements of the bridge. The directed arcs depart from the nodes that represent the minor elements of the bridge, and end at the nodes representing the major elements of the bridge. The major elements, however, influence the health state of the whole bridge. Therefore, they are parents of the node representing the condition of the health state of the whole bridge, the *BridgeHealthState* node in Figure 3-9.

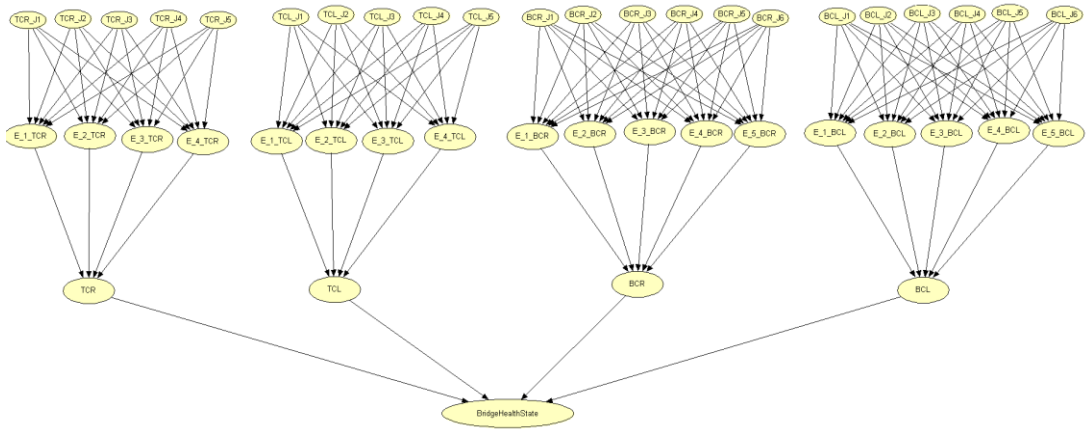

Figure 3-9. *First draft of the BBN of the steel truss bridge*

3. **Upgrade the BBN model to take account of interdependencies among major/minor elements**. A more detailed BBN is developed next by considering the influence among minor (major) elements. Further nodes are introduced into the BBN, as shown in Figure 3-10 by the nodes ending with "***_1***". For example, the nodes *E_j_TCR_1* are introduced to assess the interdependencies among the minor elements of the top chord on the right-hand side. Nodes *TCR_1*, *TCL_1*, *BCR_1* and *BCL_1* are introduced with the aim of considering the influences among major elements.

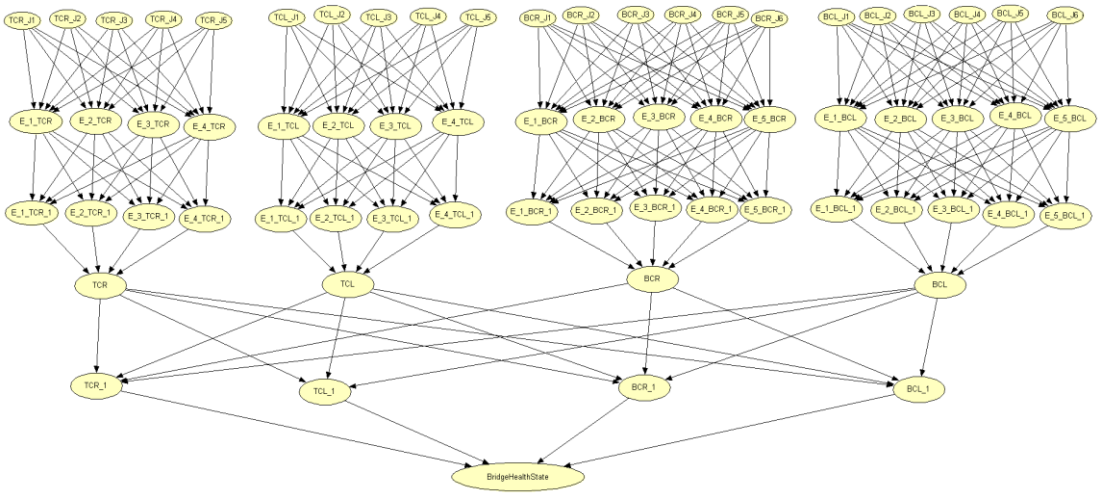

Figure 3-10. *BBN that considers the interdependencies among minor (major) bridge elements*

4. **Review the BBN structure by analysing the bridge behaviour.** A database of bridge behaviour is needed to carry out this step and optimize the structure of the BBN. Displacement of the joints is used as an input to the BBN nodes, i.e. the displacements is used to assess the condition of the bridge elements. The analysis of the bridge behaviour in different conditions of the bridge elements can provide information about the strength of the influence between different bridge elements, and the structure of the BBN can be updated accordingly. The strength of the influence of a degrading bridge element (*A*) on the health state of another healthy bridge element (*B*) is assessed by computing the percentage of variation (with respect to the healthy bridge) of the displacement of the element *B*. We assume a threshold of 0.5% to take account of a possible influence between different bridge elements. The value of the threshold is retrieved by analysing the behaviour of the developed FEM in different health states of the bridge elements. The FEM displacements are 6mm generally, and as a result the resolution of a real displacement measurement system, which best resolution is up to is 0.08mm, is not considered during the threshold definition process [Vicente et al., 2018]. For example, Figure 3-11 shows the percentage of variation of the *BCR* joints displacement, when joint 1 or joint 2 of *BCR* are degrading. When joint 1 is degrading, i.e. the cross-sectional area of the first *BCR* element is decreased at the joint location, the displacements of the other BCR joints are slightly influenced (the maximum percentage variation is equal to 0.25%). Therefore,

the influence of joint 1 of the BCR on the health state of the other BCR elements is negligible, and thus *BCR_J1* and *E_1_BCR* can be removed from the BBN structure. Conversely, the degradation of joint 2 (second row of Figure 3-11) influences the health state of joint 2 and 3, whose displacements show a percentage variation of 1% and 0.8%, respectively. The influence of the degradation of joint 2 on the other BCR elements (joint 3 and 4) is negligible. As a result, *E_2_BCR* influences only the health state of itself (E_2_BCR_1) and its neighbour *E_3_BCR_1*, and the arcs with the other BCR elements (which are shown in Figure 3-10) can be removed from the BBN. It is worth noting in Figure 3-11 that the displacement of Joint 1 and Joint 6 of *BCR* are equal to zero: these joints are assumed to be fixed in order to represent the support of the bridge.

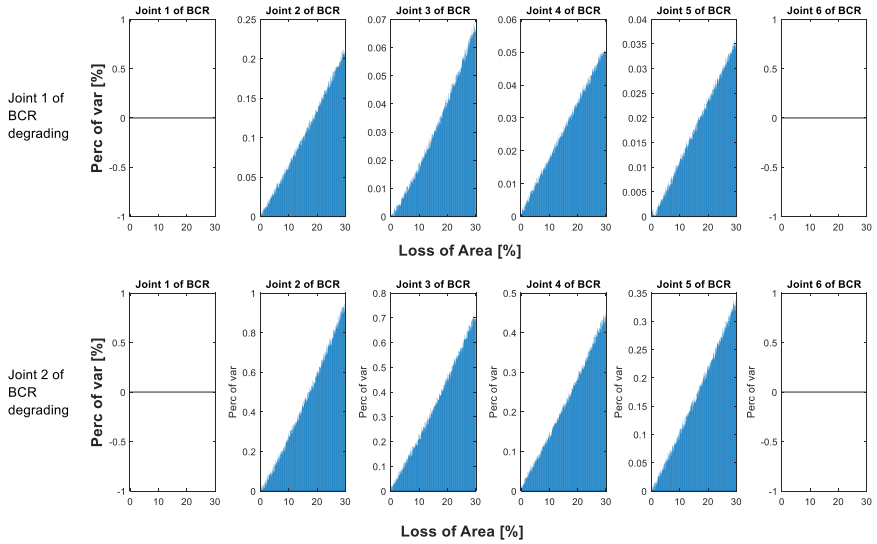

Figure 3-11. *Percentage of variation of the displacement of TCR elements, when E_1_TCR is degrading*

Similarly, Figure 3-12 shows the influence of the degradation of TCR joints on the health state of the other major elements, i.e. *TCL*, *BCR* and *BCL*. Particularly, the mean percentage variation of the displacement of each major element of the bridge, which is induced by the gradual degradation of the joints of *TCR*, is depicted in Figure 3-12. The percentage of variation of the displacement of the major elements on the left-hand side of the bridge, *TCL* and *BCL*, is lower than 0.5%. Consequently, we can assume that the health state of *TCL* and *BCL* is not influenced by the degradation of *TCR*. Hence, the arcs

that depart from *TCR* and goes to *TCL_1* and *BCL_1* (Figure 3-10) can be deleted. Finally, Figure 3-13 shows the updated BBN, which is developed by analysing the bridge behaviour when different bridge elements are degrading gradually.

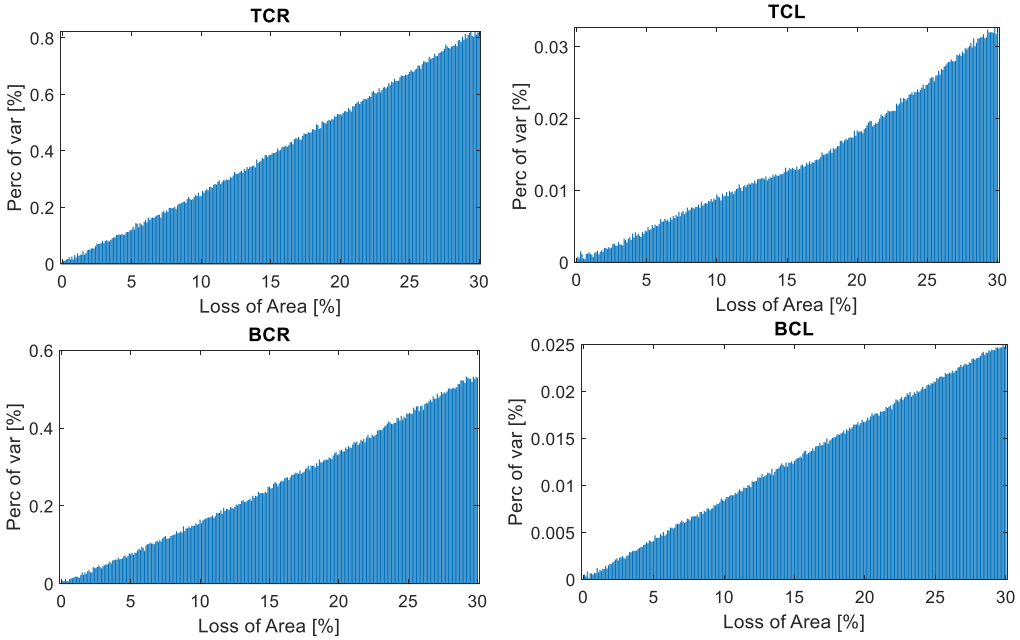

Figure 3-12. *Influence of TCR degradation on TCL*

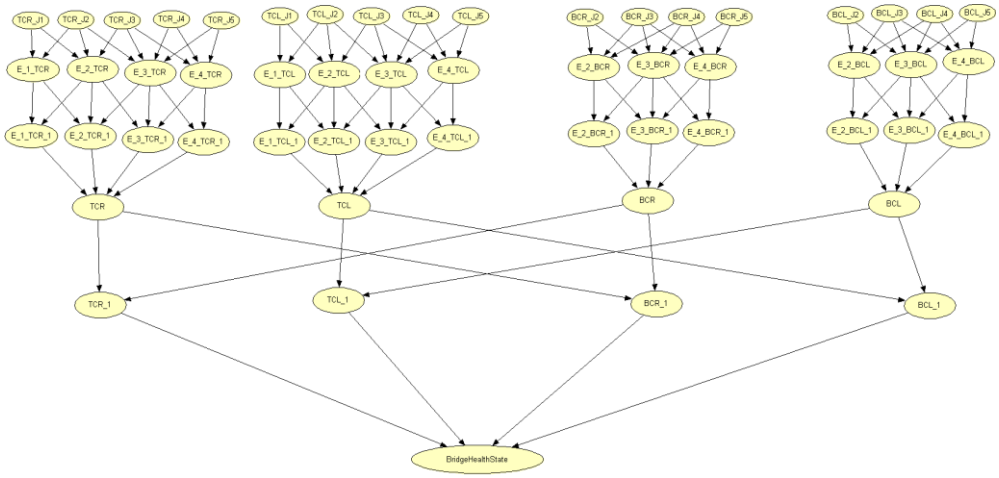

Figure 3-13. *Updated BBN after the bridge behaviour analysis*

5. **Define nodes to represent the measurement system of the bridge.** The measurement system of the FEM is represented by the virtual displacement sensors at the joint location as shown by dark circles in Figure 3-7, 5 displacement sensors are represented on each top chord, and a node for each

sensor is added to the BBN accordingly, as depicted by the S_l_TCR and the S_l_TCL nodes in Figure 3-14, where l=1, 2, 3, 4, 5. Particularly, the nodes representing the 5 sensors are introduced as parent nodes of the joint elements on which the sensors are installed. A similar approach is adopted for the bottom chords, as shown in Figure 3-14. Every time when evidence of the bridge behaviour is available, it is used as an input to the sensor nodes, which assesses the health state of the bridge joints by analysing the evidence of the bridge behaviour. Consequently, the health state of the bridge and its elements is updated accordingly.

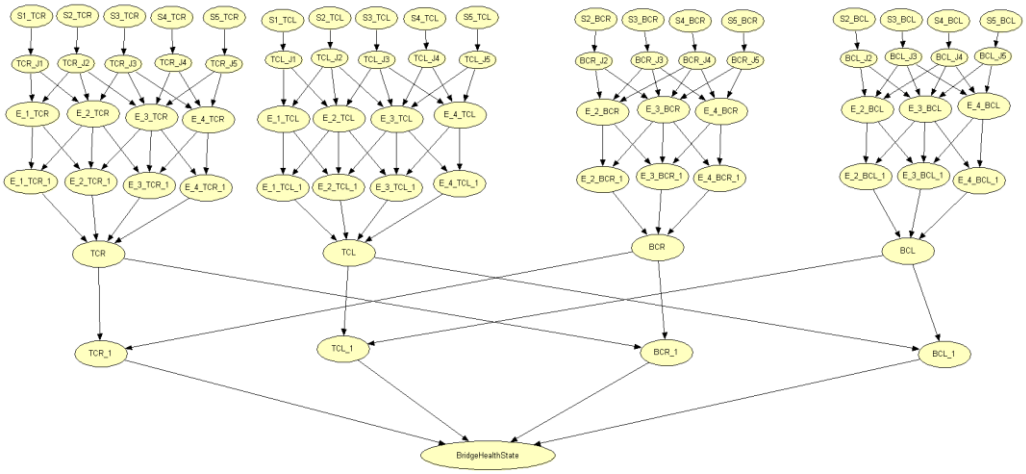

Figure 3-14. *Final BBN for condition monitoring and degradation diagnostics of the steel truss bridge*

6. **Choose the number of health states of each node.** Three mutually exclusive health states are defined for each node of the BBN: *a)* a healthy state (H), where the elements of the truss bridge are in a good condition; *b)* a partially degraded state (PD), where the element of the bridge can require a maintenance action; *c)* a severely degraded state (SD), where the elements of the bridge need to be maintained [Rafiq et al., 2015].
7. **Obtain the final BBN structure.** The final BBN for condition monitoring and degradation diagnostics of the steel truss bridge is shown in Figure 3-14.

3.4.2.2 **Development of CPTs**

The CPTs of the BBN are evaluated by adopting the expert knowledge elicitation process, described in Section 3.3.2:

a) **Identify the experts**. Three bridge experts were interviewed: *i)* Expert 1 is a principal engineer of an engineering firm with 8 years of experience in SHM; *ii)* Expert 2 is a director of an engineering consultancy group with over 28 years of experience in structural assessment of civil infrastructure; *iii)* Expert 3 is a professor of structural engineering in a top ranked UK university, with more than 25 years of experience in SHM.

b) **Identify the degraded scenarios**. The experts were interviewed to evaluate 4 scenarios: *i)* the influence of the degradation of a minor element on the health state of a neighbouring minor element; *ii)* the influence of the degradation of a minor element on the condition of a major element; *iii)* the influence of the degradation of a major element on the health state of a different major element; *iv)* the influence of the degradation of a major element on the health state of the whole bridge.

c) **Present the scenarios to the experts**. The four scenarios are presented to the experts by the means of questions. Without loss of generality, the influence of a major element on the condition of the other major elements is hereafter discussed and analysed, i.e. scenario *iii)* is investigated using questions to the experts. For instance, the influence of the top chord on the right hand side on the health state of other major elements (scenario *iii)*) can be analysed by the means of three questions: *let us consider a truss steel bridge, shown in Figure 3-7. The bridge can be divided into major elements (top and bottom chords) and minor elements (such as an individual steel beam).*

   1. *Referring to your expertise, if essential maintenance actions, such as repair, are required in the top chord on the right-hand side, i.e. the maintenance cannot be postponed, how likely would the overall condition of the bottom chord on the same hand side of the bridge be influenced by the degraded state of the top chord on the right-hand side?*
   2. *Referring to your expertise, if essential maintenance actions, such as repair, are required in top chord on the right-hand side, i.e. the maintenance cannot be postponed, how likely would the overall condition of the top chord on the left-hand side of the bridge be influenced by the degraded state of the top chord on the right-hand side?*
   3. *Referring to your expertise, if essential maintenance actions, such as repair, are required in the top chord on the right-hand side, i.e. the*

maintenance cannot be postponed, how likely would the overall condition of the bottom chord on the left-hand side of the bridge be influenced by the degraded state of the top chord on the right-hand side?

d) **Provide a scale for answers**. The linguistic scale of Table 3-2 is provided to the experts with the aim of obtaining linguistic answers.

e) **Merge the individual analyses**. The triangular fuzzy membership function of Figure 3-6 is used to estimate the linguistic analysis numerically. The three experts have provided the answers for the three questions, given in Table 3-3. For example, Table 3-3 shows that the analysis of the most experienced expert, i.e. Expert 2, for question 1 provides *unlikely* as a result, whilst Expert 1 and 3 provide *likely* and *even chance*, respectively. Table 3-3 shows also the triangular fuzzy membership value for each analysis of the experts in square brackets. The individual analyses of each expert are merged by taking account of the experience of each expert. Therefore, the analysis of each expert is weighted by using Eq. (3-10), where β is equal to 0.91.the value of β has been optimized by using the sensitivity analysis in order to avoid a single member judgment. Table 3-3 shows that the aggregated analysis is based on the information retrieved by the whole group of experts, i.e. the analysis of the most senior expert is not dominant over the analyses of other experts.

Table 3-3. *Individual and aggregated FAHP results*

	Result of the analysis		
Expert	**Question 1**	**Question 2**	**Question 3**
Expert 1	Likely [2, 5/2, 3]	Likely [2, 5/2, 3]	Likely [2, 5/2, 3]
Expert 2	Unlikely [1, 3/2, 2]	Unlikely [1, 3/2, 2]	Very unlikely [1/2, 1, 3/2]
Expert 3	Even chance [3/2, 2, 5/2]	Even chance [3/2, 2, 5/2]	Even chance [3/2, 2, 5/2]
Aggregated analysis	Even chance [3/2, 2, 5/2]	Even chance [3/2, 2, 5/2]	Unlikely [1, 3/2, 2]

f) **Assess the influence of each parent node on its child**. The aggregated answers of the experts can be seen as a fuzzy pairwise comparison matrix. Table 3-4 shows the fuzzy pairwise comparison matrix with respect to the

influences among the major elements of the bridge. The FAHP is then used to evaluate the weight of a major element on the health state of other major elements of the bridge. The fuzzy synthetic extend (Eq. (3-11)), which was computed by using Eq. (3-12) for the first term of Eq. (3-11) and the modified Chang extend for the second term [Wang et al., 2006; Kabir et al., 2014], of TCR is equal to:

$$S_{TCR} = (4,\ 5,\ 6) \otimes (0.055,\ 0.060,\ 0.055) \approx (0.222,\ 0.300,\ 0.333) \tag{3-19}$$

The integral value of each synthetic extend is computed by using Eq. (7). The integral value for the TCR is equal to:

$$I_{TCR} = \frac{1}{2}(\alpha\ 0.333 + \ 0.300 + (1-\alpha)0.222) = 0.2889 \tag{3-20}$$

where α= 0.5.

Finally, the weight of each major element on the health state of another major element is obtained by applying Eq. (3-14), and thus $w = (0.3007,\ 0.2497,\ 0.2497,\ 0.200)^T$.

Table 3-4. *Pairwise comparison matrix with respect to the influences among the bridge major elements*

	TCR	*TCL*	*BCR*	*BCL*
TCR	[1, 1, 1]	[1, 3/2, 2]	[1, 1, 1]	[1, 3/2, 2]
TCL	[1/2, 2/3, 1]	[1,1,1]	[1, 3/2, 2]	[1, 1, 1]
BCR	[1,1,1]	[1/2, 2/3, 1]	[1, 1, 1]	[1, 3/2, 2]
BCL	[1/2, 2/3, 1]	[1, 1, 1]	[1/2, 2/3, 1]	[1, 1, 1]

g) **Assess the consistency of the expert analysis.** The consistency of the expert analysis is verified by evaluating the *CR*. For the comparison matrix of Table 3-4, the CR index is equal to:

$$CR = \frac{CI}{RI} = \frac{4.0837 - 4}{3} \cdot \frac{1}{0.9000} = 0.03 \tag{3-21}$$

where $\lambda_{\max}$ = 4.0837 is retrieved by using the maximum centroid of area method to defuzzify the pairwise matrix. RI is equal to 0.9 and is obtained by

using a table from literature [Kabir et al., 2014]. Eq. (3-21) shows a *CR* ratio lower than 0.1, and thus the analysis of the experts is consistent.

h) **Compute the conditional probabilities for the bridge element nodes**. The first step is to define the conditional probability that the condition of a child node of the BBN is influenced by knowledge of the health state of its parents, $P(x_i | \bigcap_{k=1}^{N} Y^k = y_k = 1)$, with *i* = H, PD, SD. This means that the probability of having a child node in a state *i*, conditional on the knowledge that its parent nodes are in the healthy state (no degradation is present). In this thesis, we assume that the health state of each node of the BBN when no degradation is present is equal to $P(x_i | \bigcap_{k=1}^{N} Y^k = y_k = 1) = [P(x_H | \bigcap_{k=1}^{N} Y^k = y_k = 1) = 0.95, P(x_{PD} | \bigcap_{k=1}^{N} Y^k = y_k = 1) = 0.025, P(x_{SD} | \bigcap_{k=1}^{N} Y^k = y_k = 1) = 0.025]$. For example, the CPTs of the *TCR_1* node of the BBN is shown in Table 3-5. The states of the node *TCR_1* are influenced by two parent nodes, the *TCR* and *BCR* nodes, as shown in Figure 3-14. Each node is described with 3 health states, and thus the CPT requires 24 entries $(3 \cdot 2^3)$. The probability of having *TCR_1* in state *i*, conditional on the knowledge that both its parents are in the healthy state, is defined as $P(TCR\_1_i | \bigcap_{k=1}^{N} Y^k = y_k = 1) = [0.95,\ 0.025,\ 0.025]$. The CPT is then thoroughly defined by using Eq. (3-17), where p_i and f_{p_m} depend on the health state of the parent nodes *k*:

$$p_i = \begin{cases} [1, 0.7, 0.3]^T & if \quad k = PD \\ [1, 0.25, 0.75]^T & if \quad k = SD \end{cases} \tag{3-22}$$

$$f_{p_m} = \begin{cases} 1 & if \quad k = H \quad or \quad PD \\ 1.1 & if \quad k = SD \end{cases} \tag{3-23}$$

Eq. (3-22) shows that p_i is equal to 1 if *TCR_1* is in state *i=H, 0.7* if *i=PD,* etc. In this way, the decrease of $P(TCR\_1_i | \bigcap_{k=1}^{N} Y^k = y_k = 1)$ is shared between the states PD and SD, and the whole probability is normalized to 1.

An example of this process is presented in Eq. (3-24) and Eq. (3-25). The weight of the parent nodes on the child node is equal to $w = (0.3007,\ \ 0.2497)$, as shown in step *f)*. For instance, the bold probabilities of Table 3-5 are computed by using Eq. (3-17), where the number of degraded parent nodes is equal to 1, *M*=1, Eq. (3-24), or 2, *M*=2, Eq. (3-25), respectively:

$$\begin{cases} P(TCR\_1_H \left| Y_{k=PD}^{TCR}, Y_{k=H}^{BCR} \right.) = 0.95 + 0.95 \cdot 0.3007 \cdot 1 \cdot (-1) \cdot 1 = 0.6647 \approx 0.66 \\ P(TCR\_1_{PD} \left| Y_{k=PD}^{TCR}, Y_{k=H}^{BCR} \right.) = 0.025 + 0.95 \cdot 0.3007 \cdot 0.7 \cdot (1) \cdot 1 = 0.2250 \approx 0.25 \\ P(TCR\_1_{SD} \left| Y_{k=PD}^{TCR}, Y_{k=H}^{BCR} \right.) = 0.025 + 0.95 \cdot 0.3007 \cdot 0.3 \cdot (1) \cdot 1 = 0.1107 \approx 0.11 \end{cases} \quad (3\text{-}24)$$

$$\begin{cases} P(TCR\_1_H \left| Y_{k=SD}^{TCR}, Y_{k=PD}^{BCR} \right.) = 0.95 + 0.95 \cdot (0.3007 \cdot 1.1 + 0.2497 \cdot 1) \cdot 1 \cdot (-1) = 0.3986 \approx 0.39 \\ P(TCR\_1_{PD} \left| Y_{k=SD}^{TCR}, Y_{k=PD}^{BCR} \right.) = 0.025 + 0.95 \cdot (0.3007 \cdot 1.1 + 0.2497 \cdot 1) \cdot 0.25 \cdot (1) = 0.1629 \approx 0.16 \\ P(TCR\_1_{SD} \left| Y_{k=SD}^{TCR}, Y_{k=PD}^{BCR} \right.) = 0.025 + 0.95 \cdot (0.3007 \cdot 1.1 + 0.2497 \cdot 1) \cdot 0.75 \cdot (1) = 0.4386 \approx 0.43 \end{cases} \quad (3\text{-}25)$$

Table 3-5*. CPT of a child node with three health states and two parent nodes with 3 health states each*

	BCR	H			PD			SD		
	TCR	H	PD	SD	H	PD	SD	H	PD	SD
TCR_1	H	0.95	**0.66**	0.63	0.71	0.42	**0.39**	0.68	0.40	0.3
	PD	0.025	**0.22**	0.10	0.19	0.39	**0.16**	0.09	0.16	0.16
	SD	0.025	**0.11**	0.26	0.09	0.18	**0.43**	0.22	0.43	0.45

3.4.3 **BBN model usage for detection and diagnostics of bridge deterioration**

The 28 simulated degradation scenarios are presented randomly to the BBN. In this way, the nature of the scenario is not known a-priori, and the BBN needs to assess the health state of the bridge. The displacement of the bridge joints is used to monitor the bridge condition, and thus as an input to the BBN nodes. Three health states of the bridge are defined, by assessing the percentage of the joint displacement variation during the degradation process. A bridge manager can interact with the BBN during the bridge condition monitoring process. As a result, when a change of the condition of the bridge is identified, the bridge manager can diagnose the causes of such change. The bottom-up diagnostic process of the BBN can be a one-step process, i.e. the bridge manager can directly observe the most degraded element of the bridge, or a step by step process, i.e. the bridge manager diagnoses the cause of the change of the bridge condition by analysing the health state of each node of the BBN. In this example, this

latter approach is described, in order to both monitor the bridge health state and diagnose its health state change. For these reasons, Figure 3-15 shows the evolution of the health state of the whole bridge (*BridgeHealthState* node in Figure 3-14) over time. At the beginning, the bridge is in the healthy condition due to the fact that the degradation mechanism is not yet initiated, or the size of the micro-cracks is small. Consequently, the bridge is in the healthy state (grey area in Figure 3-15). When the size of the micro-cracks of the degraded joint increases, as shown in Figure 3-8, the health state of the whole bridge changes: the probability of the partially degraded (PD) state and the severely degraded (SD) state suddenly increase around time 100 (light and dark grey areas, respectively, in Figure 3-15). The size of the micro-cracks continues to increase over time, and as a consequence the health state of the whole bridge degrades, i.e. the yellow and red areas increase over time, as shown in Figure 3-15. Hence, the proposed BBN method is able to monitor the health state of the bridge over time, by detecting unexpected bridge behaviour as soon as it occurs.

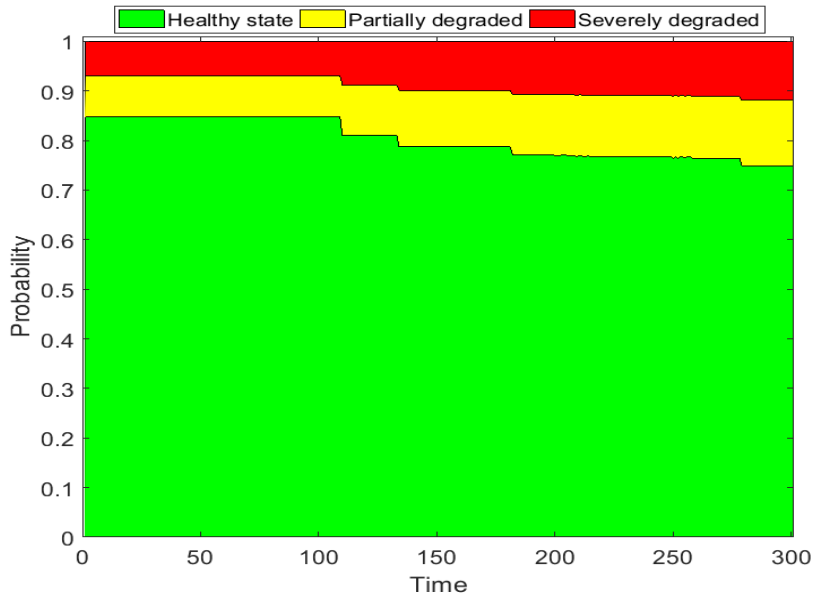

Figure 3-15. *Evolution over time of the health state of the whole bridge (BridgeHealthState node). The time represents consecutive simulations*

The BBN is able to diagnose the cause of the unexpected behaviour of the bridge. Therefore, a bridge manager, who monitors the health state of the bridge by checking Figure 3-15, can point out which element(s) of the bridge is (are) deteriorating. Figure 3-16 shows the evolution of the health states of the whole bridge (*BridgeHealthState* node in Figure 3-14) and of its parent nodes: the top and bottom chords of Figure 3-14.

Figure 3-16 allows to identify directly that the top chord on the right-hand side of the bridge (*TCR_1*) is more degraded than the other major elements, i.e. the light and dark grey areas of *TCR_1* are higher than those of the other chords.

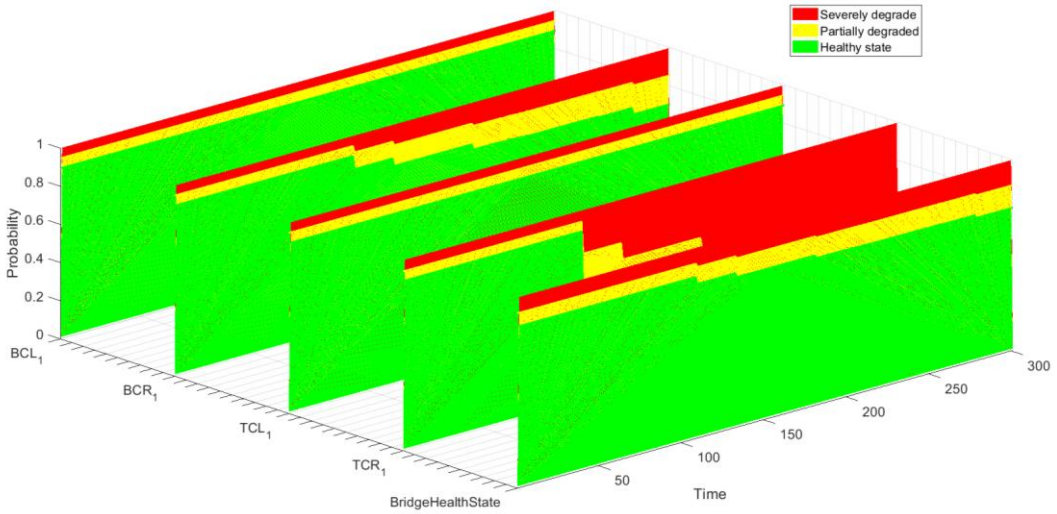

Figure 3-16. *Evolution over time of the health state of the whole bridge (BridgeHealthState node) and its parent nodes, i.e. the top and bottom chords nodes*

The diagnostic property of the BBN allows to investigate the degradation level of the bridge elements at each level of the BBN. For example, Figure 3-17 shows the evolution of the health state of the *TCR_1* node and its parent nodes, which are the top and bottom chord on the right-hand side of the bridge, *TCR* and *BCR* node in Figure 3-14, respectively. Figure 3-17 depicts that the top chord on the left-hand side of the bridge is more degraded than the right one. The cause of the decrease of the bridge health state can be thus identified among the elements of the top chord on the right-hand side of the bridge. The probability of each parent node of the top chord on the right-hand side of the bridge can be then observed and analysed by the bridge manager, with the aim of pointing out the most degraded element of the chord. Figure 3-18 shows the evolution of the health state probabilities of the most degraded element of the top chord, i.e. the joint between the third and fourth elements of the top chord on the right-hand side of the bridge. Therefore, the element of the bridge that was degrading is identified correctly, due to the fact that the degradation of the joint between the third and fourth elements of the top chord on the right-hand side of the bridge was simulated using the FEM. The oscillations of the conditional probability of the health states of the most degraded element in Figure 3-18 are due to the added noise of the data. It should be noted that the proposed approach allows the bridge

manager to interact with the monitoring and diagnostic process. As a result, the bridge manager can analyse the influence of a degradation mechanism of the bridge element on the health state of other elements of the bridge. Simultaneously, the bridge manager can avoid the step-by-step diagnostic process, and identify the most degraded element of the bridge directly.

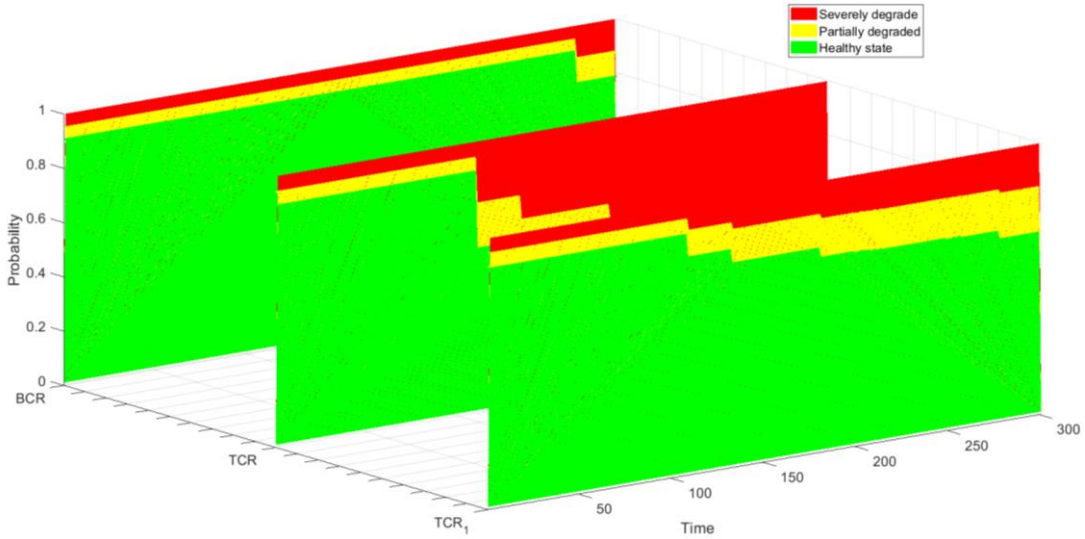

Figure 3-17. *Evolution over time of the health state of the TCR_1 node and its parents, i.e. the top and bottom chords on the right-hand side of the bridge, respectively*

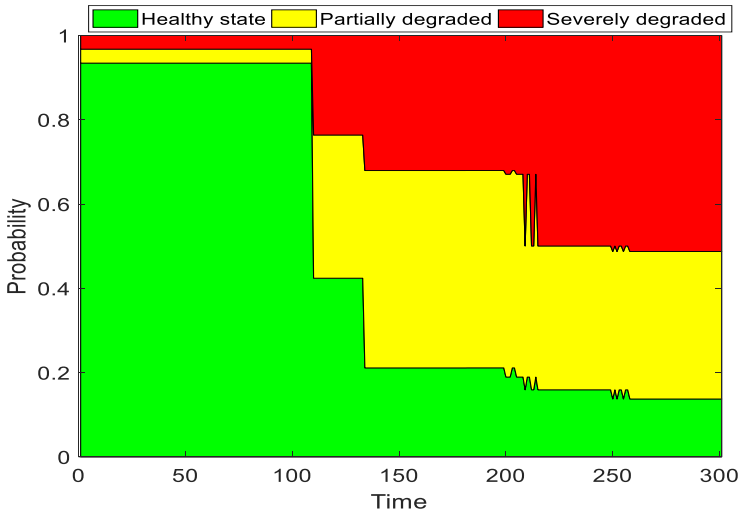

Figure 3-18. *Evolution over time of the health state of the fourth element of the top chord on the right-hand side of the bridge, which is the degraded element of the bridge*

3.4.4 Analysis of the performance of the BBN model

The 28 degraded scenarios are used as an input to the BBN in order to investigate the performance of the proposed method. As a result, the BBN identifies the most degraded element(s) of the bridge by the means of high probability of the degraded

health states. The results of the diagnostic process of the BBN are presented in Table 3-6, on which the most degraded element of the bridge identified by the BBN is compared with the actual degraded element. When a single element of the bridge is degrading, the BBN is able to correctly identify 18 out of 22 major elements that contain a degrading minor element. At the same time, when multiple minor elements are degrading, the BBN correctly identifies 10 out of 12 major elements that contain degrading minor element(s), i.e. the 6 multiple degradation scenarios simulate the degradation of 12 different major elements. A good accuracy of the BBN in diagnosing the degrading major element(s) of the bridge is demonstrated. Conversely, the analysis of the 6 misclassified scenarios can point out limitations of the BBN method. 5 scenarios are misclassified when the element at the ending part of a bottom chord is degrading, i.e. the joint at the ending of the bottom chords is degrading. Indeed, these joints represent the support of the bridge, and thus they are fixed having zero displacement (as shown in Figure 3-11). Furthermore, the displacement of all bridge elements is slightly influenced by the degradation of these joints, i.e. an increase of 0.1% is caused by the degradation of these joints (as shown in Figure 3-11). As a consequence, the BBN is not able to point out the ongoing degradation of the bridge during these 5 scenarios. The BBN seems not able to identify ongoing degradation that leads to small changes of the bridge behaviour. However, the location of the degradation has been proven to be an issue for SHM analysis due to small changes of the bridge behaviour when the lateral parts of the bridge are degrading [Shu et al., 2013]. The last misclassification of the major element occurred when the bottom chords were degrading, but the TCL was identified as the most degraded major element of the bridge. This behaviour of the BBN can be due to the definition of the CPTs, which allow a high influence among minor (major) elements of the bridge.

In a similar way, the performance of the BBN in identifying the degraded minor element(s) allows to analyse the pros and cons of the proposed approach. The BBN shows good accuracy in identifying and diagnosing the ongoing degradation of the bridge: the minor elements that are subject to the degradation process are correctly diagnosed 32 out of 40 times. When an individual minor element of the bridge is degrading, the BBN results in 5 misclassifications, due to the degradation of the elements at the ending part of a bottom chord. At the same time, when multiple minor elements of the bridge are subject to a degradation process, the BBN correctly identifies 15 out of 18 minor degrading elements (where 18 is the number of minor

elements that are degraded during the 6 scenarios). The BBN misclassifies 3 minor elements where the most degraded minor elements are not identified correctly. Particularly, when multiple minor elements of both bottom chords are degraded, the BBN incorrectly identifies the mid-span of the bridge as the most degraded element. Hence, the elements on the central part of the bridge are detected as the most degraded elements, rather than the real degrading elements of the bridge on the lateral part of the bottom chords. Finally, the BBN identifies as degraded also 17 elements that are not degrading, due to the influence between different bridge elements.

This performance of the BBN is influenced by the definition of the qualitative and quantitative structures of the BBN: *i)* qualitative: a more detailed description of the bridge elements can lead to an increase of the accuracy of the BBN in locating the ongoing bridge degradation, by introducing a higher number of nodes to describe the bridge elements; *ii)* quantitative: a more robust definition of the CPTs can lead to more accurate results by avoiding the false alarms that are raised due to high influence among minor (major) bridge elements.

Table 3-6. *Damage detection and diagnostic performance of the proposed BBN method*

Degraded scenario	**Number of scenarios**	**Number of correct identification of the degraded major element**	**Number of correct identification of the degraded minor element(s)**	**Number of false identification of the degraded minor element(s)**
A Single element	22	18/22	17/22	10/22
Multiple elements	6	10/12	15/18	7/18
Total	28	28/34	32/40	17/44

3.4.5 Discussion of the proposed BBN method

The proposed BBN method has demonstrated good performance in monitoring the health state of the steel truss bridge continuously, by identifying changes of the bridge condition and diagnosing the causes of such changes. The BBN is developed by taking account of the physical characteristics of the bridge structure, and the expertise of the bridge engineers. Bridge managers can assess the condition of the bridge continuously by monitoring the health state of each element of the bridge. In fact, the proposed BBN updates the condition of the bridge, and its elements, every time when new evidence of the bridge behaviour is provided by the sensors. In this way, the BBN is able to

detect and diagnose unexpected behaviour of the bridge as soon as it occurs. However, some drawbacks have been found:

1. The FEM of the steel truss bridge has been developed with the aim of testing and stressing the BBN ability of monitoring a bridge under ongoing degradation mechanisms. As a result, assumptions have been made during the development of the FEM: *i)* only a static uniform load has been applied to the FEM; *ii)* fixed environmental conditions; *iii)* the traffic is not present, and thus interactions between the bridge and the vehicles that are passing over the bridge are neglected. Therefore, the good performance of the BBN might not be guaranteed in a more complex case study, where the bridge is subject to traffic, for example. Traffic and changing environmental conditions can lead to a noisy response of the bridge, due to different vehicles that run over the bridge, and thus misclassifications of the bridge health state might be obtained. The effects of traffic and changing environmental conditions on the performance of the proposed BBN approach are investigated in the next section, by analysing an FEM that is excited by moving vehicles rather than static loads.
2. The accuracy of the BBN damage detection process decreased when the degradation of the bridge elements led to small changes of the bridge displacements. As a consequence, the BBN was not able to detect small changes of the bridge behaviour. The behaviour of a real in-field bridge is expected to experience small changes when a degradation mechanism is ongoing on some bridge elements. Therefore, the BBN should be able to detect small changes of the bridge behaviour, which may be hidden by the noise of the data, in order to accurately assess the health state of the bridge. A pre-processing analysis of the bridge behaviour can tackle this problem, by providing crisp information about the bridge behaviour to the BBN.
3. The diagnostics performance of the BBN seems to depend on the number of nodes that are used to describe the bridge elements of interest, i.e. the higher the number of nodes of the BBN, the higher the accuracy of the BBN in identifying the degraded element(s) of the bridge. In fact, the discussion of the performance of the BBN in section 3.4.4 has shown that when the number of degraded elements of the bridge increases, the BBN identifies the central elements of the bridge as degraded. These issues can be resolved by introducing more nodes, i.e. by describing each element of the bridge with

more than one node in the BBN network. In this way, the diagnostics ability of the BBN is expected to improve. Furthermore, the CPTs are defined by the means of an expert knowledge elicitation process, which can be subjective and incomplete. For that reason, the definition of the CPTs can be improved by merging the expert knowledge elicitation process with the analysis of the bridge behaviour. An improvement of the CPTs can lead to more accurate performance of the BBN in terms of accuracy of the diagnostics process.

These drawbacks are addressed in the next sections of the thesis, with the aim of developing a reliable condition monitoring and damage diagnostic method, which is able to provide robust results under changing environmental condition of the bridge. Indeed, the FEM presented in this section was excited only by static load to stress the updating ability of the BBN. However, before addressing the drawbacks of the BBN-based SHM approach, it is worth testing the proposed method in a dynamic case study, with the aim of investigating the properties of the proposed method. In what follows, an FEM of a beam-and-slab bridge is introduced, and the application of the BBN method for monitoring the health state of the bridge is presented.

3.5 BBN model for a beam-and-slab bridge

In this section, the BBN method is applied to an FEM of a beam-and-slab bridge, which is developed in order to assess the damage detection and diagnostics ability of the SHM methods. The FEM of the beam-and-slab highway bridge is developed by the University College of Dublin [González et al., 2015]. The damage detection and diagnostic properties of the BBN are assessed by analysing scenarios where the health state of the bridge changes suddenly, i.e. the degradation mechanism does not lead to a gradual decrease of the condition of the bridge, but rather to a sudden change of the bridge behaviour. The FEM of the beam-and-slab bridge provides a challenging case study due to the fact that: *i)* the FEM is developed by structural engineers that provide only limited information about the bridge; *ii)* the traffic that goes over the bridge is simulated, by studying the run of different vehicles; *iii)* changing environmental conditions of the bridge are investigated, by modifying the road and vehicles properties. In this way, the BBN needs to monitor the health state of a bridge, whose behaviour is noisy and unknown due to changing environmental conditions.

In what follows, the beam-and-slab bridge is described (section 3.5.1), then a BBN method is developed to assess the health state of the bridge under changing environmental conditions (section 3.5.2). The results of the performance of the BBN are presented in section 3.5.3. Finally, the discussion on the performance of the proposed BBN methods are presented in section 3.5.4.

3.5.1 **The FEM of the beam-and-slab bridge**

The FEM of a beam-and-slab bridge is developed by considering a 20 m long and 10 m wide structure (Figure 3-19). The FEM is developed by [González et al., 2015] in order to test the performance of SHM methods during real and unknown environmental condition. The bridge is modelled with 0.9 m deep precast concrete beams and a 0.16 m thick continuous structural slab on top of them. Two lanes of traffic, one for each direction, are modelled: lane 1, where a vehicle is running, and lane 2, with no vehicle runs. 10 longitudinal beams are used to represent the deck of the bridge. The longitudinal beams are spaced by 1 meter and placed symmetrically with respect to the bridge centreline. The bridge deck is discretized into 1 m x 1 m plates, with the exception of the plate at the edge, which have a size of 1 m (longitudinal) x 0.5 m (transversal). Therefore, the bridge has a total of 220 plate elements and 200 beam elements. The health state of the bridge is monitored by analysing the acceleration of the bridge that is provided by 9 accelerometers, installed in the positions depicted by circles in Figure 3-19.

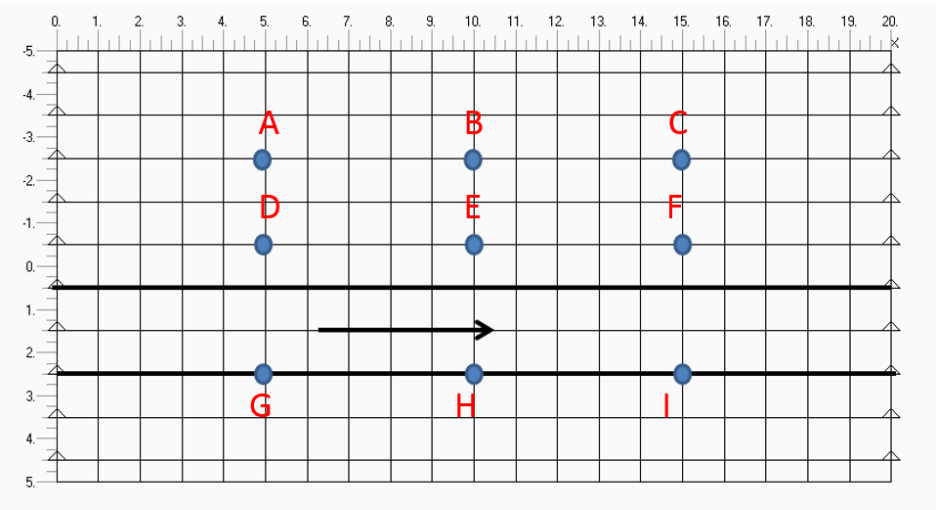

Figure 3-19. *Plan view of the beam-and-slab bridge*

3.5.1.1 **The model of the vehicle**

A model of a typical European 5-axle articulated truck is modelled in order to simulate the traffic over the bridge. The length of the truck is assumed to be 14.9 m, and the direction of the truck is assumed to be from left to right, with inner and outer wheels located along the path at 0.5 m and 2.5 m, respectively, from bridge centreline, as shown in Figure 3-19 [González et al., 2015]. A single tyre is assumed for the 1st axle while two tyres are considered for other axles. The distances between the consecutive axles is 3.6, 6.33, 1.31 and 1.31 m, respectively. The transverse distance between two wheels of an axle is 2 m. Two different Gross Vehicle Weights (GVWs) are tested: *i)* a fully-loaded condition, where the GVW is equal to 40 tons (truck A); *ii)* a half-loaded condition, where the GVW is 25 tons (truck B).

3.5.1.2 **Degradation mechanism**

The degradation of the bridge is modelled as a sudden loss of stiffness at selected beam elements. The location and magnitude of the simulated damages of the bridge is presented in Table 3-7. The damage location in Table 3-7 corresponds to the distance from the first support of the bridge on the left-hand side. The loss of stiffness extends 1.5 m longitudinally at both sides of the location shown in Table 3-7, and its width is given in Table 3-7. The percentage of loss of stiffness in Table 3-7 represents the loss of stiffness of the entire damaged area of the bridge. The 16 damage scenarios illustrate that the change of the bridge behaviour can be caused by: *i)* loss of stiffness of bridge element(s); *ii)* changes of the road roughness, i.e. the bridge is in a healthy condition, but the roughness of the road is changed, as shown by the road type column in Table 3-7; *iii)* changes of the vehicle properties (such as dynamic properties, speed, mass), i.e. the bridge is in the good condition, but the properties of the vehicles are changed, as shown by the vehicle type column in Table 3-7. Therefore, the BBN needs to be able to manage these different environmental conditions in order to assess the condition of the bridge correctly, by detecting and diagnosing its damaged health states.

Table 3-7. *Degraded scenarios of the beam-and-slab bridge*

Test number	Vehicle speed	Vehicle type	Road type	Damage location (m)	Damage width (m)	Damage severity (%)	Damaged lane
1	20	A	2	15	5	8	2
2	30	B	3	Healthy	Healthy	Healthy	Healthy
3	30	A*	1	5	5	6	2
4	20	B*	2	Healthy	Healthy	Healthy	Healthy
5	20	A	1	12.5	5	8	1
6	30	B	1	2.5	5	12.1	1
7	30	A	1	10	5	10	2
8	20	B	1	10	5	6	2
9	20	A	1	7.5	5	12.1	1
10	30	B	1	13.3	10	16	1, 2
11	22.5	A	1	6.6	10	20.1	1, 2
12	27.5	B	1	6.6	5	10	1
13	30	A	1	12.5	5	8	2
14	20	B	1	12.5	10	16	1, 2
15	20	A	1	6.6	10	11.9	1, 2
				15	5	12.1	1
16	30	B	1	7.5	10	24.2	1, 2
				13.3	5	8	2

**The dynamic properties of the vehicle are modified in test 3 and 4 by modifying the values of the stiffness of the suspensions.*

3.5.2 **The BBN of the beam-and-slab bridge**

The BBN is developed by following the methodology described in section 3.3. The aim of this section is to analyse the performance of the proposed method, and thus the step-by-step process that leads to the development of the BBN is briefly described in section 3.5.2.1 (BBN structure) and section 3.5.2.2 (CPTs of the BBN), whereas the performance of the BBN is analysed in detail in section 3.5.3.

3.5.2.1 **The structure of the BBN**

The step-by-step process presented in section 3.3.1 is adopted in order to develop the structure of the BBN to assess the health state of the beam-and-slab bridge. Major and minor elements of the beam-and-slab bridge are identified as follows: each longitudinal beam is identified as a major element of the bridge, whereas two

consecutive smaller elements of the longitudinal beams are identified as the minor elements of the bridge. As a result, two consecutive 1m small elements of a longitudinal beam of bridge are merged together into a node of the BBN. Influences between minor elements of different longitudinal beams are neglected. The size of the developed BBN is large, due to the high number of nodes. As a consequence, an individual BBN is developed for each longitudinal beam in order to provide a compact visualization of the final BBN, which assesses the condition of the whole bridge. The final BBN is then developed by merging together the ten individual BBNs into an OOBN. In fact, an OOBN allows to have a BBN as a part of another BBN. The OOBN is used to have a more compact representation of the network, which is able to assess the condition of the whole bridge by considering the health state of each bridge element, both major and minor.

Figure 3-20 shows the BBN for a longitudinal beam, whose health state is evaluated by taking account of the condition of its 10 smaller elements (2 smaller elements for each node). Influences between neighbour minor elements of the longitudinal beam are considered, as shown by "*_1*" ending nodes of Figure 3-20. The grey circle on the *Beam_1* node represents the fact that the health state of this node is used as evidence of the beam condition into the OOBN of the whole bridge.

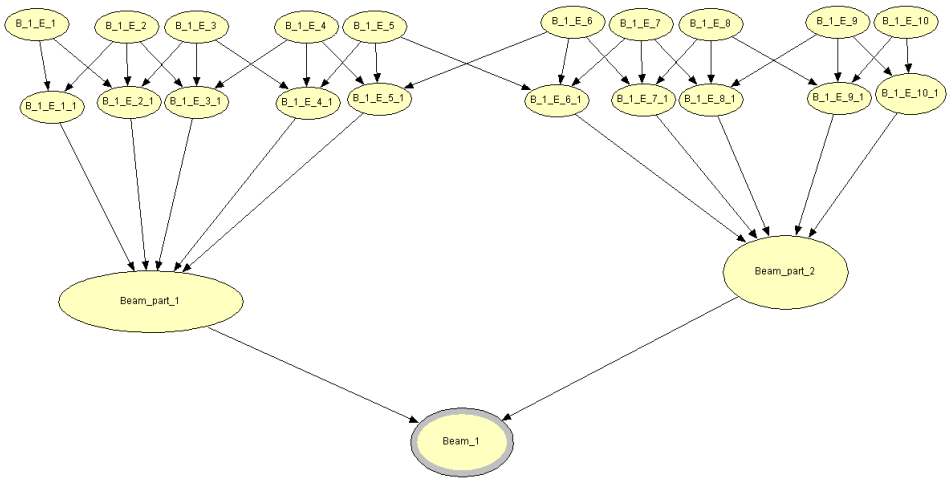

Figure 3-20. *BBN of a longitudinal beam of the bridge*

Figure 3-21 shows that the health state of the whole bridge is evaluated by taking account of the health state of each longitudinal beam. Each rectangular node of Figure 3-21 represents the evidence of the health state of the corresponding longitudinal beam, i.e. the BBNs representing each longitudinal beam of the bridge (Figure 3-20)

are used as a part of the OOBN, in order to assess the health state of the whole bridge. Influences between adjacent longitudinal beams are considered as shown by the "*_1*" ending nodes of Figure 3-21. Finally, the health state of the whole bridge is evaluated by taking account of the health state of each element of the bridge.

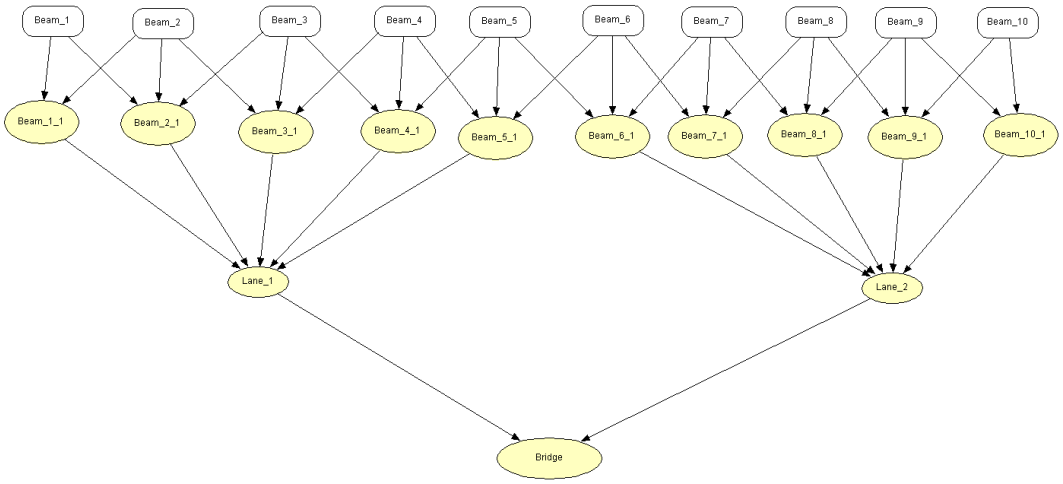

Figure 3-21. *OOBN of the beam-and-slab bridge*

3.5.2.2 **The CPTs of the BBN**

The quantitative part, i.e. the CPTs of the BBN, is defined by using discrete conditional probability distributions. Three discrete and mutually exclusive health states are used to define the conditional probabilistic relationships between two connected nodes: *i)* a healthy state, where the element of the bridge is in a good condition and no degradation is present; *ii)* a partially degraded state, where a degradation mechanism is present on the bridge element, but maintenance activities can be postponed; and *iii)* a severely degraded state, where the degradation mechanism of the bridge element is severe, and maintenance activities are required as soon as possible. The CPTs are defined by adopting a process of expert knowledge elicitation, as described in section 3.3.2. In this way, the systematic knowledge of bridge engineers is used to assess possible influences between different elements of the bridge.

3.5.3 **Analysis of the BBN performance in detecting and diagnosing damage of the beam-and-slab bridge**

The behaviour of the beam-and-slab bridge is not provided continuously, but instead the 16 scenarios of Table 3-7 are provided as evidence of the bridge behaviour. As a result, the damage detection and diagnostics properties of the BBN are tested in

this case study. A Damage Potential Indicator (DPI) is assessed from each sensor of the bridge, i.e. every time when a new evidence of the acceleration of the bridge is available, the DPI is assessed. The DPI is then used as an input to the BBN in order to assess the health state of the bridge. The DPI is a vibration-based index that takes account of the frequency content of the bridge acceleration in the time interval *t*, and of the bridge vibration energy [Moughty & Casas, 2017]. The DPI is assessed as follows:

$$D_{pi} = \frac{\frac{\pi}{2g}\int_0^t a(t)^2 dt}{\upsilon_0^2} \tag{3-26}$$

where *a(t)* is the acceleration of the bridge in the time interval *t*, *g* is equal to the gravity constant and υ_0^2 represents the number of zero crossings per unit of time of the bridge acceleration. The bridge response frequency and energy absorption are represented by the DPI.

The performance of the BBN in analysing the 16 test scenarios of the bridge behaviour are presented in Table 3-8. It is shown that in most cases the BBN is able to detect and diagnose damages of the bridge correctly. However, two false alarms are raised by the BBN, as shown by test 2 and 4 in Table 3-8: tests 2 and 4 simulate a change of the environmental condition of the bridge (road roughness and dynamic properties of the vehicle), but the BBN assigns such changes to the change in the health state of the bridge. The lane where the loss of stiffness occurred is correctly identified in 13 out of 14 remaining damaged test scenarios. The lane is identified correctly partially in Test 16: the BBN is able to correctly identify the damage from 5m to 7m that extends over the complete width of the bridge, whereas the loss of stiffness of lane 2 at 11.5m is not identified. The longitudinal damaged elements of the bridge are correctly identified on average, but, in some test scenarios healthy elements of the bridge, which are close to the damaged ones, are identified as damaged by the BBN. For example, the transversal extension of the damage of Test 9 is correctly identified, as well as the longitudinal extension from 6.5m to 9m. However, the healthy longitudinal elements from 5.5m to 6.5 and from 9m to 12m are also identified as damaged by the BBN. This behaviour of the BBN can be caused by the definition of

its structure, i.e. number of nodes that describe the bridge elements. Finally, the magnitude of the damage is assessed through the probability of the element of being in the severely degraded health state. Table 3-8 shows that the lower the loss of stiffness, the lower the probability of being in the severely degraded state. If the loss of stiffness is higher than 10%, the probability is equal to or higher than 0.4. However, a more accurate identification of the damage magnitude can be achieved by improving the definition of the CPTs, and by increasing the number of the mutually exclusive states of each node of the BBN.

Table 3-8. *Performance of the proposed BBN method in monitoring the beam-and-slab bridge*

Test number	Real damage location (m)	Real damage width (m)	Damaged longitudinal part identified by the BBN (m)	Damaged width elements identified by the BBN (m)	Probability of being in the severely degraded state
1	15	5	10.5 to 15.5	-4.5 to -0.5	0.35
2	Healthy	Healthy	10.5 to 13.5	-0.5 to 2.5	0.40
3	5	5	3 to 6	-2.5 to -0.5	0.30
			10 to 13	-2.5 to -0.5	0.30
4	Healthy	Healthy	10 to 12	-0.5 to 2.5	0.40
5	12.5	5	10.5 to 13.5	-0.5 to 2.5	0.35
6	2.5	5	7 to 15	-0.5 to 2.5	0.40
7	10	5	8 to 11	-2.5 to -0.5	0.40
8	10	5	9 to 12	-2.5 to -0.5	0.35
9	7.5	5	5 to 12	1.5 to 3.5	0.35
10	13.3	10	10 to 14	-4.5 to 4.5	0.40
11	6.6	10	4.5 to 12.5	-3.5 to -1.5	0.35
				0.5 to 2.5	
12	6.6	5	4.5 to 12	0.5 to 2.5	0.50
13	12.5	5	10.5 to 13.5	-3.5 to 2.5	0.35
14	12.5	10	10.5 to 13.5	-3.5 to 2.5	0.40
15	6.6	10	11 to 14	1.5 to 2.5	0.40
	15	5	7 to 10	-2.5 to -0.5	0.30
16	7.5	10	5 to 7	-3.5 to 2.5	0.40
	13.3	5	10 to 13	1.5 to 2.5	0.30

The real location of the damage extends 1.5 m at both sides of the location shown

3.5.4 Discussion of the proposed BBN method for the beam-and-slab bridge

The proposed BBN method has shown good performance in analysing the beam-and-slab bridge, which consisted in challenging and realistic damaged scenarios. In fact, the health state of the bridge was modified at the same time with changes of the environmental conditions of the bridge. Therefore, a change of the bridge behaviour can be caused either by a damage or (and) by a change of the environmental conditions. However, the method has confirmed the drawbacks identified in section 3.4.5:

1. False alarms have been activated when the environmental conditions of the bridge changed. A pre-processing analysis of the bridge behaviour would improve the performance of the BBN analysis by allowing to analyse only the structural behaviour of the bridge. In this way, the proposed BBN-based SHM method can assess the health state of the bridge under changing environmental conditions.
2. The accuracy of the damage detection and diagnostic process was inaccurate in some scenarios. The performance of the BBN can be enhanced by improving the method for defining the CPTs, e.g. if a database of bridge behaviour, such as bridge acceleration, displacement, natural frequencies, etc., is available, such data would help to define the influences between different elements of the bridge more accurately, and, as a consequence, the diagnostics process of the BBN could be more accurate. At the same time, a higher number of the discrete mutually exclusive states, which describe the node of the BBN, can lead to a more accurate diagnosis of the magnitude of the damage. However, the size of the CPTs increases with the number of the mutually exclusive health states.

3.6 Summary

A BBN-based method for bridge condition monitoring has been presented in this chapter. The BBN model is composed of two parts: *i)* a structural part, which is defined by analysing the structure of the bridge, represents the connection between the different elements of the bridge; *ii)* a quantitative part, which is defined by using an expert knowledge elicitation process, defines the influences between different connected elements of the bridge.

The method has been demonstrated to be able to monitor the health state of a bridge continuously, by updating the health state of the bridge, and its elements, every time when new evidence of the bridge behaviour becomes available. In this way, when the

health state of the bridge changes, the BBN allows to diagnose the causes of such a change, by pointing out the degrading element(s) of the bridge.

At the same time, the damage detection and diagnostics abilities of the BBN have been investigated, by analysing damaged scenarios of a bridge. The results of the analysis have shown that the proposed method allows to accurately detect and diagnose damage of the bridge structure, however false alarms and misclassification have been detected.

The analysis of the BBN results suggest that its performance can be improved by:

1. Introducing pre-processing of the data with the aim of managing the noise of the data and taking account of the effects of the changes in the environmental condition experienced by the bridge.
2. Updating the CPTs by merging together the expert knowledge with the analysis of the bridge behaviour. In this way, the CPTs of the BBN can be defined in a more robust way, and, thus, the accuracy of the diagnostics analysis of the BBN is expected to improve.
3. Introducing a higher number of nodes in order to describe the bridge elements in a more detailed manner. Similarly, the increase of the number of the mutually exclusive discrete states, which describe each node of the BBN, can lead to an improvement of the diagnostics property of the BBN. However, the increase of both number of nodes and health states would lead to an increase in the size of the CPTs.

In what follows, these drawbacks are handled by proposing a robust and reliable BBN-based method for SHM in the further chapters.

Chapter 4 A data analysis methodology and a machine learning approach for processing the data on bridge behaviour

4.1 Introduction

The analysis of the BBN performance in Chapter 3 has shown that pre-processing of the bridge behaviour is needed to improve the accuracy of the BBN analysis. Particularly, the data on the behaviour of the bridge needs to be processed to remove noise of the data, which then can be used to identify the condition of bridge elements. In this way, the results of the pre-processing data analysis can be used as an input to the BBN nodes in order to select the condition of the bridge element in a reliable way. The BBN is then able to update the health state of the bridge by taking account of the condition of its elements. The pre-processing of the bridge behaviour is of particular importance when an in-field bridge is analysed, due to the noise and uncertainties that affect its behaviour.

In this chapter, monitoring data from a post-tensioned concrete in-field bridge is analysed with the aim of identifying the bridge health state. Consequently, a data analysis methodology for pre-processing the bridge behaviour is proposed by relying on a multi-step method that is presented in section 4.2. Since, sensors can provide large amounts of data, the adoption of machine learning methods in the SHM of infrastructure is becoming more popular. For this reason, a machine learning approach is proposed in section 4.5 to achieve an automatic assessment of the health state of the bridge elements, by the means of a NFC [Cetişli & Barkana, 2010]. The assessment of the health state of the bridge elements provided by the NFC can be used as an input to the BBN nodes, in order to update the health state of the whole bridge.

In what follows, the proposed data analysis methodology is introduced in section 4.2, then the methodology is applied to the post-tensioned concrete bridge in section 4.3. The summary of the data analysis methodology is presented in section 4.4. The NFC machine learning method to automatically identify the health state of the bridge

element is presented in section 4.5, whereas the influence of the size of the feature training set on the performance of the NFC is discussed in section 4.6. The conclusive discussion of the results is given in section 4.7.

Finally, it is worth noting that the proposed data analysis methodology is also applied to an in-field steel truss bridge, which is subject to a progressive damage test, in order to identify and diagnose the health state of the steel truss bridge. In this way, the proposed data analysis methodology and its performance are verified using a different in-field bridge, which shows a different behaviour from the post-tensioned concrete bridge, e.g. the steel truss bridge is excited by a moving vehicle rather than changing environmental condition. However, only a small amount of data is available for the steel truss bridge, and thus the NFC cannot be verified for this second case study. The results of the data analysis methodology of this latter case study are presented in section 4.8.

4.2 The proposed data analysis methodology

Several methods for analysing the raw data of bridge behaviour are presented in literature, such as clustering techniques, PCA and ANN models [Fan et al., 2011; Moughty et al., 2017; Vagnoli et al., 2018]. These methods showed promising performance in identifying the health state of bridge elements, however two main drawbacks are: *a)* the methods are often verified by using an FEM, which is unable to reproduce all the data noise and uncertainties affecting an in-field bridge [Limongelli et al., 2017]; *b)* modal parameters of the bridge are usually monitored [Han et al., 2014; Sadhu, 2017; Khan et al., 2018]. To expand on the second point, modal parameters of the bridge can be difficult to assess in a fast and reliable manner. In fact, lower modal parameters of the bridge, i.e. the first natural frequencies and mode shapes, are both strongly influenced by changes in environmental conditions and usually are of low sensitivity to bridge infrastructure damage. Higher modal parameters of the bridge are more sensitive to damage, but more difficult to extract from the measured bridge data in a reliable manner [Kim et al., 2007; Casas et al., 2017]. For these reasons, in this thesis a data analysis methodology is proposed to process the bridge behaviour by removing noise of the data and to identify the health state of bridge elements. The methodology rely on two main steps: *i)* extraction of statistical, frequency-based and vibration-based features from the bridge behaviour, to reduce the dimension of the bridge behaviour data into valuable information, with respect to the bridge condition

[Moughty & Casas, 2017; Lei et al., 2018]; *ii)* assessment of the features' trend and of bridge HIs, by applying the EMD method to the extracted features [Huang et al., 1998]. The main novelty of the proposed data analysis methodology lies on the second step of the methodology *ii)*. In fact, the EMD is generally adopted in the SHM framework to identify structural changes by analysing the bridge dynamic behaviour directly, i.e. the dynamic behaviour of the bridge is used as input to the EMD process [Cahill et al., 2018; Han et al., 2014]. Such applications have shown good results when an FEM is analysed [Han et al., 2014; Aied et al., 2016]; conversely, misclassifications of the bridge health state were observed due to a mode-mixing problem when an in-field large structure was monitored [Barbosh et al., 2018; Khan et al., 2018]. Variations of the EMD process, such as Ensemble EMD (EEMD) and Multivariate EMD (MEMD), can be adopted in order to overcome the mode-mixing problem and achieve good assessment of the bridge condition [Wu & Huang, 2009; Rehman & Mandic, 2010]. The application of the EEMD and the MEMD to a large bridge structure provides better results than the EMD, by being able to detect changes of the bridge health state (but not to diagnose the nature of the occurred damages) and reducing the mode-mixing problem. However, the EEMD and the MEMD require higher computational time than the EMD, and the mode-mixing problem is not fully addressed [Sadhu, 2017; Barbosh et al., 2018]. For these reasons, we adopt the EMD method to assess the trend of the extracted features, not the raw data, of the bridge behaviour. Indeed, several studies showed that the trend of statistical, frequency-based and vibration-based features can provide valuable information with respect to the level of degradation of components of rotary machinery [Mosallam et al., 2014; Cannarile et al., 2017]. Furthermore, the literature review of Chapter 2 has shown that when the health state of a bridge has been evaluated by monitoring raw bridge behaviour, or slightly processed (e.g. transformation of the bridge acceleration to symbolic values based on a frequentist analysis [Cury et al., 2012]), promising results were obtained in a fast and reliable way [Langone et al., 2017].

The proposed methodology is developed and optimized by analysing the acceleration of the bridge, which is provided by accelerometers installed on the bridge infrastructure. Therefore, if different parameters are monitored, such as displacements of the bridge, some of the features introduced in the next sections cannot be adopted due to their nature that aims to analyse bridge vibration only. As a consequence, if

different parameters are monitored, the proposed methodology can be still applied to the bridge, but the set of extracted features needs to be defined accurately.

In what follows, the proposed methodology is presented in section 4.2.1, and each step of the methodology is discussed in the following sections.

4.2.1 **Overview of the methodology**

The proposed data analysis methodology is depicted in Figure 4-1. The vibration behaviour (i.e. acceleration) of the bridge is recorded by a measurement system (accelerometers) that is installed on the bridge infrastructure. Every time when a new set of raw bridge acceleration is provided by the sensors, the raw acceleration is pre-processed with the aim of removing outliers of the data (i.e. the noise) and obtaining the free vibration behaviour of the bridge. This data allows to assess the condition of the bridge by avoiding any potential noise from excitation sources [Chang & Kim, 2016; Cao et al., 2017]. A feature extraction process is then developed, to reduce the dimensionality of the free-vibration bridge behaviour. Indeed, the sensors can provide thousands of values of the bridge acceleration at each time second, whereas features can extract relevant information regarding the bridge health state, by merging together the thousands sensor values into a lumped assessment [Chalouli et al., 2017]. Statistical features (such as mean value, standard deviation, kurtosis, root mean square, etc.), frequency-domain features (such as peaks and amplitudes of the bridge frequencies that are obtained by using the Fast Fourier Transform (FFT)) and vibration parameters (such as peak acceleration, Arias intensity, cumulative absolute velocity, etc.) are assessed at each τ time step in order to extract information from the free-vibration behaviour of the bridge [Mosallam et al., 2014; Moughty & Casas, 2017]. The obtained features usually show a high level of oscillations, and a robust and reliable assessment of the bridge condition can be threatened. A further step of data processing is introduced in this thesis with the aim of computing the feature trend over the time interval τ^*, by assessing the residuals of the EMD of each extracted feature. A set of bridge HIs, which provides information with respect to the health state of the monitored bridge, can then be obtained by calculating statistical parameters (such as standard deviation and skewness) of the feature trend.

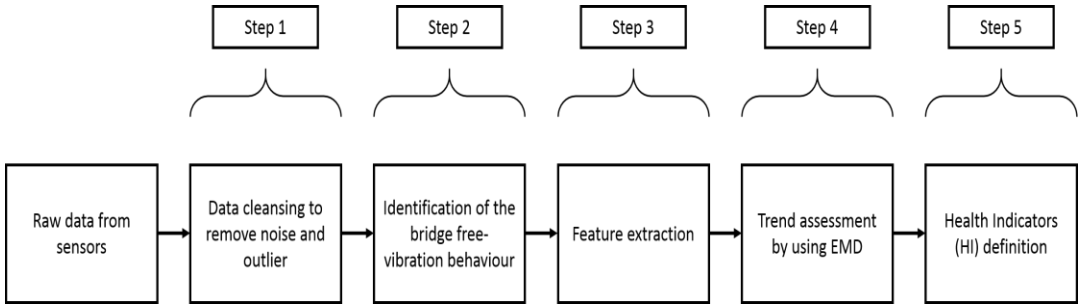

Figure 4-1. *Flowchart of the proposed methodology*

4.2.2 **Step 1 - Data cleansing**

A data cleansing process is required to remove noise from the raw bridge behaviour [Moughty et al., 2017]. Several methods are presented in literature to reduce the measurement noise, such as PCA [Žvokelj et al., 2011], Singular-Value Decomposition (SVD) [Zhao & Jia, 2017], wavelet analysis [Katicha et al., 2017] and machine learning method [Bao et al., 2018]. In this thesis, the median filtering statistical process is used to detect and correct outliers, due to its fast and robust analysis in detecting and correcting outliers [Liu et al., 2004]. Given the data of the raw bridge behaviour X from the sensors and the size of a time interval k, the median filtering process can be defined as follows:

$$if \ \left|x_i - m_i\right| > n_{st} \cdot \sigma \quad \Rightarrow \quad x_i = m_i \tag{4-1}$$

where m_i and σ represent the local median and the standard deviation of the data belonging to a time window of size $2k+1$, respectively. n_{st} represents the number of standard deviations by which a data x_i of X must differ from the local median to be considered an outlier. The median (m_i) and the standard deviation (σ) are defined as follows:

$$m_i = median(x_{i-k}, x_{i-k+1}, \ldots, x_i, \ldots, x_{i+k-1}, x_{i+k}) \tag{4-2}$$

$$\sigma = \sqrt{\frac{\sum_{j=i-k}^{i+k} (x_j - \bar{x})^2}{n-1}} \tag{4-3}$$

Eq. (4-1) shows that a value x_i that differs from the median (m_i) by more than n_{st} standard deviations, is recognized as an outlier and replaced with the median (m_i) of

that time window of size $2k+1$. The size of the time interval k is defined by the user depending on the nature of the considered case study, e.g. the sampling rate of the sensors influences the definition of k: a higher sampling rate would require a smaller size of k. Indeed, the higher the number of data points provided by the sensors, the higher the number of possible outliers that can influence the assessment of the local median (m_i). The number of standard deviations (n_{st}) that defines the acceptable deviation of a point from the local median is defined by the user according to the chosen confidence interval.

4.2.3 **Step 2 - Identification of the bridge free-vibration behaviour**

The free-vibration behaviour of the bridge is analysed with the aim of assessing the bridge health state, and avoiding any influence of the excitation source, which can lead to incorrect condition assessment [Chang & Kim, 2016; Cao et al., 2017]. The bridge free-vibration, which can be defined as the vibration of the bridge that decays in an approximately exponential form following an external excitation, can be extracted from the vibration data by analysing the available information: *i)* if a bridge is excited by a moving vehicle, the free-vibration behaviour can be identified by knowing when the vehicle leaves the bridge [Chang & Kim, 2016]; *ii)* if the bridge is excited by changing environmental condition, such as wind, the free-vibration behaviour of the bridge can be identified as the decreasing bridge vibration behaviour that follows a peak value of the bridge vibration behaviour [Cunha et al., 2001]. This second approach can also be used when information about moving vehicles is not available.

4.2.4 **Step 3 - Feature extraction**

Large data storage capacity and high computational power are required to efficiently store and analyse the data provided by the sensors: each sensor provides N values of the bridge behaviour for each second, i.e. each sensor has a sampling rate of N Hz. Conversely, the dimension of the bridge behaviour data can be reduced into more valuable information, with respect to the bridge health state, by extracting features from the acceleration data. For this reason, 18 features are extracted from the free-vibration behaviour of the bridge every τ seconds, by reducing the dimensionality of the data from $N \bullet \tau$ to 18 for each sensor, i.e. every τ seconds the 18 features are evaluated for each sensor and stored to monitor the evolution of the bridge condition over time. τ can be defined by optimizing the monotonicity and trendability values of the features. The features are extracted from both time domain (such as mean value,

standard deviation, etc.) and the frequency domain by using an FFT approach (such as amplitude and peak of the first harmonic). In this way, statistical, frequency-based and vibration parameters of the bridge are evaluated in order to assess the condition of the bridge. In fact, changes in statistical and vibration features of the bridge behaviour can identify a damage of the bridge structure: an increase of the bridge vibration behaviour can be caused by a reduction of bridge stiffness, which leads to a lower structural ability in resisting to external excitation in a static and stable manner [Moughty & Casas, 2017]. Similarly, a change in the frequency-based feature, which estimates modal and vibration characteristics of the bridge, can represent changes in bridge physical characteristics, such as stiffness, mass, etc. [Han et al., 2014; Khan et al., 2018]. The 18 features are chosen due to their ability in describing the health state of a system during different system health states [Mosallam et al., 2014; Moughty & Casas, 2017].

The 18 features are defined as follows:

1. **Mean value** (statistical) is the mean value of the bridge acceleration in the interval τ;
2. **Standard deviation** (statistical) represents how much the bridge acceleration in the interval τ differs from the mean value;
3. **Skewness** (statistical) measures the asymmetry of the bridge acceleration in the interval τ;
4. **Kurtosis** (statistical) measures the shape of the distribution of the bridge acceleration in the interval τ;
5. **Root Mean Square (RMS)** (statistical) is the root mean square of the bridge acceleration in the interval τ;
6. **Median** (statistical) is the median value of the bridge acceleration in the interval τ;
7. **Coefficient of variation** (statistical) is the ratio between the standard deviation and the mean value of the bridge acceleration in the interval τ;
8. **Euclidean Norm** (statistical) is the length of the bridge acceleration vector in the interval τ;
9. **Frequency of the first harmonic** (frequency-based) represents the frequency value of the first harmonic of the FFT spectrum, which is obtained by using the bridge acceleration in the interval τ as input to the FFT algorithm;

10. **Amplitude of first harmonic** (frequency-based) represents the amplitude of the first harmonic of the FFT spectrum, which is obtained by using the bridge acceleration in the interval τ as input to the FFT algorithm;
11. **Mean period of the bridge behaviour** (frequency-based) in the interval τ is defined as follows:

$$T_m = \frac{\sum_i A_i^2 (1/f_i)}{\sum_i A_i^2} \qquad for\ 0.25Hz \le f_i \le 20Hz \tag{4-4}$$

where A_i represents the amplitude values of the discrete frequencies f_i that belong to the interval between 0.25Hz and 20Hz. T_m evaluates a weighted average period of the bridge between 0.25Hz and 20Hz [Rathje et al., 2004].

12. **Mean frequency of the bridge behaviour** (frequency-based) is the inverse of the mean period value determined by applying Eq. (4-4);
13. **Cumulative velocity of the bridge** (vibration) computes the approximate velocity of the bridge in the interval τ;
14. **Peak acceleration** (vibration) is the maximum value of the bridge acceleration in the interval τ;
15. **Peak displacement** (vibration) is the maximum value of the bridge displacement in the interval τ, which is estimated by integrating the bridge acceleration twice;
16. **Arias intensity** (vibration) represents the cumulative value of the bridge vibration energy in the interval τ. The Arias intensity index is evaluated as follows:

$$I_A = \frac{\pi}{2g} \int_0^t a(t)^2 dt \tag{4-5}$$

where *a(t)* is the acceleration of the bridge in the time interval τ and g is equal to the gravity constant. The Arias intensity has been defined by [Arias, 1970] in order to describe the potential destructiveness of an earthquake, by assessing the energy content of the earthquake. Therefore, the Arias intensity of the bridge represents the energy content of the bridge when the bridge is excited.

17. **Damage Potential Indicator (DPI)** (vibration) is an adaptation of Arias Intensity, which takes account of the frequency content of the bridge acceleration in the time interval τ, in addition to the bridge vibration energy [Moughty & Casas, 2017]:

$$D_{pi} = \frac{\frac{\pi}{2g}\int_0^t a(t)^2 dt}{\upsilon_0^2} \tag{4-6}$$

where υ_0^2 represents the number of zero crossings per unit of time of the bridge acceleration. The bridge response frequency and energy absorption are represented by the Damage Potential Indicator.

18. **Cumulative Absolute Velocity (CAV)** (vibration) is the sum of all absolute bridge acceleration values in the interval τ:

$$CAV = \int_0^t \left|a(t)\right|^2 dt \tag{4-7}$$

4.2.5 Step 4 - Assessment of the feature trend

The features extracted from the bridge acceleration every τ seconds can show a high level of oscillations, due to changing response of the bridge and noisy data provided by the sensor. [Mosallam et al., 2014; Cannarile et al., 2017] have shown that a robust and reliable assessment of the system health state can be threatened if noisy features are evaluated. Similarly, the assessment of the bridge health state can be threatened by evaluating features that show oscillation. Hence, a further step of data processing is introduced in this thesis by using the features as an input to the EMD process. The features that are extracted during an interval [0, τ*] are used as an input to the EMD process to assess their trend. The interval [0, τ*] is chosen to monitor the health state of the bridge continuously, i.e. the trend of the features is evaluated and updated each time when τ* new features are extracted from the free-vibration of the bridge. The value of τ^* can be identified by maximizing the monotonicity and trendability values of the features.

The EMD is able to provide a smooth monotonic trend of the features, and as a consequence, the health state of the bridge can be assessed in a robust way. The EMD is a data-driven decomposition method that is able to decompose the feature pattern (F) in the interval τ^* into multiple simple harmonics of various frequencies, called Intrinsic Mode Functions (IMFs) [Huang et al., 1998]. The EMD process can be applied to any oscillatory and non-stationary time series as follows:

I. Identify all maxima and minima of the feature pattern (F) to be decomposed in the interval τ^*.
II. Connect peaks using a polynomial spline fitting to enhance interpolation.
III. Assess the mean value of both maxima and minima spline envelope.
IV. Subtract the mean of the envelope from the original feature pattern.
V. Perform steps I to IV until the following two criteria are satisfied: *i)* the number of extrema and number of zero crossings is either equal or differ at most by one; *ii)* a zero-mean of the envelope is obtained. The resulting time-series is the first IMF, denoted as h_1.
VI. Perform steps I to V to the obtained IMFs, known as shifting process, until a monotonic function remains, or a stopping criterion is reached. This final time-series is known as residuals (r) which represent the trend of the decomposed feature pattern.

In this thesis, the shifting process of the EMD is stopped when the difference between residuals of successive IMFs is lower than a predetermined threshold, which is set to equal to 0.2 on the Matlab® data processing toolbox.

The EMD decomposition can be represented as shown in Eq. (4-8): the feature pattern, denoted as F, in the interval τ^* is decomposed into multiple IMFs (h_i) and a residual curve (r).

$$F = \sum_{i=1}^{M} h_i + r \tag{4-8}$$

where M is the number of IMFs.

4.2.6 **Step 5 - Definition and selection of the bridge Health Indicators (HIs)**

The trend of the proposed feature provides information about the condition of the bridge. Such information can be lumped into a set of HIs, which represent the health state of the bridge by defining a set of parameters. The HIs are defined by evaluating four statistical parameters of each feature trend: *a)* the standard deviation of the trend (HI_1), in order to take account of the variability of the feature trend; *b)* the intercept of a linear polynomial fitting of the feature trend (HI_2), which has demonstrated to be informative with respect to the heath state of a system [Cannarile et al., 2017]; *c)* the normalized cumulative sum of the feature trend (HI_3), to take account of the positive/negative monotonicity of the feature trend; *d)* the skewness of the feature trend (HI_4), in order to take account of the trend asymmetry. A set of 72 HIs (18 feature trends and 4 statistical parameters for each trend) is computed each time τ^* when a new assessment of the feature trend is carried out. The HIs are selected to consider the variability of the features trend, the trend monotonic behaviour over time and the trend shape. Other HIs can be used to represent other characteristics of the features trend in a lumped manner. For example, both the trendability and monotonicity, which are introduced in what follows, can be used directly to monitor the evolution the bridge health state over time.

Some of the 72 HIs can be non-informative in respect to the health state of the bridge [Hoell & Omenzetter, 2017]. In a similar way, the value of τ and τ^* can influence the performance of the proposed method, due to the amount of data of the bridge behaviour that are considered to assess the features and the HIs.

The HI selection process and the optimization of τ and τ^* is carried out by maximizing the HIs trendability and monotonicity. In fact, the trendability (Eq. (4-9)), which belongs to the interval [-1, 1], represents the correlation between the feature trend and the time: a feature with constant trend has a zero correlation, whereas a feature with a trend that linearly increases over time has a strong positive correlation. The monotonicity (Eq. (4-10)), which belongs to [0, 1], represents the positive or negative trend of a feature trend: the higher the monotonicity, the higher the monotonic behaviour of the feature trend, i.e. the feature increases (decreases) as the degradation of the bridge increases. Both trendability and monotonicity are important in the health monitoring framework due to the fact that a system is generally unable to repair itself after that a degradation process is initiated, and thus the HIs should be able to represent the decreasing condition of the system in a monotonic manner [Duan et al., 2018]:

$$Trendability = \frac{n\left(\sum xt\right) - \left(\sum x\right)\left(\sum t\right)}{\sqrt{\left[n\sum x^2 - \left(\sum x\right)^2\right]\left[n\sum t^2 - \left(\sum t\right)^2\right]}} \tag{4-9}$$

$$Monotonicity = \frac{no.of\ {}^{d}\!/_{dt} > 0}{n-1} - \frac{no.of\ {}^{d}\!/_{dt} < 0}{n-1} \tag{4-10}$$

where x is the value of the HI, t is the time, n is the length of the available data being analysed, and $no.of\ {}^{d}\!/_{dt}$ represents the number of points such that the first derivative of the HI is positive/negative.

The higher the trendability and monotonicity of a HI, the higher the ability of that HI in representing the changing health state of the bridge. Hence, we merge these two metrics into a Goodness Index (GI) that accounts for both trendability and monotonicity, as shown in Eq. (4-11). The HIs with the highest value of GI are chosen as the optimal bridge HIs, whilst the values of τ and τ^* that allow to maximize the GI of the HI set are set as optimal values.

$$GI = Trendability + Monotonicity \tag{4-11}$$

The health state of the bridge is monitored by assessing the value of the optimal HIs every τ^* time when a new set of feature assessment is available. A set of HIs is adopted to monitor the health state of the bridge with the aim of tackling the uncertainties that can affect the assessment of the bridge HIs. Indeed, an HI can provide reliable information about the health state of the bridge in terms of healthy or damaged bridge but can be unable to diagnose the nature of the bridge damage. On the contrary, if a set of optimal HIs is used to monitor the condition of the bridge, each HI can provide valuable information about the condition of the bridge and the characteristics of its damage scenarios. Finally, the application of this data analysis methodology within the BBN approach is expected to improve the performance of each individual method in terms of both damage detection and diagnostics ability.

In what follows, the proposed method for data processing is applied to a post-tensioned concrete bridge that is subjected to a progressive damage test, and as a

consequence, the ability of the proposed method in monitoring the health state of the bridge by identifying the health state of the bridge elements is tested.

4.3 Application of the proposed data analysis methodology to an in-field post-tensioned concrete bridge

The performance of the proposed data analysis methodology is verified by assessing the condition of a post-tensioned concrete bridge [Siringoringo et al., 2013]. The bridge is subjected to a damage test, i.e. the infrastructure of the bridge is intentionally damaged in order to study how the bridge behaves in different conditions. The post-tensioned concrete bridge is excited by changing environmental conditions. The aim of the proposed method is to monitor the behaviour of the bridge and detect and diagnose the damaged bridge elements.

4.3.1 Description of the post-tensioned concrete bridge and the progressive damage test

The post-tensioned concrete bridge has the main span of 32 m, side spans of 12 m, and its width is 6.6 m (Figure 4-2a). The bridge was subject to a vibration measurement test before being demolished in order to obtain the bridge behaviour in different health states. The acceleration of the bridge was monitored by a measurement system made of 2 reference sensors, and 4 sensors that were moved periodically along the bridge length to obtain a complete modal description of the bridge. In this thesis, we consider the acceleration provided by the 2 reference sensors, which were kept fixed throughout the duration of the test that allows a robust calibration of the data analysis methodology by providing the behaviour of the same section of the bridge throughout the progressive damage test. The sampling rate of the sensors was 100 Hz and they were installed at locations, shown by circles in Figure 4-2b. The main excitation source of the bridge was due to changing environmental conditions. A progressive damage test was performed by cutting a pier of the bridge, as shown in Figure 4-2c. The bridge acceleration of during 6 different health states of the bridge were monitored (Figure 4-2c):

- Class 1, the undamaged (healthy) condition of the bridge was monitored for 50 minutes;

- Class 2, the pier was cut by 5cm and a steel column was installed to have a temporary support of the bridge, while studying different damage scenarios. This state was monitored for 5 minutes.
- Class 3, the pier was cut by 5 additional cm, and the bridge health state during this scenario was monitored for 20 minutes.
- Class 4, the steel column was lowered by 1 cm and the bridge deck settled at 1 cm lower of its starting position. This scenario was monitored for 20 minutes.
- Class 5, the steel column was further lowered by 1 cm and the bridge deck settled at 2 cm lower of its starting position. The acceleration of the bridge during this scenario was recorded for 50 minutes.
- Class 6, the steel column was lowered by 3cm and the bridge deck settled at 2.7 cm lower of its starting position. The bridge acceleration was monitored during this scenario was recorded for 20 minutes.
- Class 7, the pier of the bridge was retrofitted by installing a steel plate to fill the gap between the pier and footing. The bridge acceleration was monitored for 20 minutes during this scenario.

The behaviour of the bridge in the different scenarios was recorded for different time intervals. For this reason, Class 2 is not considered in this thesis due to the low amount of data available, which does not allow to adequately assess the bridge health state. Class 7 is also not considered due to the focus on the fault detection and diagnostic ability of the proposed methods. Furthermore, 20 minutes of acceleration data are considered for each remaining class, in order to analyse scenarios that have the same amount of data and to verify the ability of the proposed method in identifying different health states of the bridge. The retrieved database of bridge behaviour is divided in two smaller groups of data: *a)* the first group (group 1) contains 10 minutes of data, and is used in this chapter, and also chapter 5 to present the proposed data analysis method and define the CPTs of the bridge BBN; *b)* the second group (group 2) is made of 10 minutes of data, and is used to verify the performance of both the NFC (section 4.5) and the BBN method (Chapter 6) in identifying the bridge condition. This second group of data is not labelled, i.e. the class of the data is not

known a-priori, and thus the ability of the proposed method in assessing the health state of the bridge can be verified.

Finally, all groups of data are used as an input to the proposed methodology, in order to remove the data noise (step 1), extract the features (step 2), define the features (step 3) and their trend (step 4) and compute the bridge HIs set (step 5).

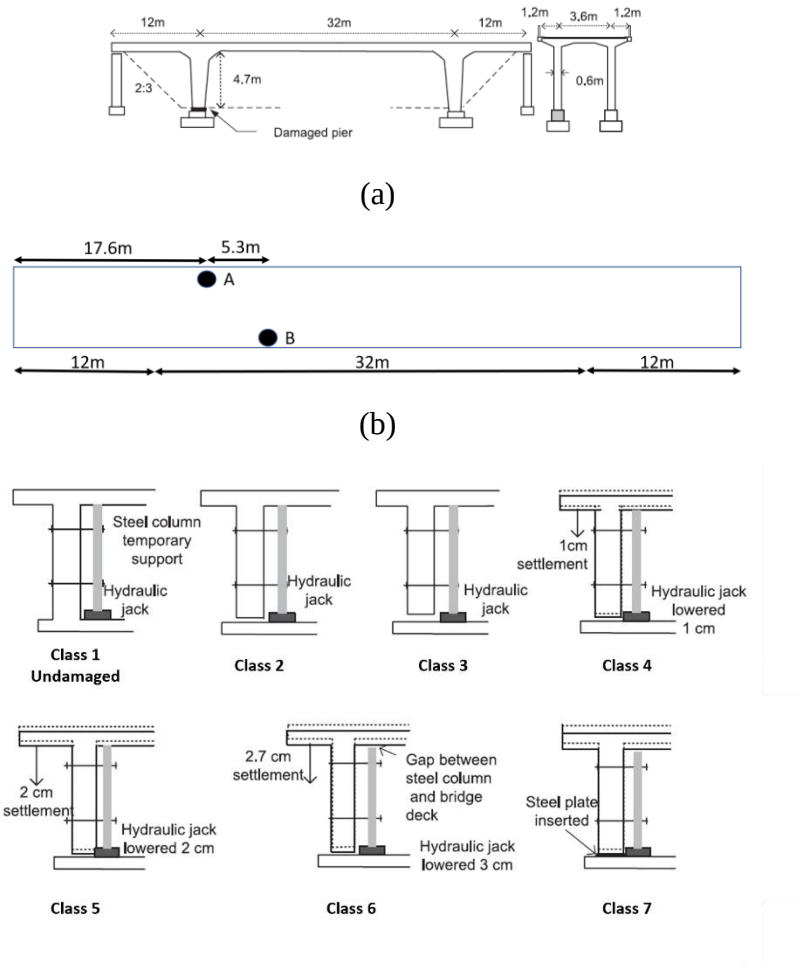

Figure 4-2. *The post-tensioned concrete bridge [Siringoringo et al., 2013]*

4.3.2 **Step 1- Data cleansing**

The bridge is excited randomly by unknown changes in wind and traffic, which is passing on the road under the bridge. As a result, the bridge acceleration can show sudden spikes due to external unknown sources of excitation. For example, Figure 4-3 (top) shows the raw data of the bridge acceleration provided by a sensor during a time interval of 300 seconds. The raw acceleration shows high level of noise, such as sudden increases and spikes, e.g. the spike at time 240 seconds, where the acceleration of the

bridge reaches 10cm/s^2 for few measurements before returning to an equilibrium position. The noise of the acceleration is reduced by applying the median filtering statistical process, presented in section 4.2.2. Figure 4-3 (bottom) shows the processed acceleration of the bridge, i.e. after the outlier removal process. The response of the bridge to external excitations is not changed, i.e. the induced acceleration of the bridge is not changed in terms of time position, but rather the noise of such induced acceleration is reduced.

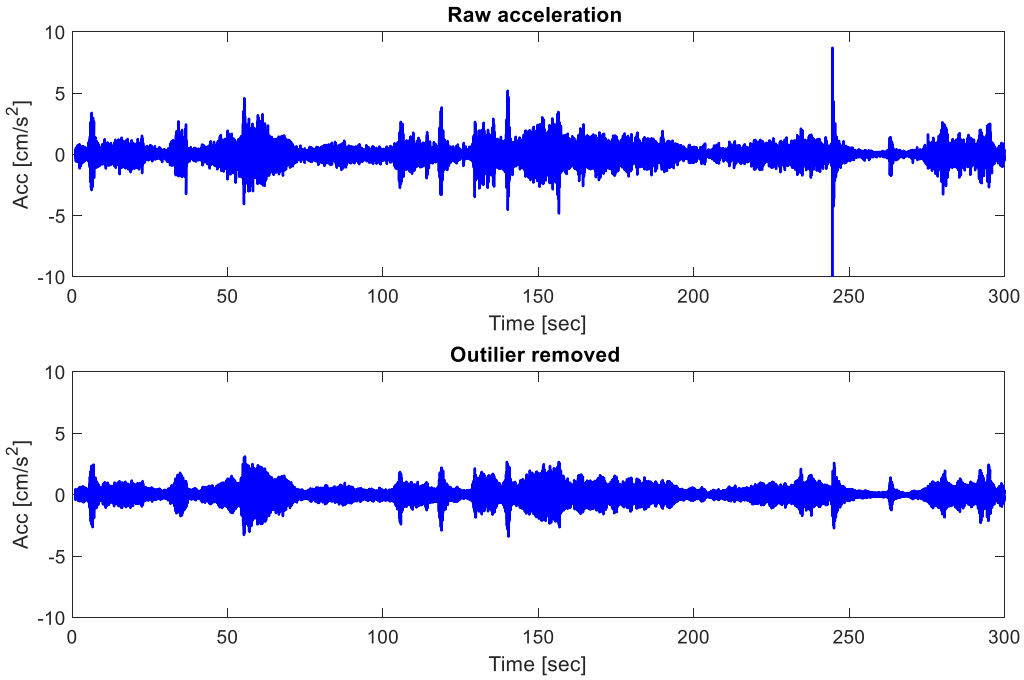

Figure 4-3. *Raw and processed acceleration of the bridge*

4.3.3 Step 2 - Identification of the bridge free-vibration behaviour

The next step (step 2) of the method aims to identify the free-vibration of the bridge, with the aim of analysing the bridge behaviour without considering the potential influence in the external excitation source. The free-vibration of the bridge is identified by looking for peaks in the acceleration. In fact, when an external force excites the bridge, the bridge usually shows its maximum vibration when the external force is acting (or just acted) on the bridge, whereas the bridge behaviour decays by following an exponential function when the action of the external force is ended. Figure 4-4 shows the typical behaviour of the bridge when an external force acts on the bridge structure: the bridge is in an equilibrium position up to 2 seconds, then an external force excites the bridge, and the acceleration of the bridge increases. When the influence on the bridge is over, the acceleration decreases towards the equilibrium

point. The dots in Figure 4-4 represent the extreme values of the bridge acceleration, which are removed from the acceleration data, i.e. the acceleration data within the dotted-box are removed. In this way, any potential effect from the external source of vibration is not considered in the assessment of the bridge health state.

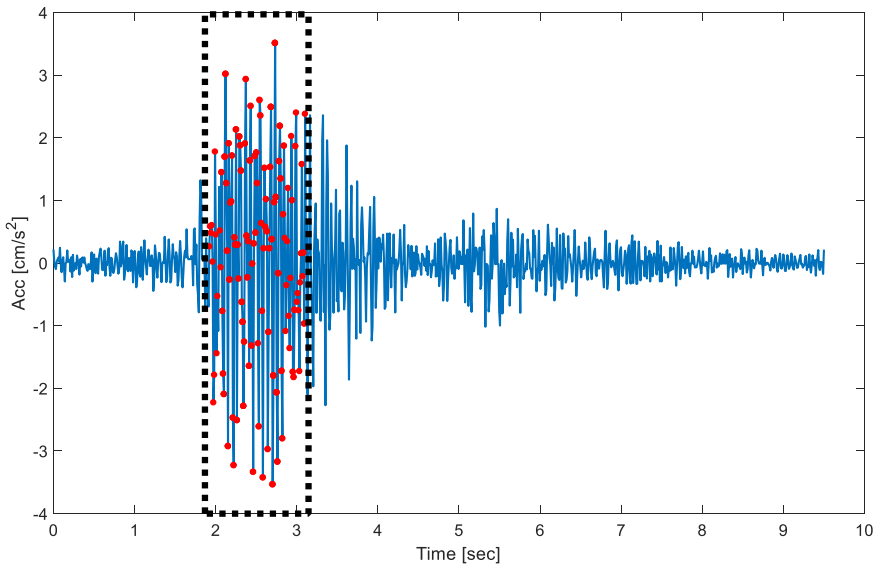

Figure 4-4. *Identification of the bridge free-vibration behaviour*

4.3.4 **Step 3 - Feature extraction**

The feature extraction process allows to extract valuable information about from the bridge free-vibration behaviour. Therefore, the 18 features are extracted from the free-vibration behaviour of the bridge every τ seconds. For example, Figure 4-5 shows the evolution over time of three (out of 18) features, when τ is equal to 3.5 seconds, and 10 minutes of data for each class are considered. The value of τ is optimized by maximizing the value of the GI. The three features in Figure 4-5 represent a statistical feature (kurtosis), a frequency-based feature (frequency of the first harmonic) and a vibration feature (Arias intensity). Each class of the bridge condition is depicted in Figure 4-5, by the means of: *i)* a cross-marked line to represent class 1 (healthy state of the bridge); *ii)* a circle-marked line to represent class 3; *iii)* a dot-marked line to represent class 4; *iv)* a diamond-marked line to depict class 5; *v)* a square-based line to show class 6. Although the features show some outliers when the bridge is damaged, on average the three features of the different classes are overlapping and noisy, and they have a high level of oscillations. A robust and reliable assessment of the bridge is not possible by analysing such features directly. For this reason, a further step of data processing is introduced by using the EMD, in order to retrieve the HIs of the bridge.

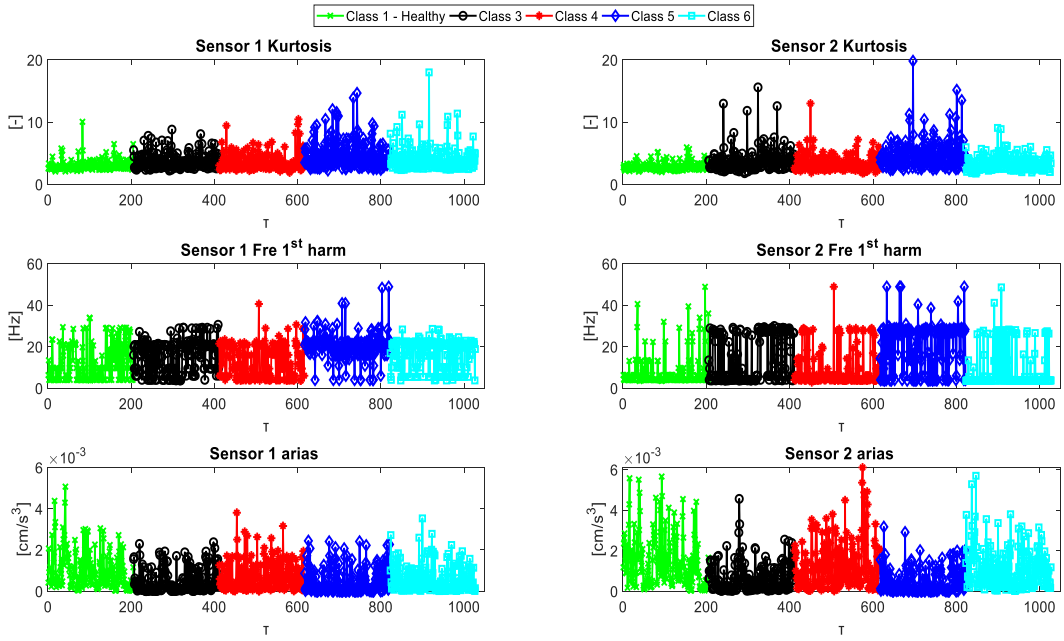

Figure 4-5. *Example of feature extracted from the free-vibration behaviour of the bridge*

4.3.5 **Step 4 - Assessment of the feature trend**

The trend of the features during an interval [0, τ^*] is assessed by using the features as an input to the EMD process. The EMD process decomposes the feature pattern over the interval [0, τ^*] into IMFs and the residuals, which represent the trend of the feature in the interval. Figure 4-6 shows the residual of the kurtosis of Figure 4-5 during three consecutive time windows [0, $4\tau^*$], [0, $5\tau^*$] and [0, $6\tau^*$], with τ^* =45 τ when the bridge health state is changing: *i)* the bridge is healthy in [0, $4\tau^*$] (solid line in Figure 4-6); *ii)* the pier of the bridge is cut during [0, $5\tau^*$] (dashed line in Figure 4-6); *iii)* the pier is completely cut in [0, $6\tau^*$] (dotted line in Figure 4-6). It should be noted that the residuals change as τ^* increases and the health state of the bridge is modified. Therefore, the trend of the kurtosis, which is retrieved by using the kurtosis as an input to the EMD process, allows to point out the different bridge health states, as shown by the different lines of Figure 4-6. However, the size of the feature trend increases over time, due to its definition in the interval [0, τ^*], and thus the different behaviour of the feature trend over time is lumped into HIs, which represent the health state of the bridge by the means of single value parameters, as shown in the following section.

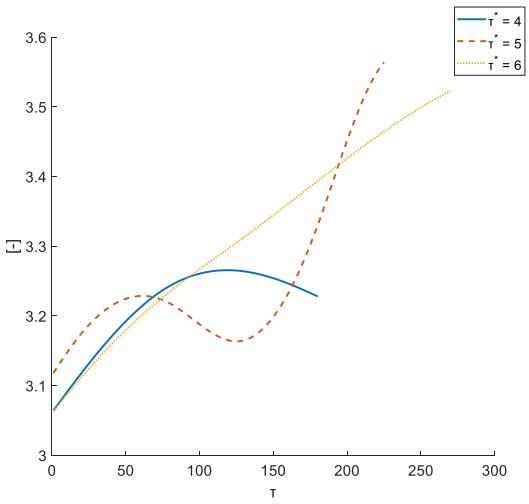

Figure 4-6. *Example of a feature trend at consecutive τ^**

4.3.6 **Step 5 - Bridge Health Indicators definition**

The trend of the features is then lumped into the 4 HIs, presented in section 4.2.6. The value of τ and τ^* influences the ability of the method in identifying the different health states of the bridge, due to the amount of the data that represents the behaviour of the bridge used to assess both the features and the bridge HIs. Therefore, the value of τ and τ^* needs to be optimized. The GI value of the 72 HIs is assessed by modifying the value of τ and τ^* in order to assess the optimal value of these time interval, which allows to maximize the value of GI. Figure 4-7 shows the variation of the maximum value of GI when τ and τ^* are modified between [0, 5] sec and [15, 45] τ, respectively. The intervals of τ and τ^* are chosen by considering the size of the data of group 1, by having at least two values of the HIs for each bridge health state. The maximum possible value of GI is equal to 2, due to the fact that 1 is the maximum value of both the monotonicity and trendability. The maximum value of GI is reached when τ = 3.5 sec and τ^* = 45 τ, which are chosen as optimal values in this case study. The HIs that allow to obtain the maximum value of GI are: *i)* HI_3 of the frequency of the first harmonic and *ii)* HI_3 of the kurtosis of the bridge acceleration, as shown in Table 4-1. Hence, the normalized cumulative sum of the two features is the optimal HI to monitor the evolution of the bridge condition over time.

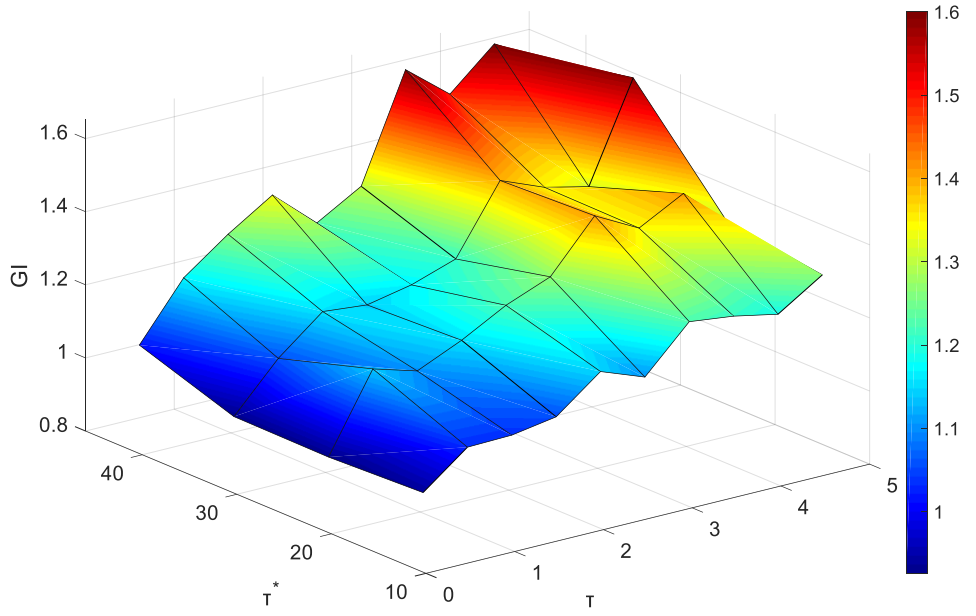

Figure 4-7. *GI values at varying τ and τ**

Table 4-1. *Optimal HIs to assess the health state of the bridge*

Optimal HI	**GI**
HI_3 of the kurtosis	1.59
HI_3 of the frequency of the first harmonic	1.27

Figure 4-8 shows the evolution of the 4 HIs of the 2 optimal features. Particularly, Figure 4-8(a) shows the HIs that are extracted by using the frequency of the first harmonic as an input to the EMD, whilst Figure 4-8(b) shows the HIs that are retrieved from the trend of the kurtosis of the bridge acceleration. It worth noting that HI_3 allows to identify the different classes of the bridge health state clearly. Therefore, the use of the EMD to extract the trend of the statistical, frequency-domain and vibration-based features, which is the main novel aspect of the proposed methodology, is able to point out the different health states of the bridge in a clear and well-separated manner. At the same time, however, some HIs are not able to identify the different bridge health states (e.g. HI_1 of the frequency of the first harmonic and HI_4 of the kurtosis show almost a constant value throughout the monitored interval). Therefore, an accurate assessment of the bridge health state might not be achieved by monitoring the evolution of such HIs. This latter result explains the reason why an HIs selection process in needed to select the optimal HIs that allow to monitor the evolution of the bridge health state. Furthermore, the HI_3 of both features allow to identify the different

health states of the bridge: HI_3 of the kurtosis allows to identify in a clear way the difference between class 3 and 4 due to higher value of HI_3 value of class 4, whereas HI_3 of the frequency of the first harmonic allows to point out in an easier way the difference between class 5 and 6. As a consequence, the health state of the bridge can be monitored by using these two HIs. Finally, this information as an input to the BBN nodes to assess the health state of the whole bridge, by taking account of the health state of the bridge elements.

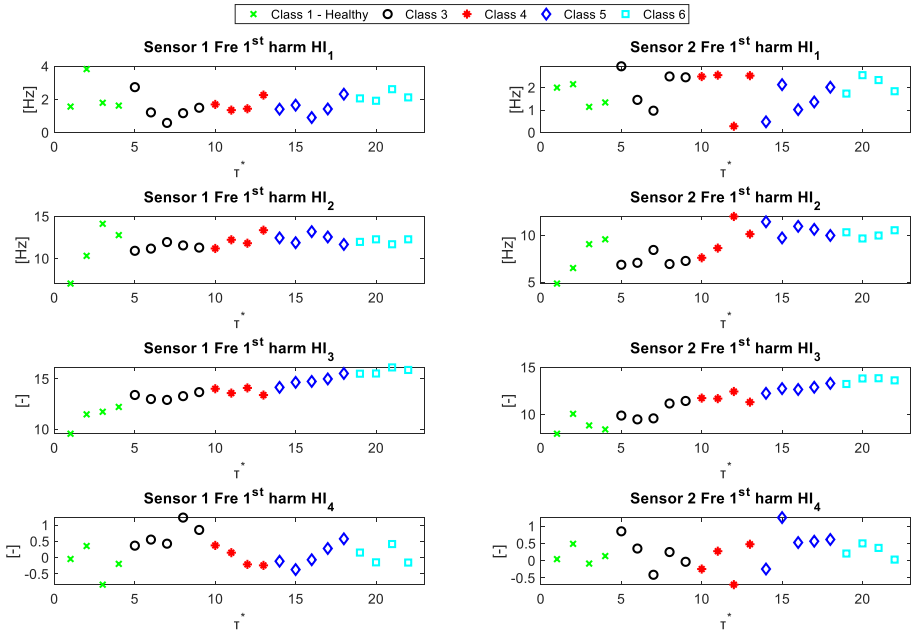

(a)

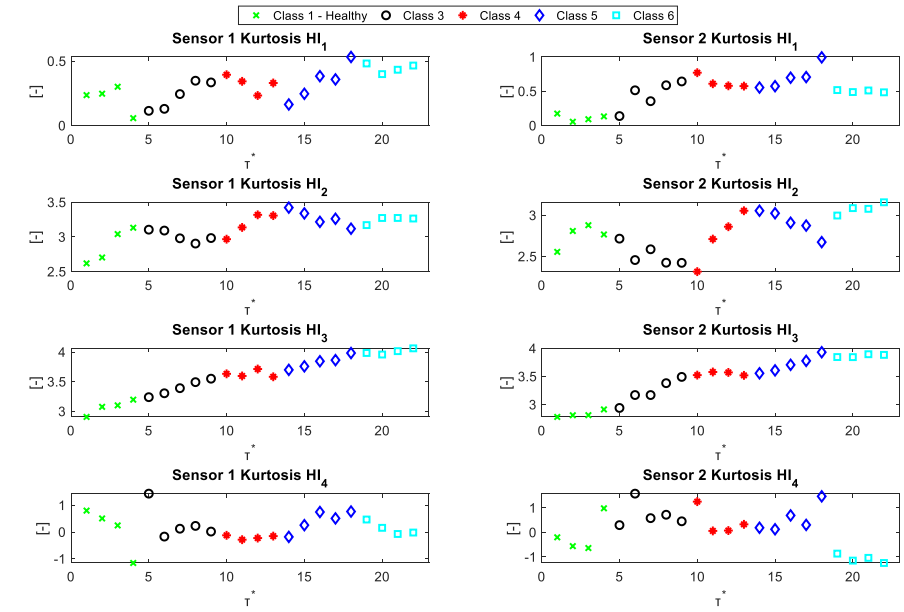

(b)

Figure 4-8. *HIs evolution of the optimal features*

Finally, it should be noted that the evolution of the HIs for each feature is presented in Appendix D.

4.4 Summary of the data analysis methodology

The proposed data-driven methodology allows to monitor the condition of the post-tensioned concrete bridge elements by relying on the data analysis of its vibration behaviour. Statistical, frequency-based and vibration-based features are extracted from the data, and the trend of these features is assessed by the means of the EMD approach. HIs of the bridge are evaluated by computing four statistical parameters of the features trend. The optimal HIs to monitor the bridge health state are identified by optimizing the value of a GI, which allows to identify the HIs with the highest values of monotonicity and trendability over time. In this way, the degrading health state of the bridge is monitored by monotonic HIs that are able to clearly represent the different conditions experienced by the bridge. Different health states of the bridge are identified by the proposed HIs, and therefore such information can be used as an input to the BBN nodes in order to select the state of the BBN nodes in a reliable manner. In this way, the BBN can assess the condition of the whole bridge, by taking account of the health state of each element of the bridge, by monitoring the optimal HIs that allow to point out the changing health state of the bridge.

The proposed methodology relies on vibration parameters of the bridge, which can be assessed only when the vibration behaviour of the bridge is monitored by the measurement system that is installed on the bridge. Hence, if other behaviour of the bridge is monitored, the methodology needs to be modified accordingly, by computing different features of the bridge behaviour. Furthermore, the proposed HIs can be replaced by other statistical parameters that assess other characteristics of the features trend. In fact, the proposed HIs do not represent the optimal set of HIs for monitoring the health state of any bridge, due to the fact that each bridge presents unique characteristics and behaviour, and thus its different health states can be represented by different optimal HIs. However, when the proposed data analysis methodology is applied to different bridges, the changing health state of the bridges can be identified by the proposed methodology, as shown in section 4.8. Future research activities should consider these initial results in order to identify an optimal set of HIs for SHM. The proposed data analysis methodology is represented by a deep data analysis, which starts using raw bridge acceleration data and their features, and results in HIs whose

physical meaning is not straightforward to explain. For example, HI_3 of the kurtosis represents the normalized cumulative sum of the trend of the kurtosis of the bridge acceleration over time. The increase of this HI of the kurtosis represents the increase of the trend of the kurtosis of the bridge acceleration over time, and consequently an increase of the outliers of the bridge acceleration. Hence, the extreme values of the bridge vibration are increasing over time, which can be expected due to the cut of the pier of the bridge that leads to a reduced capacity of the bridge in responding to external forces. The optimal value of τ and τ^* and the optimal set of HIs depend on the case study and the available data. Therefore, an optimization process needs to be carried out in order to point out the optimal value of these parameters.

Finally, although the retrofitting of the bridge, i.e. when the cut pier is repaired, allows to restore the condition of the bridge, it can be worth adding the data of class 7 when analysing the data in future work, in order to verify if the maintenance action is able to restore the as-good-as-new condition of the bridge.

The proposed data analysis method is used in Chapter 6 of this thesis to process the raw acceleration of the bridge and be incorporated in the BBN method. The proposed methodology can be integrated with a machine learning method, which allows to automatically assess the health state of the bridge elements by relying on the analysis of the bridge HIs, as shown in the next section.

4.5 A machine learning approach for automatic identification of the bridge health state

4.5.1 Introduction

An automatic assessment of the bridge health state is proposed by the means of an NFC, which is trained in a supervised manner by using a dataset of bridge behaviour in different health states [Cetişli & Barkana, 2010]. Machine learning methods are being used more frequently in different data analysis frameworks, such as system health monitoring, infrastructure health monitoring, natural language processing, etc. due to the availability of large quantities of data. For this reason, we propose a NFC-based method to assess the health state of the bridge elements in a fast and automatic manner. In this way, the proposed machine learning method can provide information about the health state of the bridge elements to the BBN, which is then able to propagate such information throughout the BBN network and update the health state of the whole bridge.

The NFC is adopted to automatically assess the health state of the bridge by using an optimal subset of HIs as an input to the NFC. Conversely to the HI selection process of section 4.2.6, here the optimal subset of HIs is retrieved by using an optimization differential evolution algorithm [Di Maio et al., 2016], which aims to optimize the accuracy performance of the NFC. The NFC is selected among the machine learning classifiers due to the fact that it combines fuzzy classification techniques with learning capabilities of the Neural Networks. As a consequence, the network structure is developed by the means of if-then fuzzy rules, which are initially defined by using a K-means clustering algorithm. Conversely to ANNs, which require the optimization of the number of hidden layers and hidden nodes, the NFC requires only the optimization of the number of clusters of the K-means algorithm, and the performance of the NFC is slightly influenced by the number of the cluster. Moreover, good performance can also be achieved with a small dataset of the system behaviour [Cetişli & Barkana, 2010]. NFC has been adopted to diagnose the damage of system components, such as wind turbine blades [Hoell & Omenzetter, 2017] and rotor bars [Dias & De Sousa, 2018], but not for bridge damage diagnostics, where ANNs and clustering techniques have been mostly applied, as discussed in Chapter 2 . The NFC can be used to automatically assess the health state of the bridge by providing robust results without requiring a time-consuming trial and error procedure to optimize its parameters, as a step needed in the ANN method. The proposed method of automatic health state identification based on the NFC also contributes to the novelty of this thesis.

In what follows, the NFC is introduced (section 4.5.2), followed by the HIs selection process (section 4.5.2.2) and the analysis of the post-tensioned bridge using this method (section 4.5.3). Finally, the influence of different datasets and of the size of the HIs set on the performance of the NFC method is investigated (section 4.6).

4.5.2 **The Neuro-Fuzzy Classifier (NFC)**

The NFC requires a database of historical behaviour of the bridge in different health states, in order to perform the training process. The NFC is trained by using a supervised process, that is, the condition of the bridge is known when the database of bridge behaviour is analysed. The NFC is trained with the HIs values that represent each health state experienced by the bridge. In this way, when a new set of unknown HIs is available, it is used as an input to the NFC, which is able to assess the health

state of the bridge elements automatically. An HIs selection process is necessary to find, among the HIs, a subset of optimal HIs that are informative with respect to the health state of the bridge [Hoell & Omenzetter, 2017]. In what follows, the main steps of the NFC are presented in section 4.5.2.1, whereas the HIs selection process is presented in section 4.5.2.2.

4.5.2.1 **The main steps of the NFC**

The detail description of the NFC is out of the scope of this thesis, and an interested reader can find more information in [Cetişli & Barkana, 2010]. An example of the NFC structure is depicted in Figure 4-9, for an NFC with 3 fuzzy rules (clusters of the K-means algorithm) and two classes. In what follows the main steps of the NFC (Figure 4-9) are presented:

1) a database of set of HIs is used as an input to the NFC. The target class of each set of HIs, i.e. the bridge health state corresponding to each set of HIs, is also provided to the NFC due to the fact that a supervised training process is carried out.
2) a K-means clustering method is applied to the HI data of each class with the aim of defining fuzzy if-then rules. This means that the HIs of each health state class are separated into different clusters, in order to describe the relation between HIs belonging to the same class. For example, a fuzzy rule can be defined as follows: if the HI_1 belongs to cluster 1, and the HI_2 belongs to cluster 2, then the bridge health state belongs to class 1.
3) the weight of each cluster of each class is assessed by evaluating the ratio between the size of each cluster with respect to the size of that class.
4) a Gaussian probability density membership function is defined for each cluster, by using the centre of each cluster as the mean value of the Gaussian distribution, whereas the standard deviation of the membership function is equal to the standard deviation of the HIs that belong to that cluster.
5) a fuzzification process is developed by assessing the membership value of each HI to each Gaussian probability distribution.
6) a defuzzification and normalization process is finally carried out in order to assign each HI to a class, i.e. each HI is assigned to the class with the higher membership value.

7) the accuracy of the process is assessed, by counting the number of correct classifications, i.e. the number of HI values that have been assigned to the correct class.
8) the performance of the NFC is assessed by computing an objective function, which represents the inverse of the accuracy of the NFC. Steps 4 to 7 are repeated iteratively with the aim of minimizing the objective function, maximizing the accuracy of the NFC and identifying the optimal value of the mean and standard deviation of the membership functions.

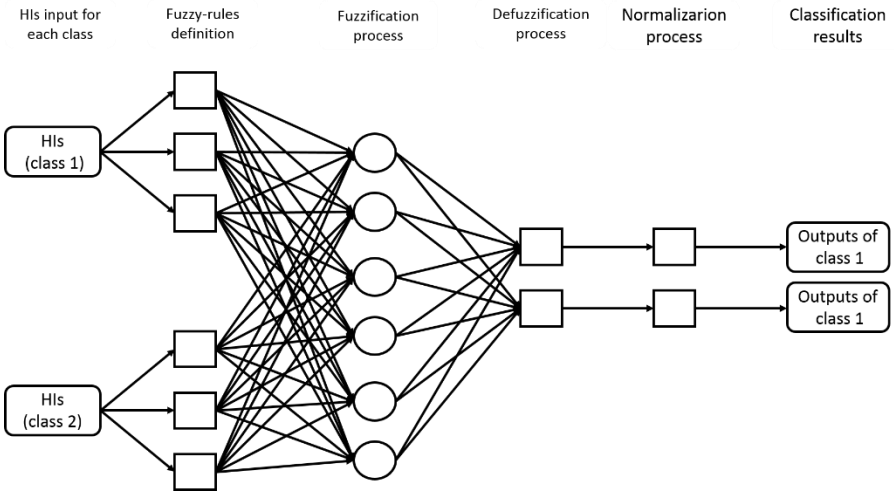

***Figure 4-9**. Example of NFC algorithm*

When the training process of the Neuro-Fuzzy classifier is complete, the NFC can be tested on a new and unknown set of bridge behaviour data. The testing process is also used to select the optimal subset of HIs that allows to maximize the accuracy of the NFC.

4.5.2.2 **The HI selection process**

The accuracy of the NFC is influenced by the quality of the HIs, because some of the HIs can be redundant or non-informative in respect to the health state of the bridge. An HI selection process is carried out to find a subset of HIs that guarantee high accuracy of the NFC, by minimizing false alarms and the degree of misclassification. An optimization algorithm is adopted by using a Modified Binary Differential Evolution (MBDE) algorithm [Di Maio et al., 2016]. A detailed description of the MBDE is provided in Appendix A. The optimization algorithm allows to select a

subset of HIs iteratively, and assess the accuracy of the NFC by using only the selected subset of HIs as an input to the NFC both during the training and testing phase, as shown in Figure 4-10. The group of possible subsets of HIs is comprehensively represented by $2^{\#HIs}$-1, where #HIs represents the number of HIs used to describe the condition of the bridge. A multi-objective optimization process is performed to minimize the fitness function, which is defined as follows:

$$fit = \left\{ \left(\frac{\sum_{i=1}^{T_{Train}} \left(L_{Real}^{Train} - L_{NFC}^{Train} \right) \times 100}{T_{Train}} \right)^{-1}, \left(\frac{\sum_{i=1}^{T_{Test}} \left(L_{Real}^{Test} - L_{NFC}^{Test} \right) \times 100}{T_{Test}} \right)^{-1} \right\} \quad (4\text{-}12)$$

where T_{Train} and T_{Test} represent the size of the target vectors for the training and test processes, respectively, $L_{\mathrm{Real}}^{Train}$ and L_{Real}^{Test} represent the real health state of the bridge for each bridge behaviour belonging to the training and testing target vectors, respectively. L_{NFC}^{Train} and L_{NFC}^{Test} represent the health state assigned to each bridge behaviour by the NFC during the training and testing process, respectively. Eq. (4-12) shows that the fitness function is minimized when the performance of the NFC is maximized, i.e. the higher the number of correct classification of the NFC, the lower the value of the fitness function. The training process is carried out in a supervised manner, whereas the test process is carried out by analysing a new and unknown set of bridge data. The optimization algorithm proceeds iteratively until a maximum number of iterations is reached, the accuracy of the NFC is maximised and the optimal subset of HIs is fixed. The optimal set of HIs can then be used to validate the proposed NFC, by monitoring the health state of the bridge when new and unknown behaviour of the bridge is provided by the sensors.

In the next sections, the proposed NFC method is tested in monitoring and assessing the health state of an in-field bridge.

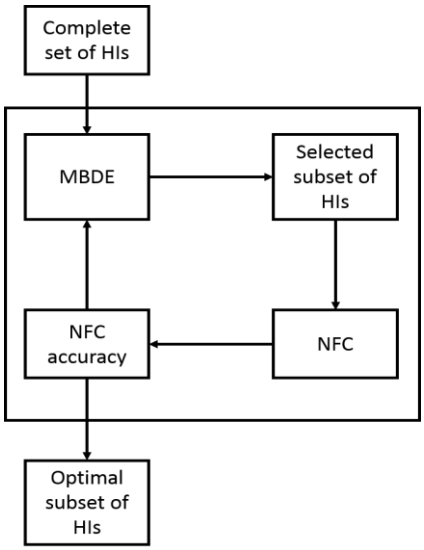

Figure 4-10. *Iterative algorithm to select the optimal HIs*

4.5.3 Application of the NFC to the post-tensioned concrete bridge

The performance of the proposed data-driven methodology is verified by monitoring and assessing the health state of the post-tensioned concrete bridge, presented in section 4.3.1. The two groups of bridge behaviour data presented in section 4.3.1 are used to train, test and validate the performance of the NFC: the 20 minutes of acceleration data allows to train the NFC in a balanced way. Indeed, an unbalanced amount of data between different classes, e.g. using different size of data for each class, can lead to misleading results due to the fact that the NFC is mainly trained with the data of the class that has the largest amount of data. Thus, the NFC can provide good performance in identifying such class, but poor performance in identifying different bridge behaviours. The retrieved two groups of data of section 4.3.1 are divided in three smaller groups of data: *a)* the first group (group A) contains 10 minutes of data, and is used to train the NFC; *b)* the second group (group B) is made of 3 minutes of data, and it is used to test the NFC and select the optimal set of HIs in order to monitor the health state of the bridge; *c)* the third set of data (group C) made of 7 minutes of data, which is used to verify the proposed methodology. This third group of data is not labelled, i.e. the class of the data is not known a-priori, and thus the ability of the proposed NFC in assessing the health state of the bridge automatically is verified.

All groups of data are used as an input to the proposed data analysis methodology first, in order to remove the data noise (step 1), extract the features (step 2), define the features (step 3) and their trend (step 4) and compute the bridge HIs set (step 5). Then,

the HIs are used as an input to the NFC that assesses the health state of the bridge (step 6).

The performance of the NFC strongly depends on the quality and amount of data available for the training process and on the selection of the subset of HIs performed by the MBDE. The amount of data is limited in this case study and the set of 72 HIs is represented by 2^{72}-1 possible combinations. Such large set of combination would require a large number of iteration in order to point out the optimal subset of HIs, and thus in this section only two HIs are considered to train, test and validate the NFC to obtain faster results based on the analysis of the HIs. Hence, HI_1 and HI_3 of the features trend are considered to monitor the health state of the bridge over time, and to train, test and validate the NFC. These two HIs are chosen due to their ability in identifying the different health states of the bridge, as discussed in section 4.3.6. Section 4.6 discusses the performance of the NFC when the whole set of bridge health state classes and of the 72 HIs are used to train, test and validate the NFC, and demonstrates that such performance is comparable to the results of other machine learning methods presented in literature.

In what follows, the performance of the NFC when only 2 HIs are used as an input to the method is investigated, by discussing the NFC training process (section 4.5.3.1), the HIs selection process (section 4.5.3.2) and the performance of the NFC (section 4.5.3.3).

4.5.3.1 **NFC training**

The NFC is adopted to automatically assess the health state of the bridge, by analysing the extracted HIs. The data of group A are used to train the NFC in a supervised manner, i.e. the health state of the bridge during the training process is known, and it is used as target results for the NFC. The training process aims to set the NFC parameters (number of clusters, mean and standard deviation of the Gaussian membership functions) to optimize the accuracy of the classification process. The number of clusters is assumed to be equal to the number of classes used as input to the NFC (5) and it is kept constant during the analysis. At the same time, the parameters τ and τ^* are optimized during the training process: the HIs of the data in group A are used as an input to the NFC by modifying either τ or τ^*, as shown in Figure 4-11. For example, when τ^* is equal to 30 τ, the NFC shows higher accuracy. The highest

accuracy is achieved when τ is equal to 2 seconds, which is chosen as the optimal τ. The optimal values of τ^* and τ are then used for the HIs selection process, to train the NFC with a dataset of 100 values of each HIs and to monitor the health state of the bridge.

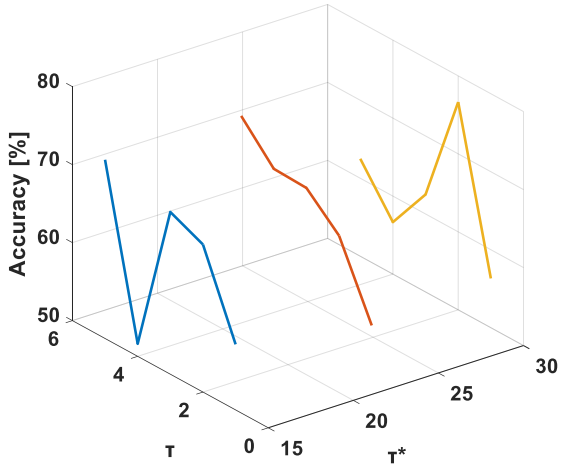

Figure 4-11. *NFC accuracy values at varying τ and τ**

4.5.3.2 **HIs selection process**

The selection process of the HIs is carried out by adopting the MBDE optimization algorithm, presented in section 4.5.3.2 and given Appendix A. The MBDE performs an iterative optimization by selecting a subset of HIs and evaluating the NFC performance by using the selected subset of HIs as an input to the NFC during both training and testing phases. The training process is carried out in a supervised manner, and the testing process is performed by using unlabelled data of group B, which are used as an input of the proposed method to assess the HIs values during these time intervals. A dataset of 30 values for each HIs is used for the HIs selection process. The aim of the MBDE is to maximize the accuracy of the NFC, and, thus, to identify the subset of HIs that allows to monitor the health state of the bridge reliably. The iterative process of the MBDE terminates when the maximum number of 2500 iterations is reached. The MBDE parameters (weighting factor, control parameter and size of the population as shown in Appendix A) are chosen by performing a trial and error procedure, and are equal to 0.8, 0.3 and 20 respectively, whereas 2500 iterations are chosen as trade-off between the high computational-time required by the MBDE and the number of iterations performed.

The evolution of the inverse of the fitness function of Eq. (4-12) is depicted in Figure 4-12: the higher the number of iteration, the higher the accuracy of the NFC (the lower the fitness function of the MBDE). Therefore, the MBDE is able to select subsets of HIs that lead to an improvement of the NFC accuracy. The dotted line in Figure 4-12 shows the improvement in the performance of the NFC during the testing phase: the accuracy of the NFC during the first iteration of the MBDE, when the subset of HIs is randomly selected by the MBDE, is 27%, whereas at generation 2500 it is 77%, due to the MBDE search that is able to select the possible optimal HIs.

The dotted line in Figure 4-12 shows a rapid increase of the NFC accuracy during the first 400 iterations, which is followed by 1000 ca. iterations that do not improve the accuracy of the NFC. This result can be due to the definition of the MBDE parameters, that lead the optimization research into a local minimum of the fitness function. The local minimum is erroneously identified as a global minimum of the MBDE fitness function, and the population of the selected HIs is slightly modified during these iterations. However, at iteration 1500 the MBDE is able to leave the local minimum, and the NFC accuracy increases accordingly. Finally, at iteration 2300 a new subset of HIs that allows to increase the accuracy of the NFC is found.

The accuracy of the NFC during the supervised training phase is always close to 98%. This latter performance of the NFC can be explained by considering the fact that, for each subset of HIs chosen by the MBDE, the NFC is able to set the value of its parameters in order to optimize the classification of the data during the training phase. The optimal subset of HIs is identified during the testing phase, as shown in Figure 4-13. The optimization algorithm, which is implemented in Matlab, requires 1 hour and 10 minutes to be completed by using an Intel core i3-4130 with CPU @ 3.4Hz.

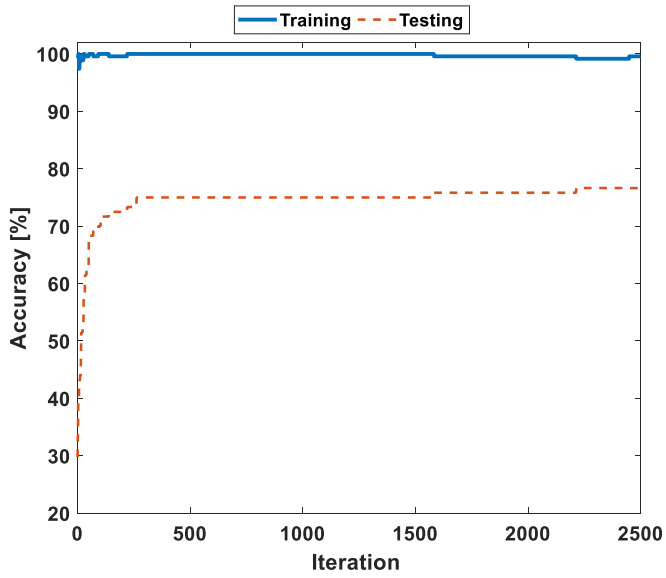

Figure 4-12. *Evolution of the fitness function during the HIs selection process*

Figure 4-13 shows the subset of selected optimal HIs (shadowed areas in Figure 4-13). HI_1 is the most selected HI for 6 features (out of 18), and HI_3 is selected for 5 features. This result of two HIs is expected due to the fact that both HIs show good performance in identifying the different health states of the bridge, as shown in Figure 4-8. It should be noted that the set of the 36 HIs is comprehensively represented by 2^{36}-1 possible combinations, and the MBDE might not have reached the best subset of HIs due to the large number of possible combinations of the HIs. However, the optimal subset of HIs in Figure 4-13 is identified by reaching a balance between computational time and accuracy of the NFC. This subset of HIs of Figure 4-13 is used to verify the proposed methodology in analysing unknown and unlabelled data of the bridge behaviour.

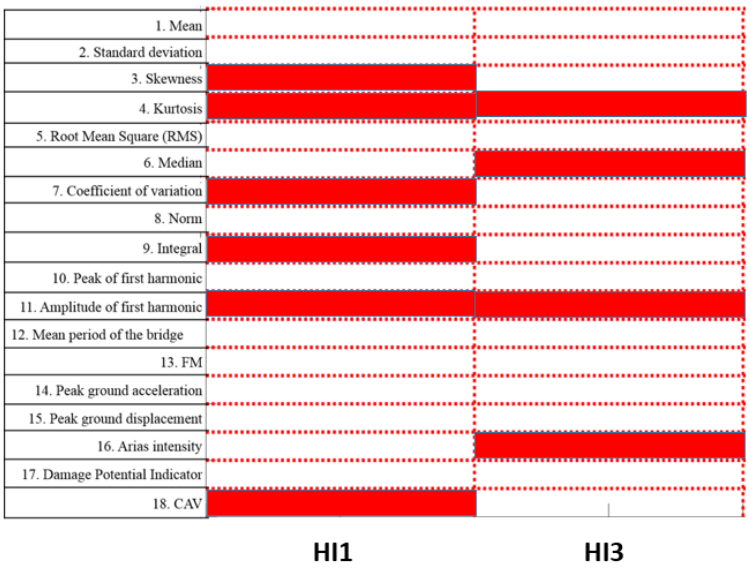

Figure 4-13. *Selected HIs by using the optimization algorithm for bridge condition monitoring and damage diagnostics*

4.5.3.3 **Results of the proposed methodology for bridge condition monitoring and damage diagnostics**

The unlabelled data of group C are used to verify the accuracy of the proposed methodology. The acceleration of the bridge of group C are used in the methodology in the chronological order, i.e. the 7 minutes of acceleration of the healthy bridge (class 1), followed by the 7 minutes of acceleration of class 3, etc. In this way, the real-time monitoring of the bridge is simulated. A dataset of 70 values for each optimal HI is used to assess the performance of the NFC. The accuracy of the methodology is assessed by comparing the health state of the bridge assigned by the NFC with the real bridge health state.

Table 4-2 shows the results of the accuracy of the NFC as a condition monitoring and diagnostic tool. The overall accuracy of the NFC is 78.3%, i.e. 78.3% of the considered scenarios of group C are correctly identified by the proposed NFC. The lowest accuracy of the NFC is obtained for class 3 and 5, i.e. the fully cut of the pier, and when the pier is fully cut, and the deck is settled 2 cm lower of its starting position, respectively. The fully cut of the bridge pier (class 3) is correctly recognized with 66.67% accuracy, and as a result 37.4% of class 3 scenarios are misclassified as class 4 scenarios. Class 5 is misclassified 41.6% of times to be either class 3 or class 6. Therefore, the NFC is able to identify the damage of the bridge structure, however,

some misclassifications of the nature of the damage are shown due to small changes of the bridge structural behaviour during these scenarios, i.e. a small loss of stiffness of the bridge, as pointed out by the modal analysis of the bridge by [Siringoringo et al., 2013].

Table 4-2 suggests that the proposed NFC can be used as both bridge condition monitoring and damage diagnostic tool, in order to identify anomalies in bridge behaviour and point out their causes. In fact, the accuracy of identifying the presence of the damage is higher than 90% (class 1), whereas the nature of the bridge damage is correctly identified 75% of times (average of results for classes 3 and higher).

Table 4-2. *Accuracy performance of the NFC for bridge condition monitoring and damage diagnostics*

Case study	Overall accuracy	Class 1	Class 2	Class 3	Class 4	Class 5	Class 6
Condition monitoring and diagnostics	78.3%	91.67%	n/a	66.67%	83.33%	58.34%	91.67%

4.6 Influence of the size of bridge behaviour data and of the HIs set on the performance of the NFC

In this section, the post-tensioned concrete bridge of presented in section 4.3.1 is analysed by using the NFC approach where a set of four HIs is considered. Particularly, the NFC is applied to each class of the bridge health state that has at least 20 minutes of data, and consequently, the data of class 1 (healthy bridge), class 3, 4, 5, 6 and 7 are used to train, test and validate the NFC in this section. In this way, the influence of different amount of data on the performance of the NFC is investigated. At the same time, the whole set of HIs is used as an input to the NFC, with the aim of assessing how a different set of HIs influences the performance of the NFC.

The data of the bridge health states are divided into the three groups of section 4.5.3 and are used as an input to the proposed data analysis methodology to assess the HIs, which are then used as input to the NFC.

In what follows, the influence of the size of the HIs set on the performance of the NFC is investigated in section 4.6.1, where how the size of the bridge behaviour data influences the NFC performance is analysed in section 4.6.2.

4.6.1 NFC performance analysis by using the whole set of bridge health states and HIs

The data of group 1 are used to train the NFC in a supervised manner, with a number of clusters equal to the number of classes (6), which is kept constant during the analysis. The optimal value of τ and τ^* needs to be identified due to the fact that a different set of data (which consists of all classes of bridge behaviour) is analysed. At the same time, a new HIs selection process is performed to identify the optimal subset of HIs that allows to monitor the health state of the bridge in a reliable way (section 4.6.1.1). The health state of the bridge is monitored by the means of the selected subset of HIs (section 4.6.1.2).

4.6.1.1 HIs selection process

The parameters τ and τ^* are optimized during the NFC training process: the HIs of the data in group 1 are used as an input to the NFC by modifying either τ or τ^*, as shown in Figure 4-14. When τ^* is equal to 20 τ, the NFC shows higher and more stable accuracy for varying values of τ. The highest accuracy is achieved when τ is equal to 3 seconds, which is chosen as the optimal τ. The optimal values of τ^* and τ are then used for the HIs selection process, to train the NFC with a dataset of 108 values of each HIs and to monitor the health state of the bridge.

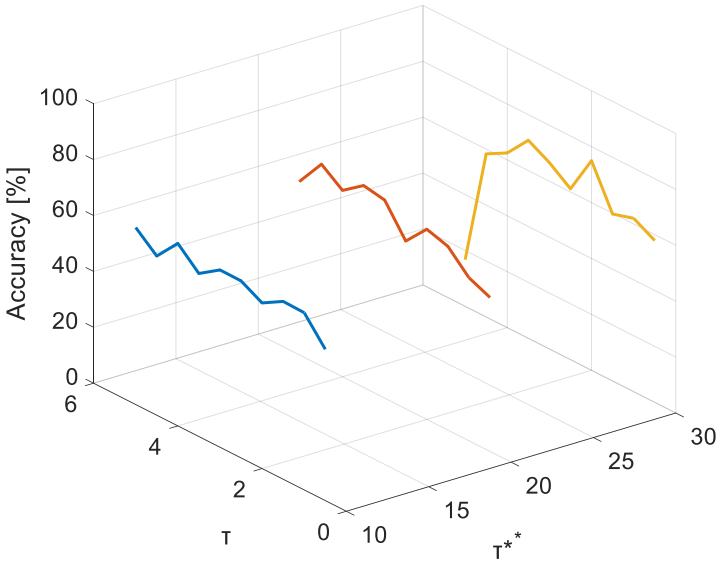

Figure 4-14. *NFC accuracy values at varying τ and τ**

The selection process of the HIs is carried out by adopting the MBDE optimization algorithm. A dataset of 30 values for each HIs is used for the HIs selection process. The iterative process of the MBDE terminates when a maximum number of 5000 iterations is reached. The MBDE parameters (weighting factor and control parameter, as shown in Appendix A) are kept constant to the previous analysis, and are equal to 0.8 and 0.3 respectively, whereas 5000 iterations are chosen as trade-off between the high computational-time required by the MBDE and the number of iteration performed. A higher number of MBDE iteration, with respect to the analysis of section 4.5.3, is chosen in order to take account of the increased set of HIs.

The evolution of the inverse of the fitness function is depicted in Figure 4-15. The dotted line in Figure 4-15 shows the improvement in the performance of the NFC during the testing phase: the accuracy of the NFC during the first iteration of the MBDE, when the subset of HIs is randomly selected by the MBDE, is equal to 27%, whereas at generation 5000 it is equal to 76%, due to the MBDE search that is able to select the possible optimal HIs. Furthermore, the dotted line in Figure 4-15 shows a rapid increase of the NFC accuracy during the first 1100 iterations, which is followed by a 3000 ca. iterations that do not improve the accuracy of the NFC. This result can be due to the definition of the MBDE parameters, that lead the optimization research into a local minimum of the fitness function. The local minimum is erroneously identified as a global minimum of the MBDE fitness function, and the population of the selected HIs is slightly modified during these iterations. However, at iteration 4000 the MBDE is able to leave the local minimum, and the NFC accuracy increases accordingly.

The accuracy of the NFC during the supervised training phase is always close to 98%. This latter performance of the NFC can be explained by considering the fact that, for each subset of HIs chosen by the MBDE, the NFC is able to set the value of its parameters in order to optimize the classification of the data during the training phase. The optimal subset of HIs is identified during the testing phase, as shown in Figure 4-16. The optimization algorithm, which is implemented in Matlab, requires 3 hours and 40 minutes to be completed by using an Intel core i3-4130 with CPU @ 3.4Hz. It should be noted that, despite an increase of the number of iteration of the MBDE, the accuracy of the NFC during the testing process is lower than the performance shown in section 4.5.3.2. Furthermore, the increase of the maximum number of generation,

the size of the bridge behaviour and the set of HIs leads to an increase of the computational time of the MBDE.

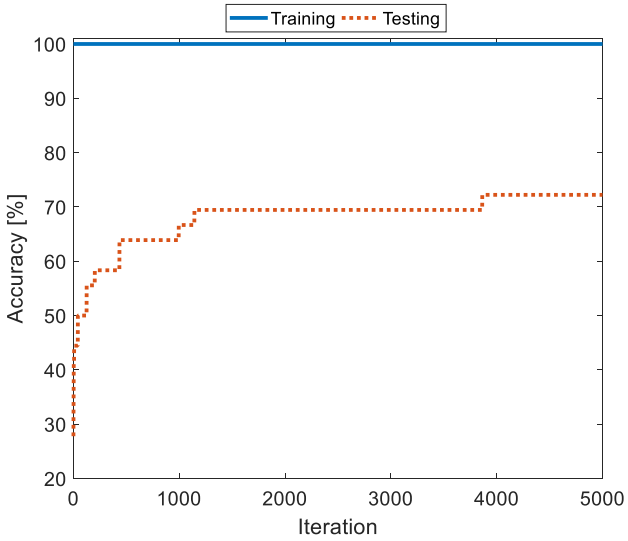

Figure 4-15. *Evolution of the fitness function during the HIs selection process*

Figure 4-16 shows the subset of selected optimal HIs. HI_3 is the most selected HI by being selected for 8 features (out of 18). This result is expected as discussed in section 4.3.6. In addition, HI_4 is the second most selected HI by being selected for 7 features, whereas HI_2 and HI_1 are selected for only 4 features each. The set of the 72 HIs is represented by 2^{72}-1 possible combinations, and as a result the MBDE might not have reached the best subset of HIs due to the large number of possible combination of the HIs. The subset of HIs of Figure 4-16 is used to verify the proposed methodology in analysing unknown and unlabelled data of the bridge behaviour in order to investigate how the increased number of HIs and bridge health states influences the performance of the NFC.

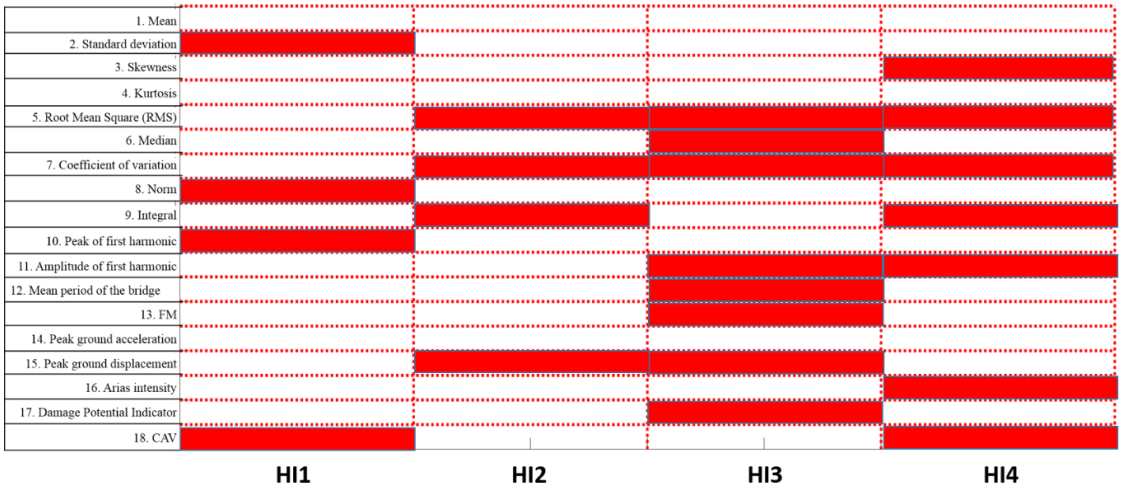

Figure 4-16. *Selected HIs by using the optimization algorithm for bridge condition monitoring and damage diagnostics*

4.6.1.2 Performance of the NFC by analysing the whole set of HIs for bridge condition monitoring and damage diagnostics

The unlabelled data of group 3 are used to verify the accuracy of the NFC. A dataset of 78 values for each optimal HI is used to assess the performance of the NFC. The accuracy of the methodology is assessed by comparing the health state of the bridge assigned by the NFC with the real bridge health state.

Table 4-3 shows the results of the accuracy of the NFC as a damage detection and diagnostic tool. The overall accuracy of the NFC is equal to 72.2%, i.e. 72.2% of the considered scenarios of group 3 are correctly identified by the proposed NFC. The lowest accuracy of the NFC is obtained for class 1 and 6, i.e. the healthy state of the bridge and when the pier is fully cut, and the deck is settled 2.7 cm lower of its starting position, respectively. The healthy state of the bridge (class 1) is correctly recognized with 66.6% accuracy, and as a result 37.4% of the healthy scenarios are misclassified as damaged scenarios. Class 6 is misclassified to be class 3. The misclassification of class 6 is not straightforward to explain due to the fact that class 6 represents a scenario in which the pier of the bridge is completely suspended, whereas class 3 represents a scenario in which the pier is completely cut but not suspended. Therefore, the structural behaviour of the bridge is expected to be different in these two scenarios. The misclassification of class 6 can be caused by both non-optimal HIs and small changes of the structural behaviour of the bridge.

It should be noted that, although an accuracy equal to 72.2% is lower than the NFC accuracy of the previous section, it is similar to (or higher than) other similar machine learning methods that have been presented in literature, as discussed in section 4.7.

Table 4-3. *Performance of the NFC for bridge condition monitoring and damage diagnostics*

Case study	Overall accuracy	Class 1	Class 2	Class 3	Class 4	Class 5	Class 6	Class 7
Condition monitoring and diagnostics	72.2%	66.6%	n/a	83.3%	100%	100%	0%	83.3%

4.6.2 NFC performance analysis by using the damage health state of the bridge and the whole set of HIs for damage characterization

The accuracy of the NFC in identifying the correct nature of the bridge damages is higher than 83.3%, (except for class 6), as shown in Table 4-3. Hence, the NFC can be used as a damage characterization tool, in order to point out the nature of anomalies in bridge behaviour. The diagnostic analysis of the damage of the bridge is of particular interest, due to the fact that previous studies of the same post-tensioned concrete bridge have shown that damages of the bridge can be detected, but the identification of the damage nature is challenging due to similar modal behaviour of the bridge during the different damage scenarios [Siringoringo et al., 2013; Moughty & Casas, 2017]. The damage characterization analysis requires to perform the training phase of the NFC again, in order to set the NFC parameters by considering only the damage classes, i.e. without considering the healthy state (class 1) of the bridge. Hence, the training and testing phases of the NFC are carried out by considering only the damage scenarios of the bridge behaviour of group 1 and 2, respectively. τ, τ^* and the parameters of the MBDE are kept constant, in this way we assess the ability of the NFC in diagnosing the nature of the bridge damage, without changing any parameters in the methodology. The performance of the NFC as damage characterization method is discussed in the following sections.

4.6.2.1 HIs selection process

Figure 4-17 represents the optimal subset of HIs that is selected by the MBDE for the diagnostics process, which is very different from the optimal set of Figure 4-16.

HI_1 is the most selected HI, followed by HI_2, whereas HI_3 and HI_4 are chosen only to represent three and two features, respectively. The number of HIs that belong to the optimal subset is also different: for the damage characterization case study 18 HIs represent the optimal subset, whilst 23 HIs represent the optimal subset for the damage detection and diagnostics case study. The different subset of optimal HIs is due to the different case study being considered.

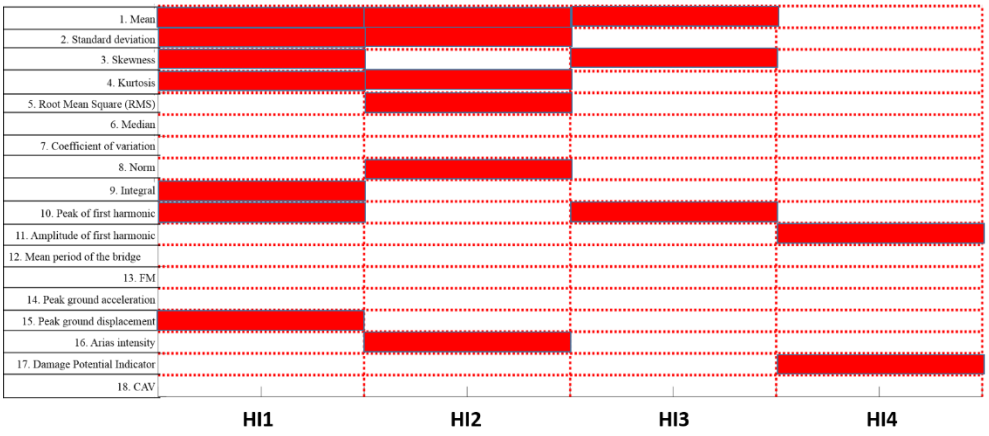

Figure 4-17. *Selected HIs by using the optimization algorithm for bridge damage diagnostics*

4.6.2.2 **Performance of the NFC by analysing the whole set of HIs for bridge damage characterization**

The unlabelled data of the damages of group 3 are used as an input to the methodology, in order to automatically characterize the nature of a bridge damage by the means of the NFC. Table 4-4 shows the accuracy of the NFC in diagnosing the nature of the bridge damage. The overall accuracy is equal to 85%: 3 out of 5 classes (class 3, 4 and 7) of the bridge damage are correctly identified all the time, whilst class 5 is correctly identified with an accuracy of 75% and class 6 with an accuracy of 50%. The analysis of the misclassifications points out that class 5 is misclassified as class 3, and class 6 as class 4. The misclassifications can be explained due to a low change of the bridge structural behaviour between the two classes.

The accuracy of the NFC in this case study outperforms the accuracy of the previous sections. This result can be explained by pointing out that when only the damage scenarios of the bridge are analysed, the proposed data analysis methodology provides HIs values of the damage scenarios that are different from each other. Furthermore, as the healthy state is not considered in the damage characterization analysis, the

misclassifications of the healthy state that the NFC showed in section 4.6.1.2 are not present.

Table 4-4. *Performance of the NFC for damage characterization*

Case study	Overall accuracy	Class 1	Class 2	Class 3	Class 4	Class 5	Class 6	Class 7
Diagnostics	85%	n/a	n/a	100%	100%	75%	50%	100%

4.7 Summary of the NFC

The NFC for bridge elements condition monitoring and damage diagnostics showed a good accuracy in identifying and diagnosing the damages of the bridge structure automatically. It should be noted that an overall accuracy that ranges from 72.2% to 85% is a good result in assessing the health state of an in-field bridge, due to the unknown source of uncertainty and changing environmental conditions. Indeed, similar machine learning methods, which are based on ANNs and verified on FEMs by adding white Gaussian noise to the simulated bridge behaviour, have shown an average accuracy of 65% [Shu et al., 201352; Zhou et al., 2014; Yeung et al., 2005], whereas clustering techniques, which were verified on in-field bridges, have shown an average accuracy of 68%, with a maximum accuracy of 75% [Alves et al., 2016]. At the same time, [Siringoringo et al., 2013] performed a modal analysis of the bridge during each health state of the bridge, and showed that the modal parameters of the bridge are slightly modified by the first inflicted damages (class 2 to class 5), whereas the most severe damage (class 6) modified the modal parameters of the bridge significantly, and, as a consequence, it is possible to identify such a damage clearly, and the accuracy for class 6 is high.

The performance of the NFC strongly depends on the quality and amount of data available for the training process, which is limited in this case study. As a consequence, the performance of the proposed NFC is expected to improve by increasing the size and quality (in terms of different behaviour of the bridge) of the training (group A), testing (group B) and validation (group C) sets. At the same time, as the size of data of the bridge behaviour and the set of HIs increases, the time required to identify the optimal set of HIs increases, due to the increases of the set of possible optimal solutions of the optimization problem. Therefore, a balance between the amount of data and the

size of the HIs set needs to be reach in order to guarantee robust results without being penalizing by large computational time of the analysis.

The NFC approach is proposed in this thesis as a possible method to assess the health state of the bridge elements automatically, and then use such information as an input to the BBN. Due to the limited amount of data that is available in this case study, in the remaining of this thesis the data analysis approach of section 4.2 is used to process the raw bridge behaviour with the aim of identifying the health state of the bridge elements. The main drawback of the NFC is that it requires a large amount of data for the training and testing processes, and, as a result, it can be used in case study with large amount of data. Furthermore, the bridge behaviour for different health states of the bridge is required to adequately train the NFC. Such data are not usually available, and the NFC is only able to identify and diagnose available bridge damages, i.e. the damages of the bridge whose behaviour is available within the training data set. However, the larger the availability of the data, the more accurate the results provided by the NFC, due to its learning ability.

4.8 Application of the proposed data analysis methodology to an in-field steel truss bridge

4.8.1 Introduction

In this section, the proposed data analysis methodology to process the raw bridge behaviour and assess the health state of the bridge is applied to an in-field steel truss bridge. The bridge is subjected to a progressive damage test that aims to study the bridge behaviour during different health states of the bridge. The bridge is excited by a moving vehicle that runs over the bridge at almost constant speed throughout the test. Three runs of the vehicle for each health state of the bridge are available, and thus a very limited amount of data is available in this case study. Despite the limited availability of data of the bridge behaviour, the proposed data analysis methodology is able to point out the different health states of the bridge. Finally, it should be mentioned that the machine learning approach that relies on the NFC is not applied to this case study due to the limited amount of data.

The steel truss bridge is described in section 4.8.2, and the steps of the proposed method for analysing the bridge behaviour are presented in the following sections.

4.8.2 **Description of the steel truss bridge and the progressive damage test**

A simply-supported steel Warren truss bridge is considered in this analysis. The length of the bridge is 59.2 m, with 3.6 m width and 8 m of maximum height, as shown in Figure 4-18 [Chang & Kim, 2016]. The bridge was demolished in 2012. However, progressive damage tests were carried out while the bridge was closed to the public in order to develop a dataset of bridge behaviour under changing health states of the bridge. The dynamic behaviour of the bridge was collected by 8 accelerometers, denoted as A_i (i = 1, 2, …, 8) circles in Figure 4-18, whose sample rates was equal to 200 Hz. Five different health state classes of the bridge were analysed by damaging the bridge infrastructure progressively (Figure 4-18): *i)* intact bridge scenarios, with no damage of the bridge infrastructure (healthy bridge); *ii)* a half cut of the mid-span vertical member (DMG1); *iii)* a complete cut of the mid-span vertical member (DMG2); *iv)* retrofitted scenarios in which the cut of the mid-span vertical member is repaired (RCV, retrofitted); *v)* a complete cut of the vertical member at 5/8th span (DMG3). The data of the bridge behaviour during the five health states are analysed in two separated groups: *a)* the first group (group A) considers the intact bridge scenarios (healthy), followed by DMG1 and DMG2; *b)* the second group (group B) consists of the data of the bridge during the retrofitted and the DMG3 scenarios. The separation between the two groups is assumed due to the repair of the bridge damage that retrofits the bridge to a healthy state after DMG2. Indeed, the repair of the bridge after DMG2 considers that the damage scenarios of the bridge are identified, and maintenance actions are taken on the bridge. Finally, the scenarios of the bridge are analysed by considering the chronological order of the events, i.e. the healthy scenarios are the first data to be used as an input to the data analysis methodology, followed by DMG1 and DMG2 data, respectively, etc. In this way, the evolution over time of the bridge health state is considered.

For each health state, the vehicle used for the experiment was a two-axle vehicle, with a total weight of about 21kN. The vehicle was driven across the bridge three times for each scenario at a speed ranging from 36 to 41 km/hr to induce excitation.

The acceleration of the bridge is recorded by the 8 sensors and used as an input to the proposed data analysis method.

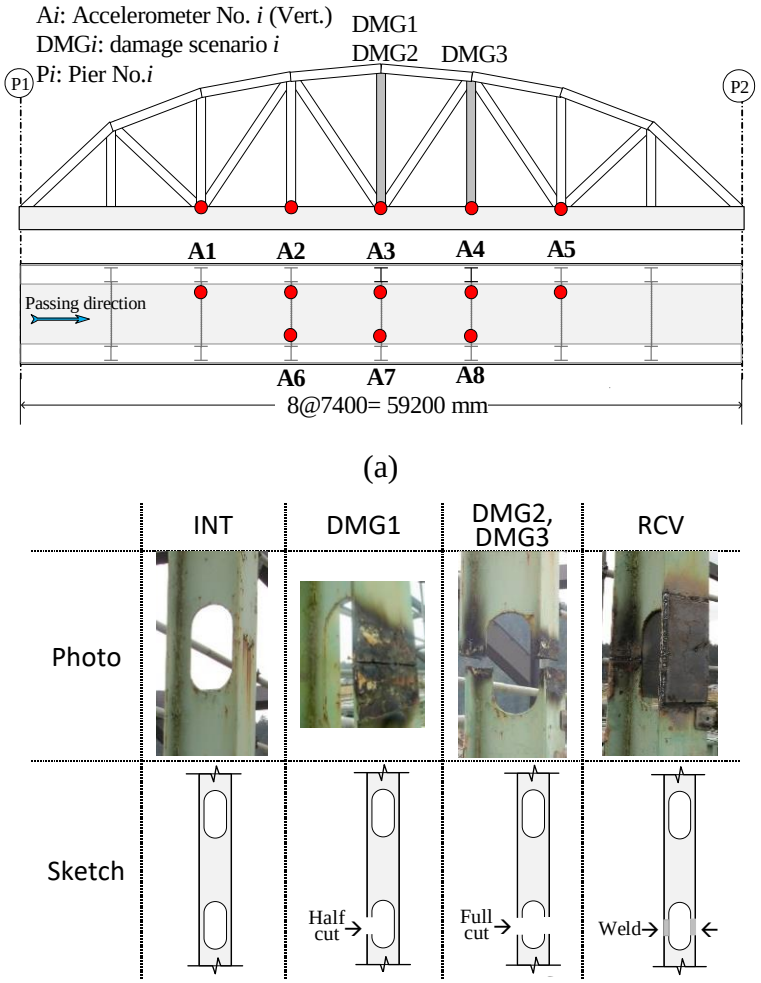

Figure 4-18. *The truss steel bridge*

4.8.3 Step 1 and 2 - Data cleansing and free-vibration bridge behaviour identification

An example of the raw data of the bridge acceleration is shown in Figure 4-19. The acceleration is quite smooth without showing outliers. Therefore, the median filtering statistical process, which is applied to the acceleration data, do not correct any outliers. The second step of the methodology is the identification of the free-vibration of the bridge, in order to assess the health state of the bridge without considering the influence of the vehicle running over the bridge. In this case study, the nature of the bridge excitation is known (the vehicle that runs over the bridge), and such information can be used to identify the free vibration of the bridge by knowing the vehicle speed and the time when the vehicle approached the bridge, as shown in Figure 4-19. In a similar way, the free-vibration of the bridge can be identified also by recognising the maximum values of the acceleration and then analysing the decreasing bridge acceleration that follows the maximum values of the acceleration.

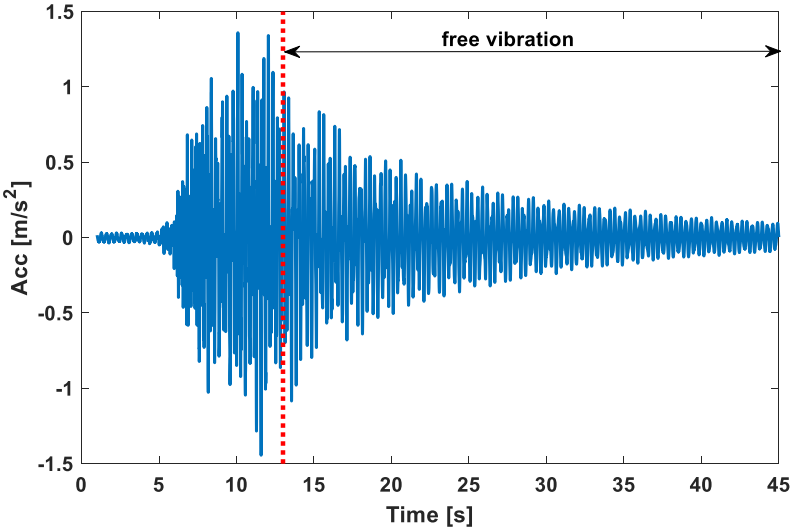

Figure 4-19. *Bridge acceleration and free vibration identification*

4.8.4 **Step 3 - Feature extraction**

The free-vibration of the bridge gathered from the 8 sensors consists of 1600 data points for each second (8 sensors, with a sampling rate of 200 Hz), and as a consequence large data storage capacity and high computation power are required to efficiently store and analyse such amount of data. Conversely, the dimension of the bridge behaviour data can be reduced into more valuable information, with respect to the bridge health state, by extracting informative features from the raw acceleration data. Therefore, the 18 features of section 4.2.4 are extracted from the bridge acceleration every τ seconds, by reducing the dimensionality of the data from 1600 • τ to 144 (18 features • 8 sensors), i.e. every τ seconds the 18 features are evaluated for each sensor and stored in order to monitor the evolution of the bridge condition over time. In this case study, τ is equal to 2 seconds, and consequently 3200 values are lumped into 144 values, which are updated every 2 seconds. The value of τ is optimized by maximizing the GI of the bridge HIs, as shown in Figure 4-20 and discussed in the next section.

Without loss of generality, Figure 4-20 shows 1 of the 18 features that is evaluated for the free vibration acceleration of the bridge during the five health states experienced by the bridge. The Mean period of the bridge behaviour (T_m) is depicted in Figure 4-20. It should be noted that the feature is noisy, by presenting a high level of oscillations, and furthermore it is not possible to identify the different health states of the bridge due to the fact that the magnitude of the features is equal throughout the monitored period. As a consequence, a robust and reliable assessment of the bridge

condition can be threatened by the oscillating behaviour of the feature. For this reason, a further step of data processing is introduced by using the EMD, in order to retrieve the trend of the feature, and, thus, to assess the health state of the bridge in an accurate way.

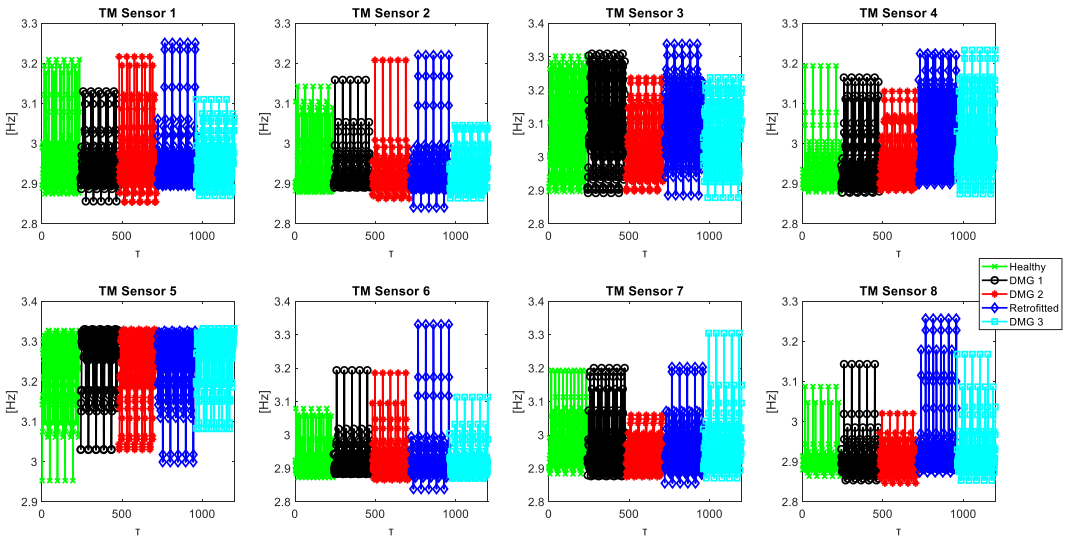

Figure 4-20. *Example of features extraction*

4.8.5 Step 4 and 5- Feature trend, Health Indicators (HI) definition and selection

The features extracted in an interval [0, τ*] are used as an input to the EMD process, i.e. the values of each feature in the interval [0, τ*] are used to assess the feature trend. The interval [0, τ*] is chosen to monitor the health state of the bridge continuously, and as a result the trend of the features is updated each time τ* new features are extracted from the free-vibration of the bridge. The trend of the features is then lumped into the 4 HIs of the bridge health state, presented in section 4.3.6. The value of τ and τ* is optimized by looking for the maximum value of the GI. Figure 4-21 shows the variation of the maximum value of GI when τ and τ* are modified between [0, 2] sec and [10, 20] τ, respectively. The interval of variation of τ and τ* are chosen by considering the amount of data available, which is very limited in this case study and thus it requires to consider small interval for both the feature extraction and the feature trend assessment. The two groups of data, i.e. group A and B, are analysed separately, however the GI value is maximized by taking account of both groups in order to identify the optimal values of τ and τ* and point out the optimal HIs that allow to assess the health state of the bridge in a reliable manner. As a result, the maximum value of

GI is equal to 4, i.e. the monotonicity and trendability of the two groups are summed into the GI. Figure 4-21 shows that the maximum value of GI is reached when τ = 2 sec and τ^* = 20 τ, which are chosen as optimal values. The HI that allows to obtain the maximum value of GI is the HI_3 of the Mean period of the bridge behaviour (T_m), as shown in Table A. 1.

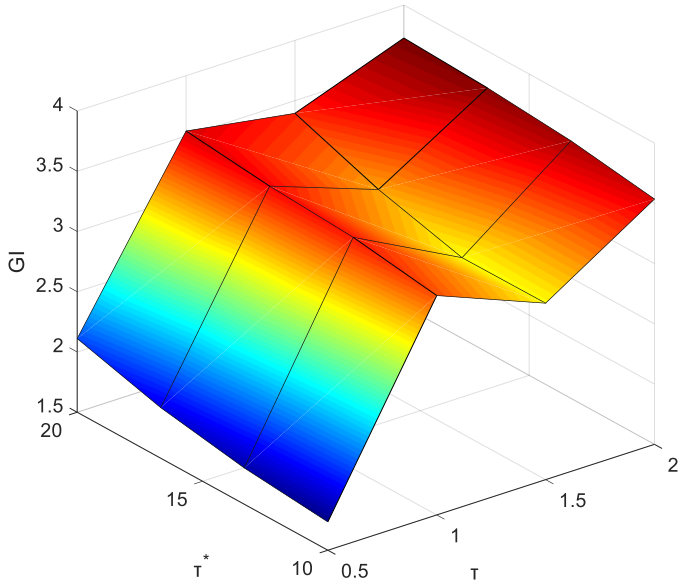

Figure 4-21. *GI values at varying τ and τ**

Table A. 1. Optimal HIs to assess the health state of the steel truss bridge

Optimal HI	**GI**
HI_3 of the mean period of the bridge behaviour (T_m)	3.5811

Figure 4-22 shows that the HI_3 of T_m for both groups of data is able to point out clearly the different health states of the steel truss bridge for both groups of data, i.e. each damage scenario of the bridge (DMG1 and DMG2 of group A, and DMG3 of group B) is identified by the optimal HIs, due to an increase of its value with respect to the healthy (retrofitted) value of the HI. The HI_3 of T_m allows to identify the location of the damages: the maximum value of the HI is shown by sensor 5 and sensor 3 for damages DMG1 and DMG2, which are installed at the damage location, whereas the maximum value for damage DMG3 is shown by sensor 4 that is exactly the location where the cut of the vertical element is applied.

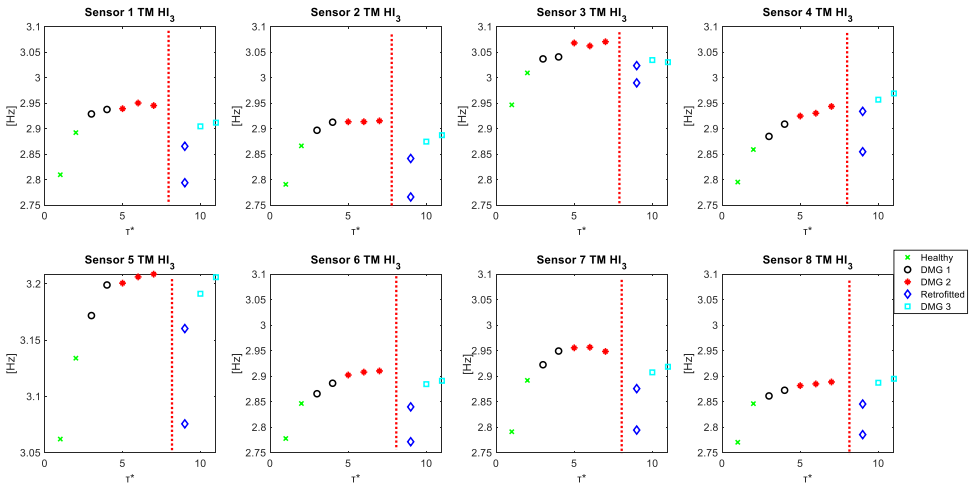

Figure 4-22. *Evolution of the optimal HIs*

4.8.6 Summary of the application of the proposed data analysis methodology to an in-field steel truss bridge

The proposed data-driven methodology allows to monitor the health state of the steel truss bridge by analysing its vibration behaviour. The optimal HI is identified by optimizing the value of the GI and is able to point out the different health states of the bridge by showing a monotonic behaviour. The optimal HI is able to point out the magnitude and the location of the bridge damage. Some of the proposed features rely on the analysis of the vibration behaviour of the bridge, and thus when a different bridge behaviour is monitored, such features cannot be extracted from the available data. Therefore, the proposed methodology needs to be modified in order to extract appropriate features. Similarly, the set of HIs can be improved by defining other statistical parameters of the feature trend: e.g. the trendability and monotonicity of the feature trend can be used directly as HIs rather than using them only to select the optimal HIs among the HIs set.

4.9 Summary

The proposed data-driven methodology is able to monitor the health state of in-field bridges by relying on the data analysis of their vibration behaviour. Statistical, frequency-based and vibration-based features are extracted from the data, and the trend of these features is assessed by the means of the EMD approach. A set of HIs of the bridge are evaluated by computing four statistical parameters of the features trend. The optimal HIs, which allow to assess the health state of the bridge elements by the means

of a monotonic behaviour that increases/decreases according to the degradation of the bridge elements, are identified by optimizing the value of a GI.

The proposed methodology is able to provide optimal HIs to clearly identify the different health states of the bridge elements, and such information can be used as an input to the BBN nodes to assess the state of the BBN nodes in a reliable manner. As a consequence, the BBN can assess the health state of the whole bridge, by taking account of the health state of each element of the bridge, by monitoring the optimal HIs that allow to point out the changing health state of the bridge.

The proposed methodology shows some drawbacks:

1. The vibration features that are extracted from the bridge behaviour can be assessed only when the vibration behaviour of the bridge is monitored by the measurement system. Hence, if other behaviour of the bridge is monitored, the methodology needs to be modified accordingly, by computing different features of the bridge behaviour.
2. The feature trend is lumped into four HIs, which do not represent the optimal set of HIs for monitoring the health state of any bridge. In fact, other statistical parameters (such as the trendability and monotonicity of the feature trend) of the feature trend can be used in order to monitor the health state of the bridge in a reliable and effective manner.
3. The optimal values of τ and τ^* and the optimal set of HIs depend on the case study and the available data, and, as a result, an optimization process needs to be carried out in order to point out the optimal value of these parameters for each case study.

The information provided by the proposed data analysis methodology, by using the HIs can be used as an input to a machine learning method, in order to identify the health state of the bridge elements automatically. The proposed NFC showed a good accuracy in identifying and diagnosing the damages of the bridge structure automatically. However, the NFC shows some drawbacks:

- The performance of the NFC relies on the quality and amount of data available for the training process, which need to be as high as possible, in order to train the NFC with lot of data of different behaviour of the bridge.
- The set of possible HIs is identified by applying the MBDE algorithm, whose computational time increases when the set of possible optimal solutions of the optimization problem increases.

The NFC approach is proposed in this thesis as a possible method to automatically asses the health state of the bridge elements, and then use such information as an input to the BBN. Due to the limited amount of data that is available in this case study, in the remaining of this thesis the data analysis methodology of section 4.2 is used to process the raw bridge behaviour with the aim of identifying the health state of the bridge elements.

In what follows, the optimal HI is used to define the CPTs of the BBN of the bridge, by merging the expert judgement analysis with the analysis of the bridge behaviour in order to define reliable CPTs.

Chapter 5 CPTs updating method by merging expert judgment and bridge behaviour analysis

5.1 Introduction

The CPTs represent the quantitative part of the BBN and allow to define the dependencies between connected nodes of the BBN, by using conditional probabilities. The analysis of bridge behaviour, if a database of information about the past behaviour of the bridge is available, or an expert elicitation process, if such database is unavailable, can be used to define the CPTs. In Chapter 3 the latter approach has been used to define the CPTs of the BBN by interviewing three experts. However, the results of the BBN analyses in Chapter 3 showed that the diagnostic performance of the BBN was limited. Therefore, an increase of the BBN diagnostic performance is expected when the CPTs are defined in a more accurate manner, by using the bridge behaviour data to assess the influences between different elements of the bridge. For this reason, an approach to update the CPTs by merging the expert elicitation process, which allows to define the CPTs at first, with the analysis of the bridge behaviour is proposed in this thesis. The proposed method requires the availability of bridge behaviour data for different known health states of the bridge elements, in order to assess the dependencies between different bridge elements, using CDFs.

However, when a database of behaviour of the infrastructure is analysed, the infrastructure health state is not always known a-priori. As a consequence, a method to analyse the database of infrastructure behaviour is also proposed in this chapter with the aim of identifying the point when the health state of the infrastructure changes. At the same time, the characteristics of this change, in terms of change duration and possible causes, are pointed out.

In what follows, the method to define the CPTs by merging the expert judgement elicitation process and the analysis of the bridge behaviour is presented in section 5.2. The proposed method is applied to the presented post-tensioned bridge in section 5.3, and the results of the method for updating the CPTs are summarized in section 5.4.

The method to analyse the database of the infrastructure behaviour to point out changes of the infrastructure behaviour is presented in section 5.5. Finally, a summary of the chapter is given in section 5.6.

5.2 The method to merge expert judgment and bridge behaviour analysis

The CPTs of a BBN are usually defined by using an expert elicitation process, due to a lack of system behaviour data. However, when a large database of the system behaviour are available, the CPTs can be defined by analysing the system behaviour by the means of learning algorithms [Sun et al., 2006; Loughney & Wang, 2017]. When a limited amount of data of system behaviour is available, learning methods can show difficulties in defining the CPTs, and thus the use of both expert judgment and data analysis is required [Mkrtchyan et al., 2016]. In fact, the two approaches, i.e. the expert knowledge elicitation process and the system behaviour data analysis approach, are complimentary: the data of the system behaviour provide information about the current health states of the system, whereas the expert elicitation process is able to provide information about the behaviour of the system by relying on expert knowledge, that can analyse what if scenarios (such as assumed possible damaged scenarios). Therefore, in this thesis a method to merge the two approaches is proposed in order to define the CPTs in a robust and continuous manner, by using the systematic knowledge of bridge engineers and the measured behaviour of the bridge. The proposed method is depicted in Figure 5-1: *i)* the expert elicitation process is carried out in order to define the CPTs of the BBN of the bridge. This analysis is performed before using the BBN to monitor the health state of the bridge (i.e. off-line analysis), as discussed in section 3.3.2; *ii)* an off-line analysis of a database of bridge behaviour is used in order to evaluate the CDF that models the relationship between different elements of the bridge by the means of the optimal HI. The analysis of the optimal HI is used to define the CDF of the influences between different bridge elements due to its ability in monitoring the health state of the bridge elements (as discussed in section 4.2); *iii)* when a new measurement of the bridge behaviour is available during the on-line monitoring of the bridge, the CPTs are updated by taking account of the current health state of the bridge elements, and merging the expert judgement with the analysis of the bridge data. Figure 5-1 shows the two steps of the proposed method for updating the CPTs of the BBN: *a)* an off-line process, which is depicted within the dotted box in Figure 5-1, that aims to initially define the CPTs by using the expert knowledge

elicitation process, and to identify the CDF of the optimal HI; *b)* an on-line process, which is depicted by the means of dashed boxes in Figure 5-1, that aims to continuously update the CPTs.

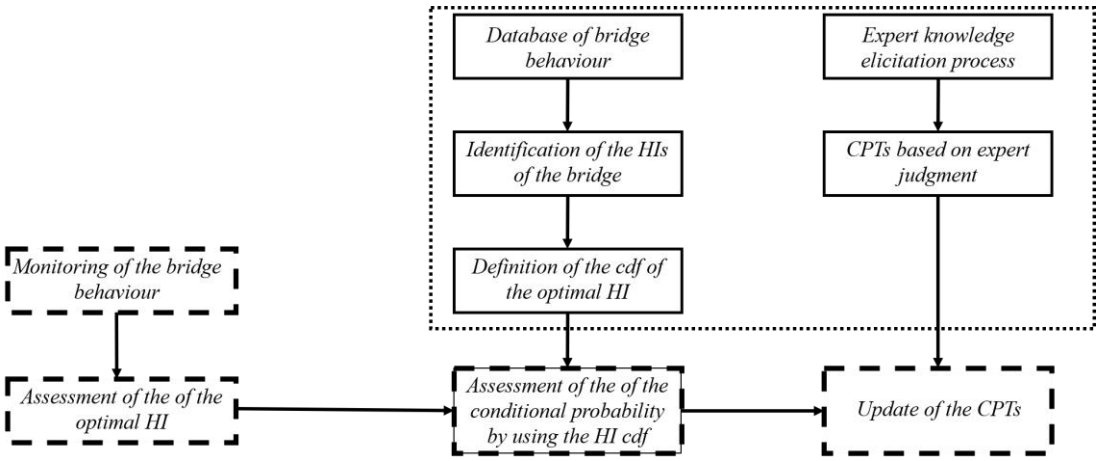

Figure 5-1. *Flowchart of the proposed method to continuously updating the CPTs*

The proposed method for merging the two approaches to define the CPTs is presented in section 5.2.1, whereas the analysis of the optimal HI that allows to evaluate the CPTs by relying on the analysis of the bridge behaviour is presented in section 5.2.2.

5.2.1 **The method**

The CPTs assess the conditional probability $P(x_i \left| Y^k = y_k \right.)$ of a child node *X* being in state x_i, with a condition that its parent nodes are in a condition y_k. $P(x_i \left| Y^k = y_k \right.)$, can be computed every time when a new measurement of the bridge behaviour is available, by taking account of the expert elicitation process and the bridge behaviour analysis as follows:

$$P(x_i \left| Y^k = y_k \right.) = \alpha P(x_i^{BA} \left| Y_{BA}^k = y_k^{BA} \right.) + (1-\alpha) P(x_i^{EJ} \left| Y_{EJ}^k = y_k^{EJ} \right.) \tag{5-1}$$

with the weight of the linear combination α that is evaluated by following equation:

$$\alpha = \frac{\#knownBridgeHealthState}{\#knownBridgeHealthState + 1}(1\text{-e}^{-\tau^*}) \tag{5-2}$$

Eq. (5-1) shows that the conditional probability that the child node *X* is in state x_i, with a condition that its parent nodes are in a condition y_k, is evaluated by a linear combination with weight $\alpha \in [0, 0.9]$, of the conditional probabilities assessed by analysing the bridge behaviour, $P(x_i^{BA} \left| Y_{BA}^k = y_k^{BA} \right.)$, and considering the expert knowledge elicitation process, $P(x_i^{EJ} \left| Y_{EJ}^k = y_k^{EJ} \right.)$. The process to assess the conditional probability, $P(x_i^{BA} \left| Y_{BA}^k = y_k^{BA} \right.)$, is presented in the following section, whereas the approach to compute the conditional probability $P(x_i^{EJ} \left| Y_{EJ}^k = y_k^{EJ} \right.)$ has been introduced in section 3.3.2.

Eq. (5-2) displays that the weight of the linear combination, $\alpha \in [0, 0.9]$, depends on both the number of the identified health states experienced by the bridge (which are labelled as $\#knownBridgeHealthState$) and the time interval $\tau *$ during which the bridge behaviour is monitored. In fact, the larger the monitoring interval of the bridge behaviour, the more reliable the assessment of $P(x_i^{BA} \left| Y_{BA}^k = y_k^{BA} \right.)$, and thus the higher the weight α of $P(x_i^{BA} \left| Y_{BA}^k = y_k^{BA} \right.)$. Conversely, the smaller the length of the monitoring time, the smaller the weight α and the higher the importance of $P(x_i^{EJ} \left| Y_{EJ}^k = y_k^{EJ} \right.)$. Furthermore, Eq. (5-2) shows also that the weight of the linear combination α increases when the number of known health states experienced by the bridge increases. In fact, the definition of α assumes that the knowledge acquired by analysing the bridge behaviour data can reach a saturation level, if different health states of the bridge are not monitored. This assumption is introduced to consider the ability of the expert knowledge elicitation process in investigating what-if scenarios, i.e. the scenarios in which the influence of a supposed damaged element of the bridge on the health state of other elements is evaluated. Indeed, although data analysis methods (such as Expectation Maximization) can estimate the value of the CPTs for missing data, when an off-line CPTs definition is carried out, a continuous CPTs definition requires a low computational-time approach. Consequently, the traditional data analysis methods for retrieving CPTs values from incomplete database might not be applied [Ji et al., 2015].

For example, Figure 5-2 depicts the evolution of α when the monitoring time $\tau *$ increases (where $\tau *$ can have the time unit of interest to the user). At the beginning of

the monitoring time, α increases due to the fact that new information about the bridge behaviour are available. The health state of the bridge is constant during this first time interval, and thus at time $\tau^* = 6$, α reaches a saturation level, due to a complete assessment of the information provided by the analysis of the bridge behaviour for this first bridge health state. At time $\tau^* = 9$, a change of the health state of the bridge is identified, and as a consequence, α increases due to the analysis of the bridge behaviour during a new, and previously unknown, health state of the bridge. As the monitoring time increases, α reaches a new saturation level at time $\tau^* = 12$, which is caused by the complete analysis of the two experienced health states of the bridge. Again, at time $\tau^* = 16$ a new health state of the bridge is identified, and consequently α increases.

It is worth noting that the definition of α relies on two assumptions: *1)* there is a new and unknown health state of the bridge that has not been experienced and analysed yet; *2)* the maximum value of α is equal to 0.9. This latter hypothesis is introduced in order to take account both the expert judgment and the analysis of the bridge behaviour during the continuous definition of the CPTs.

Finally, a conservative approach would consider α to be constant and as low as possible in order to give more weight to the expert knowledge. Therefore, later in Chapter 6 the influence of different strategies for defining α on the performance of the BBN is analysed.

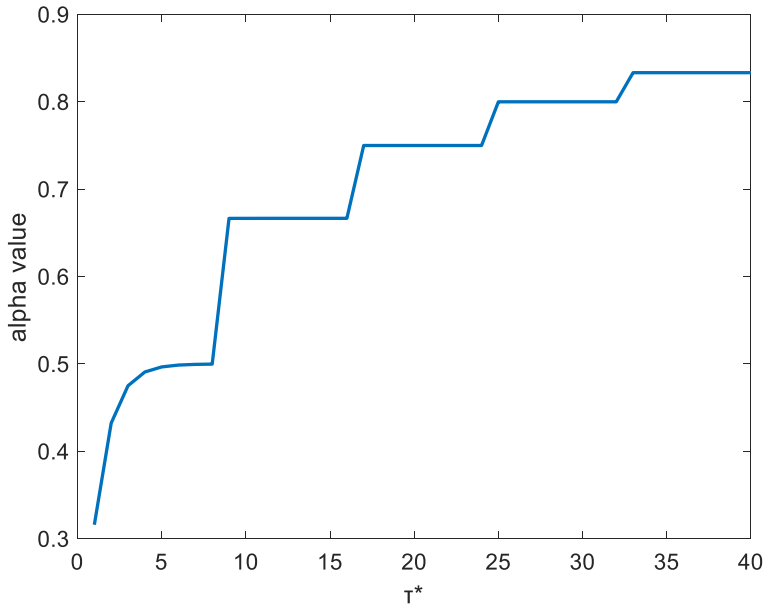

Figure 5-2. *Example of increase of the linear combination weight*

In what follows, the approach to calculate the conditional probability, $P(x_i^{BA} \middle| Y_{BA}^k = y_k^{BA})$, which relies on the analysis of the bridge behaviour is presented, with the aim of presenting the steps required to adopt the proposed approach to continuously update the CPTs.

5.2.2 The definition of the HI cumulative distribution function

The data analysis methodology introduced in Chapter 4 is able to find an HI to monitor the health state of a bridge element, by identifying different health states of the bridge elements. Hence, when a database of bridge behaviour is available, the proposed data analysis methodology can be adopted in order to retrieve values of the optimal HI during different health states of the bridge. In this way, the values of the optimal HI can be used to define the CDF of the HI, which describes the conditional probability, $P(x_i^{BA} \middle| Y_{BA}^k = y_k^{BA})$, that a bridge element x_i is influenced by the known health state of the monitored bridge element Y^k.

The CDF can be obtained by retrieving the probability density function (pdf) of the optimal HI. Generally, a pdf can be fitted to a set of data by using a parametric or non-parametric approach. The former requires the knowledge of the pdf nature, i.e. the assumption, that the HI are drawn from one of a known parametric family of distributions, is made. The latter does not assume the nature of the pdf of the HI but estimates the pdf by analysing the HI value and assuming only that a pdf of the HI exists, and it is differentiable [Silverman, 2018]. Furthermore, this latter approach requires more data than a parametric approach to estimate the properties of the pdf [Li & Racine, 2006]. Therefore, a parametric approach is selected in this thesis due to the limited amount of data available. The nature of the pdf of the HI is not known a-priori, and, as a result, a group of possible pdfs is considered in order to identify the pdf that fits the HI in the best manner. Three possible distributions (uniform, normal and Weibull) are considered in what follows. These distributions have been adopted in the past to study and model bridge degradation, even if with a very different aim of structural health monitoring [Frangopol et al., 2004; Le & Andrews, 2014; Saeed et al., 2017; Manafpour et al., 2018]. The process adopted to identify the CDF of the HI is depicted in Figure 5-3:

1) the three pdfs (uniform, normal and Weibull) are fitted to the available HIs that are retrieved by analysing a database of bridge behaviour data. A Maximum Likelihood Estimation (MLE) method is adopted to estimate the parameters of each distribution;
2) the goodness of the fitting is assessed by evaluating the performance of two criterion: *i)* the Akaike Information Criterion corrected (AICc) [Akaike, 1974; Burnham & Anderson, 2004]; and *ii)* the quantile-quantile (Q-Q) plot [Djurovic et al., 2000; Loy et al., 2016]. The two criteria are selected due to their ability in comparing different fitting models when a small dataset is used (AICc) and representing the goodness of each fitting model graphically (Q-Q plot);
3) the pdf that outperforms the others in terms of AICc (i.e. the pdf with the lowest AICc) and Q-Q plot is selected as a possible best available pdf;
4) the Kolmogorov-Smirnov test (K-S test) [Zeng et al., 2015] is adopted to verify if the available sample of HI data can be described by the selected best pdf. If the null hypothesis that the HI values belong to the selected pdf is not rejected, then the pdf is verified as optimal and its CDF is assessed. Otherwise, when the null hypothesis is rejected, the pdf with the second lowest value of AICc is tested by using the K-S test. This process is assumed to reliably identify a pdf to fit the HI data. In fact, a small difference of the AIC value between two possible pdfs can show some evidence that both pdfs perform a good fit [Burnham & Anderson, 2004].

The iterative process in Figure 5-3 is introduced due to the limited amount of data available for this thesis, which can lead to misinterpretation of the selected pdf. Therefore, the robustness of the pdf selection is expected to increase by evaluating the performance of three criteria to assess the goodness of the fitting process.

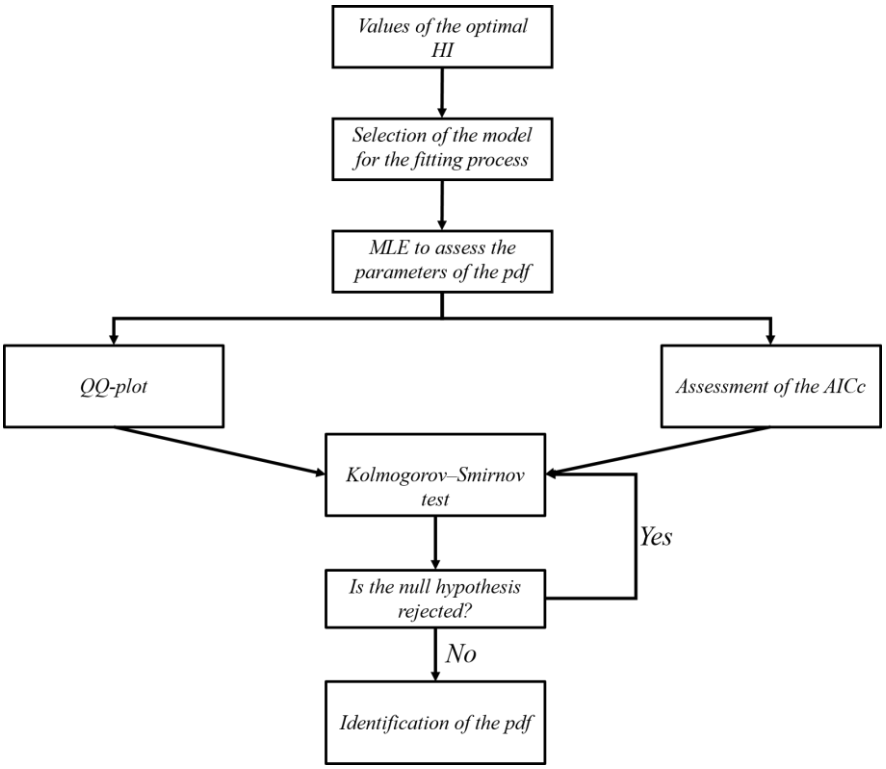

Figure 5-3. *Flow-graph of the method to identify the pdf that describes the optimal HI*

A wider group of distributions, which has been considered as a possible fit for the HI data, are presented in appendix B. The considered group of pdfs is not comprehensive, as 9 pdfs are considered. However, it should be noted that the aim of the method proposed in this chapter is to present a way to merge together the expert judgments with the knowledge acquired by analysing the bridge behaviour. Identifying the most suitable pdf to describe the HI falls outside the scope of this thesis.

In what follows, the three criteria are presented by describing the AICc in section 5.2.2.1, the Q-Q plot in section 5.2.2.2, and, finally, the K-S test in section 5.2.2.3.

5.2.2.1 **The AICc**

The Akaike Information Criterion (AIC) was introduced by Akaike [Akaike, 1974] with the aim of estimating the discrepancy between an unknown model, generating the data (i.e. the unknown model generating the HI data in this thesis), and a fitting model (i.e. the model that is a candidate to represent the unknown model). The AIC allows to rank the possible fitting models, by pointing out the model that best fits the available data, using the mean of the lowest AIC value. The AIC shows good performance in comparing the goodness of different fitting models when the size of the available data

is large. However, when only few data are available the AIC shows incorrect performance by usually choosing the model with the highest number of parameters [Burnham & Anderson, 2004]. Hence, the AIC corrected (AICc) can be introduced in order to take account of a low amount of data. Generally, AICc is recommended when $\frac{n}{k} < 40$, where n is the number of available data from the unknown generating model and k is the number of parameters of the fitting model (e.g. k= 2 for the normal distribution, where the mean value and the standard deviation need to be evaluated to represent the distribution) [Burnham & Anderson, 2004].
The AICc is defined as follows:

$$AICc = 2k - 2\ln(L) + \frac{2k^2 + 2k}{n - k - 1} \tag{5-3}$$

where k is the number of parameters of the fitting model, L the maximum likelihood of the fitting model and n the number of available data. The correction factor is represented by the last positive term of Eq. (5-3), which tends to zero as the number of available data increases.

Eq. (5-3) shows that AICs depends linearly on the number of parameters of the fitting model, k, and consequently, the higher the number of parameters of the fitting parameters the higher the value of AICc. Therefore, AICc aims to reward fitting models that are described by a low number of parameters.

5.2.2.2 **The Q-Q plot**

The Q-Q plot is probably the most commonly used graphical method to assess if a set of data belongs to a specified distribution. The Q-Q plot aims to plot the sorted data to be fitted, i.e. the data generated by the unknown model are sorted in an ascending order, against the expected quantile of the theoretical specified distribution [Loy et al., 2016]. Therefore, given a dataset of n values, e.g. the n values of the optimal HI in this thesis, a Q-Q plot can be constructed by: *i)* sorting the n values in an ascending order, i.e. from the smallest to the largest, in order to obtain the quantiles of the dataset to be fitted; *ii)* finding the quantile of the theoretical specified distribution by dividing its area into n+1 equally-sized areas, i.e. find the quantile of the theoretical distribution; iii) plot the quantile of the data (y-axis) against the quantile of the theoretical specified

distribution (x-axes). If the plotted points belong to a straight line $y = x$, then the data can be represented by the selected distribution, i.e. if Q-Q plot shows a linear behaviour, the selected distribution fits the data accurately [Djurovic et al., 2000].

5.2.2.3 **The K-S test**

The K-S test is a nonparametric test that aims to verify the null hypothesis that a dataset belongs to a selected CDF [Zeng et al., 2015]. Given a dataset of *n* data, the K-S test is carried out as follows:

- Define the null hypothesis (H_0) that the *n* data are described by a specified CDF G^*. Therefore, if H_0 is not rejected, the *n* data actually belong to the specified CDF.
- Find the empirical CDF, $F_o(n_i)$, of the *n* data of the dataset, by considering that for any value n_i of the dataset, $F_o(n_i)$ is proportional to the number of data of the dataset having a value lower or equal to n_i. Formally, the empirical CDF, $F_o(n_i)$, is obtained as follows:

$$F_o(n_i) = \begin{cases} 0, & if\ n_i < n_1 \\ \dfrac{n_{par}}{n}, & if\ n_{par} < n_i < n_{par+1} \\ 1, & if\ n_i \geq n_N \end{cases} \tag{5-4}$$

  where n_1 is the lowest value of the dataset, n_{par} is any data of the database between the minimum and maximum dataset value, and n_N is the maximum value of the dataset.
- Assess the K-S test statistic, *D*, which is defined as:

$$D = \sup_{n_1 < n_i < n_N} \left(\left| F_o(n) - G^*(n) \right| \right) \tag{5-5}$$

  Eq. (5-5) shows that the K-S test statistic is equal to the maximum (vertical) distance between the empirical CDF, $F_o(n_i)$, and the specified CDF G^*.
- Compare the computed K-S test statistic with the critical value of the K-S test statistics, *D**, which is obtained from tables defined in literature, for specified

CDF and significance level α_{sl}. In this thesis, a significance level of 5% is chosen, due to the fact that $\alpha_{sl} = 0.005$ is commonly adopted. The null hypothesis H_0 is rejected if the computed H-S test statistics D is greater than the critical value D^*, i.e. if $D>D^*$, and, as a consequence, the p-value of the dataset is lower than the significance level. Otherwise, if the null hypothesis is not rejected, the data belong to the hypothesized CDF, G^*, which can be then used to fit the data and model the system under study.

The K-S test allows to find out whether if the data belong to a specified CDF.

In what follows, the proposed method for continuously updating the CPTs of an BBN is applied to the post-tensioned concrete bridge, which was presented in Chapter 4.

5.3 Analysis of the HI of the post-tensioned bridge

The data of the first group (group 1) of the post-tensioned concrete bridge are used as an input to the data analysis methodology presented in Chapter 4 , with the aim of retrieving the optimal HIs to monitor the condition of the bridge elements over time. The analysis of the bridge behaviour in Chapter 4 showed that two optimal HIs are able to point out the different health states of the bridge elements clearly: the HI_3 of the Kurtosis of the free vibration of the bridge, and HI_3 of the frequency of the estimated first harmonic of the bridge. In what follows, only the HI_3 of the Kurtosis of the free vibration of the bridge, which is the HI of the bridge that shows the highest GI index, is considered in order to monitor the evolution of the health state of the bridge elements. The adoption of a single HI allows to have a simpler method for bridge condition monitoring, rather than using two (or more) HIs. However, a single HI can increase the number of misclassifications of assessment of the bridge health state, due to oscillations of the HI, which could be damped by using two (or more) HIs to monitor the bridge health state.

The health states of the bridge, which have been introduced in section 4.3.1, are grouped as depicted in Figure 5-4: *a)* the data of the HI_3 of the Kurtosis of class 1, i.e. the healthy state of the bridge, represent the healthy state of the bridge, as shown by the solid box in Figure 5-4; *b)* the data of HI_3 of the Kurtosis of class 3 and class 4, i.e. when the pier of the bridge has been cut by 10cm and the deck has been lowered by 1 cm (class 4), represent a partially degraded health state of the bridge, as shown by the dotted box in Figure 5-4; and *c)* the data of HI_3 of the Kurtosis of class 5 and class 6, i.e. when the pier of the bridge has been cut by 10 cm and the deck has been lowered

by 2 and 4 cm respectively, represent a severely degraded health state of the bridge, as shown by the dashed box in Figure 5-4. The assumption of merging different health states of the bridge into three classes is made in order to represent the health state of the bridge by using three categories, due to the fact that bridge owners usually adopt this three health state representation, e.g. Network Rail, which is the owner of the UK railway infrastructure [Rafiq et al., 2015].

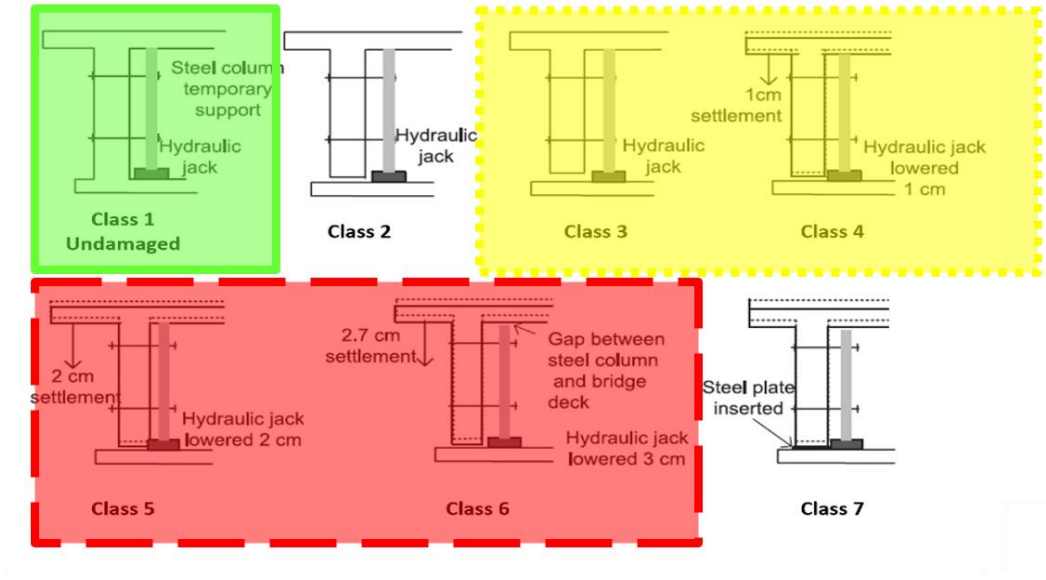

Figure 5-4. *Considered health states scenarios of the post-tensioned bridge for the BBN analysis*

The data of the HI_3 of the Kurtosis are retrieved by analysing the free-vibration of the bridge as described in section 4.3: the noise of the bridge behaviour is removed (step 1), the free-vibration of the bridge is identified (step 2), the Kurtosis of the free-vibration of the bridge is extracted every τ = 3.5 sec (that is the optimal τ) (step 3) and its trend is assessed every $\tau^* = 15\ \tau$ (step 4). It is worth noting that $\tau^* = 15\ \tau$ is not the optimal value of τ^*, which is equal to 45 τ. The decrease of τ^* is needed due to the low amount of available bridge behaviour data. The adoption of $\tau^* = 15\ \tau$ allows to increase minimally the number of data of the HI_3 of the Kurtosis that are used to fit and construct the pdf. Such a decrease in τ^* leads to a reduction of the GI index, i.e. the monotonicity and trendability of the HI_3 of the Kurtosis is decreased, and, as a consequence, the evolution of the optimal HI shows some oscillations, as illustrated in Appendix C. The change of τ^* implies that the pdfs of the optimal HI are fitted by considering a wider set of data, which shows a higher number of outliers compared to

the optimal value of τ^*. However, the different health states of the bridge can be still pointed out by using this definition of τ^*.

In what follows, the data of HI_3 of the Kurtosis are used to estimate the parameters of the three pdfs, and then the goodness of the fit is evaluated in order to identify the optimal CDF to update the CPTs of the BBN.

5.3.1 **The assessment of AICc and Q-Q plot**

The three considered models (uniform, normal and Weibull) are adopted as possible distributions to fit the data of the optimal HI. Therefore, the possibility that the optimal HI is described by one of these three CDF is investigated. The data of each health state of the bridge elements, i.e. healthy state, partially degraded and severely degraded states of the bridge elements, are used as an input to the MLE algorithm in order to assess the parameters of each model. As a result, three pdfs for each health state of the bridge are fitted. The goodness-of-fit process is analysed by assessing the AICc of the three pdfs for each health state of the bridge elements. Similarly, the Q-Q plot of the three pdfs for each health state of the bridge elements is analysed in order to graphically point out which selected pdf fits the data in the best manner.

Figure 5-5 shows the three pdfs fitted on the HI values retrieved by analysing the bridge behaviour provided by sensor A. Figure 5-5a, i.e. the three Q-Q plots on the top within the solid line box, represents the analysis of the HI of the healthy bridge. The uniform distribution shows the lowest AICc and almost linear behaviour on its Q-Q plot, with a small deviation from the linearity at the centre of the HI data, i.e. at the middle of the Q-Q plot. The Weibull distribution shows the second lowest AICc, but its Q-Q plot departs from the linearity at high values of the HI. Finally, the normal distribution shows the highest AICc and almost linear behaviour on its Q-Q plot. The analysis of Figure 5-5a shows that the uniform distribution seems to be the distribution that fits the HI values in the best possible way. However, the AICc of the three distributions is similar, and thus the K-S test needs to be adopted in order to verify whether the HI values really belong to the uniform distribution.

Similarly, Figure 5-5b, i.e. the three Q-Q plots on the middle within the dotted line box, represents the analysis of the HI of the partially degraded bridge. Again, the normal distribution shows the lowest AICc and a linear behaviour on its Q-Q plot, whereas the Weibull distribution shows the second lowest AICc and non-linear behaviour of the Q-Q plot for large values of the HI. Finally, the normal distribution

shows the highest value of AICc and quasi-linear behaviour on its Q-Q plot. The difference between the three AICc is larger than in the healthy state analysis, and as a consequence, the uniform distribution seems to outperform both Weibull and the normal distribution.

Finally, Figure 5-5c, i.e. the three Q-Q plots on the bottom within the dashed line box, represents the analysis of the HI data of the severely degraded health state. The three pdfs are ranked in the same order as the previous analyses, i.e. the uniform distribution shows the lowest AICc, followed by the Weibull and the normal distribution, respectively. The Q-Q plot of the uniform distribution departs from the linearity for low values of the HI, whereas the Q-Q plot of the Weibull departs from the linearity at high values of the HI. The Q-Q plot of the normal distribution shows almost linear behaviour, with non-linear behaviour for both low and high values of the HI. Figure 5-5c shows also that the AICc of the three distributions are very similar, and consequently each fitted pdf has evidence to be a good fit for the HI data. For this reason, the K-S test is applied to verify if the HI values of the partially degraded state of sensor A belong to a uniform distribution.

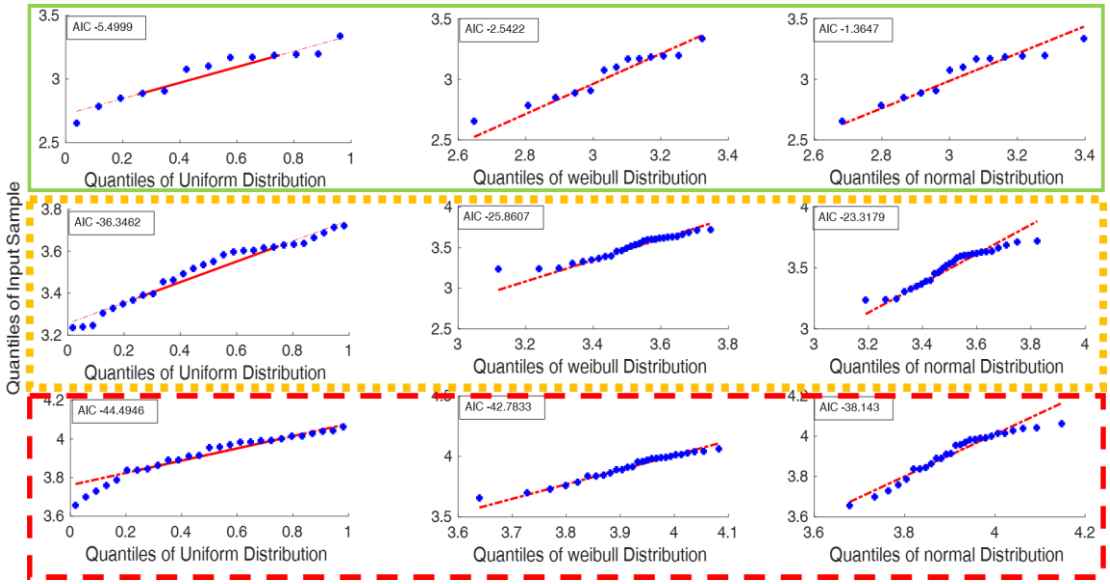

Figure 5-5. *AICc values and Q-Q plots of the three health states of the bridge for sensor A.*

In the same way as Figure 5-5, Figure 5-6 depicts the Q-Q plots and the AICc values for the three pdfs, which are used to fit the HI values of the three health states of the bridge elements obtained by sensor B. Figure 5-6a, i.e. the three Q-Q plots on the top within the solid line box, represents the analysis of the HI of the healthy bridge

provided by sensor B. The Weibull distribution shows the lowest AICc, even though its Q-Q plot shows non-linear behaviour at low values of HI. The uniform distribution provides the second lowest AICc and almost linear Q-Q plot, and the normal distribution shows the highest AICc and a Q-Q plot that departs from the linearity at low values of the HI. Figure 5-6a suggests that the Weibull distribution is the pdf that best fits the HI values for the healthy state of the bridge recorded by sensor B. However, the three AICc values are close, and therefore the K-S test needs to be applied in order to verify if these HI values can be represented by a Weibull distribution.

Figure 5-6b and Figure 5-6c, i.e. the three Q-Q plots in the middle within the dotted line box and the three Q-Q plots on the bottom within the dashed line box, respectively, show the analysis of the HI values for the partially degraded and the severely degraded health states. In both health states of the bridge elements, the uniform distribution shows the lowest AICc and almost linear behaviour in the Q-Q plot, whereas the partially degraded health states (Figure 5-6b) show a departure from the linearity on the middle of the Q-Q plot. The Weibull distribution provides the second lowest values of AICc in both Figure 5-6b and Figure 5-6c. However, the analysis of the partially degraded health state of the bridge in Figure 5-6b shows that the AICc of the Weibull distribution is much higher than the AICc of the uniform distribution. Furthermore, the Q-Q plot of the Weibull in Figure 5-6b depicts a departure from the linearity at high values of the HI. As a result, the uniform distribution seems to outperform the other two distributions in terms of fitting model for the partially degraded health state values. The K-S test in the next section would verify if the HI of this health state of the bridge can be effectively represented by the uniform distribution. Finally, the AICc of the pdfs in Figure 5-6c is similar, and thus the K-S test will help in assessing which pdf allows to fit the HI vales in the best way.

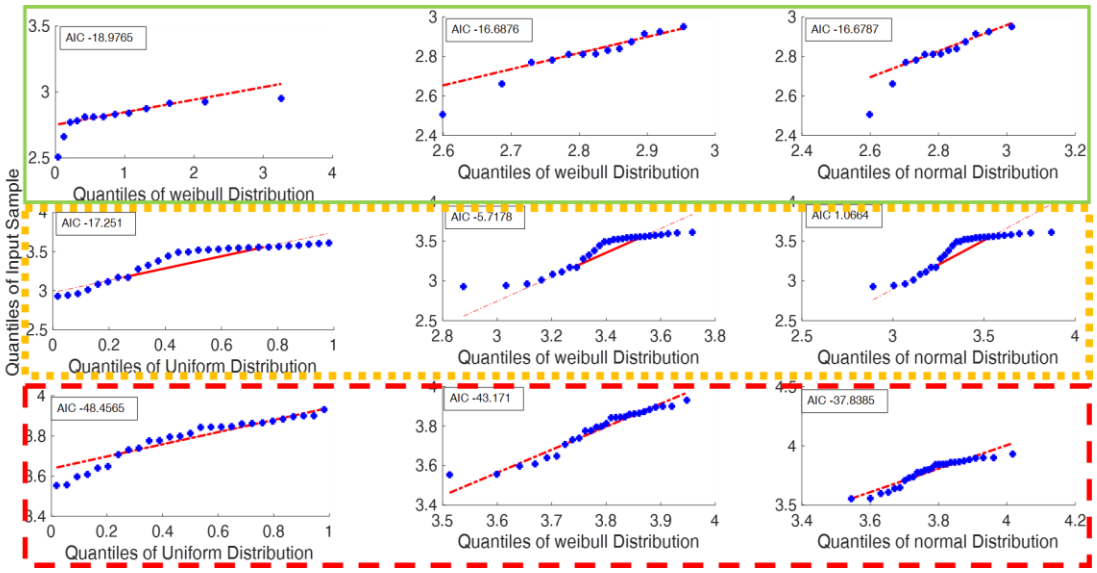

Figure 5-6. *AICc values and Q-Q plots of the three health states of the bridge for sensor B.*

Figure 5-5 and Figure 5-6 show that the pdf with the lowest AICc value and linear behaviour of the Q-Q plot is the possible best pdf to fit the HI values for each health state of the bridge and for each sensor. Figure 5-7 and Figure 5-8 depict the possible best pdf and CDF for each health state of the bridge element for sensor B and sensor A, respectively. Figure 5-7 shows that the HI values, which are obtained by monitoring the health states of the bridge by sensor 1, are modelled by uniform distributions. Particularly, the plots on the left-hand side of Figure 5-7 show the pdf of the uniform distributions, whereas the plots on the right-hand side depict the CDF of the uniform distributions. Figure 5-7 also shows that the value of the HI, i.e. the HI_3 of the kurtosis of the acceleration of the bridge, increases as the health state of the bridge decreases. In fact, the values of the HI (x-axis range) on the plots of Figure 5-7 increase by moving from the healthy to the partially degraded and severely degraded health states.

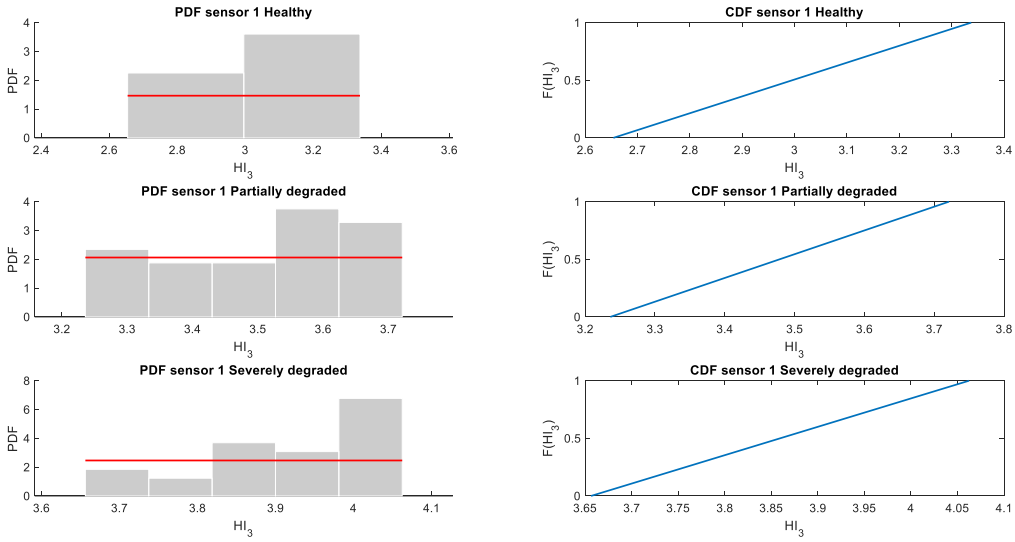

Figure 5-7. *Possible best fitting pdfs and CDFs according to the AICc and Q-Q plot analysis to model the HI values for sensor A*

Figure 5-8 depicts the optimal distributions to model the HI values obtained by monitoring the health states of the bridge by sensor B, according to the AICc and Q-Q plot analysis. The HI values of the healthy state of the bridge are modelled by Weibull distribution, whereas the partially degraded and severely degraded health states are modelled by using the uniform distribution. Similarly to Figure 5-7, the HI values of the bridge health state obtained by analysing the data of sensor B increase as the health state of the bridge decreases, as shown in Figure 5-8 by the x-axis of the plots.

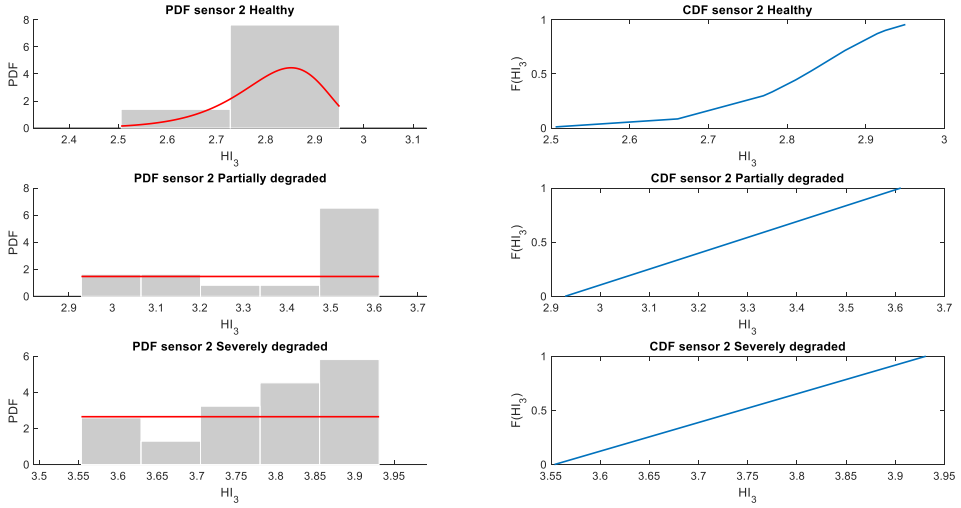

Figure 5-8. *Possible best fitting pdfs and CDFs according to the AICc and Q-Q plot analysis to model the HI values for sensor B*

Finally, Table 5-1 shows the parameters of the distributions shown in Figure 5-7 and Figure 5-8. Parameter 1 (Par 1) of the uniform distribution is the minimum value of the distribution, whereas Parameter 2 (Par 2) of the uniform distribution represents the maximum value of the distribution. Conversely, Par 1 of the Weibull distribution represents the scale parameter, whereas Par 2 represents the shape parameter (usually known as β). The values of the uniform distribution for sensor A show that the distributions of the different health states of the bridge are overlapped on their tails. This behaviour can be due to both reasons: low amount of data available to assess the distributions, and oscillations of the HI values during the monitoring of the bridge behaviour. The high value of the shape parameter of the healthy state of the Weibull distribution of sensor B shows that the higher the HI value, the more degraded the health state of the bridge. The high value of the shape parament can be explained as follows: *i)* the dispersion of the values of the HI in the healthy state is extremely low [Jian & Murthy, 2011]; *ii)* the Weibull distribution peaks around Par 1 location, and then decreases rapidly to zero. This shape of the distribution can be represented by a limited peaked distribution, such as a Generalized Extreme Value distribution. However, the performance of the BBN would be slightly influenced by using a Generalized Extreme Value distribution, as discussed in Appendix B. This result can suggest that the set of considered pdfs needs to be increased in order to identify a robust CDF to fit the data. At the same time, when a higher number of HI values is available, the fitting process would be more robust and reliable [Sobanjo et al., 2010]. However, Chapter 6 shows that the performance of the BBN is slightly influence by the nature of the CDF, whereas the proposed updating process of the CPTs improves the performance of the BBN dramatically.

Table 5-1. *Parameters of the best distributions according to AICc and Q-Q plots analysis*

Scenario	**Distribution**	**Parameters**	
		Par 1	**Par 2**
Sensor A – healthy state	Uniform	2.65	3.3
Sensor A – partially degraded state	Uniform	3.23	3.72
Sensor A – severely degraded state	Uniform	3.65	4
Sensor B – healthy state	Weibull	2.85	34.57
Sensor B – partially degraded state	Uniform	2.92	3.61
Sensor B – severely degraded state	Uniform	3.65	3.93

In what follows, the K-S test is applied to the possible best pdf for each health state of the bridge of each sensor, i.e. the pdf that provides the best AICc value is assumed to be the best pdf, and this hypothesis is verified by the means of the K-S test.

5.3.2 The K-S test to verify the hypothesis of using the best fitting pdf

The CDF of Figure 5-7 and Figure 5-8 are used as an input to the K-S test in order to verify if the HI values can be represented by the considered CDF. Hence, the K-S test is carried out for each health state of the bridge and each sensor, by assuming that for each health state of each sensor, its HI values belong to the corresponding CDF shown in Figure 5-7 and Figure 5-8.

The K-S test verifies the null hypothesis (H_0) that the HI values of the specified health state of the bridge follow the selected CDF. If H_0 is not rejected, then the HI values can be modelled by the CDF shown in Figure 5-7 and Figure 5-8. Otherwise, the distribution with the second lowest AICc is used to describe the HI values, and the K-S test is then performed again in order to test if the HI values follow the second ranked distribution (in terms of AICc value).

Table 5-2 shows the results of the K-S test for each health state and for both sensors at a significance level of 5%. The null hypothesis that the HI values of the healthy state of the bridge follow a uniform distribution (sensor A) and a Weibull distribution (sensor B) is not rejected (p-values higher than the significance level for both cases), and thus the CDF of the healthy state depicted in Figure 5-7 and Figure 5-8 are used to model the HI during the healthy state of the bridge. Similarly, the null hypothesis that the HI values of sensor A of the partially degraded health state of the bridge elements follow a uniform distribution is not rejected, by obtaining a p-value higher than the significance level. Therefore, the uniform distribution shown in Figure 5-7 is adopted to model the HI of the partially degraded health state for sensor A.

The null hypothesis that the HI values of the severely degraded state for sensor A follows a uniform distribution is rejected (p-value lower than the significance level), as well as the null hypothesis that the HI values of the partially and severely degraded states for sensor B follow the uniform distributions. For these three scenarios, the values of the HI are then assumed to follow the distribution that shows the second lowest AICc, i.e. the Weibull distribution for all scenarios. The K-S test is performed

again for these three cases, in order to verify if the HI values follows the Weibull distribution.

Table 5-2. *K-S test results for the CDFs with the lowest value of AICc*

Scenario	H_0	p-value
Sensor A – healthy state	Not rejected	0.4144
Sensor A – partially degraded state	Not rejected	0.2931
Sensor A – severely degraded state	Rejected	0.0401
Sensor B – healthy state	Not rejected	0.9121
Sensor B – partially degraded state	Rejected	0.0002
Sensor B – severely degraded state	Rejected	0.0496

Table 5-3 shows the results of the K-S test for the HI values of the three health states that are rejected in Table 5-2. For each scenario, the null hypothesis (H_0) is that the HI values of the three health states of the bridge belong to Weibull distribution, which is the distribution with the second lowest AICc. The null hypothesis (H_0) is not rejected in all three cases, due to the fact that the p-values are higher than the significance level. As a result, the HI values of the degraded health state of the bridge shown in Table 5-3 follow Weibull distribution. The pdfs and CDF of Figure 5-7 and Figure 5-8 need thus to be updated in order to take account of the K-S test results.

Table 5-3. *K-S results for the CDFs with the second lowest value of AICc*

Scenario	H_0	p-value
Sensor A – severely degraded state	Not rejected	0.7544
Sensor B – partially degraded state	Not rejected	0.0790
Sensor B – severely degraded state	Not rejected	0.4125

Figure 5-9 and Figure 5-10 show the possible best pdf and CDF for the HI values of each health state of the bridge for sensor A and sensor B, respectively, by accounting for the results of the K-S test. Figure 5-9 shows that the HI values of the partially degraded health state obtained by monitoring the health states of the bridge by sensor A are modelled by the Weibull distributions. The HI values of the healthy state and

the severely degraded state are modelled by using the uniform distribution, obtained in section 5.3.1.

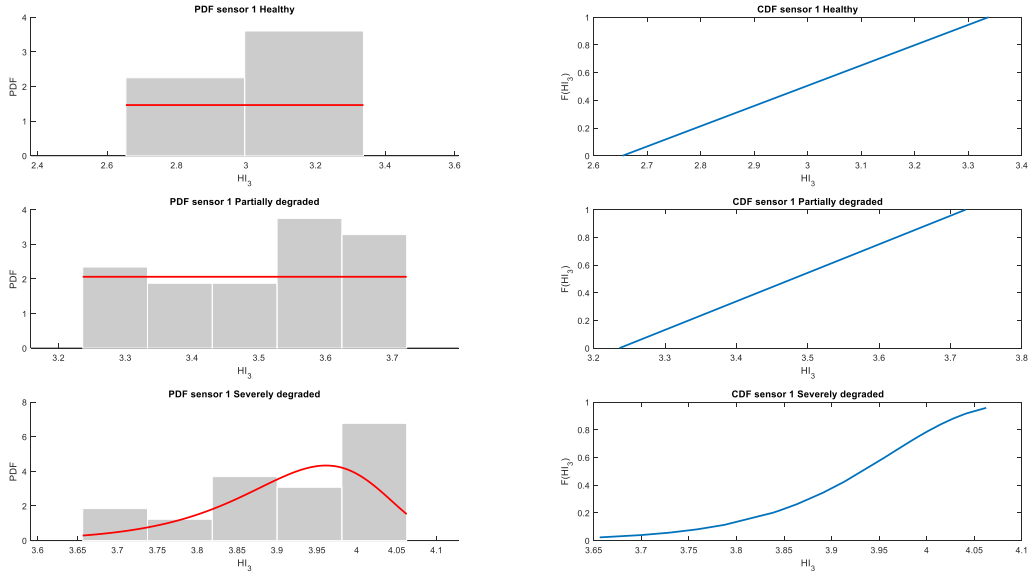

Figure 5-9. *Possible best pdfs and CDFs according to K-S test to model the HI values for sensor A*

Figure 5-10 shows that the HI values of the healthy bridge state obtained by monitoring the health states of the bridge by sensor B are modelled by using the Weibull distribution in section 5.3.1. The HI values of the partially degraded and the severely degraded states are modelled using a Weibull distribution, according to the K-S test results.

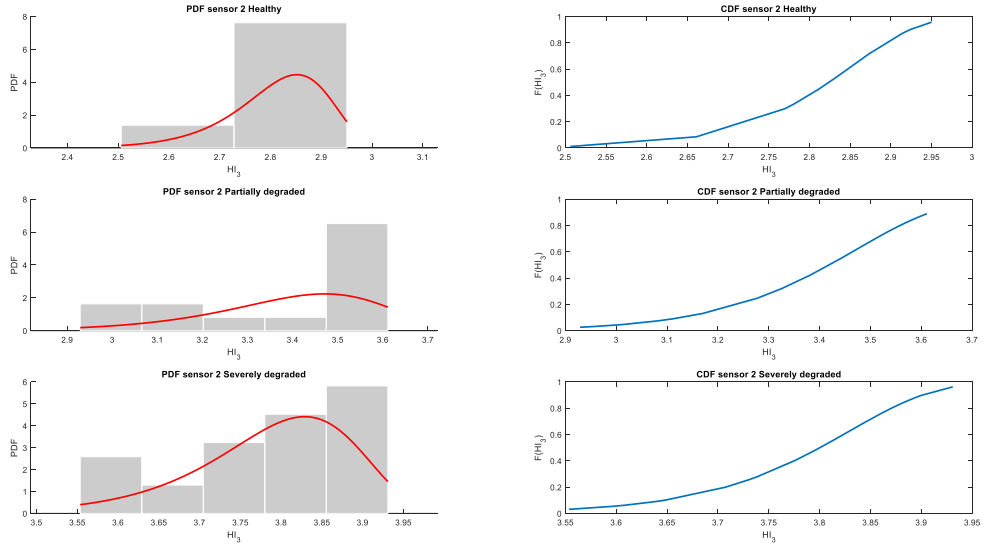

Figure 5-10. *Possible best pdfs and CDFs according to K-S test to model the HI values for sensor B*

Table 5-4 shows the values of the parameters of the best distribution according to the K-S test. The distributions of the healthy state for both sensors of the partially degraded state for sensor A are the same as in section 5.3.1. The distributions of the severely degraded state for both sensors and of the partially degraded state for sensor B are modified to Weibull distributions. Again, the high value of the shape parameter shows that the health state of the bridge decreases when the HI value increases. Furthermore, such high value of the shape parameter leads to a distribution that peaks at the location of Par 1, and then decrease suddenly to zero. The high value of the shape parameter can be caused by the low variability of the small set of HI data and due to a non-optimal selection of the set of the pdfs, which, however, influences the performance of the BBN slightly.

It is worth mentioning that, when more data of the bridge behaviour are available, the fitting process needs to be performed again, in order to point out the distribution of the optimal HI in a more reliable manner.

Table 5-4. *Parameters of the best distributions according to the K-S test*

Scenario	Distribution	Parameters	
		Par 1	Par 2
Sensor A – healthy state	Uniform	2.65	3.3
Sensor A – partially degraded state	Uniform	3.23	3.72
Sensor A – severely degraded state	Weibull	3.96	46.68
Sensor B – healthy state	Weibull	2.85	34.57
Sensor B – partially degraded state	Weibull	3.47	21.11
Sensor B – severely degraded state	Weibull	3.83	45.92

In what follows, the CDF of both Table 5-1 and Table 5-4 are used to update the CPTs in order to compare the performance of the BBN when different CDFs are adopted.

5.4 Summary of the proposed method to merge expert judgment and bridge behaviour analysis

A method to merge the expert elicitation process with the analysis of the bridge behaviour is proposed, with the aim of updating the CPTs of a BBN in a reliable and

continuous manner. The CPT values are updated by considering an α weighted combination of the expert knowledge and the bridge behaviour analysis. The expert knowledge elicitation process and the bridge behaviour analyses are carried out off-line in order to initially define the CPTs and identify a set of CDFs to model the optimal HI of the bridge elements, respectively. The expert knowledge process has been discussed in section 3.3.2. The assessment of the CDF of the HI that monitors the health state of the bridge elements is proposed by analysing the HI of different health state of the bridge elements. Particularly, for each health state of the bridge elements, its HI values are fitted to a set of three possible pdfs, and the goodness-of-fit process is then evaluated. The AICc index and Q-Q plot approaches are used to select the pdf that fits the HI values in the best manner. The selected pdf is then verified by adopting a K-S test, which aims to verify if the HI values belongs to the specified distribution.

The low amount of available data of HI led to different results, i.e. the distributions selected by analysing the AICc and the Q-Q plot are not verified by using the K-S test. Therefore, in the following of the thesis both distributions are adopted as an input to the CPTs of the BBN in order to take account of the uncertainties in the CDF distributions and to analyse how different CDFs influence the performance of the BBN.

The presented method shows some drawbacks:

- the weight of the combination α is defined by considering that the bridge behaviour data can give more reliable information than the expert knowledge. Therefore, the higher the amount of data of the bridge behaviour, the higher α and the more important the analysis of the bridge behaviour. As a consequence, the importance of the information provided by the expert knowledge process decreases over time, due to the fact that the monitoring process of the bridge provides more and more data. However, a conservative approach would suggest giving more importance to the expert knowledge, as the experts can investigate what-if scenarios and the analysis of the bridge behaviour data depends on the quality of the available data. In the following of the thesis, different strategies for the definition of α are investigated, with the aim of assessing how the performance of the BBN is affected.
- the fitting process to identify the best CDF is carried out with a parametric approach and a small amount of data. The parametric approach considered only

three different CDFs (9 CDFs considering also Appendix B). As a result, the optimal CDF to describe the optimal HI values might not be considered within the group of 9 CDFs. Therefore, future work should analyse how to identify the best CDF to model the HI of the bridge elements, in order to model the bridge behaviour changes in a reliable manner.

- the analysis of the bridge behaviour data assumes that the health state of the bridge is known a-priori, i.e. the data of bridge behaviour are labelled in order to point out the health state of the bridge at that moment. However, the health state of the bridge is not always known a-priori and such labels might be unavailable. As a consequence, a method to analyse database of infrastructure behaviour is needed in order to point out the changes of the health state of the infrastructure. In this way, this information can be used as an input to the proposed method with the aim of updating the definition of the CPTs of the BBN. Such a method is proposed in the following section. Furthermore, data of a damaged bridge is not usually available, and it might require the adoption of an FEM to retrieve data of the bridge behaviour.

In what follows, a method to analyse unknown database of infrastructure behaviour is presented in order to assess changes of the health state of the infrastructure, and investigate the characteristics of such changes.

5.5 A method to data-mine the behaviour of the infrastructure

5.5.1 Introduction

SHM systems generate a large amount of data and, as a consequence, processing and interpreting this data can be difficult and time consuming. Particularly, when decision makers need to analyse a database of infrastructure behaviour in order to analyse the past behaviour of an infrastructure, robust data mining techniques are required to analyse this data automatically, accurately and rapidly [Duan and Zhang, 2006]. Indeed, data mining techniques are able to transform the recorded data into valuable information for decision makers, by pointing out past changes of the health states of the infrastructure.

In this thesis, an ensemble-based data mining method is proposed in order to detect the past unexpected behaviour of civil infrastructure. The proposed method relies on an ensemble-based change-point detection analysis, which aims to identify the time when the infrastructure behaviour starts to change rapidly and point out the duration

of the health state change. The ensemble-based change-point detection method is needed due to the fact that single change-point methods, such as Cumulative Sum (CUSUM)-based [Carslaw et al., 2006] or probability distributions-based [Liu et al., 2013] methods, are able to detect only abrupt changes in the data, without pointing out the most severe changes. Furthermore, the longer the duration of the monitored behaviour of the system, the higher the number of the abrupt changes, which are identified by an individual change-point method. Thus, the most severe change in the data can be lost among all the change-points [Killick et al., 2012]. Individual change-point methods are also usually unable to identify the duration of the most critical system behaviour. Conversely, the proposed ensemble-based of change-point methods is able to identify the most critical change in the data, by highlighting its start and end time. In this way, only the information regarding the most critical behaviour of the tunnel is provided to the decision maker.

In what follows, the proposed data mining method is presented. First of all, the proposed method would be applied to the HI of a bridge infrastructure. Then, the past bridge behaviour would be analysed to identify the HIs of the bridge health state over time, and the optimal HI, which is the HI with the highest GI, would be analysed by the proposed data mining method in order to detect changes of the HI pattern. Therefore, when the HI changes, the health state of the bridge changes accordingly. In this way, different health state of the bridge can be identified and analysed. However, low amount of data about bridge behaviour was available for this study, and, as a consequence, the proposed data mining method was tested on a different case study of a railway tunnel. Furthermore, the case study considered in this thesis showed the potential of the proposed method, which can be applied to every system that has monotonic behaviour as the degradation increases.

For these reasons, the proposed data mining method is applied to a real in-field railway tunnel, which is subject to renewal activities. As described also above, this case study is selected due to the limitation of the scarce amount of bridge behaviour data, and due to the needs of the industrial collaborator, AECOM, to analyse a database of tunnel behaviour in order to detect when the health state of the tunnel changes. Indeed, the tunnel data shows noisy measurements that are caused by the working activities, and the decision makers need information about the changes of the tunnel health states rapidly, in order to guarantee the safety of the asset and the workforce.

The content of this chapter has been published in "*Tunnelling and Underground Space Technology Journal*" with the aim of proposing a novel ensemble-based change point detection method for identifying changes of infrastructure health state [Vagnoli & Remenyte-Prescott, 2018]. Particularly, section 5.5.2 and section 5.5.3 are extracted from [Vagnoli & Remenyte-Prescott, 2018].

5.5.2 **The proposed ensemble-based change-point detection method**

Change-point methods aim to identify the exact moment when the monitored variable of a system starts to deviate abruptly from an equilibrium level. Change-point detection algorithms are adopted in several frameworks, such as SHM and prognosis of gas turbines [Maleki et al., 2016], variation of air pollution concentration [Carslaw et al., 2006], variation of climate parameters in order to monitor climate change characteristics [Reeves et al., 2007], failure of pipes in chemical industries [Tickle et al., 2010]. However, change-point methods are usually unable to point out the most critical change-point clearly, i.e. the change-point where the monitored variable experiences the highest variation. In fact, the most critical change point is identified among all the change-points of the system. The duration of the unexpected changes is also not assessed. Furthermore, the choice of an individual change-point algorithm can jeopardize the reliability and robustness of the data analysis, due to different results of the individual change-point detection methods.

In this thesis, a novel ensemble-based change-point method is proposed to analyse database of infrastructure behaviour, by coupling the performance of four individual change-points methods. In this way, the proposed ensemble-based method is able to point out the most critical change-point of the infrastructure, providing its duration and, eventually, possible causes. As a consequence, the reliability and robustness of the data mining analysis are expected to improve accordingly. Decision makers can then schedule future monitoring and work activities by using the results of the ensemble-based change-point method.

In what follows, the theoretical background of the four individual change-point algorithms is presented briefly in section 5.5.2.1, and then the proposed ensemble-based method is introduced in section 5.5.2.2.

5.5.2.1 **Change-point methods: theoretical background**

The change-point analysis can be divided in two groups - real-time and retrospective detection: the former aims to identify a change-point of system behaviour as soon as it occurs; the latter aims to identify a change-point of system behaviour by analysing the history of the monitored parameter. The focus in this thesis is on the retrospective change-point analysis, which usually provides a more robust and accurate detection than the real-time analysis [Liu et al., 2013]. Particularly, the aim is to identify the most critical change-point of the system health state, by assessing its duration and diagnosing its possible causes. In order to achieve this aim, an ensemble-based change-point method is developed by coupling the performance of four of the most commonly adopted change-point algorithms: *i)* a change-point detection method that relies on a relative probability density ratio, which is computed by using the Relative Unconstrained Least-Squares Importance Fitting (RuLSIF) [Liu et al., 2013]. The RuLSIF method has demonstrated to provide very good results in identifying change-points through the assessment of a relative probability density-ratio; *ii)* a Cumulative Sum (CUSUM) change-point detection algorithm [Carslaw et al., 2006]. The CUSUM is one of the most popular change-point method that has been adopted in many different research framework, such as air pollution concentration [Carslaw et al., 2006], failures of computer networks [Montes De Oca et al., 2010], functionality of animal brain activity [Koepcke et al., 2016]; *iii)* a change-point detection method that relies on the identification of changes of the mean value of the monitored system behaviour, by defining a penalty cost function [Lavielle, 2005]; *iv)* a change-point detection method that relies on the identification of changes of the slope of the monitored system behaviour, by using a Pruned Exact Linear Time (PELT) method [Killick et al., 2012]. The change-point methods *iii)* and *iv)*, which rely on the same theoretical basis, have been chosen due to their efficiency and low computational burdensome. Indeed, as the length of the monitored parameters increases, the number of possible change-points also increases, and thus an efficient and fast detection of change-point is needed [Harchaoui and Levy-Leduc, 2010; Killick & Eckley, 2014].

A brief description of each individual change-point detection method is presented in what follows, by discussing the RuLSIF method in section 0, the CUSUM in section 0, the mean-based change-point detection in section 0 and the PELT-based change-point detection method in section 0.

The RuLSIF change-point detection method

This method aims to detect a change-point by assessing the probability density ratio, $\frac{p(t)}{p(t+n)}$, of samples of the monitored system behaviour, *Y(t)*, between time *t* and *t+n*, where *n* is the size of a time window. The samples *Y(t)* and *Y(t+n)* are defined as the *k* behaviour of the system within the time window *n*, such as the displacements of a tunnel that are recorded during *k* times consecutively. For example, Figure 5-11 shows the monitored behaviour of the system, such as the displacement of a tunnel, *y(t)*, which is collected at each time *t*: its samples, *Y(t)* and *Y(t+n)*, are the *k*=3 displacements of the tunnel recorded during a time window of size *n*=5, i.e. *Y(t)* is defined by the measurements recorded at time *a*, *b* and *c*, whereas *Y(t+n)* is equal to the displacements at time *f*, *g* and *h*. The ratio of the probability densities, $\frac{p(t)}{p(t+n)}$, between *Y(t)* and *Y(t+n)* can be then assessed by using the RuLSIF strategy.

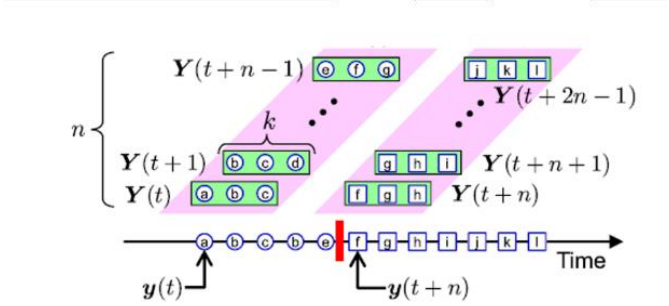

Figure 5-11. *Graphical relationship between the monitored behaviour of the system, y(t), and its samples, Y(t) [Liu et al., 2013]*

Particularly, the change-point is estimated by monitoring the evolution over time of an α-relative Pearson (PE) divergence index, which depends on the Gaussian kernel estimation of the density-ratio:

$$PE \propto \sum_{i=1}^{n} \theta_i K(Y, Y_i) \tag{5-6}$$

where the Gaussian kernel function, *K*, is computed as:

$$K(Y,Y^{'}) = \exp\left(-\frac{\|Y - Y_i\|^2}{2\sigma^2}\right) \quad (5\text{-}7)$$

σ in Eq. (5-7) is the width of the kernel.

The parameters, θ_i , are to be found from the data [Liu et al., 2013]. Eq. (5-6) and Eq. (5-7) show that the PE index increases as the distance between the samples *Y* and *Yi* increases, i.e. the probability that a change-point occurred increases as the difference between the two samples of the monitored system behaviour increases.

The CUSUM change-point detection algorithm

Given a time series of monitored behaviour of the system, such as the displacement of a tunnel at consecutive times 1, 2, …, *m*, $y(t)= [y_1, y_2, ..., y_m]$, where *m* is the size of the measured behaviour of the system, the CUSUM chart is developed by assessing the cumulated difference between each value y_i of *y(t)* and the mean value of the displacement pattern, y_{mean}:

$$S_i = S_{i-1} + (y_i - y_{mean}) \; for \; i = 1, 2, \ldots, m \quad (5\text{-}8)$$

Eq. (5-8) shows that when the system behaviour is measured, the cumulative difference, S_i, is computed as the difference between the mean value of the measured behaviour of the system, y_{mean}, (e.g. the mean value of the recorded displacement of a tunnel) and the value of the system behaviour at each time, y_i, (e.g. the displacement of the tunnel at each time step).

The difference between the maximum value of Eq. (5-8), S_{max}, and the minimum cumulated difference, S_{min}, is the maximum variation of the CUSUM, ΔS_{max}. ΔS_{max} is used in order to evaluate if a change of the monitored behaviour of the system has occurred. Indeed, once ΔS_{max} for the original recorded data is computed, the values of the monitored behaviour of the system, *y(t)*, are randomly resampled for 1000 times, and the CUSUM process is repeated for each resampled trial. As proposed by [Carslaw et al., 2006], we consider that a change has occurred on the recorded data *y(t)* when the ΔS_{max} of *y(t)* is higher than the ΔS_{max} of the 95% of the randomly resampled trials. Therefore, a change point is estimated to have occurred at the time of occurrence of the maximum CUSUM value, ΔS_{max}, if a 95% confidence level is achieved. Finally, multiple change-points can be detected by dividing the monitored behaviour data *y(t)*

in two parts, one for each side of the identified change-point, and repeating the CUSUM analysis for each part. The CUSUM analysis is terminated when no change-point is detected in each analysed part of *y(t)*.

The penalty cost function-based change-point detection method

The existence of change-points of the monitored behaviour of the system is investigated by minimising an objective cost function, *C*. Particularly, assume that the monitored behaviour, *y(t)*, shows l change-points, which occur at time $\tau_{1:l} = (\tau_1, \tau_2, \ldots, \tau_l)$. The monitored behaviour, *y(t)*, is divided in l+1 segments, $y_{(\tau_{j-1}+1):\tau_j}$. The cost function for each segment, which needs to be minimized, can be defined as follows:

$$\sum_{j=1}^{l+1}\left[C(y_{(\tau_{j-1}+1):\tau_j}) \right] + \beta f(l) \qquad (5\text{-}9)$$

where $\beta f(l)$ is a penalty function that is usually linear with the number of the change-points, $\beta f(l) = \beta \cdot l$ [Killick et al., 2012]. The cost function *C* is defined by using features of the monitored system behaviour. For example, the mean value, the root mean square, the standard deviation, the slope of a linear fitting model, etc. of the system behaviour can be used as features that define the objective of the cost function *C*. A change-point is identified at time when the cost function is minimized, i.e. at time when the chosen feature of the system behaviour changes suddenly. In this thesis, a cost function that aims to detect change-points by looking for changes of the mean value of the system behaviour is presented. The penalty parameter β is optimized by using an iterative procedure with the aim of minimizing the cost function, *C* [Lavielle, 2005]. However, the optimal choice of the penalty function, $\beta f(l)$, and the penalty parameter, β, depend on several parameters that are unknown a-priori, such as the length of the data and number of change-points [Killick & Eckley, 2014]. In this thesis, the penalty parameter, β, and the penalty function, $\beta f(l)$, are automatically selected by the software (MatLab®).

The PELT-based change-point detection method.

This method identifies the change-points of the monitored behaviour of the system, *y(t)*, by relying on the same theoretical approach described for method of section 0, i.e.

by minimizing the cost function, *C*. However, a pruning strategy is applied in order to improve the computational speed and efficiency of the change-point search. Hence, the values of the monitored behaviour of the system, *y(t)*, that cannot minimize the cost function, *C*, are removed from the analysis. In this thesis a cost function that aims to detect change-points by identifying changes on the slope of the system behaviour by considering an autoregressive linear model for the individual change-point method is presented.

5.5.2.2 **The proposed ensemble-based change-point detection method**

The individual change-point methods described in section 5.5.2.1, are able to identify efficiently abrupt change-points of the monitored variable of the system. However, the most critical change-point, which occurs when the monitored variable experiences the highest variation, is identified among all the change-points experienced by the system. The performance of each individual change-point method is different, and consequently the reliability and robustness of the change-point detection analysis is influenced by the choice of a change-point method. The duration of the change of the system is also not assessed by these individual methods. The four-individual change-point detection algorithms are then merged together in an ensemble strategy, in order to point out the most critical change-point of the monitored behaviour of the system, and identify its duration. The following criteria for identifying the start and end of the change-point are proposed Eqs. (5-10)-(5-11) and (5-12)-(5-13), respectively:

$$\max\left\{\left|\frac{\delta y_{1:\tau_1}(\tau_P)}{\delta t}\right|\right\} \tag{5-10}$$

where τ_p is defined as follows:

$$\tau_P = \left\{\min\left(\tau_1^k, \tau_1^q\right) + \Delta \mid \left|\tau_1^k - \tau_1^q\right| \le \Omega\right\}, \textit{with } k = 1, ..., M-1; q = k+1, ..., M \tag{5-11}$$

$$\min\left\{\left|\frac{\delta y_{\tau_{l-1}+1:\tau_l}(\tau_{P^*})}{\delta t}\right|\right\} \tag{5-12}$$

where τ_{P^*} is defined as follows:

$$\begin{aligned}&\tau_{P^*} = \min\left(\frac{1}{N}\sum_{n^*=1}^{N} t_{n^*} + \Phi, \max\left(\tau_l^k, \tau_l^q\right) + \Phi \mid \left|\tau_l^k - \tau_l^q\right| \le \Omega\right),\\ &with\ k = 1, ..., M-1; k^* = k+1, ..., M\end{aligned} \tag{5-13}$$

where *M* is the number of the individual change-point algorithms adopted, i.e. four in this example; *N* in Eq. (5-13) is the length of the interval, where $PE \ge \Theta$; $\tau_1^{k,q}$ and $\tau_l^{k,q}$ represent the first and *l-th* change-point identified by each individual change-point algorithm, respectively. Finally, Θ, Ω and Δ are constants that need to be defined by the user. Θ is a threshold for the PE coefficient that needs to be chosen in order to emphasise the detection ability of the most critical change-point in the behaviour of the system, by neglecting other small changes [Liu et al., 2013]. The constants Ω and Δ need to be defined by the user when considering the nature of the case study. For example, if the ensemble-based method is applied for monitoring the existence of change in behaviour in a computer network, Ω and Δ need to be as low as possible, i.e. one second or less. Indeed, a computer network system manages large amount of information continuously, at each second or a fraction of a second. On the contrary, if the ensemble-based method is to be applied to monitor possible changes of the behaviour of a civil infrastructure, such as a bridge or tunnel, Ω and Δ will be set to larger values. In fact, the SHM measurement system can provide a measurement of the infrastructure behaviour every hour. As a result, Ω and Δ require to be optimized by considering the nature of the case study and using expert knowledge elicitation.

Eq. (5-10) shows that the ensemble-based strategy is able to identify the initial change-point of the most critical unexpected behaviour of the system, by looking for the maximum variation of the monitored system behaviour at time τ_P (Eq. (5-11)). τ_P is the first change-point that is identified by at least two different individual change-point methods within Ω time of each-other, plus a constant Δ.

Eq. (5-12) shows that the final point of the most critical change-point of the behaviour of the system, i.e. the point where the critical unexpected behaviour ends, is identified by looking for time τ_{p^*}. The point, τ_{p^*}, in Eq. (5-13), is identified by looking for the minimum value between: *i)* the mean value of the time interval, where the PE coefficient is higher than the threshold Θ; *ii)* the time where a change-point is identified by at least two different individual change-point methods within Ω time of each other, plus a constant Φ. Again, Ω and Φ depend on the nature of the system analysed, and they are optimized considering the nature of the system under analysis. The ensemble-based method merges the performance of each individual change-point method in order to improve the reliability of the data analysis process. At the same time, the ensemble-based method is able to detect and diagnose the most critical change-point, by providing a robust and reliable analysis. Each individual change-point method identifies different change-points of the monitored behaviour of the system, and so a reliable and robust analysis of the system behaviour can be influenced by the choice of the change-point algorithm. On the contrary, the proposed ensemble-based change-point method is able to provide the most critical change of the system behaviour, by coupling the results of the individual change-points methods. Therefore, the reliability and robustness of the identified change-point is improved. In what follows, the performance of the individual methods is compared with the performance of the ensemble-based strategy, in order to demonstrate the more robust and reliable results of the proposed strategy.

5.5.3 **A case study: data mining technique applied to a railway tunnel**

The proposed ensemble-based change-point method is applied to a database of real-time recorded displacements of a railway tunnel, which is subjected to electrification works. Particularly, during the electrification works, the track and the ballast of the rail are removed in order to excavate the sub-formation towards a new lowered level of the track, which provides the necessary clearance for the OLE system. However, when the track and the ballast are removed, the tunnel can start to converge due to changes of its support. A real-time SHM system is thus needed with the aim of monitoring the behaviour of the tunnel. A large amount of data is available from the SHM measurement system. Hence, a robust and rapid analysis of the recorded displacements of the tunnel is needed, in order to eventually identify unexpected changes of the behaviour of the tunnel. With this aim, a data mining procedure is

proposed aiming to detect unexpected displacements of the tunnel during the works, by pointing out the time duration and the work activity at the tunnel at the moment of the unexpected behaviour. The proposed method relies on three steps:

1. **Step 1.** A data pre-processing process that aims to delete the noise of the measurements.
2. **Step 2.** A feature definition and selection process are carried out, in order to identify, by the means of a K-means clustering algorithm, the locations where unexpected tunnel behaviour is measured.
3. **Step 3.** The critical behaviour is analysed by the means of the proposed ensemble-based change-point detection method, with the aim of identifying the duration of the unexpected variation of the tunnel displacements. The work activities that are carried out at the tunnel site at that moment are also provided.

The electrification works are presented in section 5.5.3.1, and each step of the analysis in discussed in the following section, by presenting step 1 in section 5.5.3.2, step 2 in section 5.5.3.3 and, step 3 in section 5.5.3.5.

Finally, it should be noted that if a large database of bridge behaviour were available, and as a consequence a large number of optimal HI values could be calculated to represent the evolution of the health state of the bridge over time, the proposed method would be applied with the same aforementioned steps. In fact, if a high number of optimal HI values were available, such values would show oscillations due to noise of the data and biased assessment of the optimal HI. Therefore, Step 1 would be applied to smooth the optimal HI pattern over time. Similarly, when multiple sensors are used to monitor a bridge, Step 2 would be used to identify which sensors monitored a change of the bridge health state, by identifying the sensors with the highest HI value. Step 3 would be finally adopted to identify the time when the HI changes in order to point out changes of the bridge health state.

5.5.3.1 **Introduction to the tunnel electrification works and the SHM system**

The electrification process of the UK railway network aims to develop a cheaper and cleaner railway system. For example, a reduction of maintenance activities is expected due to less wear of the railway track caused by electric trains, which are lighter than diesel trains, and also carbon-free journeys are provided by electric trains [Baxter, 2015]. One of the biggest challenges of the electrification process is the

installation of the Overhead Line Equipment (OLE) system on aging railway lines. Figure 5-12(a) shows a tunnel where the OLE system cannot be installed. The following three main activities are scheduled in order to install the OLE: *i)* to remove the track, sleepers and ballast; *ii)* to excavate into the sub-formation in order to obtain a new lowered ground; *iii)* to re-establish the ballast, sleepers and track to the new lower level that provides the necessary clearance for the OLE system. The works are carried out at intervals between 20 to 100 meters on the approach of the tunnel and inside the tunnel, in order to avoid a sudden sharp step in the track level. During these works, a real-time monitoring system is needed in order to continuously monitor the behaviour of the tunnel, by comparing the real convergence movements of the tunnel with those predicted by an FEM [Ordoñez et al., 2016]. The convergence of the tunnel can be measured by the means of optical and mechanical measurement systems: the former can rely on total stations and laser scan systems [Lato & Diederichs, 2014], whereas the latter can use fiber optical sensors [Mohamad et al., 2012]. However, the electrification works are carried out by working on two sets of tracks at different times. For example, whilst the track on the right hand-side of the tunnel is lowered, the track on the left hand-side needs to be accessible by trains in order to remove the ballast and move work materials. A measurement system that requires line-of sight within the tunnel or across the tunnel, such as laser distance measurement or total station, cannot be adopted. For these reasons, Shape Accel Array (SAA) sensors [Abdoun et al., 2009] are chosen by the contractor of the monitoring, which was appointed to study and install a monitoring system of the tunnel. Ten SAA sensors are installed within the first 100 meters of the tunnel, spaced at regular intervals along the tunnel length, in order to monitor a critical area of the tunnel where a void behind a section of the tunnel wall is discovered. Each SAA sensor is made of 23 orthogonally aligned accelerometers. Particularly, the sensors provide the relative displacement of the tunnel with respect to a reference point that measures zero always and has been numbered as sensor zero, as shown in Figure 5-12(b). The frequency of the sensors is changed based on the type of the works that are carried out on the site, i.e. when the electrification works are carried out within the tunnel, the frequency is higher than when the works are carried out on the approaching of the tunnel. However, in this case-study a measurement of the displacement of the tunnel is provided for each hour, and, as a result, the frequency of the SAA is constant. An illustration of SAA sensor, which is composed of 23 accelerometers installed on the control points of the tunnel

perimeter, is sketched in Figure 5-12(b), where the dotted line represents the SAA sensor. The available database, which is analysed by the proposed method, consists of the hourly measurements of the 230 sensors over a real-time monitoring period of 40 days.

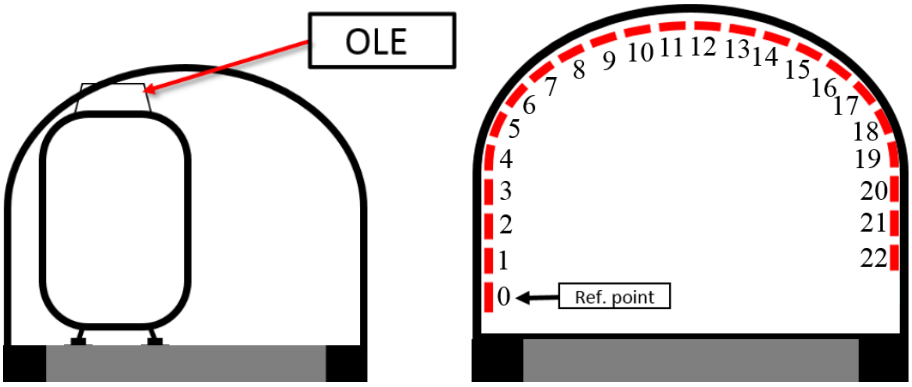

(a) (b)

Figure 5-12. *Example of clearance problem (a), and SAA monitoring system (b)*

5.5.3.2 **Step 1 - Pre-processing of the displacements of the tunnel**

A pre-processing of the measured displacements is needed in order to correct an off-set value problem of the sensors, which can occur during the monitoring period. The off-set problem can be caused by accidental knocks of the sensor during the works, and as a result, it needs to be corrected. The pre-processing is carried out by assessing the difference between two consecutive measurements of the tunnel displacements, which are recorded by the same sensor. Indeed, the analysis of the expected tunnel behaviour, which has been carried out by the experts of the works contractor by using an FE model, showed that the expected displacement of the tunnel should remain around the value of zero during each phase of the works. However, if the tunnel would converge, the displacement would increase at a rate of 0.001 mm/h. The experts suggested that if the tunnel displacement increases in one hour more than 0.3 mm, i.e. the difference between two consecutive measurements of the tunnel displacement provided by the same sensor is higher than 0.3 mm, an off-set problem of the sensor has occurred. The measurements need to be corrected by restoring the off-set of the previous hours accordingly. For example, Figure 5-13(a) shows the raw data provided by a sensor with a wrong off-set value at time 578 h, where the displacement of the tunnel jumps from -0.56mm to 16.14mm in one hour. This behaviour is extremely unlikely to be caused by a real movement of the tunnel, and, more likely, it is caused

by a knock of the sensor during the works. The off-set problem of the displacements leads to an incorrect assessment of the health condition of the tunnel. A pre-processing procedure is needed in order to re-establish the correct value of the displacement of the tunnel. Figure 5-13(b) depicts the processed displacement, where the wrong off-set at time 578h is removed by adding an off-set of -15.58 mm (d_{577} - d_{578} = -15.58mm) at time 578h. A pre-processing analysis is carried out on the displacements of the whole database, in order to correct the off-set problem, and consequently analyse the correct behaviour of the tunnel. Similarly, Figure 5-13(c) shows an off-set error where the relative displacement drops at time 588h from -0.04mm to -2.6mm. After the pre-processing of the data the correct displacement of the tunnel can be analysed, as shown in Figure 5-13(d).

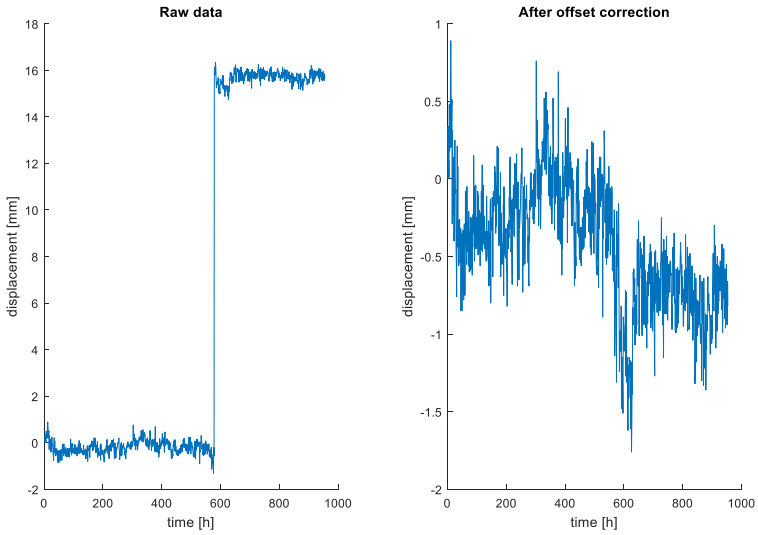

(a) (b)

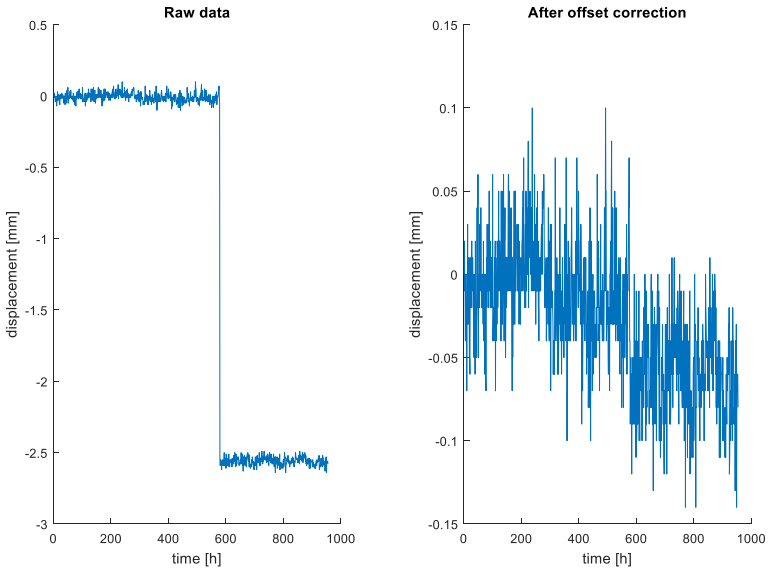

(c) (d)

Figure 5-13*. Displacements before (a-c) and after the off-set correction (b-d)*

5.5.3.3 **Step 2 - Identification of critical location of the tunnel**

In order to point out the critical locations of the tunnel, which need to be analysed by the means of the proposed ensemble-based change-point detection method, a feature definition and selection process is developed, as shown in Figure 5-14. In this way, the critical locations can be identified by selecting the features that optimize the performance of a K-means clustering algorithm. The displacements of each SAA in the tunnel are used as an input to a feature definition problem, where 11 statistical features (such as mean value, standard deviation, peak value, minimum, kurtosis, skewness, root mean square, median, interquartile range, 5% and 95% percentile) of the displacements of the tunnel are evaluated. The 11 statistical features of the displacement of each SAA sensor are then used as an input to an iterative process, which aims to optimize the performance of a K-means clustering in terms of the compactness and separation of the clusters. The iterative process aims to maximize the silhouette index [Rousseeuw, 1987] of the tunnel behaviour belonging to each cluster, by grouping similar behaviour of the tunnel in the same cluster (compactness), and dissimilar behaviour in different clusters (separation). A group of candidate optimal features is selected by a Genetic Algorithm (GA) engine [Di Maio et al., 2016], and then it is used as an input to the K-means algorithm, where the features are grouped by evaluating the different number of clusters (the number of cluster is assumed to be between 2 and 5). The performance of the clustering algorithm is evaluated by

assessing the silhouette index of the clusters, i.e. for each behaviour of a cluster, the silhouette index is computed by assessing its similarity with the other behaviours of the same cluster (compactness) compared to those of other clusters (separation). The iterative process is repeated until the silhouette index is maximized, and thus, the optimal features and the clusters are identified.

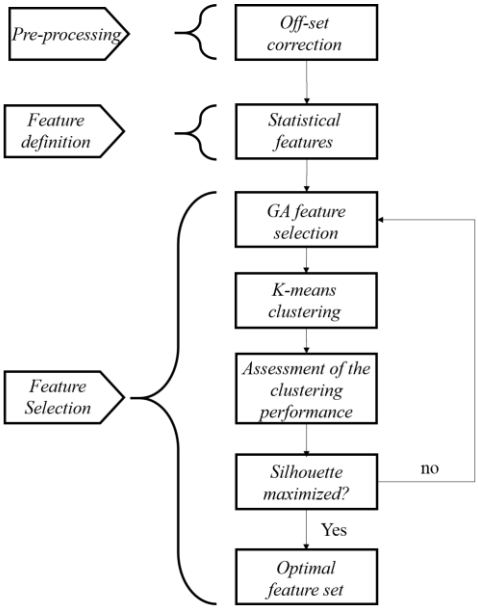

Figure 5-14. *Feature definition and selection process*

7 of the 10 SAAs, which are installed along the tunnel, show displacements that are around the value of zero for most of the time of the observation, or slow increase over time of the works by respecting the prediction of the FE model. For that reason, these SAAs are excluded from further analysis. On the contrary, 3 SAAs show unexpected behaviour of the tunnel, and they need to be thoroughly analysed by the means of the proposed change-point method. In this way, we can investigate when and why the tunnel started to depart from the predicted displacement. The three critical SAAs are installed at 30, 40, and 80 meters inside the tunnel, respectively. Figure 5-15 and Figure 5-16 show the optimal features and clusters for the SAAs 30 and 80, by highlighting that the optimal number of clusters for each critical SAA is 5. The optimal set of features is different for each critical SAAs, i.e. the different behaviour of the tunnel, which is recorded by different SAA sensors, is clustered optimally by different statistical features.

SAA installed 30m inside the tunnel (SAA30)

Figure 5-15(a) shows that the standard deviation, the peak value and the median are the best features in order to cluster the measurements of the tunnel recorded by the SAA installed 30m inside the tunnel. The most critical clusters are those with the highest values of these features, i.e. cluster 1, 3 and 4, which are represented by circles, points and pointing-up triangles respectively in Figure 5-15 (a). Accordingly, the measurements of the tunnel, which have the highest variability, the maximum value of displacement and median, are those belonging to the most critical clusters, as shown in Figure 5-15 (b), where the displacements of clusters 1, 3 and 4 show an unexpected fast increase at the beginning of the works. The displacements of the tunnel, Figure 5-15(b), are reported in order to verify the results of the K-means clustering in identifying the most critical sensors of the tunnel, which are further analysed in Step 3. Clusters 1, 3 and 4 (and the related sensors, as shown in Figure 5-15(b)) require to be analysed with the proposed ensemble-based change-point detection method, in order to detect the exact point when the tunnel started to converge rapidly. The duration of this unexpected behaviour and the works that are carried out at that time also need to be identified.

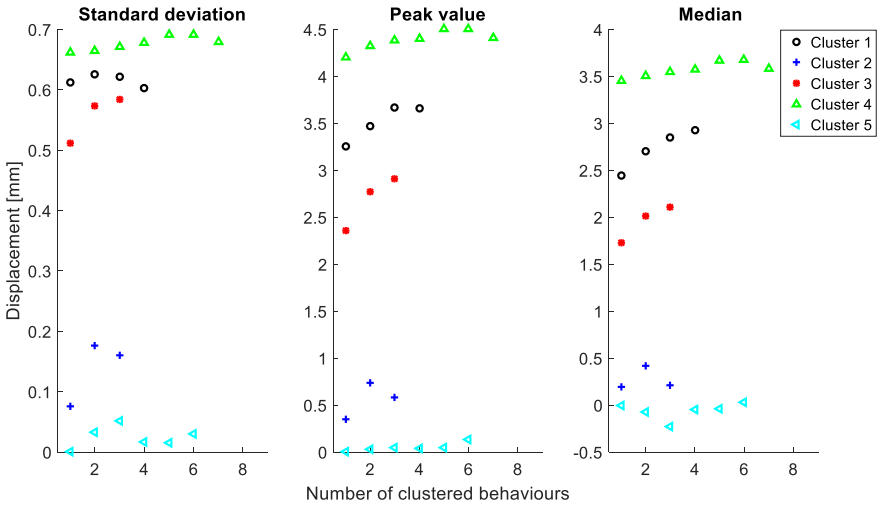

(a)

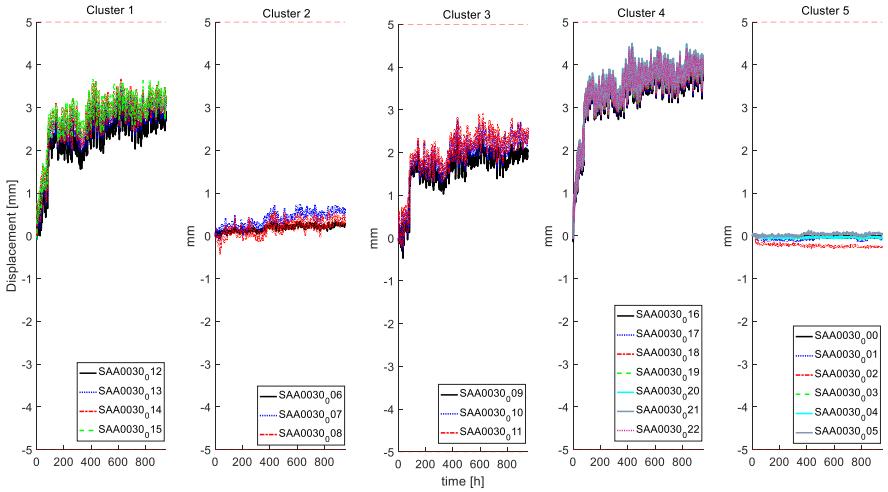

(b)

Figure 5-15. *Optimal features (a) and grouped behaviours of the tunnel (b) measured by the SAA installed 30m inside the tunnel*

SAA installed 80m inside the tunnel (SAA80)

Unexpected behaviours of the tunnel are also measured by the SAA installed at 80 meters inside the tunnel. For this SAA, the optimal features that allow to obtain compact and well separated clusters are the mean value, the root mean square and the median of the displacements. Therefore, the most critical clusters are those with the extreme values of these features, as shown by circles, points, pointing-up and pointing-backwards triangles in Figure 5-16(a) for clusters 1, 3, 4 and 5, respectively. The tunnel behaviours that belong to these four clusters show an increase of the convergence of the tunnel at the beginning of the works, and consequently the analysis with the ensemble-based change-point detection method of these behaviours is needed.

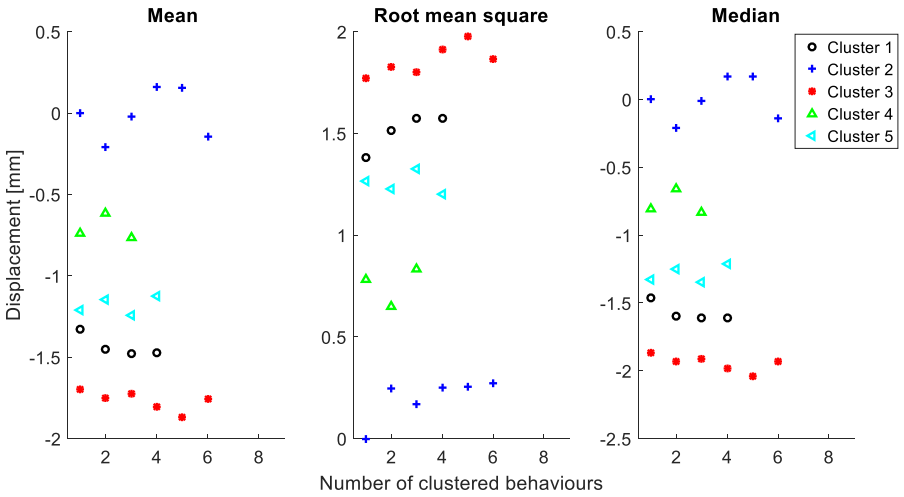

(a)

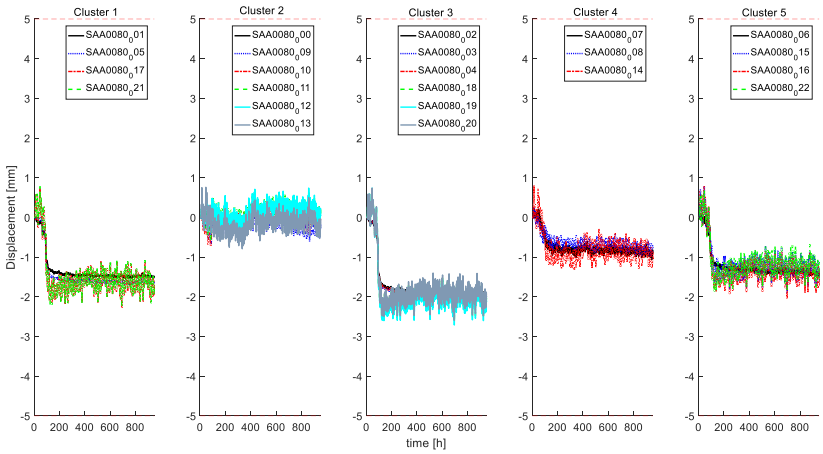

(b)

Figure 5-16. *Optimal features (a) and clustered behaviours of the tunnel (b) measured by the SAA installed 80m inside the tunnel*

5.5.3.4 **Discussion about the identification of critical SAAs of the tunnel**

The critical locations of the tunnel, i.e. those SAA sensors that have measured unexpected displacement of the tunnel, are identified by developing the feature definition and selection problem. The identified critical behaviour is further analysed in order to identify the duration of the unexpected critical behaviour, and the kind of works that are carried out at the worksite at that time.

The characteristics of the identified locations of the tunnel are summarized in Table 5-5, where the optimal features, the number of critical clusters and sensors, and the location of the critical sensor in the SAA are described.

Table 5-5*. Analysis of the critical SAAs*

SAA location [meter]	**Optimal features**	**Number of critical clusters**	**Number of critical sensors**	**Numbering label of the critical sensors**
30	Standard deviation Peak value Median	3	14	From 9 to 22
40	Mean value Root mean square Median	3	13	From 7 to 13 and from 16 to 20
80	Mean value Root mean square Median	4	16	From 1 to 8 and from 14 to 22

The analysis of the critical clusters of the three SAAs shows that the sensors that have high numbering label (from 9 to 22), i.e. those on the right hand-side of the tunnel, as shown in Figure 5-12(b), are those with the higher value of displacement, as shown in Table 5-5. However, the SAA installed at 80m inside the tunnel, Figure 5-16(b), shows high values of displacement on both sides of the tunnel, and as a result the infrastructure of the tunnel might have unknown critical issues at this point. This common behaviour can mean that the works are carried out on the right-hand side of the tunnel, and as a result the displacement of the tunnel on the right hand-side is higher than on the left-hand side, due to the temporary lack of the track and the excavation process. However, such detail information is not available on the database of the work activities, as only the information about the main work activity (e.g. excavation of the zone between 80 and 100 meters) is available.

In what follows, the behaviour of the critical clusters, which are identified by using the feature definition and selection process, are analysed further, in order to point out the time of occurrence, the duration and the possible causes of the unexpected fast convergence of the tunnel.

5.5.3.5 **Step 3 – Change-point identification using the proposed ensemble-based methodology**

The measurements that have been identified to describe the critical behaviour of the tunnel are further analysed with the aim of identifying the time when the unexpected behaviour of the tunnel has started, its duration and pointing out its possible causes. The duration of the unexpected tunnel behaviour is identified by the means of the proposed ensemble-based change-point detection method, whose performance is compared with the results of each individual change-point method. Once the most critical change-point is identified, the works that are carried out at the tunnel site are investigated by automatically analysing the database of the work activities. However, hard copies of the spreadsheets of the works are usually used by the contractor of the works, and an electronic version is prepared only at a later date. Hence, some information about the works might be omitted. Other possible causes that can lead to unexpected behaviour of the tunnel, such as geophysics of the ground around the tunnel or geometry of the tunnel, are neglected due to the lack of such technical

information about the tunnel. The works that are carried out at the tunnel are investigated by using the results of each change-point algorithm.

In this case study, the values of the time constants Δ, Φ, Ω, and Θ, which have been introduced in section 5.5.2.2, are optimized by expert knowledge elicitation, and they are equal to -7h, 15h, 10h and 0.75, respectively.

In this thesis, two particular penalty functions are considered in order to detect change-points of the monitored variable:

- a cost function, *C*, that aims to detect change-points by identifying changes on the mean value of the monitored variable:

$$C(y_{(\tau_{j-1}+1):\tau_j}) = \frac{1}{m}\sum_{j=1}^{l+1}\sum_{q=\tau_{j-1}+1}^{\tau_j}\left(y_q - \bar{y}_j\right)^2 \tag{5-14}$$

  where $\bar{y}_j$ is the empirical mean value of the monitored behaviour of the tunnel in the segment *j*, y_q is the monitored variable of the tunnel at time *q*, *m* is the time duration of the monitored behaviour of the tunnel and τ_j is a change-point of the tunnel behaviour.

- a cost function, *C*, which aims to identify change-points of the tunnel behaviour by pointing out changes on the slope of the system behaviour by considering an autoregressive linear model for the PELT-based individual change-point method. The cost function is then defined as follows

$$C(y_{(\tau_{j-1}+1):\tau_j}) = \frac{3}{2}\log(\tau_j - \tau_{j-1}) + \frac{\tau_j - \tau_{j-1}}{2}\log(2\pi\sigma^*(1,\tau_{j-1}+1,\tau_j)^2) \tag{5-15}$$

  where σ^* is the estimation of the variance of the monitored data in the segment $[\tau_{j-1},\tau_j]$, i.e. $y_{(\tau_{j-1}+1):\tau_j}$, τ_j is a change-point of the tunnel behaviour.

In what follows, without loss of generality, among the critical sensors of the clusters that have been identified in section 5.5.3.3, two critical scenarios of the tunnel are presented, in order to discuss the performance of the proposed ensemble-based change-point method with respect to the individual change-point methods.

Change-point analysis of SAA30

Figure 5-17(a-1) shows the displacement measured by sensor SAA30_13 (i.e. the sensor number 13 of the SAA installed at 30m inside the tunnel). An increase of the displacements around time 100h is recorded, as shown in Figure 5-17(a-1). Figure 5-17(a) depicts the performance of each individual change-point method by comparing it with the result of the proposed ensemble-based method. Each individual change-point methods is able to point out this change-point generally, as shown in Figure 5-17(a-2), (a-3), (a-4) and (a-5) by the means of vertical lines and the probability of change being higher than $\Theta = 0.75$ for the RuLSIF method. The change-point is identified around time 130h by the RuLSIF method, which results to be at a later time than the actual initial change-point (Figure 5-17(a-2)). The CUSUM, the penalty cost-function-based and the PELT-based methods are able to identify the change-point effectively around time 80h, as shown in Figure 5-17(a-3), (a-4) and (a-5), respectively. However, each individual change-point method is not able to identify the duration of the unexpected behaviour of the tunnel, i.e. the time when the unexpected behaviour ends is not found. A second and small change-point around time 400h is identified by the CUSUM, the penalty cost-function-based and the PELT-based methods, Figure 5-17(a-3), (a-4) and (a-5), and a third one at time 600h by the CUSUM method (Figure 5-17(a-3)). The change-point at time 80h can be caused by the works that are carried out in the first 50m inside the tunnel. In a similar way, the change-point at time 130h, which is identified by the RuLSIF method, is due to the works in the first 50m inside the tunnel. The change-point at time 400h can be caused by work activities that are carried out at between 340 to 420m inside of the tunnel, as reported in the database of the work activities for that time. However, the change-point at time 400h is not the most critical change-point of the tunnel behaviour, which is the one where the tunnel shows the highest change of its convergence. The most critical change-point is not identified by each individual change-point algorithm, i.e. the start and ending time and the duration of the most critical change are not identified.

Oppositely, the proposed ensemble-based change-point method is able to identify the time when the tunnel started to converge rapidly at time 74h. At the same time, the final time of the unexpected behaviour, i.e. when the fast convergence of the tunnel ends, is pointed out at time 161h, as shown in Figure 5-17(a-6). The most critical unexpected behaviour of sensor SAA30_13, and its duration, is identified by the proposed method correctly, accordingly to the safety reports of the tunnel. The

proposed method provides the information of the most critical behaviour of the tunnel directly, i.e. the initial time and the duration of the most critical behaviour of the tunnel are provided by the ensemble-based method in a simple and clear way. In contrast, each individual change-point method provides the information of all the change-points of the tunnel, without assessing the duration and the criticalness of each change-point. The information of the time of occurrence of the most critical tunnel displacements is used to analyse the database of the works. Figure 5-17(b) shows the works that are carried out at the tunnel site at the start and end of the fast convergence of the tunnel. It can be observed that when the track and the ballast of the rail are removed in the first 50m inside the tunnel, the tunnel starts to converge rapidly. At the same time, the ground is being drained from the extra water. On the other hand, the fast convergence of the tunnel ends around 87h later, when the base stone process is started in order to fill-back the ground with new ballast. The works at the beginning of the most critical change of the tunnel behaviour can be identified correctly by using the information provided by the individual change-point algorithms. However, three out of four individual change-point methods do not provide information about the works that are carried out at the end of the critical behaviour of the tunnel, and the RuLSIF method provides this useful information. As a consequence, the individual change-point methods results depend on the choice of the method, and as a result, the reliability of the analysis can be jeopardized.

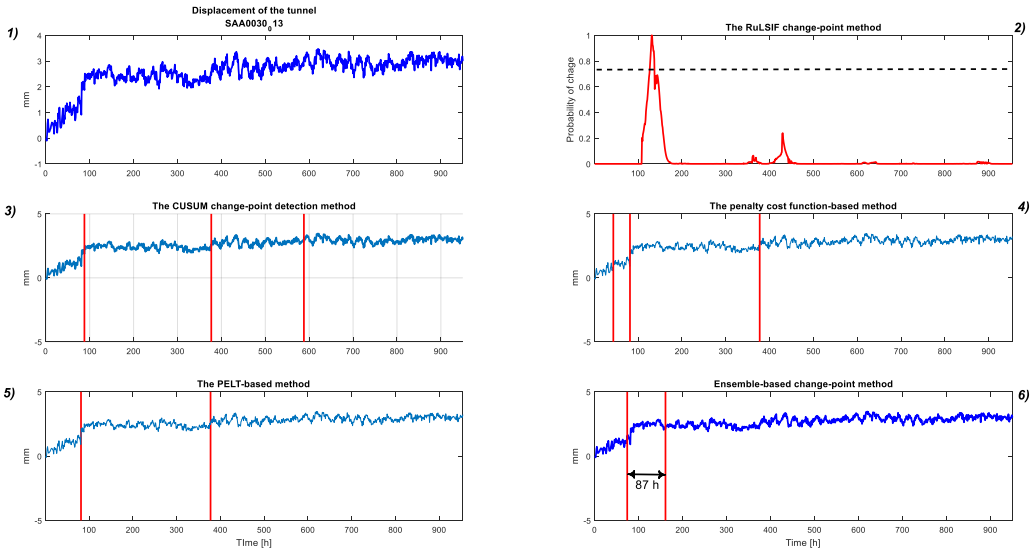

(a)

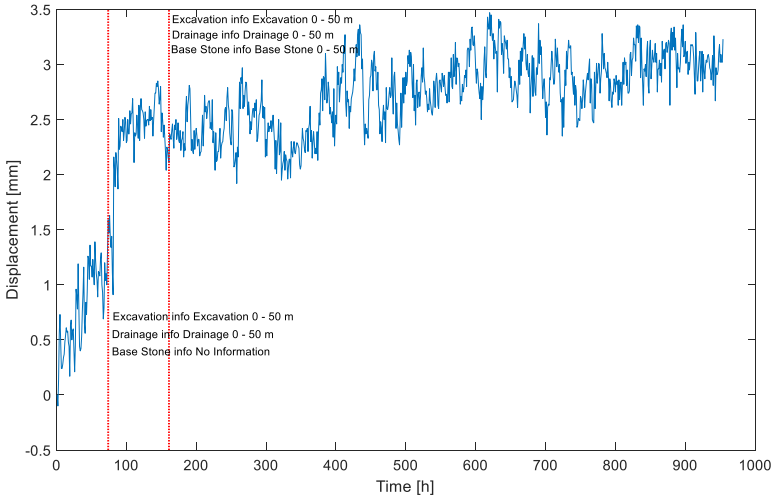

(b)

Figure 5-17. *Change-point detection of the SAA30_13 by using the proposed ensemble-based method and each individual change-point method (a), and the corresponding work activities (b)*

Change-point analysis of SAA80

An increase of the displacements of the tunnel is also measured by SAA80. The feature definition and selection process of Section 5.5.3.3 showed that the SAA80 is particularly critical, due to the fact that high values of displacement are measured all along the section of the tunnel. Indeed, almost all the sensors of the SAA80 measure an increase of the convergence of the tunnel at the beginning of the works. For example, Figure 5-18(a-1) shows the displacement recorded by sensor 19 of the SAA80. Therefore, the analysis of this behaviour with the ensemble-based change-point method is needed in order to point out the time duration of this unexpected fast convergence of the tunnel, and the works that are carried out at the tunnel at that time. Figure 5-18(a-2), (a-3), (a-4) and (a-5) show the analysis of the displacements of the tunnel by the means of each individual change-point method. Again, the RuLSIF method detects the change-point at a later time than the actual initial point of the unexpected behaviour, as shown in Figure 5-18(a-2). The CUSUM and the penalty cost-function-based agree in pointing out the first change-point around 50h (Figure 5-18(a-3) and (a-4)), whereas the PELT-based method identifies the first change-point around 80h, Figure 5-18(a-5). Furthermore, the CUSUM, the penalty cost-function-based and the PELT-based methods identifies a second change-point of the displacement of the tunnel around 100h, i.e. before that the tunnel stops to converge, as shown in Figure 5-18(a-3), (a-4) and (a-5), respectively. The analysis of the database of the work activities shows that no information is available at time 50h, when the first

change-point is identified by each individual change-point method. At time 100h, the works are carried out in the first 50m inside the tunnel, and, especially, the base stone process of this section has been started. Conversely, the proposed ensemble-based change-point method identifies a change-point interval that starts at time 50h and ends at time 169h (Figure 5-18(a-6)). In this way, the initial point where the tunnel displacement starts to increase, and the end point of the critical convergence are identified. The analysis of the database of the work activities shows that no information is available at the beginning of the critical behaviour of the tunnel. On the contrary, the tunnel stops to converge when the works are carried out at 50 to 100 meters inside the tunnel, as shown in Figure 5-18(b). The base stone process of this section of the tunnel is initiated when the fast convergence of the tunnel ends, and subsequently we can conclude that when the ground is back filled with new ballast, the tunnel stops to show the unexpected fast increase of the displacement. The works identified by using the results provided by the ensemble-based method are different from those retrieved by using the results of the individual change-point algorithms. Particularly, at time 100h, i.e. the change-point identified by the individual change-point methods, the behaviour of the tunnel is still changing rapidly, as shown in Figure 5-18, and the works are carried out in the first 50m inside the tunnel. In contrast, the ensemble-based method points out that the fast convergence of the tunnel ends at time 160h, when the works are carried out at 50 to 100 meters inside the tunnel.

Note that similar results in terms of the performance of the proposed method, described in this section, have also been achieved during the analysis of other critical sensors, as identified in Table 5-5 of Section 5.5.3.3.

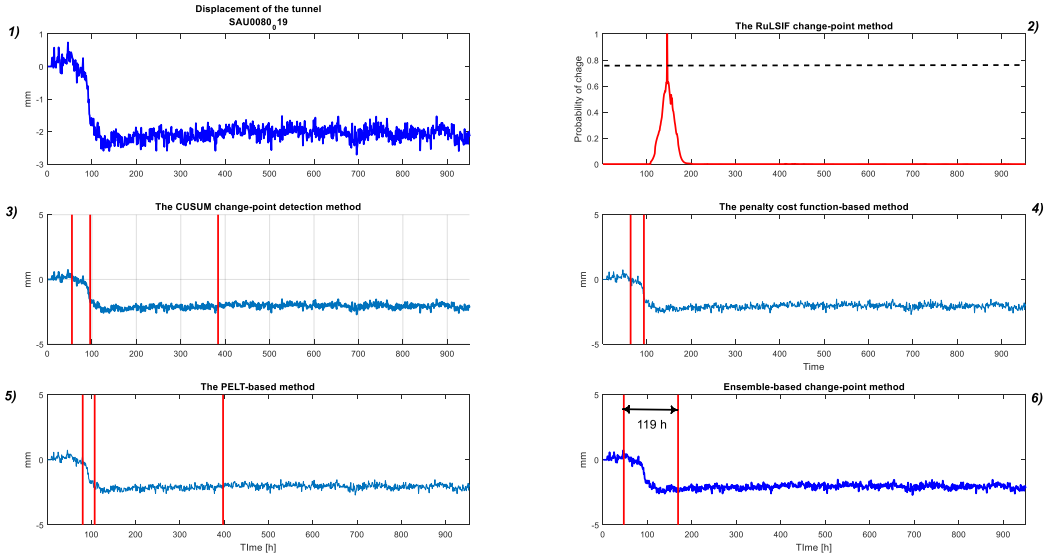

(a)

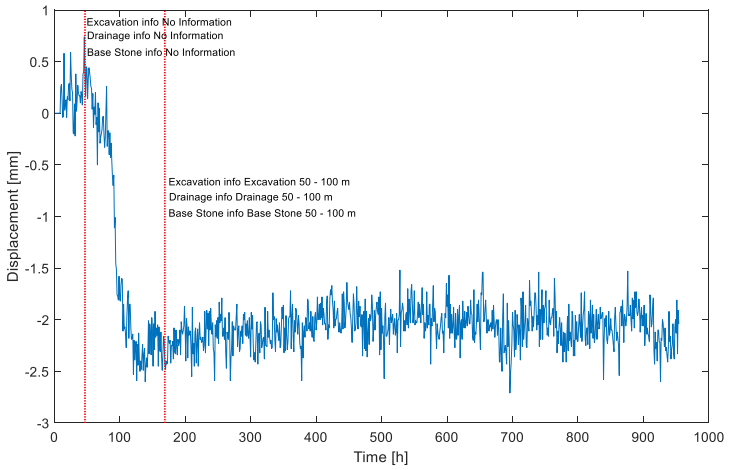

(b)

Figure 5-18. *Change-point detection of the SAA80_19 by using the proposed ensemble-based method and each individual change-point method (a), and the corresponding work activities (b).*

Discussion of the results

Table 5-6 shows the results of each individual change-point detection algorithm and the proposed ensemble-based method for the SAA 30, 40 and 80, i.e. the SAAs that show unexpected critical behaviour. It can be observed that the RuLSIF change-point method detects a change-point always a later time than the other change-point. This behaviour can be due to the optimization of the parameters, θ_i, which are learned from the data, and the definition of the size of the time window, *n*. The results of the CUSUM, penalty function and PELT change-point methods agree generally in all the three SAAs analysed. The individual change-point methods provide all the change-points of the tunnel behaviour, and so the most severe change of the tunnel behaviour

can be lost among all the change-points. Furthermore, individual change-point methods are unable to identify the duration of the most critical system behaviour. The works that might have caused the unexpected behaviour of the tunnel, which are identified by investigating the database of the work activities when a change-point is identified, demonstrate the usefulness of the proposed method. For example, the SAA30 shows the unexpected behaviour when the works are carried out in the first 50m inside the tunnel. Table 5-6 shows that the ensemble-based method is able to point out directly the works at the initial and end time of the most critical behaviour of the tunnel, whereas the individual change-point methods are not able to correctly identify the works at the initial and end time of the critical behaviour simultaneously. Indeed, the CUSUM, the penalty function and PELT are able to correctly detect only the works at the beginning of the critical unexpected behaviour, whilst the RuLSIF method is able to correctly detect only the works at the end of the unexpected critical behaviour. For this reason, the choice of an individual change-point algorithm can threaten the reliability and robustness of the data analysis, due to different results of each individual change-point detection method. The works that are identified for the SAA40 lead to similar a conclusion. In opposition, SAA80 shows that individual change-point methods are not able to point out the works correctly. In fact, each individual change-point detects the works in the first 50m inside the tunnel as a possible cause of the unexpected tunnel behaviour. However, the ensemble-based method detects that the works, which are carried out when the critical behaviour of the tunnel ends, are carried out between 50m and 100m inside the tunnel. This result, which is not acknowledged by the individual change-point methods, leads to conclude that a new equilibrium of the tunnel is reached due to the fact that the base stone process is initiated in the area where the SAA80 is installed.

Finally, the analysis of the three critical SAAs shows that all the critical SAAs show a common behaviour, i.e. a critical unexpected behaviour at the beginning of the works. This critical behaviour can be caused by the works that are carried out in the first 100m inside the tunnel, and, on the right-hand side of the tunnel.

Table 5-6. *Result for each change-point detection strategy.*

	Change-point algorithm	**Identified change-points [h]**	**Change duration [h]**	**Work activities**		
				Excavation	Drainage	Base-stone
SAA30_13	RuLSIF	From 125 to 167	Not provided	0-50m	0-50m	0-50m
	CUSUM	88	Not provided	0-50m	0-50m	0-50m
		377	Not provided	360-420m	360-380m	340-360m
		588	Not provided	620-680	580-620m	580-620m
	Penalty function	43	Not provided	No info	No info	No info
		81	Not provided	0-50m	0-50m	0-50m
		377	Not provided	360-420m	360-380m	340-360m
	PELT	81	Not provided	0-50m	0-50m	0-50m
		377	Not provided	360-420m	360-380m	340-360m
	Ensemble	74	87	0-50m	0-50m	0-50m
		161		0-50m	0-50m	0-50m
SAA40_08	RuLSIF	From 111 to 123	Not provided	0-50m	0-50m	0-50m
	CUSUM	42	Not provided	No info	No info	No info
		63	Not provided	No info	No info	No info
		625	Not provided	No info	No info	No info
	Penalty function	47.5	Not provided	No info	No info	No info
		58.5	Not provided	No info	No info	No info
		624.5	Not provided	No info	No info	No info
	PELT	33.5	Not provided	No info	No info	No info
		64.5	Not provided	0-50m	No info	No info
	Ensemble	26	105	No info	No info	No info
		131		0-50m	0-50m	0-50m
SAA80_19	RuLSIF	From 152 to 156	Not provided	0-50m	0-50m	0-50m
	CUSUM	57	Not provided	No info	No info	No info
		96	Not provided	0-50m	0-50m	0-50m
		384	Not provided	380-420m	380-400m	No info
	Penalty function	63.5	Not provided	0-50m	No info	No info
		93.5	Not provided	0-50m	0-50m	0-50m

	PELT	80.5	Not provided	0-50m	0-50m	No info
		107.5	Not provided	0-50m	0-50m	0-50m
		397.5	Not provided	380-400m	420-440m	No info
	Ensemble	50	119	No info	No info	No info
		169		50-100m	50-100m	50-100m

5.5.4 **Summary of the proposed ensemble-based change-point detection method**

An ensemble-based change-point detection method is proposed in order to identify and diagnose the most critical change of the behaviour of a railway infrastructure. For example, the proposed method can be applied both to bridge vibration behaviour with the aim of assessing when the HI of the bridge changed over time, and to infrastructure that shows monotonic behaviour over time, such as the presented tunnel case study. The proposed ensemble-based change-point detection method has been developed to overcome the limitation of the individual change-point methods. In fact, individual change-point methods can only detect abrupt changes of the behaviour of the infrastructure, without providing information regarding the severity and the duration of the identified change-points of the infrastructure behaviour.

The behaviour of a tunnel during renewal activities has been analysed to assess the performance of the proposed method. The proposed ensemble-based change-point method outperforms each individual change-point method, in identifying the most critical behaviour of the tunnel, by pointing out the time, when the tunnel starts to converge rapidly, its duration and possible causes. Particularly, the proposed method outperforms each individual method when severe unexpected behaviour is experienced, i.e. when the displacements of the tunnel increase suddenly and rapidly.

The ensemble-based change-point detection method, however, has some drawbacks:

- only the most critical change-point of the system is pointed out, without providing further information regarding other smaller change-points. Decision makers can be interested in identifying and analysing the most critical behaviour of the system firstly, and once immediate actions are taken, minor changes in the system behaviour can also be analysed. In that case, a comprehensive analysis of the data can be carried out and all the vulnerabilities of the system can be identified. If all the change-points were to be analysed, the proposed ensemble-based change-point method can be used for this purpose by modifying its rules appropriately. For example, a decision maker

can look for each change-point that has been identified by at least two individual change-point methods, rather than for the change-point where the tunnel behaviour experiences its highest variation.

- the performance of the proposed method relies on the assessment of time-constants, i.e. Δ, Φ, Ω, which are defined by using an expert knowledge elicitation process. When the time constants are set, the identification of the change-points depends on the values of these parameters, and consequently the expert knowledge elicitation process can lead to misleading results if the considered system is new and unknown for the experts.

5.6 Summary

A method to merge the expert elicitation process with the analysis of the bridge behaviour has been proposed, with the aim of updating the CPTs of a BBN in a reliable and continuous manner. The CPT values are updated by considering an α-weighted combination of the conditional probabilities obtained by analysing both: *i)* the expert knowledge; and *ii)* the bridge behaviour data. Particularly, the latter analysis requires data of different health states of the bridge elements to define a CDF for each health state of the bridge. An approach to assess the CDF by relying on the analysis of the HI of the bridge has been proposed by fitting a set of possible pdfs and choosing the optimal distribution by evaluating the goodness of the fit.

In addition, an ensemble-based change-point detection method has been introduced in order to analyse a database of past infrastructure behaviour to identify when the health state of the infrastructure changed. The results of the proposed ensemble-based method can then be used to analyse different health states of the infrastructure, and thus define the CDF of each health state to update the CPTs of a BBN.

In what follows, the CDFs that have been defined in this chapter are used in order to update the CPTs of a BBN continuously, by taking account of the actual health state of the bridge elements in Chapter 6 . The performance of the BBN by using the proposed method to update the CPTs and the performance without using the proposed method is evaluated in order to investigate the potential of the CPTs updating strategy are also analysed in Chapter 6 .

Chapter 6 The application of the BBN method to the in-field post-tensioned bridge

6.1 Introduction

In this chapter, the BBN approach that is introduced in Chapter 3 is applied to the in-field post-tensioned bridge, which is presented in section 4.3.1. In this way, the condition monitoring and damage detection capability of the BBN is verified by assessing the health state of the bridge and its elements.

The bridge behaviour data of group 2, which are not labelled (i.e. the health state of the bridge elements is assumed to be unknown), are used as an input to the data analysis methodology of section 4.2, in order to assess the optimal HI of the bridge. The HI is then used as an input to the BBN to assess the health state of the whole bridge. Therefore, a bridge manager, that is monitoring the bridge health state by the means of the proposed BBN, is able to find changes of the bridge health state, by identifying the degrading elements of the bridge.

The BBN of the bridge is developed by following the step-by-step procedure presented in section 3.3, whereas different strategies to define the CPTs of the BBN are analysed in Chapter 5 . Particularly, the CPTs are firstly defined by adopting an expert knowledge elicitation process, and then the proposed strategy to update the CPTs by merging expert judgements and bridge behaviour analysis is used.

The developed BBN is presented in section 6.2, whereas the performance of the BBN by using different CPT definition strategies is analysed in section 6.3. Conclusions and remarks are discussed in section 6.4.

6.2 The BBN of the post-tensioned bridge

In section 4.3.1, the post-tensioned concrete bridge is described. Before introducing the BBN that aims to monitor and assess the health state of the bridge, the main characteristics of the bridge are recalled. The post-tensioned concrete bridge has the main span of 32 m and two side spans of 12 m each. The bridge was subject to a vibration measurement test before being demolished to obtain the bridge vibration behaviour in different health states. The acceleration of the bridge was monitored by a

measurement system made of 2 reference sensors, with a sampling rate of 100 Hz, and they were installed at 17.6m and 22.6m from the left hand side end of the bridge, as shown in Figure 4-2b. Five different health states of the bridge elements, 1 healthy state and 4 damage states, are considered in this thesis, by dividing the available 20 minutes of data of each health state into two groups: *a)* the first group (group 1) contains 10 minutes of data, and has been used to both introduce the data analysis methodology of chapter 4 and identify the CDFs (Chapter 5) that are used to update the CPTs of the BBN; *b)* the second group (group 2), which is made of 10 minutes of data, has been used to verify the performance of the NFC (in section 4.5) and is used in this section to verify the performance of the BBN (Chapter 6). This second group of data is not labelled, i.e. the class of the data is not known a-priori, and thus the ability of the proposed BBN method in assessing the health state of the bridge can be verified.

The BBN of the post-tensioned bridge is developed by defining the BBN structure (section 6.2.1) and then completing the CPTs (section 6.2.2).

6.2.1 The BBN model building

The development of the structure of the BBN of the post-tensioned bridge is carried out by following the 7 steps proposed in Section 3.3:

1. **Identify the type of the bridge and its major and minor elements of interest.** The bridge is a post-tensioned concrete structure, and its major elements can be identified as the three spans of the bridge and the piers. The minor elements of the bridge are represented by smaller sections of the major elements: the deck of the bridge, which is made of the three spans, is arbitrarily divided into 10 smaller elements of length 5.6m each. As a result, each element of length 5.6m represents a minor element of the bridge. Hereafter, the condition of the deck is assumed to represent the health state of the whole bridge. This assumption is made due to the fact that the two sensors that monitor the behaviour of the bridge are installed on the deck. Therefore, information about the health state of the piers is obtained by analysing the nodes of the BBN at the pier location.
2. **Define the BBN structure.** The deck is made of 3 spans, two side spans of 12m and the main span of 32m. Therefore, 3 nodes are used in the BBN framework to characterize these three major elements, as shown in Figure 6-1.

The three major elements are composed of minor elements, which represent a 5.6m long section of the deck. As a consequence, each *E_j* node in Figure 6-1 represents the condition of the minor elements *j*, where *j*=1, 2, …, 10. The nodes *E_2* and *E_3* represent the nodes at the location of the left pier of the bridge, whereas nodes *E_8* and *E_9* represent the minor elements at the location of the right pier of the bridge. Similarly, the node *E_4* and the node *E_5* represent the node at the location of the two accelerometers. The directed arcs depart from the minor elements of the bridge (*E_j* nodes), and end at the nodes representing the major elements of the bridge (*Side_span_left*, *Main_span* and *Side_span_right*). The major elements influence the health state of the whole deck, and consequently they are parents of the node representing the condition of the whole deck, the *Deck* node in Figure 6-1, which is assumed to represent the health state of the whole bridge.

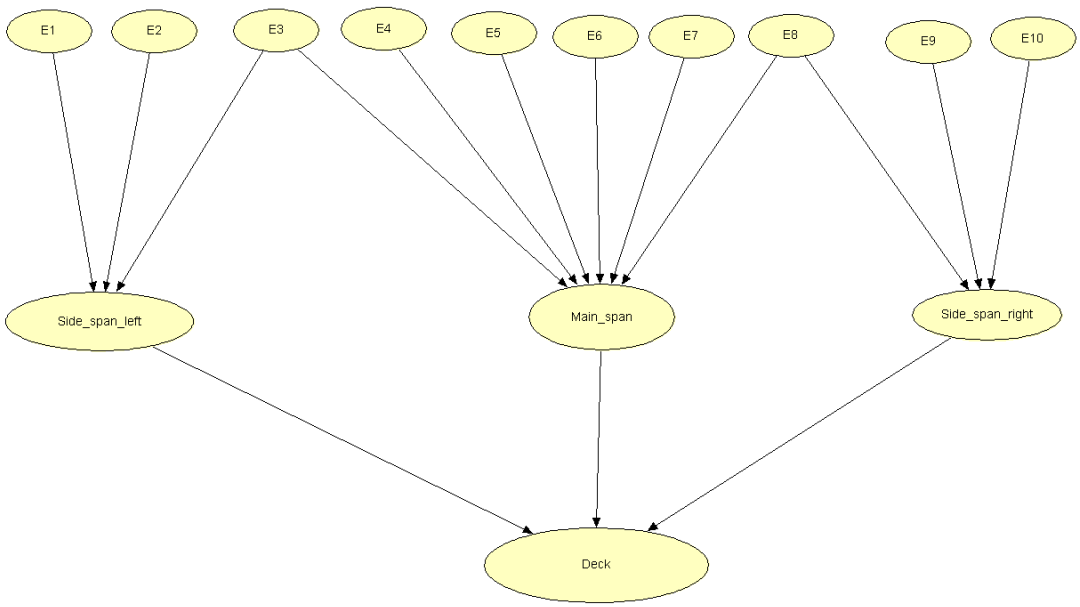

Figure 6-1. *First BBN draft of the post-tensioned concrete bridge*

3. **Upgrade the BBN model to take account of interdependencies among major/minor elements**. A more detailed BBN is developed by considering possible influence among minor (major) elements. Further nodes are introduced into the BBN, as shown in Figure 6-2 by the nodes ending with "***_1***". For example, the nodes *E_j_1* are introduced to assess the interdependencies among the minor elements of the deck. It should be noted that the interdependencies among major elements are evaluated at the minor

elements level, using *E_3_1* node to represent the interdependencies between the main and left-side spans, and node *E_8_1* for the influences of the main span on the right-side span.

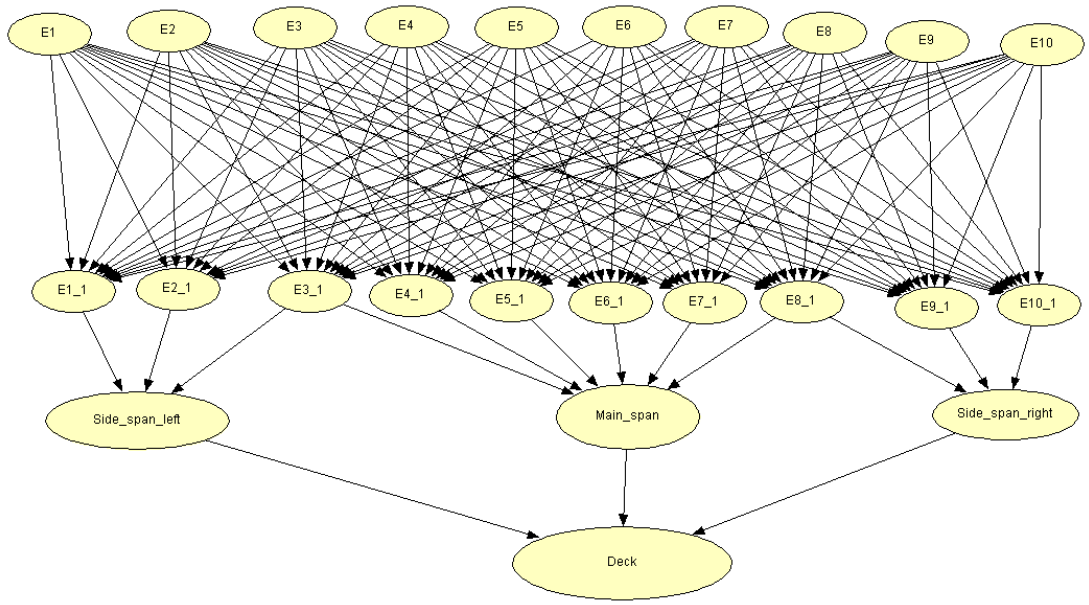

Figure 6-2. *BBN that considers the interdependencies among minor (major) bridge elements*

4. **Review the BBN structure by analysing the bridge behaviour.** This step aims to optimize the structure of the BBN and to delete unnecessary connections between nodes, and to eventually reduce the size of the BBN by deleting nodes if their contribution to the health state of the bridge is negligible. Ideally, a database of bridge behaviour would be available to carry out this step. In fact, the analysis of the bridge behaviour in different health states of each bridge elements can provide information about the strength of the influence between different bridge elements. As a consequence, the structure of the BBN can be updated accordingly. In this case study, only the behaviour of the two minor elements of the bridge is directly monitored by the means of accelerometers. At the same time, the health state of only one bridge element (the left pier of the bridge, which is assumed to be represented by the elements 3 and 4 of the network, i.e. the smaller elements at the pier location) is modified. The analysis of the bridge behaviour (which has been discussed in section 4.3) shows that the two minor elements of the bridge at the sensor location are influenced by the changing health state of the pier. Therefore, the connection between the nodes at the location of the left pier, and the nodes at

the location of the two sensors is validated. Further analysis based on the data cannot be carried out, due to a lack of bridge behaviour data. However, the BBN of Figure 6-2 is a complex model, due to all the connections between the minor elements, which lead to large CPTs of the BBN. Subsequently, only connections between neighbour minor elements are considered. This assumption is based on the performance of both the BBN of the steel truss bridge (section 3.4) and of the beam-and-slab bridge (section 3.5.2), which have shown to be able to monitor and assess the health state of each bridge. Figure 6-3 shows the BBN structure after the bridge behaviour analysis and the abovementioned assumptions.

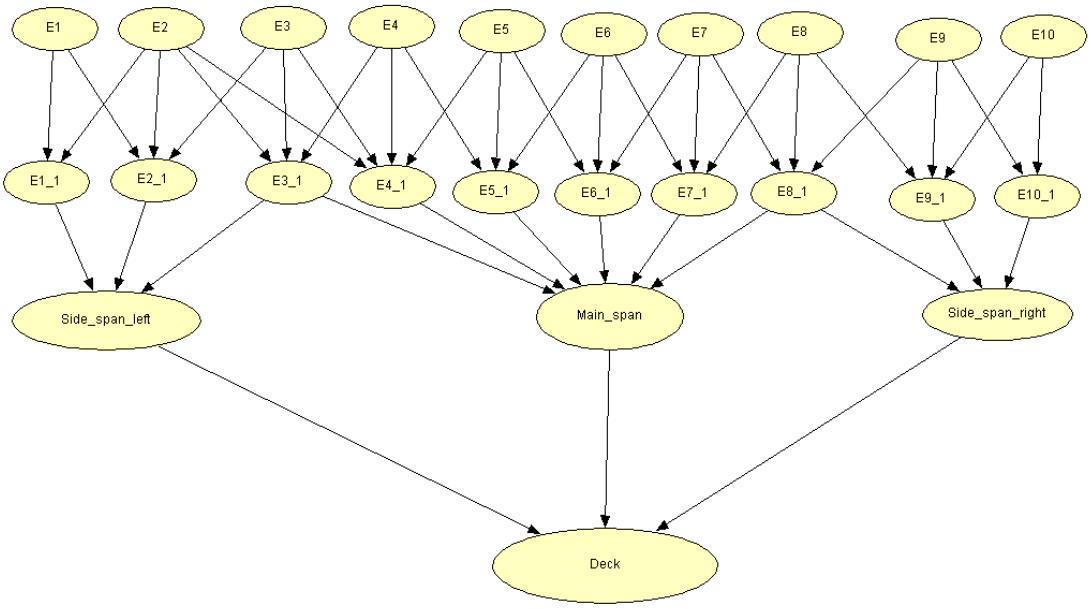

Figure 6-3. *Updated BBN of the post-tensioned bridge after the bridge behaviour analysis*

5. **Define nodes to represent the measurement system of the bridge.** The measurement system of the bridge is represented by two accelerometers that are installed at 17.6m and 22.6m from the left ending if the bridge, as shown in Figure 4-2. The two sensors are introduced into the BBN structure accordingly, as depicted in Figure 6-4. The nodes representing the 2 sensors are introduced as a parent of the minor elements on which the sensors are installed. Every time when evidence of the bridge vibration is available, it is analysed by the proposed data analysis methodology and the resulting optimal HI value is used as an input to the sensor nodes, which assess the health state

of the bridge element. Consequently, the health state of the bridge and its elements is updated accordingly.

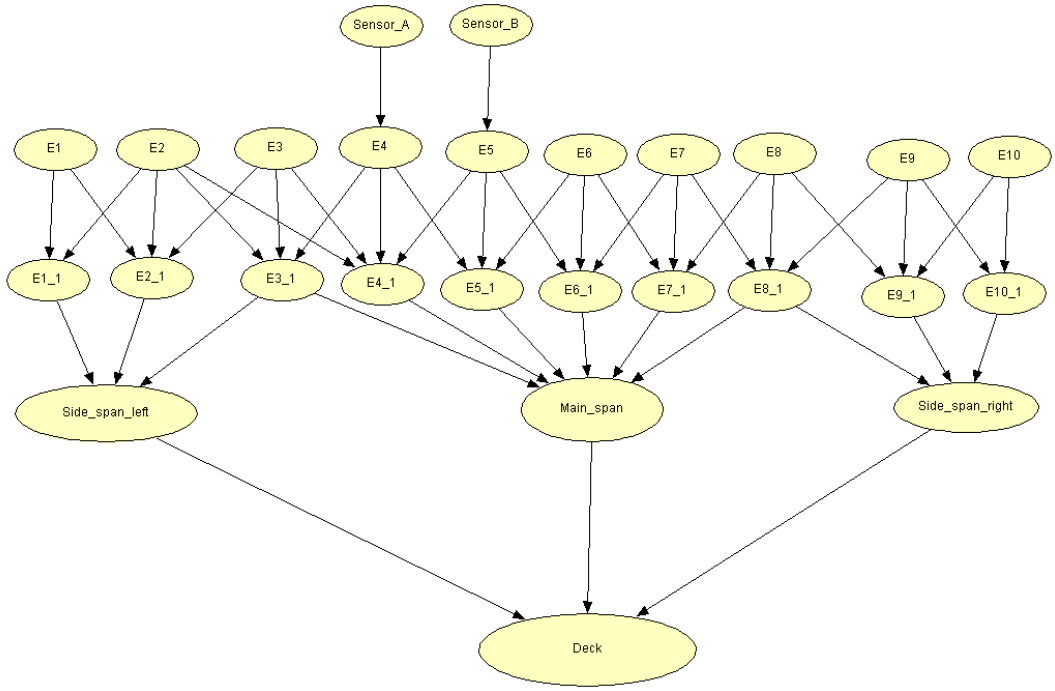

Figure 6-4. *Final BBN for condition monitoring and degradation diagnostics of the post-tensioned concrete bridge*

6. **Choose the number of states of each node.** As pointed out in Chapter 5, three mutually exclusive health states are defined for monitoring the health state of the post-tensioned bridge: *a)* a healthy state (H), where the elements of the post-tensioned bridge are in a good condition; *b)* a partially degraded state (PD), where the bridge experiences the damages described by class 3 and 4; *c)* a severely degraded state (SD), where the bridge experiences the damages described by class 5 and 6.
7. **Obtain the final BBN structure.** The final BBN for condition monitoring and degradation diagnostics of the post-tensioned concrete bridge is shown in Figure 6-4.

6.2.2 Development of the CPTs

The CPTs of the BBN are defined by adopting different strategies. At first, the CPTs are defined by adopting the expert knowledge elicitation process, described in Section 3.3.2. Then, the CPTs are updated by taking account of the health state of the bridge

elements, as described in section 5.2. The BBN is analysed by comparing its performance when both CPTs strategies are adopted

The expert knowledge elicitation process is assumed to be the same as presented in section 3.3.2. This assumption is needed due to a lack of experts to be interviewed about the post-tensioned concrete bridge. Such an assumption influences the assessment of the exact value of the probability of BBN nodes describing each state. However, the damage detection ability of the BBN is not influenced by this assumption, since the detection ability of the BBN depends on how the different states of the nodes are selected, rather than on the values the CPTs. As a consequence, this assumption allows to point out different health states of the bridge, and its elements, but it may impact the diagnostic ability of the BBN. Indeed, conservative results (such as a larger probability that the bridge is in a degraded health state than the actual health state of the bridge) or misleading results (such as a much lower probability that the bridge is in a degraded health state than the actual health state of the bridge) can be achieved due to this assumption. The updating process of the CPTs, however, is able to define the value of the conditional probabilities of the CPTs by taking account of the actual health state of the bridge elements. Consequently, the values of the updated CPTs are expected to provide an optimal assessment of the bridge health state, due to the fact that the actual health state of the bridge elements is considered during the definition of the CPTs. It should be noted that two sensors are available to monitor the behaviour of the bridge, and thus the CPTs updating strategy is performed for the two nodes where evidence are provided, i.e. nodes *E_4_1* and *E_5_1*.

Different strategies to define the CPTs are compared in what follows:

a. CPTs are defined by considering only the expert knowledge elicitation process.
b. CPTs are defined by considering the proposed updating strategy (section 5.2) with the weight of the linear combination $\alpha \in [0, 0.9]$ that varies over time, by taking account of the number of identified health states of the bridge elements and the monitoring time. In this way, the analysis of the bridge behaviour data has more importance than the expert knowledge elicitation process, due to the fact that α increases over time towards 0.9.
c. CPTs are defined by considering the proposed updating strategy (section 5.2) with the weight of the linear combination α that is constant and equals to 0.1. In this way, a possible conservative scenario is analysed by giving the more

importance to the expert knowledge rather than to the bridge behaviour analysis.

d. CPTs are defined by considering the proposed updating strategy (section 5.2) with the weight of the linear combination α that is constant and equals to 0.5. In this way, the expert knowledge elicitation process and the bridge behaviour analysis have the same importance.

The performance of the BBN in monitoring the health state of the post-tensioned bridge by using these four CPTs strategy is compared in terms of the conditional probability value of the most degraded elements of the bridge. Therefore, the aim of the comparison is to point out which strategy allows to describe the health state of the bridge, and its elements, in the most accurate way.

Finally, it is worth noting that the CDFs of the optimal HI for each sensor are used to updated the CPTs of the two minor nodes of the BBN: section 6.3.1 and section 6.3.2 show the performance of the BBN by using the CDFs that are retrieved by using the AICc to update the CPTs, and compare the performance of the BBN with the results of the BBN analysis when the CPTs are defined by using the expert knowledge elicitation process only. Then, in section 6.3.3, the performance of the BBN is evaluated by taking account of the CDFs that are retrieved by using the results of the K-S test. This latter performance of the BBN is compared to the results of the BBN that relies on the CDFs retrieved by using the AICc analysis.

6.3 BBN model usage for detection and diagnostics of bridge deterioration

The acceleration data are used as an input to the data analysis methodology presented in section 4.2, in order to assess the value of the optimal HI of the bridge. The value of the optimal HI is then used as an input to the BBN nodes, with the aim of assessing the health state of the whole bridge, by taking account of the health state of each element of the bridge.

The analysis of the BBN is presented by considering the bottom-up diagnostic process of the BBN, which allows a bridge manger to interact with the BBN to diagnose the cause of a change of the health state of the bridge. The step-by-step bottom-up diagnostic process is proposed in this section to describe the results of the BBN. In this way, the health state of the whole bridge is monitored and the causes of the change of its health state can be diagnosed.

The different strategies to update the CPTs of the BBN are analysed in what follows.

6.3.1 BBN performance when the CPTs are defined by considering the proposed updating strategy and α varies over time

The CPTs of nodes *E_4_1* and *E_5_1* are updated continuously by taking account of the health state of the bridge elements, and considering the CDFs that are retrieved by analysing the AICc. Therefore, the CDFs of Table 5-1 are used to update the CPTs. The CPTs are initially defined by adopting the expert knowledge elicitation process, and the initial CPTs of nodes *E_4_1* and *E_5_1* are presented in Table 6-1. The values of the CPTs during the proposed updating process is showed in section 6.3.2. Figure 6-5 shows the evolution of the health state of the whole bridge (Deck node in Figure 6-4) over time. At the beginning, the bridge is in the healthy condition due to the fact that the bridge has not been damaged yet. Consequently, the bridge is in the healthy state (grey area in Figure 6-5). The dashed vertical lines in Figure 6-5 represent the time when the bridge is damaged by cutting the left pier of the bridge: the first vertical dashed line at time 19min represents the partially degraded scenario of the bridge (i.e. damaged scenarios of class 3 and 4), whereas the second dashed line at time 34min represents the severely degraded scenarios (i.e. the damaged scenarios of class 5 and 6). Therefore, the increase of the probability of the partially degraded (PD) state and the severely degraded (SD) state at around time 15min (light and dark grey areas, respectively, in Figure 6-5) is due to noise of the data that leads to a misclassification of the HI value. When the data of the damaged bridge are monitored, at time 19min, the probability of the partially degraded (PD) state and the severely degraded (SD) increase (light and dark grey areas, respectively, in Figure 6-5). Finally, as new damage scenarios are inflicted to the bridge in order to increase the magnitude of the damage towards the SD state, the health state of the whole bridge slightly decreases, i.e. the yellow and red areas increase over time, as shown in Figure 6-5. Hence, the proposed BBN method is able to monitor the health state of the bridge over time, by detecting unexpected bridge behaviour as soon as it occurs.

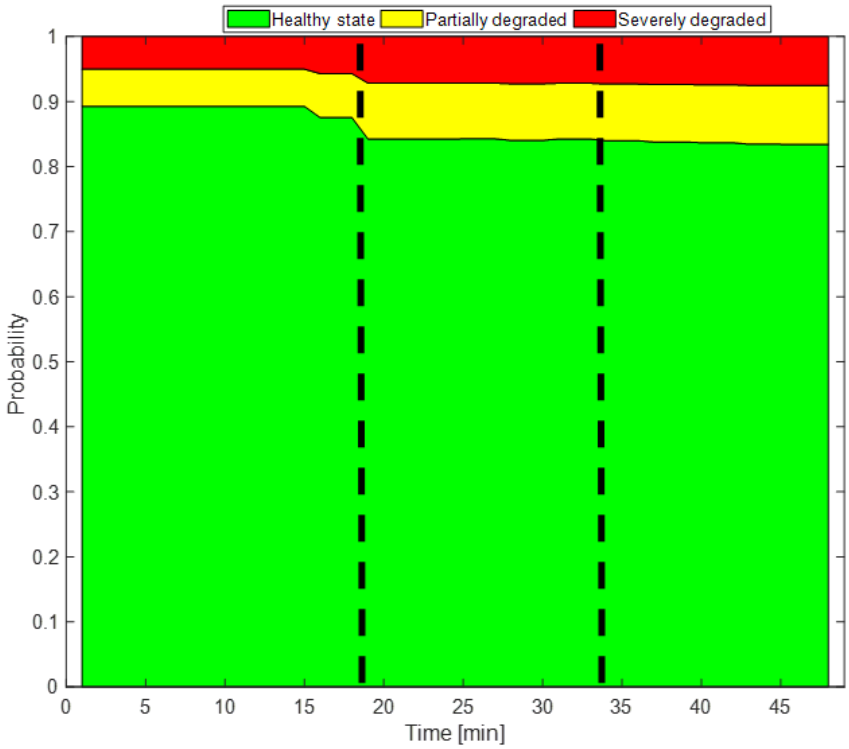

Figure 6-5. *Evolution over time of the health state of the whole bridge when* α *varies over time, as shown in Eq. (5-2) (Deck node)*

The BBN allows to diagnose the cause of the change of the bridge health state, by pointing out the evolution over time of the health state of the parent nodes of the *Deck* node (note that the *Deck* node represents the health state of the whole bridge). Figure 6-6 shows the evolution of the health states of the whole bridge (*Deck* node in Figure 6-4) and of its parent nodes: the left, main and right spans of the bridge, as shown in Figure 6-4. Figure 6-6 allows to directly identify that the left and main spans of the bridge are damaged, and that the main span is more degraded than the other major elements, i.e. the light and dark grey areas of *Main_span* node are higher than those of the other major elements. This result is because evidence of the bridge behaviour is provided by the two sensors that are installed on the main span of the bridge.

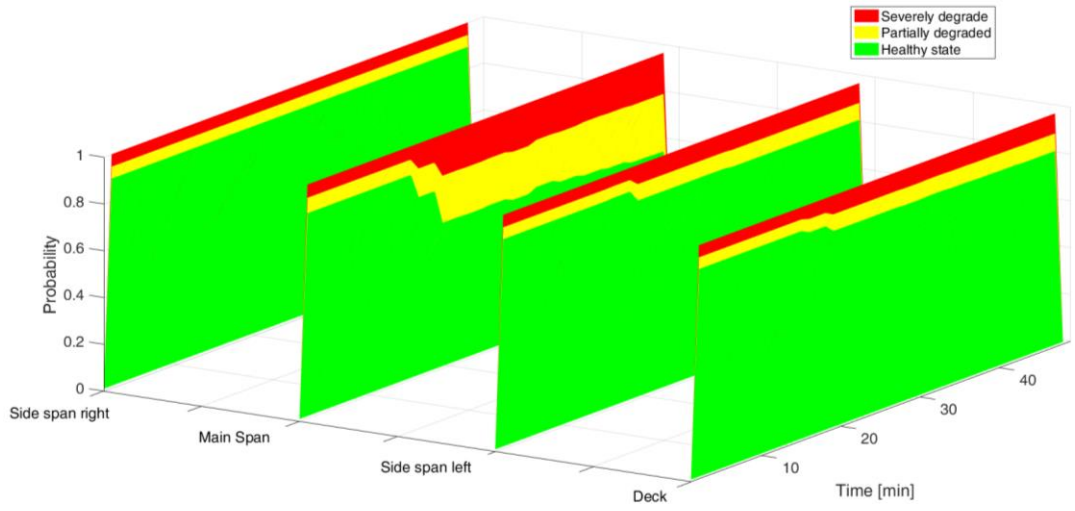

Figure 6-6. *Evolution over time of the health state of the whole bridge (Deck node) and its parent nodes, i.e. left, right and main span, when α varies over time, as shown in Eq. (5 2)*

The diagnostic property of the BBN allows to investigate the degradation level of the bridge elements at each level of the BBN. Figure 6-7 shows the evolution of the health state probabilities of the minor elements of the bridge, i.e. the 5.6m long segments of the deck of the bridge. The degrading elements of the bridge are represented by nodes *E_3_1*, *E_4_1*, *E_5_1* and *E_6_1*, i.e. the nodes that are at the location of both the left pier (*E_3_1* and *E_4_1*) and the sensors (*E_4_1* and *E_5_1*). The most degraded elements of the bridge are identified as *E_4_1* and *E_5_1*, i.e. the elements on which the sensors are installed. Again, the health state of the minor elements changes at time 15min for the first time, due to the noise of the data and misclassification of the HI value at that time. Similarly, the increase of the probability of the healthy state of node *E_4_1* at time 31min is due to misclassification of the HI value. Figure 6-7 shows that the health state of *E_4_1* and *E_5_1* get worse over time, i.e. the probability of the PD state and SD increase over time. This result is expected as each degraded state of the bridge element is made of two different damage scenarios, whose damage magnitude increases over time. The damage of the bridge element is identified correctly. However, the location of the damage is only identified partially, since the damaged element of the bridge (i.e. the left pier of the bridge) is represented by both node *E_3_1* and node *E_4_1*.

Finally, Figure 6-7 depicts that the health state of the minor elements, for which evidence of their health state is not available, does not change throughout the monitoring time. This result is due to the definition of the BBN structure, which considers only interdependencies between neighbour minor elements. When further

information about the possible interdependencies between non-neighbour minor elements (e.g. the influence of *E_1_1* on the health state of *E_10_1*) is available, the structure of the BBN can be updated. Consequently, when evidence of a bridge element is available, the health state of each minor element is updated accordingly.

In what follows, the performance of the BBN with different CPTs definition strategies is analysed.

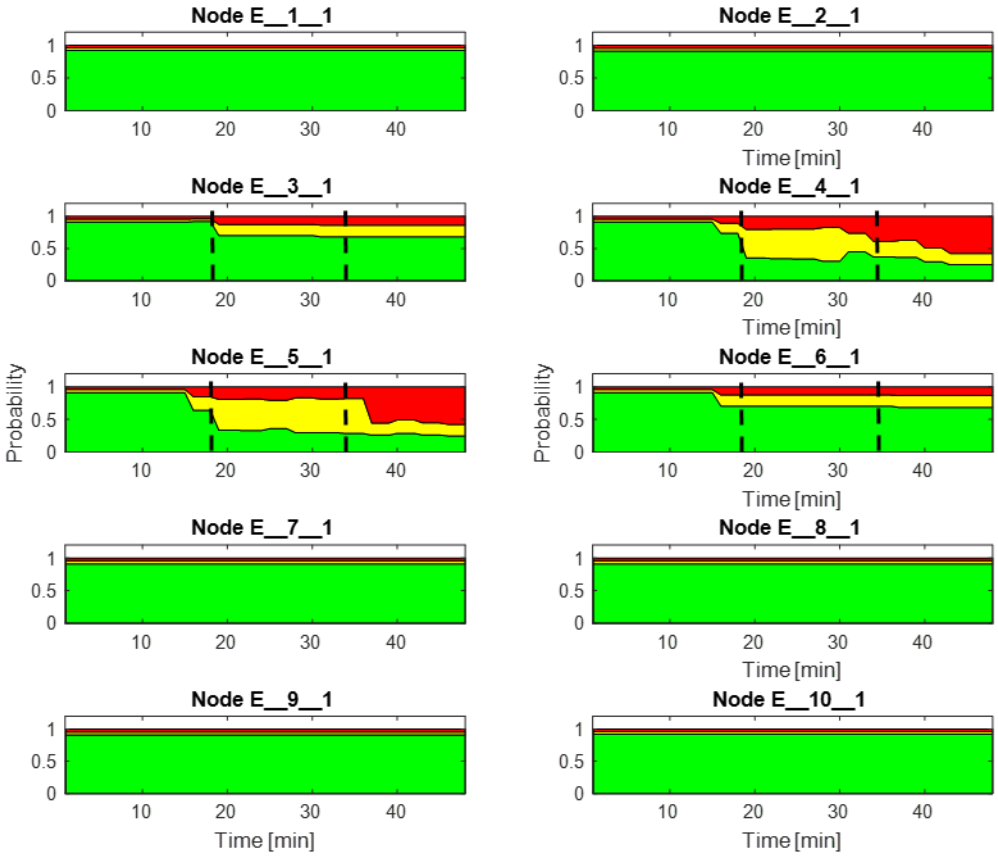

Figure 6-7. *Evolution over time of the health state of the minor elements of the post-tensioned bridge when α varies over time, as shown in Eq. (5 2)*

Table 6-1. *CPT of node E_4_1 by relying on the expert knowledge elicitation process*

E3	**H**									**PD**									**SD**								
E5	**H**			**PD**			**SD**			**H**			**PD**			**SD**			**H**			**PD**			**SD**		
E4	**H**	**PD**	**SD**	**H**	**PD**	**SD**	**H**	**PD**	**SD**	**H**	**PD**	**SD**	**H**	**PD**	**SD**	**H**	**PD**	**SD**	**H**	**PD**	**SD**	**H**	**PD**	**SD**	**H**	**PD**	**SD**
H	0,95	0,65	0,61	0,73	0,43	0,39	0,71	0,41	0,38	0,73	0,43	0,39	0,51	0,21	0,18	0,49	0,19	0,16	0,71	0,41	0,38	0,49	0,19	0,16	0,47	0,17	0,14
PD	0,025	0,20	0,17	0,16	0,34	0,25	0,17	0,35	0,25	0,16	0,34	0,25	0,29	0,47	0,33	0,30	0,48	0,34	0,17	0,35	0,25	0,30	0,48	0,34	0,31	0,49	0,35
SD	0,025	0,15	0,22	0,11	0,23	0,36	0,12	0,24	0,37	0,11	0,23	0,36	0,20	0,32	0,49	0,21	0,33	0,50	0,12	0,24	0,37	0,21	0,33	0,50	0,22	0,34	0,51

6.3.2 Comparison of BBN performance by using different CPTs definition strategies

The performance of the BBN by using the proposed strategy to update the CPTs is compared with the performance of the BBN that relies on the expert knowledge elicitation process. At the same time, the performance of the BBN is investigated by considering different strategies of α definition.

6.3.2.1 Expert knowledge elicitation process-based CPTs vs CPTs based on the proposed updating strategy with time varying α

The performance of the BBN for different scenarios is evaluated in this section. The structure of the BBN is the same during the comparison scenarios, whereas the strategy to define the CPTs is changed. Particularly, two CPTs definition strategies are compared: *i)* the expert knowledge elicitation process; and *ii)* the proposed updating strategy for CPT, by taking account of both expert judgement and bridge behaviour analysis, with a value of α that changes over time based on the health state of the bridge element. The comparison of the BBN performance is made by considering the evolution over time of the health state of the most degraded element of the bridge that has been identified, i.e. *E_4_1* and *E_5_1*.

Figure 6-8 shows the evolution of the health state of nodes *E_4_1* and *E_5_1* when the proposed strategy for updating the CPTs is used (Figure 6-8 top), and when the CPTs are defined by using the expert knowledge elicitation process (Figure 6-8 bottom). Both strategies allow to point out the different health states of the bridge elements, by increasing the probability of the PD and SD states when damages are inflicted to the bridge (light and dark grey areas, respectively, in Figure 6-8). Figure 6-8 top, i.e. when the CPTs are updated by adopting the proposed strategy, shows that the probability of the PD and SD states increases more than the correspondent PD and SD probabilities in Figure 6-8 bottom (i.e. when the CPTs are defined by using the expert judgement). Therefore, the BBN that relies on the proposed strategy to update the CPTs is able to diagnose the damage states of the bridge in a clearer manner. Furthermore, the probability of the PD and SD states increase over time in Figure 6-8 top, which means that the health state of the bridge elements decrease over time. In fact, the health state of the bridge decreases over time, due to the different damages that are inflicted to the bridge pier: both the PD and the SD state are made of two

different damage scenarios, whose magnitude increases over time. Such a decrease in the degraded states of the bridge elements is not pointed out in Figure 6-8 bottom, which means that when the CPTs of the BBN are defined by using the expert knowledge elicitation process, the diagnostic ability of the BBN decreases. The reduction of the diagnostic ability of the BBN is not caused by the assumptions made in the expert knowledge elicitation process, but rather is due to the constant value of the conditional probability retrieved by the expert judgement, which is not able to point out the increasing damage magnitude. It should be noted that the Figure 6-8top shows some oscillations of the PD and SD probability, which are due to the values of the conditional probability retrieved by using the CDF of the HI, as shown in Figure 6-9.

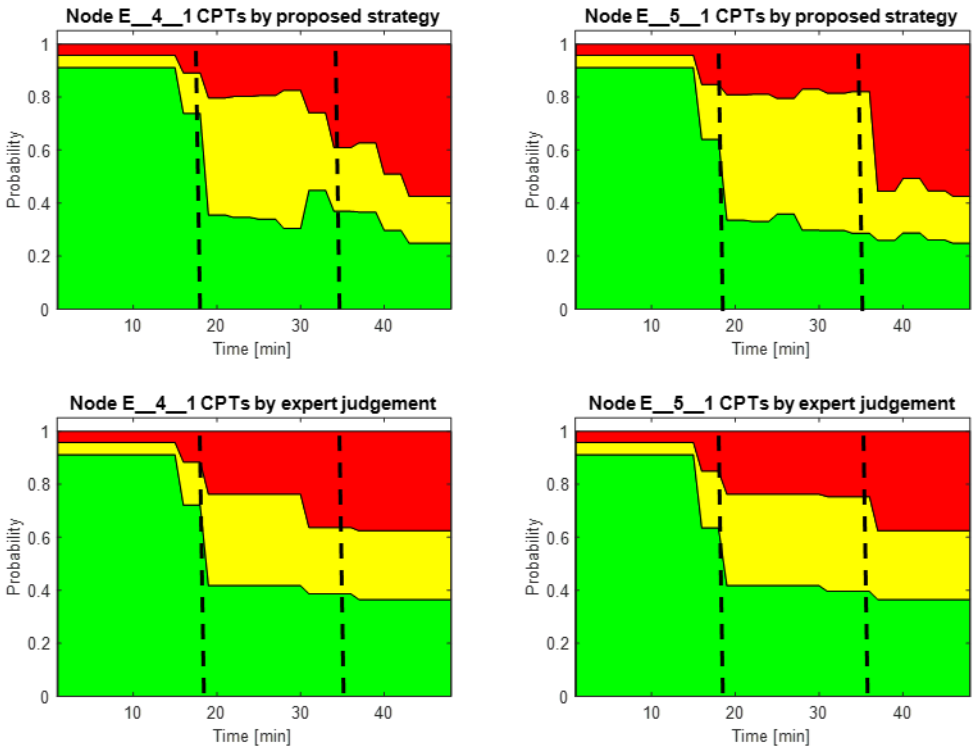

Figure 6-8. *Evolution over time of the health state of the most degraded elements of the post-tensioned bridge when CPTs are defined by the proposed updating strategy and the expert knowledge elicitation process*

Figure 6-9 explains the reason why the BBN that relies on the proposed strategy to define the CPTs is able to diagnose the damage scenarios of the bridge in a better and more reliable manner. Indeed, Figure 6-9 shows the evolution of the conditional probability of the SD state of the nodes *E_4_1* and *E_5_1* when the HI values are classified as SD state, i.e. the time when the health state of each most degraded bridge element is recognized as SD. The dashed line in Figure 6-9 depicts the conditional

probability of both *E_4_1* and *E_5_1* nodes when the CPTs are defined by the expert knowledge process: the expert judgement is a constant value, which cannot be changed during the monitoring process of the bridge. As a consequence, when the magnitude of a damaged health state of the bridge increases, the BBN is not able to point out such a decrease of the bridge health state by using an expert-based CPTs definition. Conversely, the dotted line in Figure 6-9 shows the evolution of the conditional probability of the SD state of the two nodes that is retrieved by using the CDFs of the optimal HI. This dotted line shows some oscillations due to the value of the HI, which is used as an input to the CDF. The conditional probability of the SD states that is assessed by using the CDFs of the optimal HI increases over time. Consequently, different degraded scenarios of the bridge can be pointed out by using the CDFs of the optimal HI, which are retrieved by analysing the bridge behaviour, as discussed in section 5.2. Finally, the solid line in Figure 6-9 shows the evolution of the conditional probability of the SD state of the two nodes when the expert judgement and the bridge behaviour analysis are merged by using the proposed method to update the CPTs. The value of α changes over time, according to the number of health states of the bridge and the time of the monitoring process, as shown in Eq. (5-2). Therefore, the proposed strategy to update the CPTs of the nodes of the BBN allows to diagnose different damage health states of the bridge elements, by increasing the probability of the damage states based on the actual health state of the bridge elements.

Different strategies to define the weight of the combination of the expert knowledge and the bridge behaviour analysis can be used. In what follows, three different strategies to define α are analysed and compared.

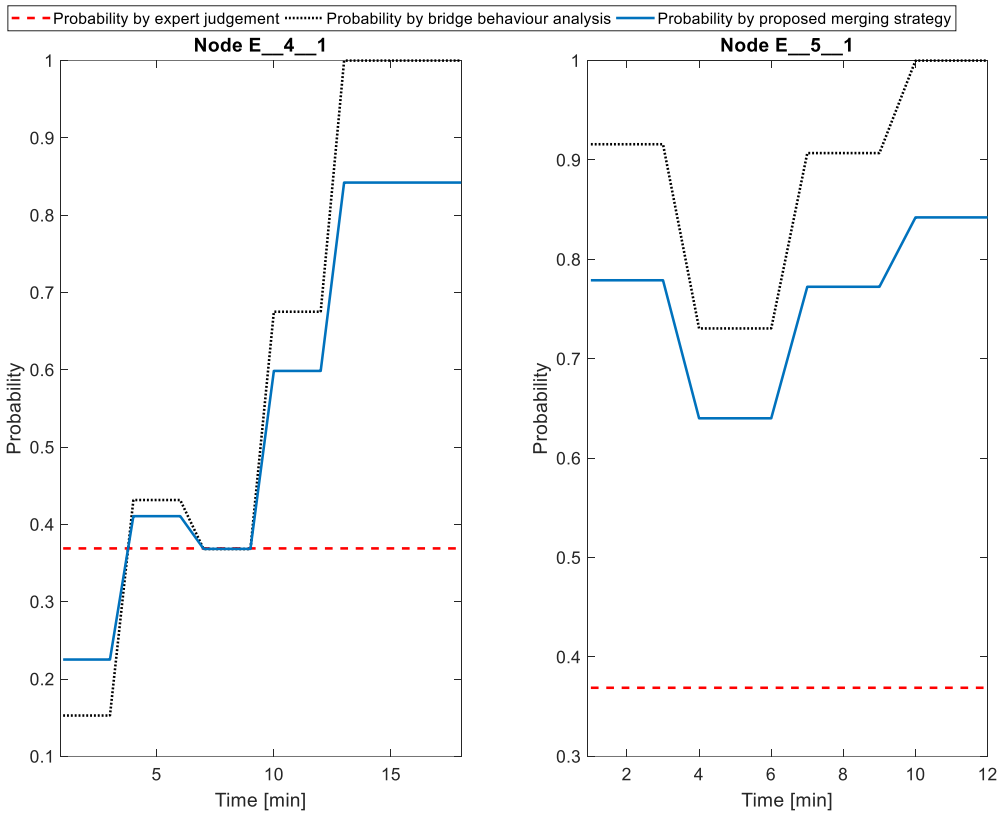

Figure 6-9. *Comparison between different CPT definition strategies for the severely degraded probability of the most degraded bridge element when* α *varies over time*

6.3.2.2 Influence of α on the performance of the BBN for bridge condition monitoring and degradation diagnostics

The proposed CPTs updating strategy gives more importance to the bridge behaviour data, than to the expert judgment, in defining the weight of the linear combination α. In fact, the higher the number of the identified health states of the bridge, and the longer the monitoring time of the bridge, the higher the value of α (as shown in Eq. (5-2)). Hence, the higher the value of α, the higher the importance of the bridge behaviour analysis over the expert judgment. Different strategies can be adopted to define α. In what follows, three different strategies for α are compared: *a)* the expert knowledge elicitation process have more importance than the bridge behaviour analysis, by considering a constant $\alpha = 0.1$; *b)* both the expert judgment and the bridge behaviour analysis have the same importance in the CPTs definition process, by considering a constant $\alpha = 0.5$; *c)* the bridge behaviour analysis has more importance than the expert knowledge elicitation process, as α increases over time. Each strategy allows to update the CPTs of the BBN by taking account of the actual health state of the bridge elements. However, strategy *a)* gives a small weight to the

information of the health state of the bridge elements and relies mainly on the expert knowledge. Such a strategy can be used, for example, when there is a lack of data of the bridge behaviour to define the CDFs, and the experts are able to provide an exhaustive what-if analysis, i.e. by considering many and different what-if scenarios, to evaluate possible damage scenarios of the bridge elements. Strategy *b)* gives the same weight to each approach to define the CPTs, and subsequently it can be adopted when there are no reasons to prefer a strategy to define the CPTs over the other.

Figure 6-10 shows the evolution of the health states of the most degraded elements of the bridge, i.e. nodes *E_4_1* and *E_5_1*, when the three different strategies to define α are adopted. Particularly, the evolution of the health state of nodes *E_4_1* and *E_5_1* are analysed by considering: *i)* the updating strategy of the CPTs when α changes over time by considering the actual health state of the bridge elements, i.e. the bridge behaviour analysis has an higher weight than the expert judgment; *ii)* the updating strategy of the CPTs when α is constant and equal to 0.5, i.e. the bridge behaviour analysis and the expert judgement have the same weight; *iii)* the updating strategy of the CPTs when α is constant and equal to 0.1, i.e. the bridge behaviour analysis has a lower weight than the expert judgment.

Each strategy for defining α is able to identify the damages of the bridge elements, as shown in Figure 6-10. However, the diagnostic ability of the BBN decreases as the weight of the expert judgement increases: Figure 6-10 shows that when the CPTs are updated by considering $\alpha = 0.1$, the conditional probability of the PD and SD states is almost constant throughout the monitoring time of the damage scenarios of the bridge. As a result, the increase of the magnitude of the damages of the bridge is not identified when the CPTs are updated by considering $\alpha = 0.1$.

On the contrary, when the CPTs are updated by considering $\alpha = 0.5$, i.e. both the expert judgment and the bridge behaviour analysis have the same weight, the BBN is able to diagnose the different magnitude of the bridge damages, by increasing the probability of the PD and SD states over time, as depicted in Figure 6-10. The difference between the adoption of a constant $\alpha = 0.5$ and a value of α that changes over time is that this latter approach leads to higher values of the conditional probability of the PD and SD states. For example, Figure 6-10 shows that the conditional probability of the SD state at the end of the monitoring time, i.e. when the magnitude of the damage of the bridge is at its maximum, is equal to 52% for the

$\alpha = 0.5$ strategy and 58% for the proposed strategy with α that varies over time. Although the difference between the value of the conditional probability is small, this can result in a change of the diagnostic ability of the BBN. In fact, when a high number of different damage scenarios of the bridge are considered, each damage scenario may be recognized by a value of the conditional probability of the SD state. Consequently, the best strategy can be the one that is able to assign the highest value of conditional probability of the SD to the most degraded scenario of the bridge.

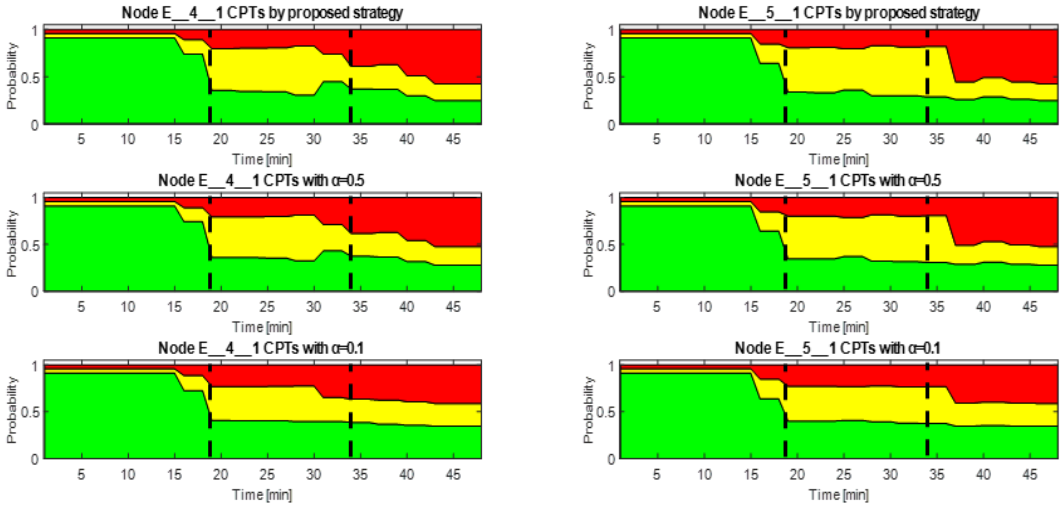

Figure 6-10. *Evolution over time of the health state of the most degraded elements of the post-tensioned bridge when CPTs are defined by the proposed updating strategy by using different α values*

Finally, Figure 6-11 and Figure 6-12 show the evolution of the conditional probability of the being in the SD state for nodes *E_4_1* and *E_5_1*, when the two strategies for updating the CPTs with a constant α are considered. Both figures show the evolution of the conditional probability of SD when the health state of the two bridge elements is recognized as SD.

Figure 6-11 shows that the conditional probability assigned by the expert knowledge elicitation process is constant during the time when the elements are identified as SD, as depicted by the dashed line in Figure 6-11. On the contrary, the conditional probability obtained by the CDFs of the optimal HI increases as the condition of the bridge elements gets worse, as shown by the dotted line in Figure 6-11. The solid line in Figure 6-11 shows the evolution of the combination of the two strategies when a constant $\alpha = 0.1$ is considered. It should be noted that the solid line is closer to the conditional probability obtained by the expert judgment, rather than to

the probability retrieved by analysing the bridge behaviour. Furthermore, the CPTs updating strategy allows to increase the probability of the SD state of the bridge elements when the magnitude of the bridge damage increases. However, the value of the PD and SD states is close to the expert judgment values, and thus the diagnostic ability of the BBN can be limited.

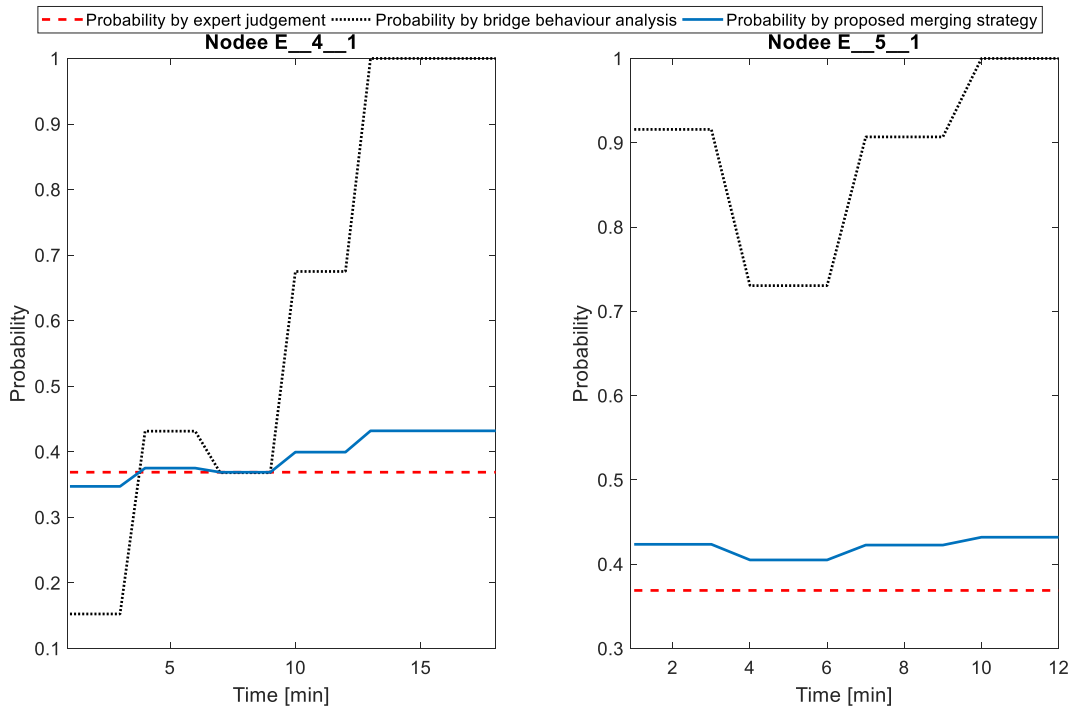

Figure 6-11. *Comparison between different CPT definition strategies for the severely degraded probability of the most degraded bridge element when α is constant and equals to 0.1*

Figure 6-12 shows the evolution of the combination of the two strategies when a constant $\alpha = 0.5$ is considered, by the means of a solid line. The conditional probability of the SD state of the two BBN nodes increases over time, as the magnitude of the bridge damages increase. Furthermore, the solid line is closer to the probability obtained by analysing the bridge behaviour (i.e. by assessing the CDFs of the optimal HI), than the solid line in Figure 6-11. However, the solid line in Figure 6-12 is closer to the probability retrieved by the expert judgment than the solid line in Figure 6-9, where α changes based on the length of the monitoring time and the number of identified health states of the bridge. Again, it is worth mentioning that the proposed strategy to update the CPTs allows to increase the probability of the SD state when the magnitude of the damages of the bridge increases.

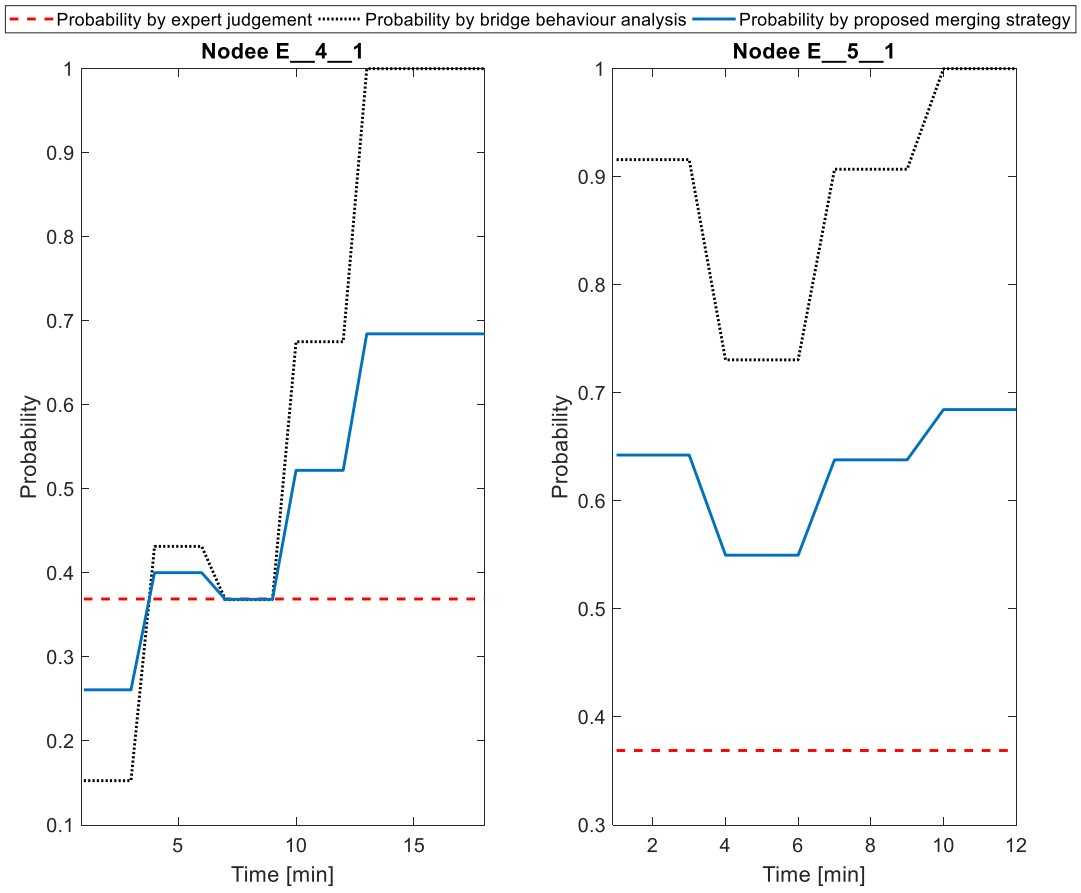

Figure 6-12. *Comparison between different CPT definition strategies for the severely degraded probability of the most degraded bridge element when α is constant and equals to 0.5*

In what follows, the performance of the BBN when different CDFs of the optimal HI are adopted to update the CPTs is analysed.

6.3.3 BBN performance by using the CDFs retrieved by the K-S test

Section 5.3.2 discussed how the K-S test can be used to verify the CDFs of the optimal HI for each sensor that is installed on the bridge. The K-S test showed that the CDFs of the PD state of sensor A and of the SD state of both sensor A and B belong to Weibull distributions, rather than to uniform distributions, as suggested by the AICc analysis. Hence, in what follows the performance of the BBN by using the Weibull distributions identified by the K-S test are used to update the CPTs of the BBN, by adopting the proposed strategy with α values that change over time. The Weibull distributions are used to update the CPTs of both nodes *E_4_1* and *E_5_1*, which are the nodes where the sensors are installed.

Figure 6-13 shows the evolution of the health state of the minor elements of the bridge, when the Weibull distribution is used to update the CPTs. Both nodes *E_4_1*

and *E_5_1* are identified as the most degraded elements of the bridge. The evolution of the health state of these minor elements of the bridge shows that the location of the damage is partially identified (i.e. the damaged pier is between nodes *E_3_1* and *E_4_1*). At the same time, the modification of the health state of the bridge elements at time before 19min is due to misclassification of the HI values. Similarly, the oscillations of the health state of the nodes are due to oscillations of the HI values that lead to different assessment of the conditional probability values by using the Weibull-based CDFs.

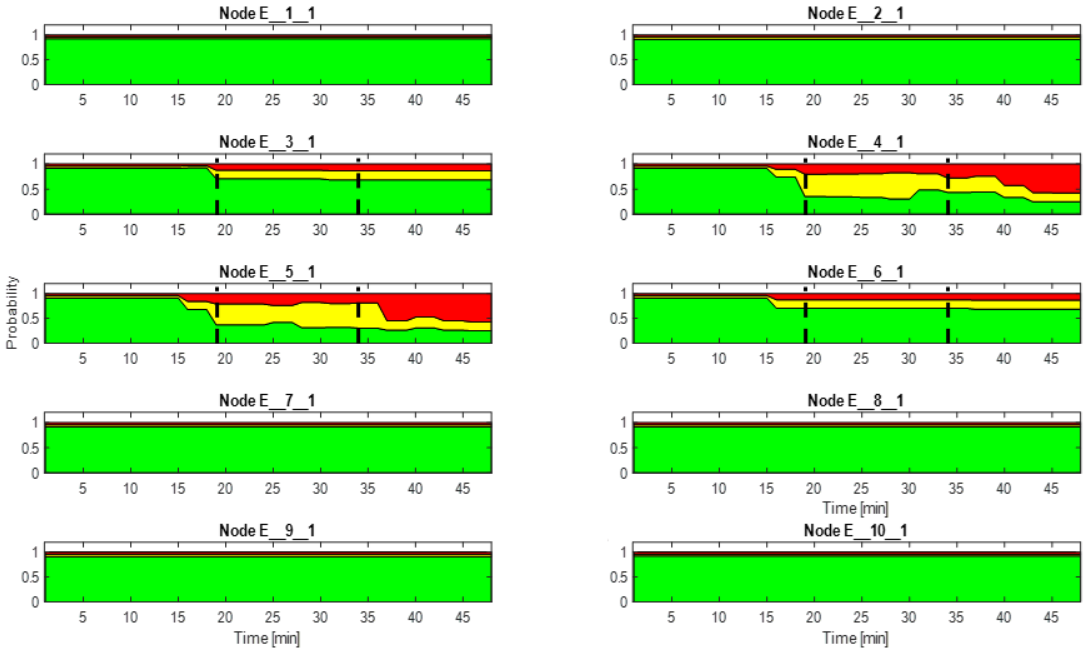

Figure 6-13. *Evolution over time of the health state of the minor elements of the post-tensioned bridge when α varies over time and Weibull distributions are used*

Finally, Figure 6-14 shows the evolution of being in state SD for both nodes *E_4_1* and *E_5_1*, when the health state of each node is identified as SD. Similarly to the previous analyses, the conditional probability that is obtained by the proposed method to update the CPTs, i.e. the solid line in Figure 6-14, increases over time due to the increase of the magnitude of the bridge damage. At the beginning of the SD time interval, the conditional probability of the SD state of the *E_4_1* node (solid line in Figure 6-14) is lower than the conditional probability obtained by the expert judgment (dashed line in Figure 6-14). However, when the magnitude of the bridge damage increases, the proposed method to update the CPTs allows to increase the probability

that the *E_4_1* bridge element is in a damaged state, and thus the solid line increases over the dashed line in Figure 6-14.

The evolution of the health state of the minor elements (Figure 6-13) looks very similar to the evolution of the health state of the element that are based on the results of the AICc analysis (Figure 6-7), i.e. the uniform distributions are used to update the CPTs of the BBN. At the same time, the evolution of the conditional probability of the SD state of Figure 6-14 looks similar to the conditional probability of the SD state by using the uniform distribution (Figure 6-9). Therefore, in what follows, a comparison between the two different sets of CDFs to update the CPTs is carried out.

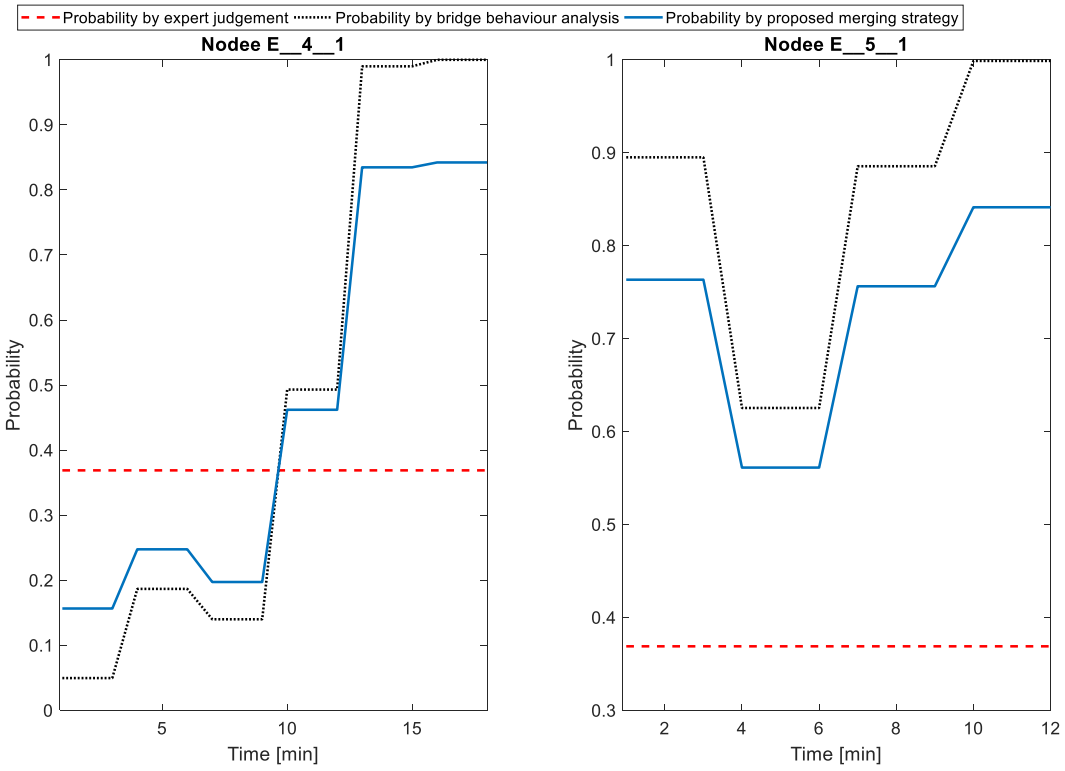

Figure 6-14. *Comparison between different CPT definition strategies for the severely degraded probability of the most degraded bridge element when α varies over time and the Weibull distributions are used*

6.3.3.1 **Influence of the nature of the CDFs on the BBN performance**

The performance of the BBN is analysed by using different CDFs to update the CPTs. The diagnosing ability of the BBN is analysed by monitoring the health state of the post-tensioned concrete bridge. The structure of the BBN is kept the same during the analysis, as well as the definition of the weight of the linear combination α, which is defined as shown in Eq. (5-2). The different performance of the BBN is due to the

different CDFs that are used to update the CPTs of nodes *E_4_1* and *E_5_1*. In fact, the CDFs of the PD state for sensor A and of the SD states for both sensor A and B are retrieved by using: *i)* the AICc analysis, which leads to three uniform distributions; *ii)* the K-S test, which leads to three Weibull distributions. The comparison between the different CDFs is carried out by analysing the evolution of the identified most degraded element of the bridge, i.e. nodes *E_4_1* and *E_5_1* of the BBN.

Figure 6-15 shows the evolution of the health states of nodes *E_4_1* and *E_5_1* when the Weibull or the uniform distributions are used to update the CPTs. The evolution of the health state of the nodes is similar when using both CDFs updating strategies. However, the evolution of the PD state for node *E_4_1* (light grey area in Figure 6-15) shows higher probability values when the Weibull distribution is used to update the CPTs of the BBN. For example, from time 32min to time 39min, the Weibull distribution provides a PD probability slightly larger than the other health states of the bridge elements. On the other hand, the uniform distribution-based BBN shows a similar value of the PD state from time 31min to time 34min, however, after time 34min, the value of the SD state (dark grey area in Figure 6-15) becomes the largest one. At the end of the monitoring time, the value of the conditional probability of each state is the same for both CDFs-updating strategies. Therefore, the updating of the health state of the bridge elements appears to happen more slowly, when the Weibull distribution is adopted. This behaviour can be due to the shape of the CDF of the Weibull distribution, which increases slowly of the tail on the distribution. On the contrary, the uniform distribution increases linearly throughout the interval of the distribution, and consequently the transition between different health states of the bridge can be faster. The evolution of the health state of node *E_5_1* is mainly the same for both CDFs strategies, as shown in Figure 6-15.

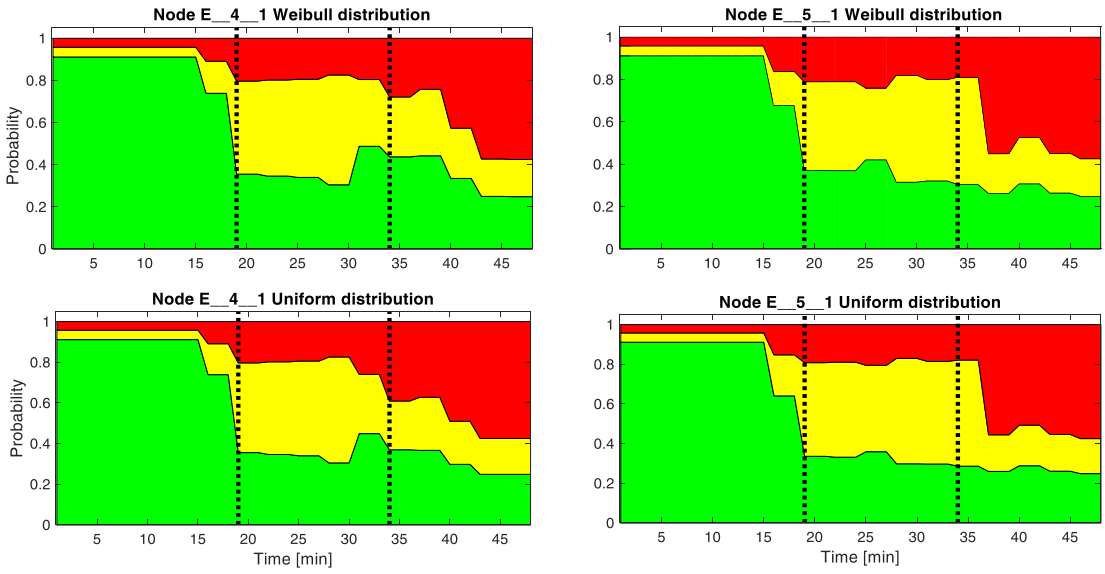

Figure 6-15. *Evolution over time of the health state of the most degraded elements of the post-tensioned bridge when CPTs are updated by using a uniform or a Weibull distribution*

Figure 6-16 shows the evolution of the SD conditional probability of nodes *E_4_1* and *E_5_1* of the BBN, when the health state of each most degraded node is identified as SD. The evolution of the SD conditional probability is depicted by considering both the Weibull distribution and the uniform distribution to update the CPTs. Both distributions allow to increase the value of the SD probability of the two nodes of the BBN during time, i.e. when the magnitude of the bridge damage increases, both distributions allows to increase the probability that the nodes of the BBN are in the SD state. However, as discussed for Figure 6-15, the increase of the SD probability is slower when the Weibull distribution is adopted. For example, the evolution of the SD probability of node *E_4*_1 when the proposed method to update the CPTs is adopted (solid line in Figure 6-16) shows that: *i)* if the uniform distribution is adopted to update the CPTs, the solid line overcomes the expert judgment-based probability (dashed line in Figure 6-16) at time 4min; on the contrary, *ii)* if the Weibull distribution is adopted to update the CPTs, the solid line overcomes the probability retrieved by the expert judgment at time 9min. Hence, the Weibull distribution requires higher values of the optimal HI to assign high value to the SD probability of the bridge. Again, this result is expected by analysing the shape of the CDFs of both distribution. Furthermore, the Weibull distribution can be considered as a more conservative approach, due to the fact that the probability of the SD state is increased only when the HI value is high. As a consequence, the adoption of the Weibull distribution can lead to a lower number of misclassification during the diagnostic process of the BBN.

Finally, both distributions allow to point out the most degraded elements of the bridge and to diagnose the different damages of the bridge elements. A more detailed analysis is required in order to identify the optimal CDFs of the HI, that allows to update the CPTs of the BBN in a reliable manner.

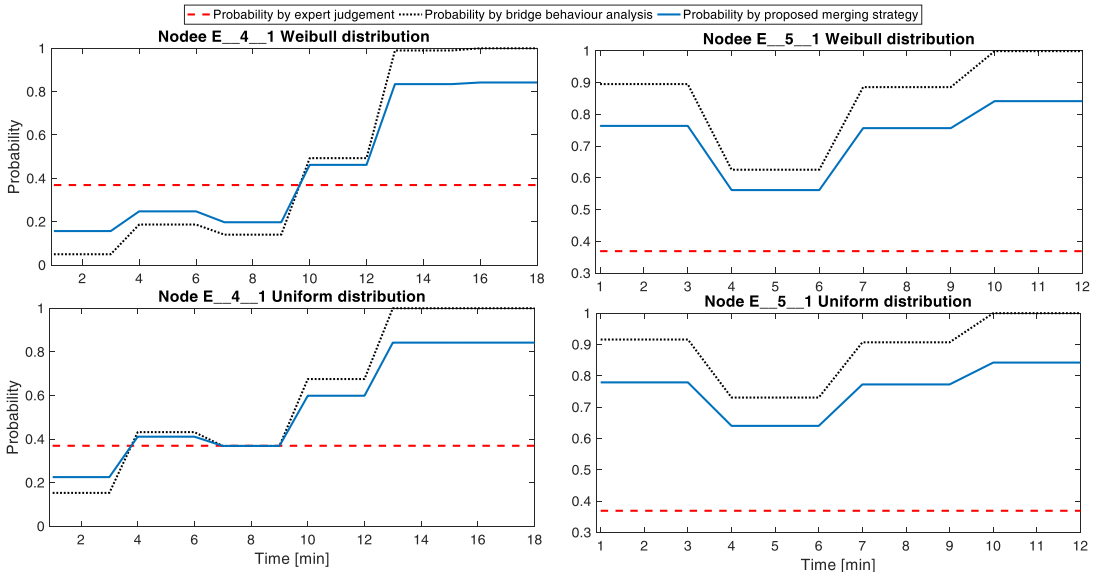

Figure 6-16. *Comparison between different CPT definition strategies for the severely degraded probability of the most degraded bridge element when uniform or Weibull distribution are adopted*

6.4 Summary

The proposed BBN-based method has been applied for monitoring the condition of the in-field post-tensioned bridge. The method has been demonstrated to be able to monitor the health state of a bridge continuously, by updating the health state of the bridge, and its elements. At the same time, damages of the bridge elements have been identified by the proposed BBN-based method. Several strategies to define the CPTs of the BBN have been analysed and compared. The analysis has pointed out the CPTs that are based on the updating strategy proposed in Chapter 5 allow to improve the diagnostics ability of the BBN significantly. In fact, when the CPTs have been defined by taking account of both the expert knowledge elicitation process and the bridge behaviour analysis, the performance of the BBN has been improved.

The analysis of the BBN results suggest that its performance can be enhanced by:

- Improving the development of the structure of the BBN. For example, a higher number of nodes can be considered in order to locate the damage of the bridge in a more accurate way. At the same time, the structure of the BBN should consider interdependencies between non-neighbour elements of the bridge.

However, a database of bridge behaviour is needed in order to validate such connections between non-neighbour bridge elements. Similarly, the number of states of the BBN nodes can be increased with the aim of improving the diagnostic ability of the BBN. However, the higher the number of state of the BBN nodes, the higher the size of the CPTs.

- Interviewing a group of experts in order to retrieve a set of CPTs that relies on the analysis of the post-tensioned bridge. In fact, this process can improve the diagnostic ability of the BBN slightly, when the CPTs are based on the expert knowledge elicitation process. However, when the CPTs are based on the expert judgements, a small deterioration of the bridge health state is not identified. For example, if the magnitude of bridge damage increases, the BBN that relies on expert judgement-based CPTs is not able to point out the decrease of the bridge health state, due to the constant value of the CPTs.
- Optimizing the definition of the CDFs of the optimal HI of the bridge. In this way, the diagnostic ability of the BBN can be optimized by taking account of the actual health state of the bridge elements.
- Optimizing the strategy to define the weight of the linear combination α. Indeed, the analysis of the BBN when different values of α have been considered showed that the diagnostic ability of the BBN strongly rely on the value of α. Therefore, a rigorous way to define α needs to be proposed in order to optimize the performance of the BBN.

In what follows, the conclusions of the thesis and future work are discussed.

Chapter 7 Conclusions and future work

7.1 Conclusions

The European transportation network has more than one million bridges. These assets are continuously deteriorating due to aging, traffic load (which nowadays exceeds original design criteria of bridges), and environmental effects, such as wind, and changing temperatures. Commonly, the health state of bridges is assessed by time-consuming, expensive and subjective visual inspections at fixed time intervals, ranging from one to six years. As a consequence, the degradation of the bridge health state can increase undetected, by reducing the safety, reliability and availability of both the bridge and the corresponding transportation network.

In this thesis, the literature review process showed that a clear majority of the analysed condition monitoring and damage detection methods have deficiencies in monitoring the health state of a bridge continuously, by taking account of the influences between different elements of the bridge. Model-based methods allow to consider interdependencies between different elements of a bridge, but a time-consuming process is required for their development. At the same time, the reviewed methods presented difficulties in managing different sources of data (such as bridge behaviour data and expert knowledge) and diagnosing the location and level of severity of the bridge damage. Furthermore, most of the reviewed non-model-based methods are verified on FEMs of bridges, which are not able to represent the data uncertainties and noise of an in-field bridge.

Several objectives have been achieved in this thesis:

- The main objective of this thesis was to develop a bridge condition monitoring and damage diagnostics method. The main element of the proposed method was to monitor and assess the health state of a bridge continuously, by taking account of the health state of each element of the bridge and without requiring a time-consuming process for its development. This method has been developed by proposing a BBN-based approach. First of all, the CPTs of the BBN have been defined by adopting an expert knowledge elicitation process. Such a BBN method has shown to be able to monitor the health state of two

bridges (a steel truss bridge and a beam-and-slab bridge), modelled using FEMs, continuously, by accounting for the interdependencies between different elements of the bridge. The BBN allowed also to identify damages of the bridge, and to diagnose the causes of such damages by pointing out the damaged minor element(s) of the bridge. However, in terms of the diagnostic ability of the BBN there were some cases of misclassification. Consequently, several methods have been introduced in this thesis to improve the performance of the BBN analysis, by pre-processing the data of the bridge behaviour and improving the definition of the CPTs, as discussed below.

- A data analysis methodology has been developed in order to pre-process the bridge behaviour data. The data analysis methodology allowed to assess HIs of the bridge elements. The HIs have been identified by using statistical, frequency-based and vibration-based features as an input to an EMD method, which allowed to assess the trend of the features over time. The optimal HI to represent the health state of the bridge elements has been identified by looking for the HI with the highest values of trendability and monotonicity. The optimal HI has been then used as an input to the BBN nodes, in order to assess the health state of the whole bridge. The proposed data analysis methodology has been verified on two in-field bridges, a steel truss bridge and a post-tensioned concrete bridge. Both bridges were subjected to a progressive damage test under unknown environmental conditions. A good performance has been achieved in monitoring the health state of the bridges and diagnosing their damages in terms of location and magnitude.
- A machine learning method, which relies on an NFC, has been introduced to assess the health state of a bridge element automatically. The results of the NFC can potentially be used as an input to the BBN nodes, to select the states of the BBN nodes. An optimal set of HIs has been identified to assess the health state of the bridge elements automatically, by relying on an MBDE method. The optimal set of HIs allowed to achieve good performance in assessing the health state of the post-tensioned concrete bridge (an in-field bridge) automatically.
- A method to update the CPTs of the BBN nodes, by merging the expert knowledge elicitation process and the analysis of a database of bridge behaviour has been proposed. This method allows to update the CPTs of the

BBN nodes by taking account of the actual health state of the bridge elements. The method has been tested on the post-tensioned concrete in-field. The analysis of the results showed that a significant improvement of the diagnostic ability of the BBN is achieved, when the proposed method to update the CPTs is adopted.

- A method to analyse database of unknown infrastructure behaviour has been proposed. This latter method relies on an ensemble-based change-point detection algorithm, which has been developed to identify the most critical change of the health state of the infrastructure. The proposed method has been confirmed by analysing the database of a real in-field tunnel infrastructure. The method allowed to identify when the health state of the infrastructure changes, by providing the characteristics of such changes of the infrastructure health state. In this way, information about different health states of the infrastructure can be identified and analysed. As a result, useful information for defining the CPTs of the BBN, by relying on both expert judgment and bridge behaviour analysis, can be retrieved.

Overall, the proposed BBN-based method, with the integration of the other developed methods, allows to monitor the health state of a bridge continuously. The health state of the bridge is assessed by taking account of the interdependencies between different elements of the bridge. Different sources of information, such as visual inspection reports and bridge behaviour data, can be used as an input to the BBN. Moreover, the proposed BBN method allows to identify and diagnose damage of the bridge elements. In this way, the health state of the bridge is monitored continuously, and consequently the safety, reliability and availability of the bridge are improved. At the same time, continuous information about the health state of the bridge, and its elements, is provided to bridge managers, who can optimize the maintenance budget by scheduling maintenance activities based on the actual health state of the bridge.

7.2 Research contributions

The developed thesis makes several contributions to the SHM framework:

- **A better understanding of the SHM needs.** A vast number of SHM methods for bridge condition monitoring and damage detection has been reviewed in this thesis. The advantages and disadvantages of each condition monitoring method have been identified and discussed. The needs of a comprehensive

bridge SHM strategy have been proposed and discussed. The output of this literature review analysis has been published in the *Structural health monitoring journal* [Vagnoli et al., 2018].

- **Assessment of the bridge health state by considering the health state of its elements.** Many bridge condition monitoring, and damage diagnostics methods do not consider the interdependencies between different elements of the bridge. Hence, the influence of a damaged element on the health state of a different bridge element is neglected. The BBN method proposed in this thesis allows to assess the interdependencies between different elements of the bridge. The BBN method can be applied directly on any infrastructure, by following the proposed step-by-step process to define both the BBN structure and its CPTs. This will allow bridge engineers to monitor the behaviour of a bridge, by pointing out and diagnosing its unexpected behaviour. The proposed method allows to satisfy the first three level of the damage detection process. However, a rigorous way to define the BBN structure, and the number of states of the BBN nodes require to be analysed further. The proposed method has been described in a paper, which is currently under review at the *Structural Control and Health Monitoring Journal*.
- **Merging the expert knowledge and the bridge behaviour analysis.** Bridge engineers and bridge managers have a lot of experience in knowing the most critical elements of a bridge, and in providing insights about possible relationships between the different elements. At the same time, the data of the bridge behaviour also provides information about interdependencies between different elements of the bridge. In this thesis, these two sources of information have been analysed together in order to improve the reliability of the condition monitoring process using the BBN. The proposed method can be applied in a framework where a BBN method is used to monitor the health state of a system. In fact, such method has been demonstrated to enhance the diagnostic performance of the BBN significantly. However, the expert elicitation process requires further analysis, in order to provide a reliable assessment of the interdependencies between different system elements. At the same time, the definition of the CDFs of the bridge behaviour needs to be analysed further, to provide a robust assessment of the CPTs. The method for analysing both the

expert judgment and the bridge behaviour is being described in a paper, which is going to be submitted to the *Reliability Engineering & System Safety journal*.

- **Assessment of the health state of the bridge elements by relying on data-driven methods.** Measurement systems are becoming cheap, and thus sensors are installed on an increasing number of infrastructures. Therefore, two data-driven methods have been proposed to assess the health state of the bridge elements in a fast and reliable manner. A data analysis methodology showed how to analyse the data of the bridge behaviour by adopting several steps: *i)* the removal of the noise; *ii)* identification of the free-vibration of the bridge; *iii)* extraction of statistical, frequency-based and vibration-based features; *iv)* assessment of the features trend by using the EMD method; *v)* assessment of the health state of the bridge elements. Features of the bridge behaviour data have been analysed. A machine learning method showed how the past behaviour of the bridge can be used to assess the health state of the bridge elements in a fast and automatic way. Furthermore, the performance of the machine learning method is expected to increase when the availability of the bridge behaviour data increases. Consequently, in the future, when more bridge behaviour data is available, machine learning methods can be applied to automatically monitor the health state of bridge infrastructure in a fast and reliable way. The two data-driven methods can be applied to any system that is monitored by the means of vibration data. Particularly, the data analysis methodology would allow to identify unexpected behaviour of the system as soon as it occurs, whereas the machine learning method would require a database of past behaviour of the system for the training process. However, the set of proposed HIs may require further analysis in order to increase the set of possible HIs to describe the health state of different systems. The developed data-driven methods have been described in a research article, which is under review at the *Structural Control and Health Monitoring Journal* .
- **Analysis of database of infrastructure behaviour for change identification.** A method to analyse vast database of past infrastructure behaviour has been proposed, in order to identify the most critical change of the health state of the infrastructure. In fact, structural engineers would use this method for identifying the most critical change of behaviour of the infrastructure. Such information can be used to analyse the critical behaviour experienced by the

infrastructure and diagnose possible causes of the changes of the infrastructure health. The proposed method can be applied to any system that has monotonic behaviour as the degradation increases. Further analysis of the time constant definition may be required in order to identify a rigorous method for their definition. The developed method has been published in the *Tunnelling and Underground Space Technology Journal* [Vagnoli & Remenyte-Prescott, 2018].

7.3 Future work

The proposed method-based on BBN is suitable for monitoring the health state of real in-field bridge continuously, by diagnosing damage of the bridge elements. At the same time, the other methods proposed in this thesis to analyse the data of bridge behaviour showed good performance in assessing changes of the health state of real infrastructures. However, there are some aspects of the proposed methods that require further analysis to improve the robustness of the methods in real applications:

- A step-by-step process to define the structure of the BBN has been proposed, by identifying major and minor elements of the bridge. Eventually, the minor elements of the bridge have been identified by dividing the major elements into smaller parts. Therefore, a rigorous method to divide major (minor) elements into smaller elements, and thus to define an optimal number of nodes of the BBN, needs to be proposed. For example, an optimization analysis can be carried out in order to evaluate how different structure of the BBN influences the BBN performance. In this way, an optimal structure of the BBN may be identified, by optimizing both the diagnostics performance of the BBN and the size of the network, which can influence the computational time of the analysis.
- The number of states of the nodes in the proposed BBN is three in this thesis: *i)* a healthy state; *ii)* a partially degraded state; and *iii)* a severely degraded state. However, a higher number of states of the BBN allows to increase the damage detection and diagnostics ability of the BBN, by pointing out small changes of the bridge damage magnitude. It should be noted that the size of the CPT increases with the number of states of the nodes, and, as a consequence, a balance between number of states and size of the CPTs needs to be obtained. A possible solution to this problem can be the adoption of continuous nodes of

the BBN, which might also help in identifying smaller changes of the health state of the bridge, by avoiding the issue of the CPTs size.

- The proposed data analysis methodology provides HIs of the health state of the bridge, by lumping together the information of the trend of the features into the HI. However, the proposed set of HIs is not exhaustive, i.e. more HIs can be used to represent the health state of the bridge. Therefore, several statistical parameters, such as the mean value, the peak value, the interquartile range, etc., could be analysed in order to identify an optimal set of HIs, which is able to monitor the health state of the bridge by minimizing the number of misclassification of the bridge health state.
- The proposed method to update the CPTs of the BBN by merging expert knowledge elicitation process and the bridge behaviour analysis requires further analysis to: *i)* improve the robustness of the expert knowledge elicitation process by interviewing a wider group of experts; *ii)* improve the definition of the weight of the linear combination α, by considering also the robustness of the expert judgment; iii) define the CDFs of the bridge behaviour in a robust manner, by considering a wider set of possible distributions to fit the optimal HI values.
- The performance of the proposed ensemble-based change-point detection method relies on the value of three time-constants, i.e. Δ, Φ, Ω. These constants are defined by using an expert knowledge elicitation process. Further analysis needs to be carried out in order to assess the value of the time constant in a more robust manner.

References

[Abdoun et al., 2009] Abdoun, T., Bennett, V., Thevanayagam, S., Dobry, R., Shantz, T., Jang, D., 2009. "Wireless MEMS-based system for real-time geotechnical instrumentation of active slopes", WIT Transactions on the Built Environment, 108, pp. 617-624.

[Rousseeuw, 1987] Rousseeuw, P.J., 1987. "Silhouettes: A graphical aid to the interpretation and validation of cluster analysis", Journal of Computational and Applied Mathematics, 20 (C), pp. 53-65.

[Adey et al., 2004] Adey, B., Hajdin, R., Brühwiler, E., "Effect of common cause failures on indirect costs", Journal of Bridge Engineering, 9 (2), pp. 200-208, 2004.

[Aied et al., 2016] Aied, H., González, A., Cantero, D., "Identification of sudden stiffness changes in the acceleration response of a bridge to moving loads using ensemble empirical mode decomposition", Mechanical Systems and Signal Processing, 66-67, pp. 314-338, 2016.

[Akaike, 1974] Akaike, H., "A New Look at the Statistical Model Identification", IEEE Transactions on Automatic Control, 19 (6), pp. 716-723, 1974.

[Alves et al., 2016] Alves, V., Cury, A., Cremona, C., "On the use of symbolic vibration data for robust structural health monitoring", Proceedings of the Institution of Civil Engineers: Structures and Buildings, 169 (9), pp. 715-723, 2016.

[Anastasopoulos et al., 2015] Anastasopoulos, I., Anastasopoulos, P.C., Agalianos, A., Sakellariadis, L., "Simple method for real-time seismic damage assessment of bridges", Soil Dynamics and Earthquake Engineering, 78, pp. 201-212, 2015.

[Andersen et al., 2006] Andersen, J.E. and Fustinoni, M., "Structural Health Monitoring Systems", L&S S.r.l. Servizi Grafici, 2006.

[Arangio et al., 2014] Arangio, S., Bontempi, F., "Structural health monitoring of a cable-stayed bridge with Bayesian neural networks", Structure and Infrastructure Engineering, Article in Press, 2014.

[Arias, 1970] A. Arias, "A Measure of Earthquake Intensity", R.J. Hansen, ed. Seismic Design for Nuclear Power Plants, MIT Press, Cambridge, Massachusetts, pp. 438-483, 1970.

[Attema et al., 2017] Attema, T., Kosgodagan Acharige, A., Morales-Nápoles, O., Maljaars, J., “Maintenance decision model for steel bridges: a case in the Netherlands”, Structure and Infrastructure Engineering, 13 (2), pp. 242-253, 2017.

[Attoh-Okine & Bowers, 2006] Attoh-Okine, N.O., Bowers, S., “A Bayesian belief network model of bridge deterioration”, Proceedings of the Institution of Civil Engineers: Bridge Engineering, 159 (2), pp. 69-76, 2006.

[Bao et al., 2018] Bao, Y., Tang, Z., Li, H., Zhang, Y., “Computer vision and deep learning–based data anomaly detection method for structural health monitoring”, Structural Health Monitoring, DOI 10.1177/1475921718757405, 2018.

[Barbosh et al., 2018] Barbosh, M., Sadhu, A., Vogrig, M., “Multisensor-based hybrid empirical mode decomposition method towards system identification of structures”, Structural Control and Health Monitoring, 25 (5), art. no. e2147, 2018.

[Başaĝa et al., 2011] Başaĝa, H.B., Türker, T., Bayraktar, A., “A model updating approach based on design points for unknown structural parameters”, Applied Mathematical Modelling, 35 (12), pp. 5872-5883, 2011.

[Bhalla et al., 2005] Bhalla, S., Yang, Y.W., Zhao, J., Soh, C.K., 2005. “Structural health monitoring of underground facilities - Technological issues and challenges”, Tunnelling and Underground Space Technology, 20 (5), pp. 487-500.

[Burnham & Anderson, 2004] Burnham, K.P., Anderson, D.R., “Multimodel inference: Understanding AIC and BIC in model selection”, Sociological Methods and Research, 33 (2), pp. 261-304, 2004.

[Cahill et al., 2018] Cahill, P., Hazra, B., Karoumi, R., Mathewson, A., Pakrashi, V., “Vibration energy harvesting based monitoring of an operational bridge undergoing forced vibration and train passage”, Mechanical Systems and Signal Processing, 106, pp. 265-283, 2018.

[Cannarile et al., 2017] Cannarile, F., Baraldi., P., Compare, M., Borghi, D., Capelli, L., Cocconcelli, M., Lahrac, A., Zio, E., “An unsupervised clustering method for assessing the degradation state of cutting tools in the packaging industry”, Safety and Reliability: Theory and Application- Proceedings of the European Safety and Reliability Conference, ESREL 2017, Portroz, Slovenia, 2017.

[Cao et al., 2011] Cao, Y., Yim, J., Zhao, Y., Wang, M.L., “Temperature effects on cable stayed bridge using health monitoring system: A case study”, Structural Health Monitoring, 10 (5), pp. 523-537, 2011.

[Cao et al., 2017] Cao, M.S., Sha, G.G., Gao, Y.F., Ostachowicz, W., “Structural damage identification using damping: A compendium of uses and features”, Smart Materials and Structures, 26 (4), art. no. 043001, 2017.

[Carslaw et al., 2006] Carslaw, D.C., Ropkins, K., Bell, M.C., “Change-point detection of gaseous and particulate traffic-related pollutants at a roadside location”, Environmental Science and Technology, 40 (22), pp. 6912-6918, 2006.

[Casas et al., 2017] Casas, J.R., Moughty, J. J., “Bridge Damage Detection Based on Vibration Data: Past and New Developments”, Front. Built Environ. 3:4., doi: 10.3389/fbuil.2017.00004, 2017.

[Catbas et al., 2008] Catbas, F.N., Susoy, M., Frangopol, D.M., “Structural health monitoring and reliability estimation: Long span truss bridge application with environmental monitoring data”, Engineering Structures, 30 (9), pp. 2347-2359, 2008.

[Cavadas et al., 2013] Cavadas, F., Smith, I.F.C., Figueiras, J., “Damage detection using data-driven methods applied to moving-load responses”, Mechanical Systems and Signal Processing, 39 (1-2), pp. 409-425, 2013.

[Cetişli & Barkana, 2010] Cetişli, B., Barkana, A., “Speeding up the scaled conjugate gradient algorithm and its application in neuro-fuzzy classifier training”, Soft Computing, 14 (4), pp. 365-378, 2010.

[Chalouli et al., 2017] Chalouli, M., Berrached, N.-E., Denai, M., “Intelligent Health Monitoring of Machine Bearings Based on Feature Extraction”, Journal of Failure Analysis and Prevention, 17 (5), pp. 1053-1066, 2017.

[Chang & Kim, 2016] Chang, K.-C., Kim, C.-W., “Modal-parameter identification and vibration-based damage detection of a damaged steel truss bridge”, Engineering Structures, 122, pp. 156-173, 2016.

[Chang et al., 2014] Chang, K.-C., Kim, C.-W., Kawatani, M., “Feasibility investigation for a bridge damage identification method through moving vehicle laboratory experiment”, Structure and Infrastructure Engineering, 10 (3), pp. 328-345, 2014.

[Chen & Pollino, 2012] Chen, S.H., Pollino, C.A., “Good practice in Bayesian network modelling”, Environmental Modelling and Software, 37, pp. 134-145, 2012.

[Cremona et al., 2012] Cremona, C., Cury, A., Orcesi, A., “Supervised learning algorithms for damage detection and long term bridge monitoring”, Bridge Maintenance, Safety, Management, Resilience and sustainability - Proceedings of the Sixth International Conference on Bridge Maintenance, Safety and Management, pp. 2144-2151, 2012.

[Cunha et al., 2001] Cunha, A., Caetano, E., Delgado, R., “Dynamic Tests on Large Cable-Stayed Bridge”, Journal of Bridge Engineering, 6. 10.1061/(ASCE)1084-0702(2001)6:1(54), 2001.

[Cury et al., 2012] Cury, A., Crémona, C., “Assignment of structural behaviours in long-term monitoring: Application to a strengthened railway bridge”, Structural Health Monitoring, 11 (4), pp. 422-441, 2012.

[Das, 2004] Das, B., “Generating conditional probabilities for Bayesian networks: Easing the knowledge acquisition problem”, arXiv preprint cs/0411034, 2004.

[Di Maio et al., 2016] Di Maio, F., Vagnoli, M., Zio, E., “Transient identification by clustering based on Integrated Deterministic and Probabilistic Safety Analysis outcomes”, Annals of Nuclear Energy, 87, pp. 217-227, 2016.

[Dias & De Sousa, 2018] Dias, C.G., de Sousa, C.M., “A Neuro-Fuzzy Approach for Locating Broken Rotor Bars in Induction Motors at Very Low Slip”, Journal of Control, Automation and Electrical Systems, 29 (4), pp. 489-499, 2018

[Djurovic et al., 2000] Djurovic, Z., Kovacevic, B., Barroso, V., “QQ-plot based probability density function estimation”, IEEE Signal Processing Workshop on Statistical Signal and Array Processing, SSAP, pp. 243-247, 2000.

[Dowling et al., 2012] Dowling, J., Obrien, E.J., González, A., “Adaptation of Cross Entropy optimisation to a dynamic Bridge WIM calibration problem”, Engineering Structures, 44, pp. 13-22, 2012.

[Duan and Zhang, 2006] Duan Z, Zhang K., “Data Mining Technology for Structural Health Monitoring”, Pacific Science Review, 8, 2006.

[Duan et al., 2018] Duan, L., Zhao, F., Wang, J., Wang, N., Zhang, J., "An Integrated Cumulative Transformation and Feature Fusion Approach for Bearing Degradation Prognostics", Shock and Vibration, 2018, art. no. 9067184, 2018.

[Elmasry et al., 2017] Elmasry, M., Hawari, A., Zayed, T., "Defect based deterioration model for sewer pipelines using bayesian belief networks", Canadian Journal of Civil Engineering, 44 (9), pp. 675-690, 2017.

[Enright & Frangopol, 1998] Enright, M.P., Frangopol, D.M., "Probabilistic analysis of resistance degradation of reinforced concrete bridge beams under corrosion", Engineering Structures, 20 (11), pp. 960-971, 1998.

[European Commission, 2012] European Commission, "EU transport in figures", statistical pocketbook, 2012.

[Fan et al., 2011] Fan, W., Qiao, P., "Vibration-based damage identification methods: A review and comparative study", Structural Health Monitoring, 10 (1), pp. 83-111, 2011.

[Feng et al., 2015] Feng, D., Feng, M.Q., "Model Updating of Railway Bridge Using in Situ Dynamic Displacement Measurement under Trainloads", Journal of Bridge Engineering, 20 (12), art. no. 04015019, 2015.

[Fenton et al., 2013] Fenton, N., Neil, M., "Risk assessment and decision analysis with Bayesian networks", 1st ed. Oxford: Taylor & Francis, 2013.

[Ferdous et al., 2011] Ferdous, R., Khan, F., Sadiq, R., Amyotte, P., & Veitch, B., "Fault and event tree analyses for process systems risk analysis: Uncertainty handling formulations", Risk Analysis, 31, 86–107, 2011.

[Franchin et al., 2016] Franchin, P., Lupoi, A., Noto, F., Tesfamariam, S., "Seismic fragility of reinforced concrete girder bridges using Bayesian belief network", Earthquake Engineering and Structural Dynamics, 45 (1), pp. 29-44, 2016.

[Frangopol et al., 2004] Frangopol, D.M., Kallen, M.J. and Noortwijk, J.M.V., "Probabilistic models for life-cycle performance of deteriorating structures: review and future directions", Progress in Structural Engineering and Materials, 6(4), pp.197-212, 2004.

[Frangopol et al., 2012] Frangopol, D.M., Saydam, D., Kim, S., "Maintenance, management, life-cycle design and performance of structures and infrastructures: a brief review", Structure and Infrastructure Engineering, 8 (1), pp. 1-25, 2012.

[Galotto et al., 2015] Galotto, L., Brun, A.D.M., Godoy, R.B., Maciel, F.R.R., Pinto, J.O.P., "Data based tools for sensors continuous monitoring in industry applications", IEEE International Symposium on Industrial Electronics, 2015-September, art. no. 7281536, pp. 600-605, 2015.

[Gangone et al., 2011] Gangone, M.V., Whelan, M.J., Janoyan, K.D., "Wireless monitoring of a multispan bridge superstructure for diagnostic load testing and system identification", Computer-Aided Civil and Infrastructure Engineering, 26 (7), pp. 560-579, 2011.

[Gentile et al., 2015] Gentile, C., Saisi, A., "Continuous dynamic monitoring of a centenary iron bridge for structural modification assessment", Frontiers of Structural and Civil Engineering, 9 (1), pp. 26-41, 2015.

[González et al., 2015] González, A., Covián, E., Casero, M., "Impact of super-imposed and truck live load on modal characteristics of short-span bridges", Operational Modal Analysis Conference (IOMAC 2015); Proc. 6th intern. Confer., Gijon (Spain), 10-14 May 2015.

[Guo et al., 2012] Guo, W., Orcesi, A.D., Cremona, C.F., Santos, J.P., Yang, S., Dieleman, L., "A vibration-based framework for structural health monitoring of railway bridges", Life-Cycle and Sustainability of Civil Infrastructure Systems – Proceedings of the 3rd International Symposium on Life-Cycle Civil Engineering, IALCCE 2012, pp. 1118-1125, 2012.

[Hakim et al., 2013] Hakim, S.J.S., Abdul Razak, H., "Structural damage detection of steel bridge girder using artificial neural networks and finite element models", Steel and Composite Structures, 14 (4), pp. 367-377, 2013.

[Han et al., 2014] Han, J., Zheng, P. & Wang, H., "Structural modal parameter identification and damage diagnosis based on Hilbert Huang transform", Earthquake Engineering & Engineering Vibration, Vol. 13, (1) pp 101-111, 2014.

[He et al., 2008] He, X.-H., Yu, Z.-W., Chen, Z.-Q., "Finite element model updating of existing steel bridge based on structural health monitoring", Journal of Central South University of Technology (English Edition), 15 (3), pp. 399-403, 2008.

[Hoell & Omenzetter, 2017] Hoell, S., Omenzetter, P., "Fukunaga-Koontz feature transformation for statistical structural damage detection and hierarchical

neuro-fuzzy damage localisation", Journal of Sound and Vibration, 400, pp. 329-353, 2017.

[Holický et al., 2013] Holický, M., Marková, J., Sýkora, M., "Forensic assessment of a bridge downfall using Bayesian networks", Engineering Failure Analysis, 30, pp. 1-9, 2013.

[Hooper et al., 2012] Hooper, E., Chapman, L., "The impacts of climate change on national road and rail networks", Transport and Sustainability, 2, pp. 105-136, 2012.

[Hsu et al., 2010] Hsu, T.-Y., Loh, C.-H., "Damage detection accommodating nonlinear environmental effects by nonlinear principal component analysis", Structural Control and Health Monitoring, 17 (3), pp. 338-354, 2010.

[Huang et al., 1998] Huang, N.E., Shen, Z., Long, S.R., Wu, M.C., Snin, H.H., Zheng, Q., Yen, N.-C., Tung, C.C., Liu, H.H., "The empirical mode decomposition and the Hubert spectrum for nonlinear and non-stationary time series analysis", Proceedings of the Royal Society A: Mathematical, Physical and Engineering Sciences, 454 (1971), pp. 903-995, 1998.

[IRA, 2015] International railway association, community of European railway and infrastructure, "Rail transport and environment, facts and figure", ISBN 976-2-7461-2400-4, 2015.

[Jaishi & Ren, 2005] Jaishi, B., Ren, W.-X., "Structural finite element model updating using ambient vibration test results", Journal of Structural Engineering, 131 (4), pp. 617-628, 2005.

[Jensen & Nielsen, 2007] Jensen, F.V., Nielsen, T. D., "Bayesian Networks and Decision Graphs", Information Science and Statistics, Springer, 2007.

[Ji et al., 2015] Ji, Z., Xia, Q., Meng, G., "A review of parameter learning methods in bayesian network", Lecture Notes in Computer Science (including subseries Lecture Notes in Artificial Intelligence and Lecture Notes in Bioinformatics), 9227, pp. 3-12, 2015.

[Jian & Murthy, 2011] Jiang, R., Murthy, D.N.P., "A study of Weibull shape parameter: Properties and significance", Reliability Engineering and System Safety, 96 (12), pp. 1619-1626, 2011.

[Kabir et al., 2016] Kabir, G., Sadiq, R., Tesfamariam, S., “A fuzzy Bayesian belief network for safety assessment of oil and gas pipelines”, Structure and Infrastructure Engineering, 12 (8), pp. 874-889, 2016.

[Kan et al., 2015] Kan, M.S., Tan, A.C.C., Mathew, J., “A review on prognostic techniques for non-stationary and non-linear rotating systems”, Mechanical Systems and Signal Processing, 62, pp. 1-20, 2015.

[Katicha et al., 2017] Katicha, S.W., Flintsch, G., Bryce, J., Ferne, B., “Wavelet denoising of TSD deflection slope measurements for improved pavement structural evaluation”, Computer-Aided Civil and Infrastructure Engineering, 29 (6), pp. 399-415, 2014.

[Katipamula et al., 2005] Katipamula, S., Brambley, M.R., “Methods for fault detection, diagnostics, and prognostics for building systems - A review, Part I”, HVAC and R Research, 11 (1), pp. 3-25, 2005.

[Khan et al., 2018] Khan, I., Shan, D., Li, Q., Jie, H., “Continuous modal parameter identification of cable-stayed bridges based on a novel improved ensemble empirical mode decomposition”, Structure and Infrastructure Engineering, 14 (2), pp. 177-191, 2018.

[Killick et al., 2012] Killick, R., Fearnhead, P., Eckley, I.A., “Optimal detection of changepoints with a linear computational cost”, Journal of the American Statistical Association, 107 (500), pp. 1590-1598, 2012.

[Kim et al., 2007] Kim, J.-T., Park, J.-H., Lee, B.-J., “Vibration-based damage monitoring in model plate-girder bridges under uncertain temperature conditions”, Engineering Structures, 29 (7), pp. 1354-1365, 2007.

[Kim et al., 2015] Kim, C.-W., Morita, T., Oshima, Y., Sugiura, K., “A Bayesian approach for vibration-based long-term bridge monitoring to consider environmental and operational changes”, Smart Structures and Systems, 15 (2), pp. 395-408, 2015.

[Koepcke et al., 2016] Koepcke, L., Ashida, G., Kretzberg, J., 2016. “Single and multiple change point detection in spike trains: Comparison of different CUSUM methods”, Frontiers in Systems Neuroscience, 10 (JUN), art. no. 51.

[Lavielle, 2005] Lavielle, M., 2005. “Using penalized contrasts for the change-point problem”, Signal Processing, 85 (8), pp. 1501-1510.

[Killick & Eckley, 2014] Killick, R. and Eckley, I., 2014. “Changepoint: An R package for changepoint analysis”, Journal of Statistical Software, 58(3), pp.1-19.

[Baxter, 2015] Alan Baxter, 2015. “Network Rail A Guide to Overhead Electrification”, 132787-ALB-GUN-EOH-000001, February 2015 Rev 10.

[Ordoñez et al., 2016] Ariznavarreta-Fernández, F., González-Palacio, C., Menéndez-Díaz, A., Ordoñez, C., 2016. “Measurement system with angular encoders for continuous monitoring of tunnel convergence”, Tunnelling and Underground Space Technology, 56, pp. 176-185.

[Lato & Diederichs, 2014] Lato, M.J. and Diederichs, M.S., 2014. “Mapping shotcrete thickness using LiDAR and photogrammetry data: Correcting for over-calculation due to rockmass convergence”, Tunnelling and Underground Space Technology, 41, pp.234-240.

[Mohamad et al., 2012] Mohamad, H., Soga, K., Bennett, P.J., Mair, R.J., Lim, C.S., 2012. “Monitoring twin tunnel interaction using distributed optical fiber strain measurements”, Journal of Geotechnical and Geoenvironmental Engineering, 138 (8), pp. 957-967.

[Kosgodagan-Dalla Torre et al., 2017] Kosgodagan-Dalla Torre, A., Yeung, T.G., Morales-Nápoles, O., Castanier, B., Maljaars, J., Courage, W., “A Two-Dimension Dynamic Bayesian Network for Large-Scale Degradation Modeling with an Application to a Bridges Network”, Computer-Aided Civil and Infrastructure Engineering, 32 (8), pp. 641-656, 2017.

[Kreislova et al., 2012] Kreislova, K., Geiplova, H., “Evaluation of corrosion protection of steel bridges”, Procedia Engineering, 40, pp. 229-234, 2012.

[Lampis et al., 2009] Lampis, M., Andrews, J.D., “Bayesian belief networks for system fault diagnostics”, Quality and Reliability Engineering International, 25 (4), pp. 409-426, 2009.

[Langone et al., 2017] Langone, R., Reynders, E., Mehrkanoon, S., Suykens, J.A.K., “Automated structural health monitoring based on adaptive kernel spectral clustering”, Mechanical Systems and Signal Processing, 90, pp. 64-78, 2017.

[Laory et al., 2012] Laory, I., Hadj Ali, N.B., Trinh, T.N., Smith, I.F.C., “Measurement system configuration for damage identification of continuously monitored structures”, Journal of Bridge Engineering, 17 (6), pp. 857-866, 2012.

[Laory et al., 2013] Laory, I., Trinh, T.N., Posenato, D., Smith, I.F.C., “Combined model-free data-interpretation methodologies for damage detection during continuous monitoring of structures”, Journal of Computing in Civil Engineering, 27 (6), pp. 657-666, 2013.

[Le & Andrews, 2014] Le, B.L., Andrews, J.D., “Modelling railway bridge asset management using Petri-Net modelling techniques”, Civil-Comp Proceedings, 104, 2014.

[LeBeau et al., 2000] LeBeau, K., Wadia-Fascetti, S., “A fault tree model of bridge deterioration”, 8th ASCE conference on probabilistic mechanics and structural reliability, Indiana, USA, 2000.

[Lebeau et al., 2010] Lebeau, K., Wadia-Fascetti, S., “Predictive and diagnostic load rating model of a prestressed concrete bridge”, Journal of Bridge Engineering, 15 (4), pp. 399-407, 2010.

[Lee et al., 2005] Lee, J.J., Lee, J.W., Yi, J.H., Yun, C.B., Jung, H.Y., “Neural networks-based fault detection for bridges considering errors in baseline finite element models”, Journal of Sound and Vibration, 280 (3-5), pp. 555-578, 2005.

[Lee et al., 2014] Lee, J., Wu, F., Zhao, W., Ghaffari, M., Liao, L., Siegel, D., “Prognostics and health management design for rotary machinery systems - Reviews, methodology and applications”, Mechanical Systems and Signal Processing, 42 (1-2), pp. 314-334, 2014.

[Lei et al., 2018] Lei, Y., Li, N., Guo, L., Li, N., Yan, T., Lin, J., “Machinery health prognostics: A systematic review from data acquisition to RUL prediction”, Mechanical Systems and Signal Processing, 104, pp. 799-834, 2018.

[Li & Racine, 2006] Li, Q. & Racine, J. S., “Nonparametric Econometrics Theory and Practice”, Princeton university press, ISBN 9781400841066, 2006.

[Li et al., 2004] Li, Z.N., Tang, J., Li, Q.S., “Optimal sensor locations for structural vibration measurements”, Applied Acoustics, 65 (8), pp. 807-818, 2004.

[Li et al., 2016] Li, H. N., Ren, L., Jia, Z. G., Yi, T. H., & Li, D. S., “State-of-the-art in structural health monitoring of large and complex civil infrastructures”, Journal of Civil Structural Health Monitoring, 6(1), 3-16, 2016.

[Limongelli et al., 2017] Limongelli, M. P., Tirone, M., Surace, C., "Non-destructive monitoring of a prestressed bridge with a data-driven method", Proc. SPIE 10170, Health Monitoring of Structural and Biological Systems 2017,

1017033 (5 April 2017); doi: 10.1117/12.2258381; https://doi.org/10.1117/12.2258381, 2017

[Liu et al., 2008] Liu, W., Gao, W.-c., Sun, Y., Xu, M.-j., “Optimal sensor placement for spatial lattice structure based on genetic algorithms”, Journal of Sound and Vibration, 317 (1-2), pp. 175-189, 2008.

[Liu et al., 2013] Liu, S., Yamada, M., Collier, N., Sugiyama, M., “Change-point detection in time-series data by relative density-ratio estimation”, Neural Networks, 43, pp. 72-83, 2013.

[Loughney & Wang, 2017] Loughney, S., Wang, J., “Bayesian network modelling of an offshore electrical generation system for applications within an asset integrity case for normally unattended offshore installations”, Proceedings of the Institution of Mechanical Engineers, Part M: Journal of Engineering for the Maritime Environment, p.1475090217704787, 2017.

[Loy et al., 2016] Loy, A., Follett, L. and Hofmann, H., “Variations of Q–Q Plots: The Power of Our Eyes!”, The American Statistician, 70(2), pp.202-214, 2016.

[Lynch et al., 2006] Lynch, J. P., Loh, K. J., “A summary review of wireless sensors and sensor networks for structural health monitoring”, Shock and Vibration Digest, 38(2), pp. 91–128, 2006.

[Maleki et al., 2016] Maleki, S., Bingham, C., Zhang, Y., 2016. “Development and Realization of Changepoint Analysis for the Detection of Emerging Faults on Industrial Systems”, IEEE Transactions on Industrial Informatics, 12 (3), art. no. 7458838, pp. 1180-1187.

[Reeves et al., 2007] Reeves, J., Chen, J., Wang, X. L., Lund, R., and Lu., Q., 2007. “A review and comparison of changepoint detection techniques for climate data”, Journal of Applied Meteorology and Climatology, 46(6):900–915.

[Tickle et al., 2010] Tickle, A.J., Harvey, P.K., Smith, J.S., 2010. “Applications of a Morphological Scene Change Detection (MSCD) for visual leak and failure identification in process and chemical engineering”, Proceedings of SPIE - The International Society for Optical Engineering, 7833, art. no. 78330W.

[Montes De Oca et al., 2010] Montes De Oca, V., Jeske, D.R., Zhang, Q., Rendon, C., Marvasti, M., 2010. “A cusum change-point detection algorithm for

non-stationary sequences with application to data network surveillance", Journal of Systems and Software, 83 (7), pp. 1288-1297.

[Manafpour et al., 2018] Manafpour, A., Guler, I., Radlińska, A., Rajabipour, F., Warn, G., "Stochastic Analysis and Time-Based Modeling of Concrete Bridge Deck Deterioration", Journal of Bridge Engineering, 23 (9), art. no. 04018066, 2018.

[Mehrjoo et al., 2008] Mehrjoo, M., Khaji, N., Moharrami, H., Bahreininejad, A., "Damage detection of truss bridge joints using Artificial Neural Networks", Expert Systems with Applications, 35 (3), pp. 1122-1131, 2008.

[Meo & Zumpano, 2005] Meo, M., Zumpano, G., "On the optimal sensor placement techniques for a bridge structure", Engineering Structures, 27 (10), pp. 1488-1497, 2005.

[Mkrtchyan et al., 2016] Mkrtchyan, L., Podofillini, L., Dang, V.N., "Methods for building Conditional Probability Tables of Bayesian Belief Networks from limited judgment: An evaluation for Human Reliability Application", Reliability Engineering and System Safety, 151, pp. 93-112, 2016.

[Morales-Nápoles et al., 2014] Morales-Nápoles, O., Delgado-Hernández, D.J., De-León-Escobedo, D. and Arteaga-Arcos, J.C., "A continuous Bayesian network for earth dams' risk assessment: methodology and quantification", Structure and Infrastructure Engineering, 10(5), pp.589-603, 2014.

[Mosallam et al., 2014] Mosallam, A., Medjaher, K., Zerhouni, N., "Time series trending for condition assessment and prognostics", Journal of Manufacturing Technology Management, 25 (4): 550-567, 2014.

[Mottershead & Friswell, 1993] Mottershead, J.E. and Friswell, M.I., "Model updating in structural dynamics: a survey", Journal of Sound and Vibration, 167(2), 347–375, 1993.

[Moughty & Casas, 2017] Moughty, J.J., Casas, J.R., "Performance Assessment of Vibration Parameters as Damage Indicators for Bridge Structures under Ambient Excitation", Procedia Engineering, 199, pp. 1970-1975, 2017.

[Moughty & Casas, 2017b] Moughty, J., Casas, J., "Evaluation of the Hilbert Huang transformation of transient signals for bridge condition assessment", European Safety and Reliability Conference. "Safety and Reliability: Theory and Applications". Portoroz: CRC Press, p. 2741-2749, 2017.

[Moughty et al., 2017] Moughty, J.J., Casas, J.R., “A state of the art review of modal-based damage detection in bridges: Development, challenges, and solutions”, Applied Sciences (Switzerland), 7 (5), art. no. 510, 2017.

[Muin & Mosalam, 2017] Muin, S. & Mosalam, K., “Cumulative Absolute Velocity as a Local Damage Indicator of Instrumented Structures”. Earthquake Spectra. 33. 641-664. 10.1193/090416EQS142M, 2017.

[Nair et al., 2010] Nair, A., Cai, C.S., “Acoustic emission monitoring of bridges: Review and case studies”, Engineering Structures, 32 (6), pp. 1704-1714, 2010.

[Ni et al., 2012] Ni, Y.Q., Xia, H.W., Wong, K.Y., Ko, J.M., “In-service condition assessment of bridge deck using long-term monitoring data of strain response” Journal of Bridge Engineering, 17 (6), pp. 876-885, 2012.

[Ni, 2014] Ni, Y. Q., “Structural health monitoring of cable-supported bridges based on vibration measurements”, Proceedings of the 9th International Conference on Structural Dynamics, EURODYN 2014 Porto, Portugal, 2014.

[Noroozian et al., 2018] Noroozian, A., Kazemzadeh, R.B., Niaki, S.T.A., Zio, E., “System Risk Importance Analysis Using Bayesian Networks”, International Journal of Reliability, Quality and Safety Engineering, 25 (1), art. no. 1850004, 2018.

[Park et al., 2009] J.H. Park, J.T. Kim, D.S. Honga, D.D. Hoa, J.H. Yib, “Sequential damage detection approaches for beams using time-modal features and artificial neural networks”, Journal of Sound and Vibration, 323, 451–474, 2009.

[Pearl, 1986] Pearl, J., “Fusion, propagation, and structuring in belief networks”, Artificial Intelligence, 29 (3), pp. 241-288, 1986.

[Perkusich et al., 2013] Perkusich, M., Perkusich, A., De Almeida, H.O., “Using survey and weighted functions to generate node probability tables for Bayesian networks”, Proceedings - 1st BRICS Countries Congress on Computational Intelligence, BRICS-CCI 2013, art. no. 6855848, pp. 183-188, 2013.

[Phares et al., 2004] Phares, B. M., Washer, G. A., Rolander, D. D., Graybeal, B. A. Moore, M., “Routine highway bridge inspection condition documentation accuracy and reliability”, Journal of Bridge Engineering, 9 (4), pp. 403–13, 2004.

[Pipinato & Patton, 2016] Pipinato, A., Patton, R., “Chapter 19 – Railway bridges”, Innovative Bridge Design Handbook Construction, Rehabilitation and Maintenance, Pages 509–527, 2016

[Qin, 2012] Qin, S.J., “Survey on data-driven industrial process monitoring and diagnosis”, Annual Reviews in Control, 36 (2), pp. 220-234, 2012.

[Rafiq et al., 2015] Rafiq, M.I., Chryssanthopoulos, M.K., Sathananthan, S., “Bridge condition modelling and prediction using dynamic Bayesian belief networks”, Structure and Infrastructure Engineering, 11 (1), pp. 38-50, 2015.

[Rajabi et al., 2017] Rajabi, M., Rahmannejad, R., Rezaei, M., Ganjalipour, K., “Evaluation of the maximum horizontal displacement around the power station caverns using artificial neural network”, Tunnelling and Underground Space Technology, 64, pp. 51-60, 2017.

[Rao et al., 2017] Rao, A.S., Lepech, M.D., Kiremidjian, A., “Development of time-dependent fragility functions for deteriorating reinforced concrete bridge piers”, Structure and Infrastructure Engineering, 13 (1), pp. 67-83, 2017.

[Rathje et al., 2004] Rathje, E.M., Faraj, F., Russell, S., Bray, J.D., “Empirical Relationships for Frequency Content Parameters of Earthquake Ground Motions”, Earthquake Spectra, 20 (1), pp. 119-144, 2004.

[Rehman & Mandic, 2010] Rehman, N., Mandic, D.P., “Multivariate empirical mode decomposition”, Proceedings of the Royal Society A: Mathematical, Physical and Engineering Sciences, 466 (2117), pp. 1291-1302, 2010.

[Rigamonti et al., 2016] Rigamonti, M., Baraldi, P., Zio, E., Alessi, A., Astigarraga, D., Galarza, A., “Identification of the degradation state for condition-based maintenance of insulated gate bipolar transistors: A self-organizing map approach”, Microelectronics Reliability, 60, pp. 48-61, 2016.

[Roberts et al., 2004] Roberts, G.W., Meng, X., Dodson, A.H., “Integrating a global positioning system and accelerometers to monitor the deflection of bridges”, Journal of Surveying Engineering, 130 (2), pp. 65-72, 2004.

[Saaty et al., 2007] Saaty, T.L., Tran, L.T., “On the invalidity of fuzzifying numerical judgments in the Analytic Hierarchy Process”, Mathematical and Computer Modelling, 46 (7-8), pp. 962-975, 2007.

[Sadhu, 2017] Sadhu, A., “An integrated multivariate empirical mode decomposition method towards modal identification of structures”, JVC/Journal of Vibration and Control, 23 (17), pp. 2727-2741, 2017.

[Saeed et al., 2017] Saeed, T.U., Qiao, Y., Chen, S., Gkritza, K., Labi, S., “Methodology for probabilistic modeling of highway bridge infrastructure

condition: Accounting for improvement effectiveness and incorporating random effects", Journal of Infrastructure Systems, 23 (4), art. no. 04017030, 2017.

[Salamatian et al., 2013] Salamatian, S.A., Zarrati, A.R., Banazadeh, M., "Assessment of bridge safety due to scour by Bayesian network", Proceedings of the Institution of Civil Engineers: Water Management, 166 (6), pp. 341-350, 2013.

[Sanayei et al., 2015] Sanayei, M., Khaloo, A., Gul, M., Necati Catbas, F., "Automated finite element model updating of a scale bridge model using measured static and modal test data", Engineering Structures, 102, pp. 66-79, 2015.

[Santillán et al., 2015] Santillán, D., Salete, E., Toledo, M.Á., "A methodology for the assessment of the effect of climate change on the thermal-strain-stress behaviour of structures", Engineering Structures, 92, pp. 123-141, 2015.

[Santos et al., 2016] de Oliveira Dias Prudente dos Santos, J.P., Crémona, C., da Silveira, A.P.C., de Oliveira Martins, L.C., "Real-time damage detection based on pattern recognition", Structural Concrete, Article in Press, 2016.

[Schlune et al., 2009] Schlune, H., Plos, M., Gylltoft, K., "Improved bridge evaluation through finite element model updating using static and dynamic measurements", Engineering Structures, 31 (7), pp. 1477-1485, 2009.

[Sekkal et al., 2017] Sekkal, M.C., Berrached, N., Medjaher, K., Varnier, C., "Skeleton of a generic approach for the generation of health indicators of physical systems", Colloquium in Information Science and Technology, CIST, art. no. 7804960, pp. 621-626, 2017.

[Sekuła et al., 2012] Sekuła, K., Kołakowski, P., "Piezo-based weigh-in-motion system for the railway transport", Structural Control and Health Monitoring, 19 (2), pp. 199-215, 2012.

[Shabbir et al., 2016] Shabbir, F., Omenzetter, P., "Model updating using genetic algorithms with sequential niche technique", Engineering Structures, 120, pp. 166-182, 2016.

[Shu et al., 2013] Shu, J., Zhang, Z., Gonzalez, I., Karoumi, R., "The application of a damage detection method using Artificial Neural Network and train-induced vibrations on a simplified railway bridge model", Engineering Structures, 52, pp. 408-421, 2013.

[Silverman, 2018] Silverman, B.W., "Density estimation for statistics and data analysis", Routledge, ISBN 9781351456173, 2018.

[Siringoringo et al., 2013] Siringoringo, D.M., Fujino, Y., Nagayama, T., “Dynamic characteristics of an overpass bridge in a full-scale destructive test”, Journal of Engineering Mechanics, 139 (6), pp. 691-701, 2013.

[Sobanjo et al., 2010] Sobanjo, J., Mtenga, P., Rambo-Roddenberry, M., “Reliability-based modeling of bridge deterioration hazards”, Journal of Bridge Engineering, 15, 671-683, 2010.

[Soyoz et al., 2009] Soyoz, S., Feng, M.Q., “Long-term monitoring and identification of bridge structural parameters”, Computer-Aided Civil and Infrastructure Engineering, 24 (2), pp. 82-92, 2009.

[Stajano et al., 2010] Stajano, F., Hoult, N., Wassell, I., Bennett, P., Middleton, C., Soga, K., “Smart bridges, smart tunnels: Transforming wireless sensor networks from research prototypes into robust engineering infrastructure”, Ad Hoc Networks, 8 (8), pp. 872-888, 2010.

[Sun et al., 2006] Sun, S., Zhang, C., Yu, G., “A Bayesian network approach to traffic flow forecasting”, IEEE Transactions on Intelligent Transportation Systems, 7 (1), pp. 124-133, 2006.

[Surowiecki, 2004] Surowiecki, J., "The Wisdom of Crowds: Why the many are smarter than the few and how collective wisdom shapes business, economies, societies and nations". Brown, Little, 2004, ISBN: 0-316-86173-1, 2004.

[Tesfamariam et al., 2010] Tesfamariam, S., Sadiq, R., & Najjaran, H., “Decision-making under uncertainty – An example for seismic risk management” Risk Analysis, 30, 78–94, 2010.

[Teughels et al., 2002] Teughels, A., Maeck, J., De Roeck, G., “Damage assessment by FE model updating using damage functions”, Computers and Structures, 80 (25), pp. 1869-1879, 2002.

[Torfi et al., 2010] Torfi, F., Farahani, R.Z., Rezapour, S., “Fuzzy AHP to determine the relative weights of evaluation criteria and Fuzzy TOP-SIS to rank the alternatives”, Applied Soft Computing Journal, 10 (2), pp. 520-528, 2010.

[Vagnoli & Remenyte-Prescott, 2018] Vagnoli, M., Remenyte-Prescott, R., “An ensemble-based change-point detection method for identifying unexpected behaviour of railway tunnel infrastructures”, Tunnelling and Underground Space Technology Journal, 81, pp. 68-82, 2018.

[Vagnoli et al., 2018] Vagnoli, M., Remenyte-Prescott, R., Andrews, J., “Railway bridge structural health monitoring and fault detection: State-of-the-art methods and future challenges”, Structural Health Monitoring, 17 (4), pp. 971-1007, 2018.

[Venkatasubramanian et al., 2003] Venkatasubramanian, V., Rengaswamy, R., Yin, K., Kavuri, S.N., “A review of process fault detection and diagnosis part I: Quantitative model-based methods”, Computers and Chemical Engineering, 27 (3), pp. 293-311, 2003.

[Vicente et al., 2018] Vicente, M.A., Gonzalez, D.C., Minguez, J., Schumacher, T., “A novel laser and video-based displacement transducer to monitor bridge deflections”, Sensors (Switzerland), 18 (4), art. no. 970, 2018.

[Vileiniskis et al., 2016] Vileiniskis, M., Remenyte-Prescott, R., Rama, D., Andrews, J., “Fault detection and diagnostics of a three-phase separator”, Journal of Loss Prevention in the Process Industries, 41, pp. 215-230, 2016.

[Wang et al., 2006] Wang, Y.-M., Elhag, T.M.S., “On the normalization of interval and fuzzy weights”, Fuzzy Sets and Systems, 157 (18), pp. 2456-2471, 2006.

[Wang et al., 2009] Wang, L., Chan, T.H.T., “Review of vibration-based fault detection and condition assessment of bridge structures using structural health monitoring”, the Second Infrastructure Theme Postgraduate Conference, Queensland University, 2009.

[Wang et al., 2012] Wang, R., Ma, L., Yan, C., Mathew, J., “Condition deterioration prediction of bridge elements using Dynamic Bayesian Networks (DBNs)”, ICQR2MSE 2012, art. no. 6246298, pp. 566-571, 2012.

[Webb et al., 2015] Webb, G.T., Vardanega, P.J., Middleton, C.R., “Categories of SHM deployments: Technologies and capabilities”, Journal of Bridge Engineering, 20 (11), art. no. 04014118, 2015.

[Wellalage et al., 2015] Wellalage, N.K.W., Zhang, T., Dwight, R., “Calibrating Markov chain-based deterioration models for predicting future conditions of railway bridge elements”, Journal of Bridge Engineering, 20 (2), art. no. 04014060, 2015.

[Wu & Huang, 2009] Wu, Z. and Huang, N.E., “Ensemble empirical mode decomposition: a noise-assisted data analysis method”, Advances in adaptive data analysis, 1(01), pp.1-41, 2009.

[Xia et al., 2014] Xia, C., De Roeck, G., “Modal analysis of the Jalon Viaduct using FE updating”, Proceedings of the International Conference on Structural Dynamic, EURODYN, 2014-January, pp. 2311-2317, 2014.

[Yang & Lee, 2018] Yang, J.P., Lee, W.-C., “Damping Effect of a Passing Vehicle for Indirectly Measuring Bridge Frequencies by EMD Technique”, International Journal of Structural Stability and Dynamics, 18 (1), art. no. 1850008, 2018.

[Yeung et al., 2005] Yeung, W.T., Smith, J.W., “Fault detection in bridges using neural networks for pattern recognition of vibration signatures”, Engineering Structures, 27 (5), pp. 685-698, 2005.

[Yi et al., 2013] Yi, T.-H., Li, H.-N., Gu, M., “Experimental assessment of high-rate GPS receivers for deformation monitoring of bridge”, Measurement: Journal of the International Measurement Confederation, 46 (1), pp. 420-432, 2013.

[Yin et al., 2014] Yin, S., Ding, S.X., Xie, X., Luo, H., “A review on basic data-driven approaches for industrial process monitoring”, IEEE Transactions on Industrial Electronics, 61 (11), art. no. 6717991, pp. 6414-6428, 2014.

[Zeng et al., 2015] Zeng, X., Wang, D. and Wu, J., “Evaluating the three methods of goodness of fit test for frequency analysis”, Journal of Risk Analysis and Crisis Response, 5(3), pp.178-187, 2015.

[Zhao & Jia, 2017] Zhao, M., Jia, X., “A novel strategy for signal denoising using reweighted SVD and its applications to weak fault feature enhancement of rotating machinery”, Mechanical Systems and Signal Processing, 94, pp. 129-147, 2017.

[Zhao et al., 2015] Zhao, X., Liu, H., Yu, Y., Xu, X., Hu, W., Li, M., Ou, J., “Bridge displacement monitoring method based on laser projection-sensing technology”, Sensors, 15 (4), pp. 8444-8643, 2015.

[Zhou & Yi, 2014] Zhou, G.-D., Yi, T.-H., “A summary review of correlations between temperatures and vibration properties of long-span bridges”, Mathematical Problems in Engineering, 2014, art. no. 638209, 2014.

[Zhou et al., 2014] Zhou, X.T., Ni, Y.Q., Zhang, F.L., “Damage localization of cablesupported bridges using modal frequency data and probabilistic neural network”, Mathematical Problems in Engineering, 2014, art. no. 837963, 2014.

[Zhou et al., 2015] Zhou, F., Zhang, W., Sun, K., & Shi, B., “Health state evaluation of shield tunnel SHM using fuzzy cluster method”, Nondestructive Evaluation and Health Monitoring pp. 94371J, 2015.

[Zio et al., 2010] Zio, E., Di Maio, F., “A data-driven fuzzy approach for predicting the remaining useful life in dynamic failure scenarios of a nuclear system”, Reliability Engineering and System Safety, 95 (1), pp. 49-57, 2010.

[Zio, 2012] Zio, E., “Prognostic and health management of industrial equipment”, Diagnostic and Prognostic of Engineering Systems: Methods and Techniques, IGI Global, pp. 333-356, 2012.

[Žvokelj et al., 2011] Žvokelj, M., Zupan, S., Prebil, I., “Non-linear multivariate and multiscale monitoring and signal denoising strategy using Kernel Principal Component Analysis combined with Ensemble Empirical Mode Decomposition method”, Mechanical Systems and Signal Processing, 25 (7), pp. 2631-2653, 2011.

Appendix A – The Modified Binary Differential evolution

The Modified Binary Differential Evolution (MBDE) is an evolutionary algorithm, which has shown good performance in tackling optimization problems with high number of variables [Di Maio et al., 2016]. Given a space of size *R* of HIs (in this case study), the solution space is formed by 2^R-1 possible solutions (by excluding the solution where no HIs are chosen). Hence, each possible solution is represented by a specific combination of HIs that is represented by a binary *R*-dimensional vector $\bar{x} = (x_1, x_2, ..., x_R)$, usually called chromosome. Each x_i of the chromosome is known as gene. A chromosome $\bar{x}$ allows to choose a subset of HIs: if a 1 is present in the *i*-th gene of the vector x_i, the HIth is chosen in the possible solution $\bar{x}$; otherwise the HIth is not chosen and the value of the *i*-th gene position x_i is equal to 0.

The MBDE assess the goodness of each chromosome of each population (a group of NP chromosome) iteratively for a maximum number of generation G_{max}, where the following generation provides better results, or at least equal, to the previous generation due to the definition of the population at *G+1*. For each generation *G*, the MBDE performs three phases to define the chromosome population: *i)* mutation; *ii)* crossover; *iii)* selection.

i) **Mutation.** Given the population of *NP* different chromosomes $\bar{x}_G = (x_1, x_2, ..., x_R)_G$ at generation *G*, the chromosomes at the *G+1*-th generation are obtained by adding to gene x_i of the chromosome vector $\bar{x}_G = (x_1, x_2, ..., x_R)_G$ a noisy gene v_i of the noisy vector $\bar{v}_{G+1} = (v_1, v_2, ..., v_R)_{G+1}$. The noisy vector $\bar{v}_{G+1} = (v_1, v_2, ..., v_R)_{G+1}$ is obtained as follows: a probability estimation operator (Eq. (A.1)) is introduced to generate mutated genes, by accounting for the information of the parent population:

$$P(x_i) = \frac{1}{1 + e^{-\frac{2b \cdot \left[x_{i(l)} + F \cdot \left(x_{i(k)} - x_{i(m)} \right) - 0.5 \right]}{1+2F}}} \tag{A.1}$$

where *b* is a positive real constant, usually set to the value of *6*; $F \in [0,2]$ is known as weighting factor. *F* is defined by the user and kept constant during the optimization. Finally, $x_{i_{(l)}}, x_{i_{(k)}}$ and $x_{i_{(m)}}$, with $l,k,m \in \{1,2,...,NP\}$, are the *i*-th genes of three randomly chosen chromosome of the population *NP*.

The corresponding genes of the noisy vector $\bar{v}_{G+1}$ of the current target individual $\bar{x}_G$ are generated as follows:

$$v_i = \begin{cases} 1 & \text{if } rand \le P(x_i) \\ 0 & \text{otherwise} \end{cases} \qquad \text{(A.2)}$$

where $P(x_i)$ is the probability estimation operator of the *i-th* gene and *rand* is a random number drawn from the standard uniform distribution on the open interval (0,1).

ii) **Crossover.** The noisy vector $\bar{v}_{G+1}$ obtained by Eq. (A.2) is not directly compared with $\bar{x}_G$, but it is modified with the aim of having a diversity of chromosome inside the perturbed population *G+1*. The crossover phase aims to mix $\bar{v}_{G+1}$ and $\bar{x}_G$ according to Eq. (A.3) in order to create a trial vector $\bar{u}_{G+1}$, which is formed by different pieces of chromosome of $\bar{v}_{G+1}$ and $\bar{x}_G$. The genes of the trial individual $\bar{u}_{G+1}$ can be obtained by the crossover operator through Eq. (A.3):

$$u_i = \begin{cases} v_i & \text{if } rand \le CR \text{ or } i = irand(R) \\ x_i & \text{otherwise} \end{cases} \qquad \text{(A.3)}$$

where $CR \in [0,1]$ is known as control parameter, and it is defined by the user. *CR* influences the probability for $\bar{v}_{G+1}$ to be selected for the mutation process. *irand(R)* is a number randomly sampled from and uniform discrete distribution $\{1,2,...,R\}$.

iii) **Selection.** The objective function of the MBDE (fitness function, e.g. inverse of the accuracy of the NFC in this thesis) is evaluated by using the trail vector

$\bar{u}_{G+1}$ as input of the objective function. The aim of the MBDE is to minimize the objective function, and consequently if the objective function of $\bar{u}_{G+1}$ is lower than the objective function of $\bar{x}_G$, the trail vector $\bar{u}_{G+1}$ will be a chromosome of the next population *G+1*, by replacing the chromosome $\bar{x}_G$.

$$\bar{x}_{G+1} = \begin{cases} \bar{u}_{G+1} & \textit{if } \textit{fitness}(\bar{u}_{G+1}) < \textit{fitness}(\bar{x}_G) \\ \bar{x}_G & \textit{otherwise} \end{cases} \qquad \text{(A.4)}$$

Appendix B – Analysis of nine distributions for fitting the bridge HI values

In section 5.2.2 a set of three pdfs is introduced in order to identify a distribution to fit the data of the optimal HI of a bridge. In this way, the CPTs of a BBN can be updated by taking account of both the expert knowledge and the bridge behaviour analysis. A wider group of pdfs is analysed in this Appendix, in order to evaluate whether the HI values can be fitted by a different distribution in a better way, by providing more reliable results. The set of nine distribution contains the three distributions presented in section 5.2.2 (uniform, Weibull and normal), plus 6 arbitrarily chosen pdfs (gamma, inverse Gaussian, log-normal, logistic, log-logistic and Generalized Extreme Value (GEV)). The considered group of pdfs is not comprehensive, and further analysis could to be carried out in the future in order to identify the most suitable pdf to model the HI values of a bridge.

In what follows, the nine pdfs are fitted to the data of the optimal HI of the post-tensioned bridge for each health state of the bridge (i.e. healthy, partially degraded and severely degraded). The goodness of the fitting process is evaluated by considering both the AICc index and the Q-Q plot. The K-S test is not considered due to the fact that the three pdfs considered in section 5.2.2 outperform the other 6 distributions generally. However, the GEV distribution is selected as the possible best fitting model for three health states of the bridge. Therefore, in section B.1 Weibull vs Generalized Extreme value distribution for HIs the CDFs of the GEV and of the Weibull distribution are compared in order to show that the influence of the difference between these two distributions on the performance of the BBN is negligible.

The HI values of each health state of the bridge are analysed as follows:

1. **HI values of the healthy bridge.** The HI values obtained by analysing the bridge acceleration provided by both sensor A and sensor B are fitted by

considering the 9 pdfs. Figure B- 1and Figure B- 2 show the AICc and the Q-Q plots for sensor A and sensor B respectively. The three pdfs presented in section 5.2.2 show the best values of AICc Figure B- 1. On the contrary, Figure B- 2 shows that the GEV distribution has the lowest AIC, whereas the Weibull distribution was pointed out as the best fitting model in section 5.2.2. The AICc values of most of the pdfs are similar, and thus each pdf can potentially be a good fit for the available dataset. It is worth noting that when a larger dataset is available, the fitting process is more accurate and the difference between the AICc value of different pdfs is expected to increase.

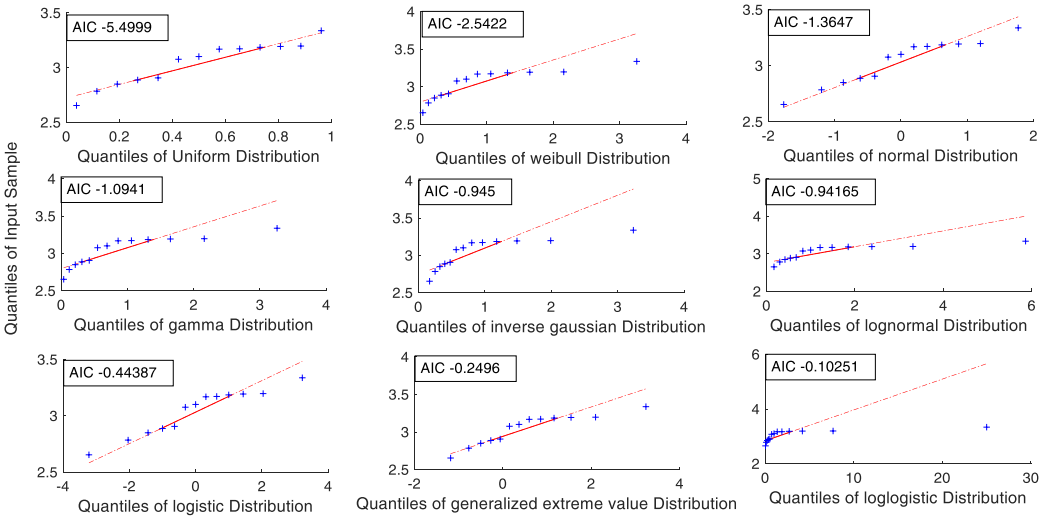

Figure B- 1. *AICc values and Q-Q plots of the healthy state of the bridge for sensor A*

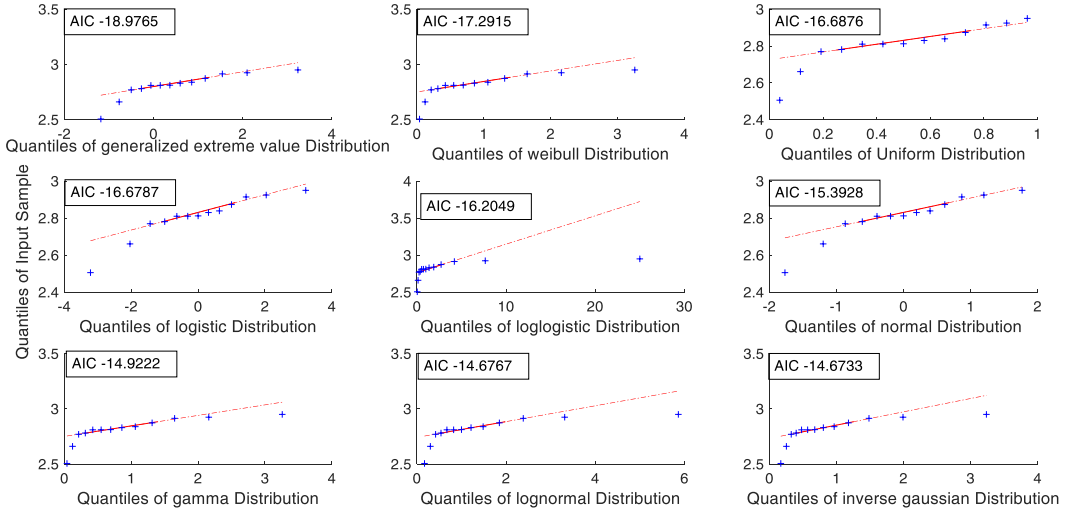

Figure B- 2. *AICc values and Q-Q plots of the healthy state of the bridge for sensor B*

2. **HI values for partially degraded states of the bridge elements.** The values of the optimal HI of the partially degraded health state of the bridge elements are fitted by the 9 pdfs. Figure B- 3and Figure B- 4 present the analysis of the goodness of the fitting process for the nine pdfs. Again, the GEV distribution is among the best fitting models in both Figure B- 3and Figure B- 4. Figure B- 3 confirms the uniform distribution as the distribution with the lowest AICc, whereas Figure B- 4. points out that the GEV distribution has the lowest AICc.

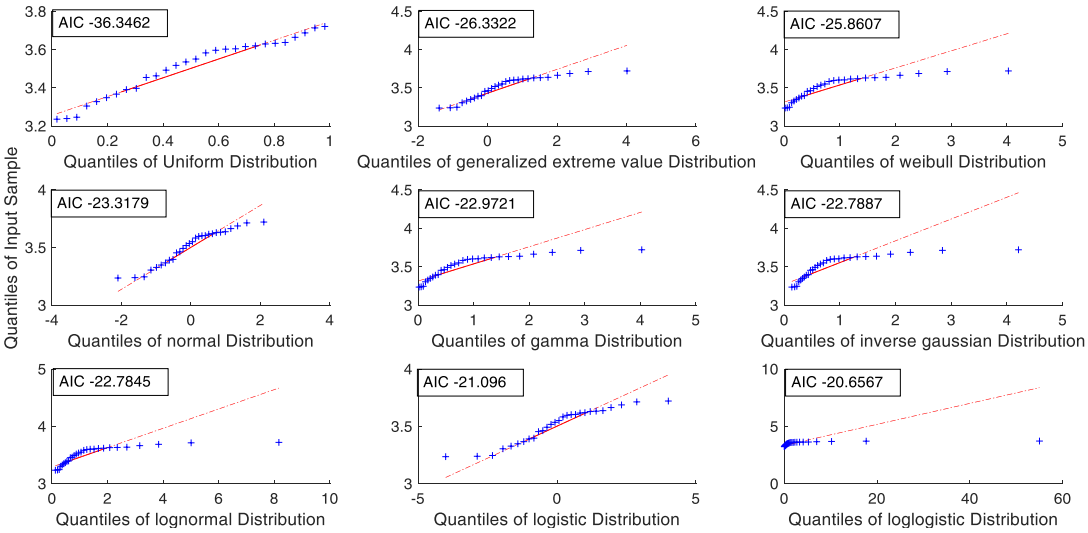

Figure B- 3. *AICc values and Q-Q plots of the partially degraded state of the bridge elements for sensor A*

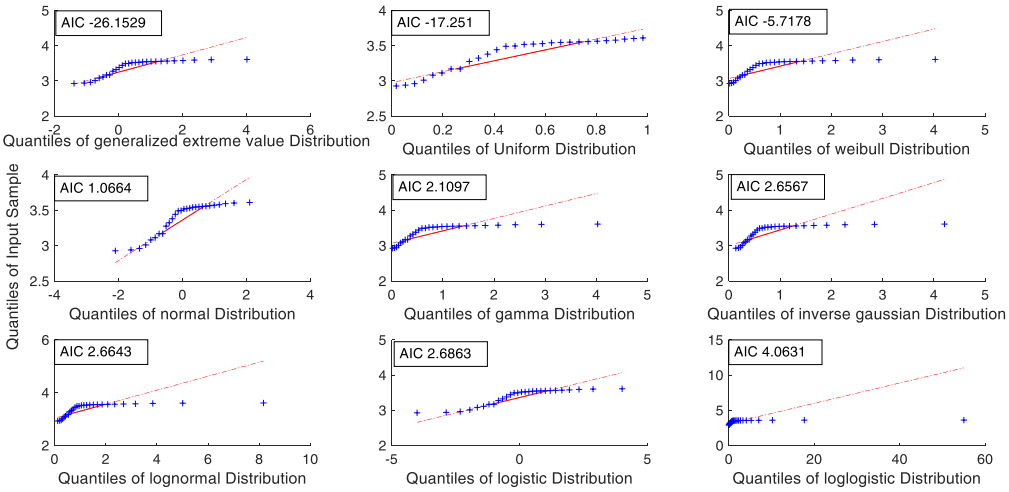

Figure B- 4. *AICc values and Q-Q plots of the partially degraded state of the bridge elements for sensor B*

3. **HI values for severely degraded states of the bridge elements.** The 9 pdfs are used to fit the data of the optimal HI of the severely degraded health state

of the bridge elements. Figure B- 5 and Figure B- 6 shows the results of the analysis of the goodness of the fitting process. The AICc of most of the pdfs is similar, and as a consequence further analysis is needed in order to assess if the HI data belongs to the pdf with the lowest AICc value. Figure B- 5 shows that the GEV distribution provides the lowest AICc, and thus it should be used to update the CPTs of the BBN. Again, when the size of the HI set increases, the difference between the AICc values of different pdfs is expected to increase due to the fact that a more reliable fitting process can be carried out.

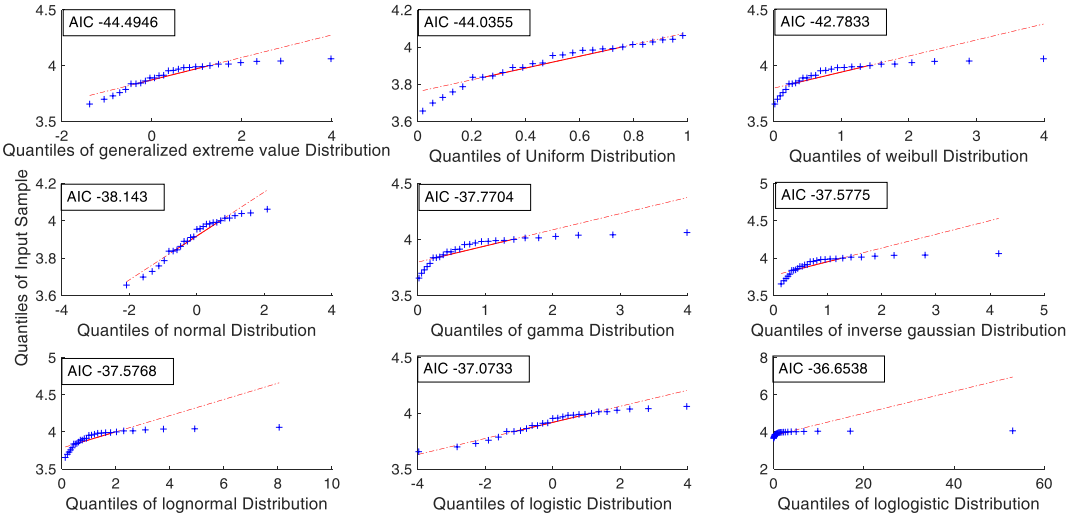

Figure B- 5. *AICc values and Q-Q plots of the severely degraded state of the bridge elements for sensor A*

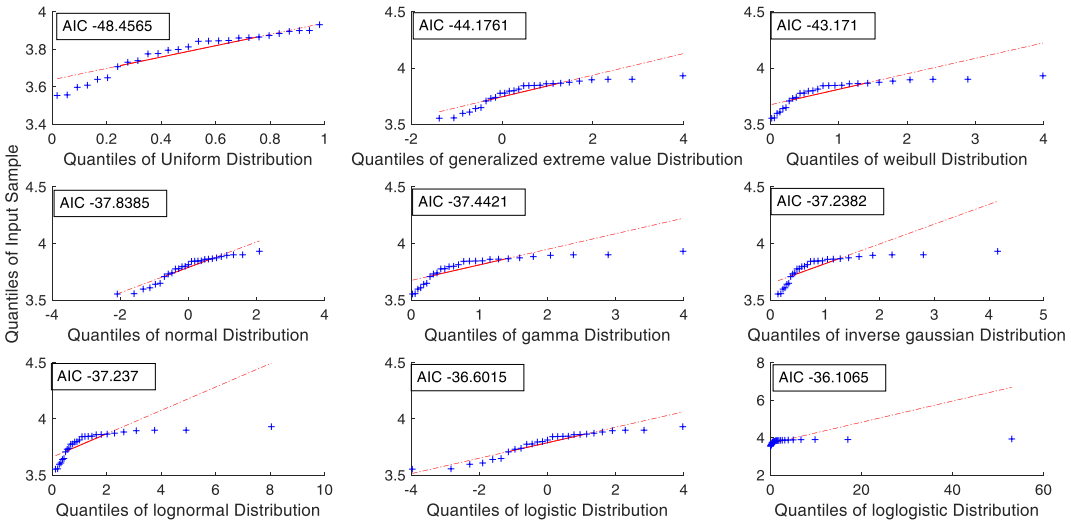

Figure B- 6. *AICc values and Q-Q plots of the severely degraded state of the bridge elements for sensor B*

B.1 Weibull vs Generalized Extreme value distribution for HIs

The GEV distribution provides the minimum value of AICc for three health states of the bridge elements: *i)* the healthy state of the values recorded by sensor A; *ii)* the partially degraded state of the values recorded by sensor B; *iii)* the severely degraded state of the values recorded by sensor B. As a consequence, the GEV distribution should be adopted to update the CPTs of the BBN, in order to assess the health state of the bridge by considering both the bridge expert judgment and the analysis of the bridge behaviour. Section 6.3.3 has discussed the performance of the BBN when the uniform and the Weibull distributions are used to update the CPTs. The analysis of the BBN performance showed that the diagnostic ability of the BBN is influenced by the shape of the CDF. For example, the CDF of the uniform distribution increases rapidly than the CDF of the Weibull, and thus the probability of the damaged BBN node of being in a degraded state is higher when the uniform distribution is adopted, rather than the Weibull CDF. Therefore, Figure B- 7 shows the CDF of the Weibull (by using a solid blue line) and of the GEV distribution (by the means of a dotted red line) for the three health states in which the GEV distribution provides the lowest AICc. The CDF of the Weibull and the GEV distribution increase in a similar manner, when the HI values increase. Therefore, the diagnostic performance of the BBN would be indistinguishable when the Weibull or the GEV distributions are adopted.

However, it is worth mentioning that the nature of the CDF needs to be pointed out in a reliable and robust manner, in order to increase the accuracy of the BBN performance. Therefore, as discussed in the future work session, the analysis of the fitting model needs to be further considered.

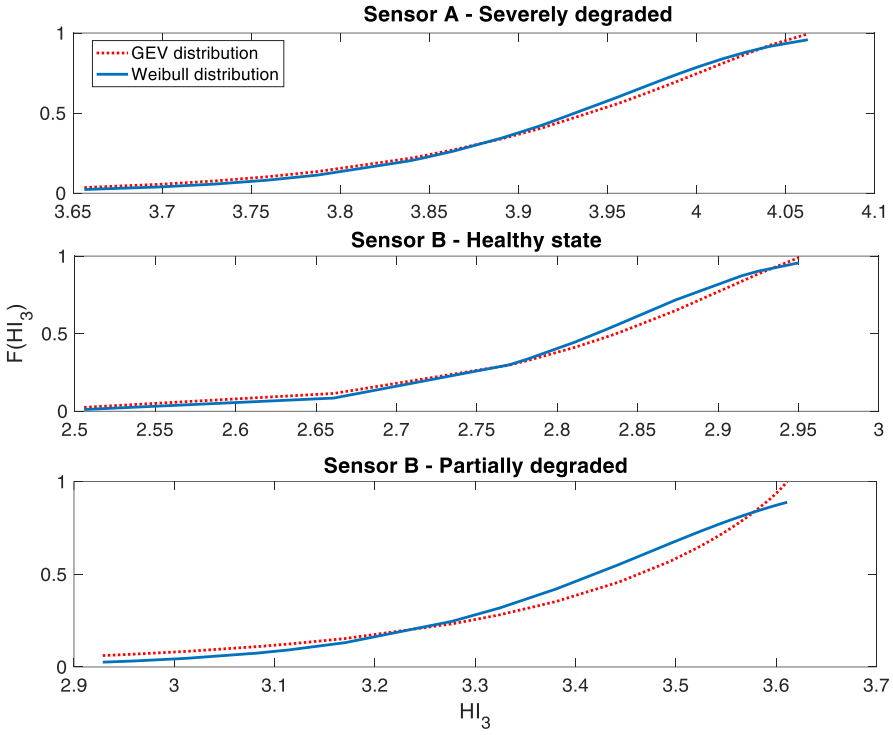

Figure B- 7. *Comparison between Weibull and GEV CDF*

Appendix C – Comparison between the optimal HI of the post-tensioned bridge for different τ^*

In section 5.3 a $\tau^* = 15\ \tau$ has been considered in order to obtain a set of HI values for updating the CPTs of a BBN. The optimal value of τ^* is equal to 45 τ, as shown in section 4.3.6. Figure C- 1 shows the evolution of the optimal HI for monitoring the health state of the post-tensioned bridge elements when different values of τ^* and τ are considered: Figure C- 1(a) shows the evolution of the HI when τ=0.5sec and $\tau^* = 15\ \tau$, Figure C- 1(b) shows the evolution of the HI when τ=3.5sec and $\tau^* = 15\ \tau$, and Figure C- 1(c) shows the evolution of the optimal HI when τ=3.5sec and $\tau^* = 45\ \tau$. Figure C- 1(c) represents the optimal configuration to monitor and assess the health state of the bridge, as shown in section 4.3.6, i.e. the definition of τ=3.5sec and $\tau^* = 45\ \tau$ allows to maximize the GI. It should be noted that the lower the value of both τ and τ^*, the higher the number of assessments of the HI. As a consequence, although the three plots are based on the analysis of the same set of data, the range τ^* decreases when both τ and τ^* increases.

The comparison between the three figures shows two main results: *i)* the higher the values of both τ and τ^*, the higher the value of the optimal HI, due to the assessment of a higher number of bridge vibration data. This can be behaviour of the HI can be due to the amount of energy of the bridge that is analysed and lumped into the assessment of the optimal HI. For example, the minimum value of the optimal HI increases from 2.2 in Figure C- 1(a) to 2.7 in Figure C- 1(c); *ii)* Figure C- 1(b) and Figure C- 1(c) show the same range of values for the HI, and a similar evolution over time of the HI, which allows to point out the different health states of the bridge elements. Figure C- 1(c) allows to point out the different health states of the bridge elements in a clearer manner than the HI values in Figure C- 1(b). However. Figure C- 1(b) shows that the evolution of the optimal HI of the bridge when τ=3.5sec and 5sec and $\tau^* = 15\ \tau$ is very similar to the evolution of the HI in Figure C- 1(c). The analysis of the two plots justify the hypothesis that the HI values of Figure C- 1(b) are used to define the CDF of the bridge health states. The main difference between Figure C- 1(b) and Figure C- 1(c) is that the HI values of Figure C- 1(b) show higher oscillations that

the values in Figure C- 1(c), which show a higher monotonicity throughout the monitoring time.

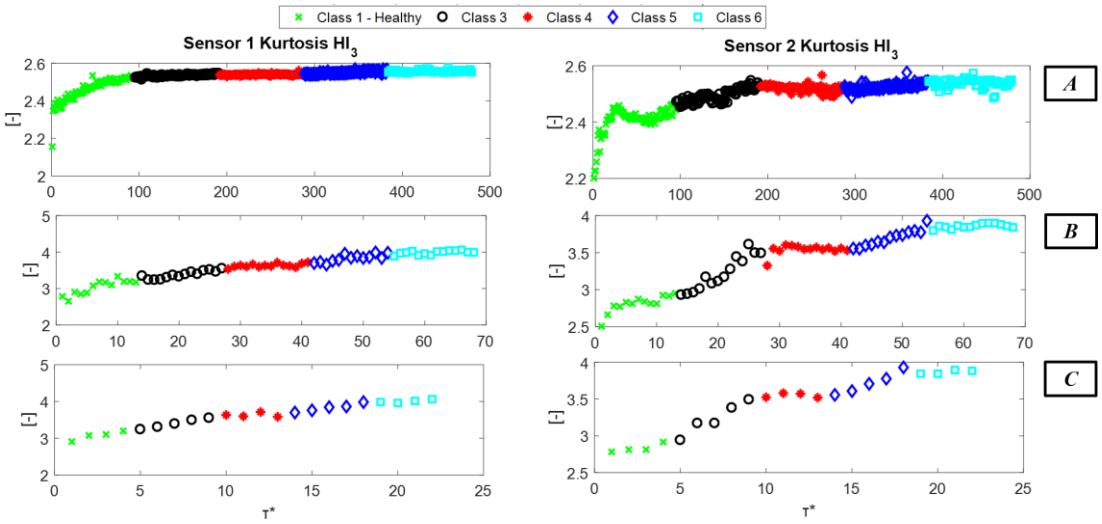

Figure C- 1. *Evolution of the optimal HI to monitor the health state of the elements of the post-tensioned bridge for different values of τ**

Appendix D – Plots of the HIs of each extracted feature for the post-tensioned concrete bridge

In section 4.2 the figure of the optimal HIs are presented, with the aim of describing how the different health states of the bridge can be identified by monitoring the evolution of the optimal HIs. In this Appendix, the plots of the HIs of each extracted feature are presented, in order to show the evolution of the all HIs computed during the progressive damage test of the post-tensioned concrete bridge. It is worth recalling that 18 features have been extracted from the free-vibration of the bridge, and 4 HIs have been assessed for evaluating the trend of each feature over time. Each plot represents on the x-axes the evolution of the monitoring time, whereas on the y-axes the value of the HI is represented.

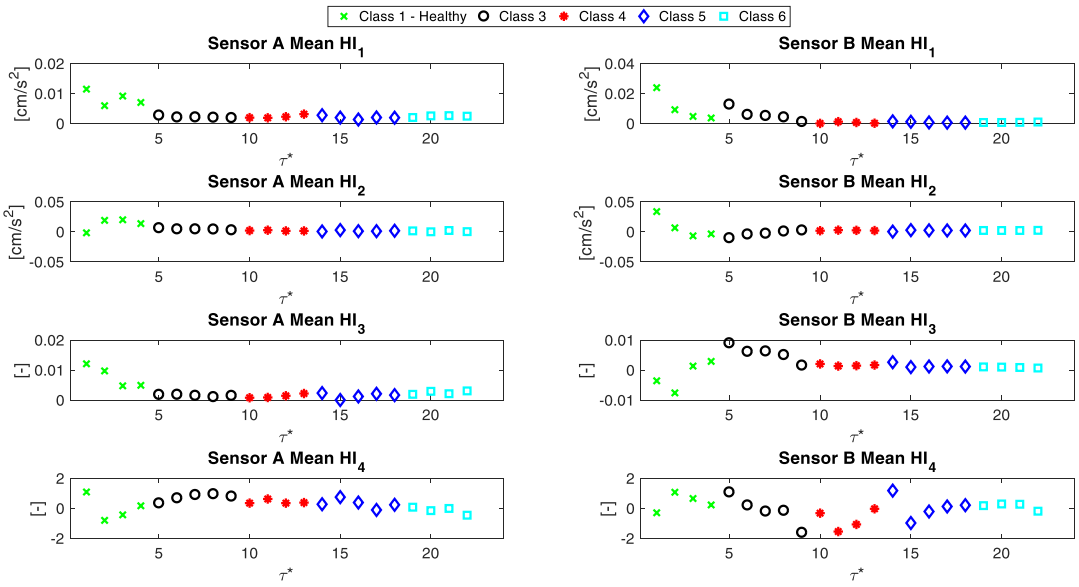

Figure D- 1. *HIs evolution of the extracted mean values*

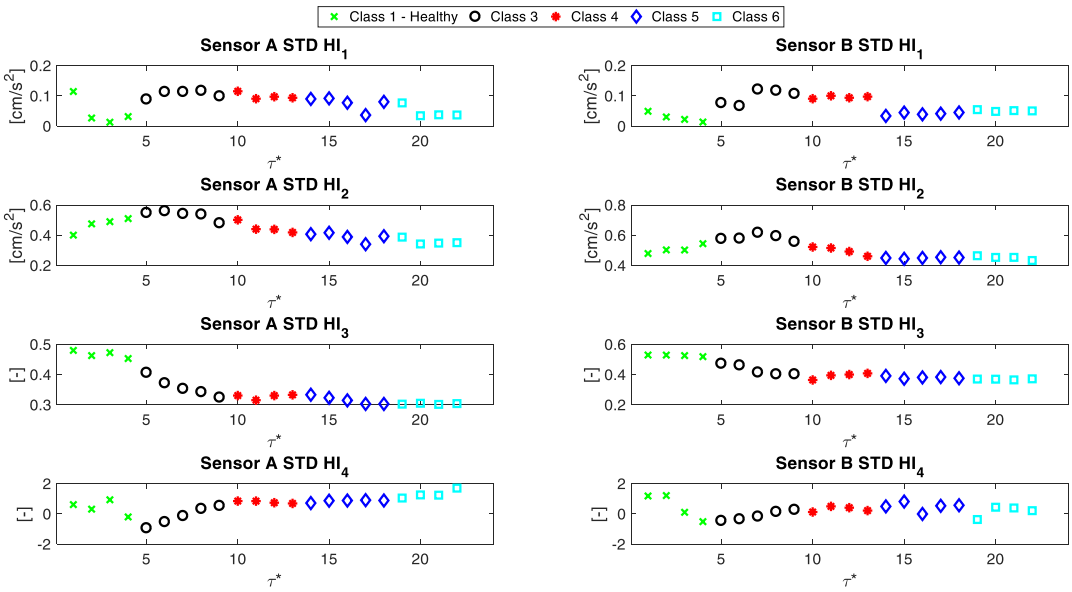

Figure D- 2. *HIs evolution of the extracted standard deviation values*

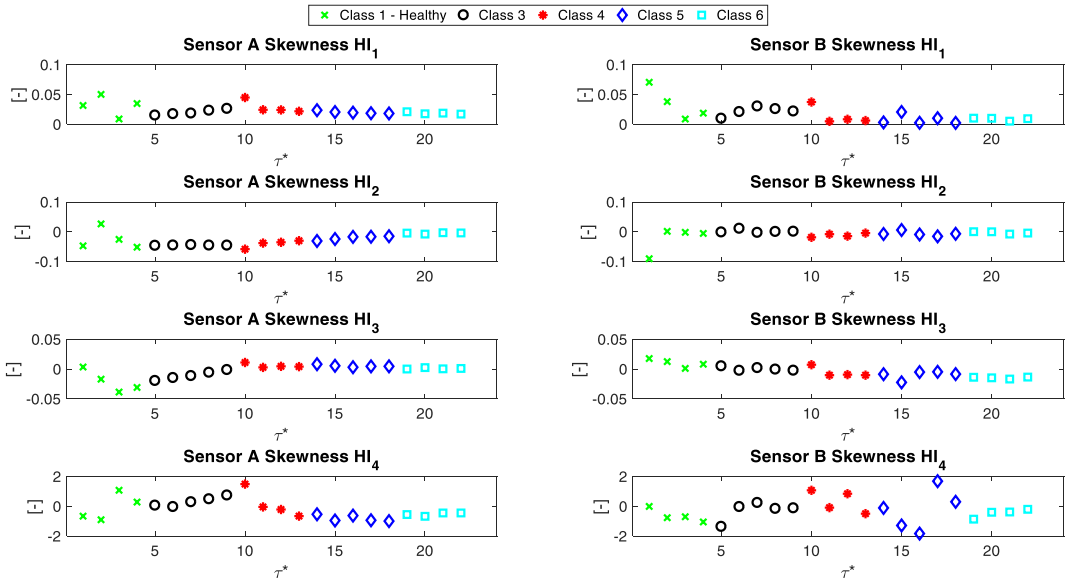

Figure D- 3. *HIs evolution of the extracted Skewness values*

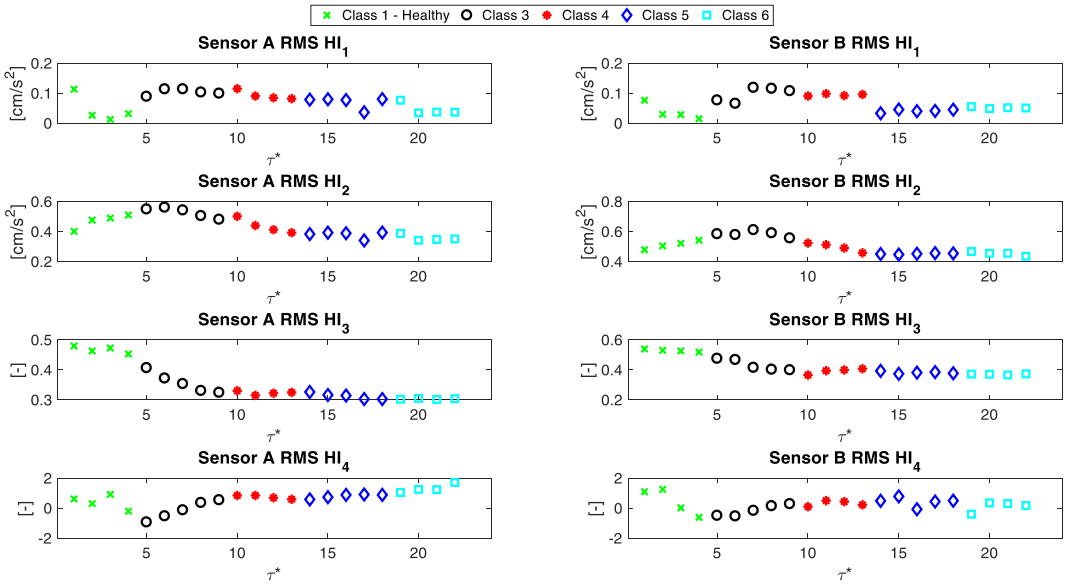

Figure D- 4. *HIs evolution of the extracted Root Mean Square (RMS) values*

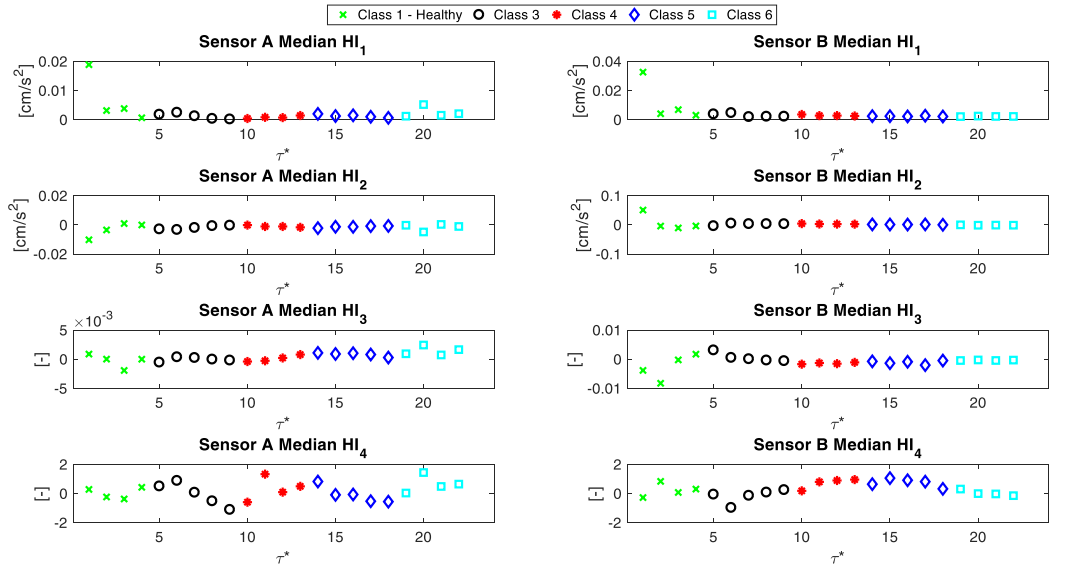

Figure D- 5. *HIs evolution of the extracted Median values*

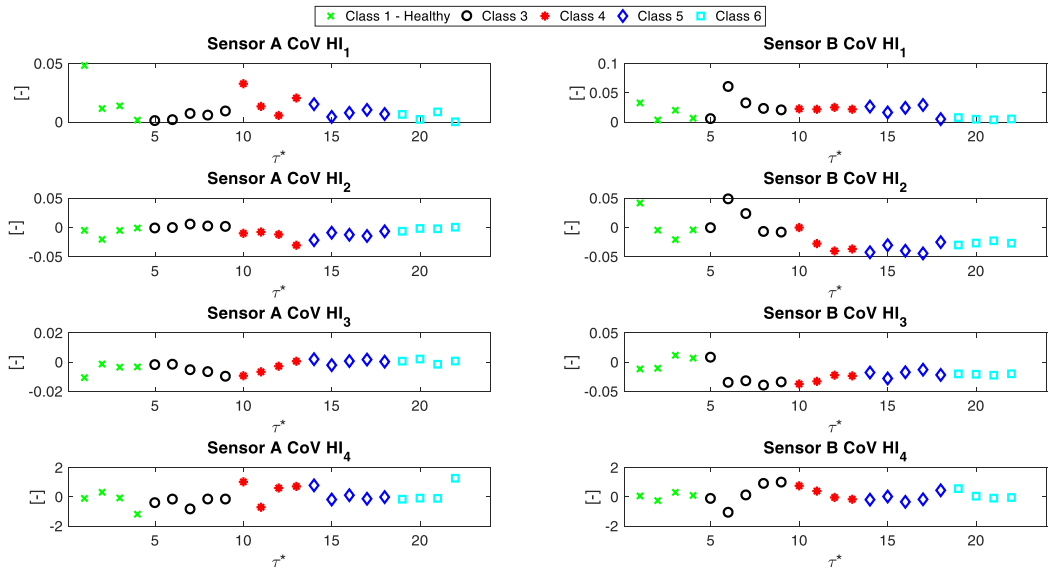

Figure D- 6. *HIs evolution of the extracted Coefficient of Variation (CoV) values*

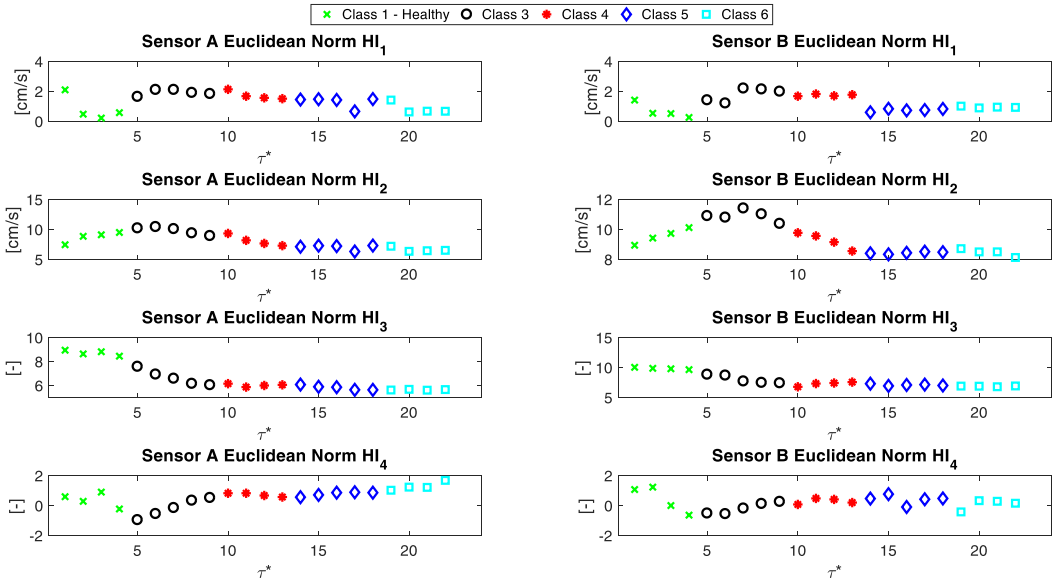

Figure D- 7. *HIs evolution of the extracted Euclidean norm values*

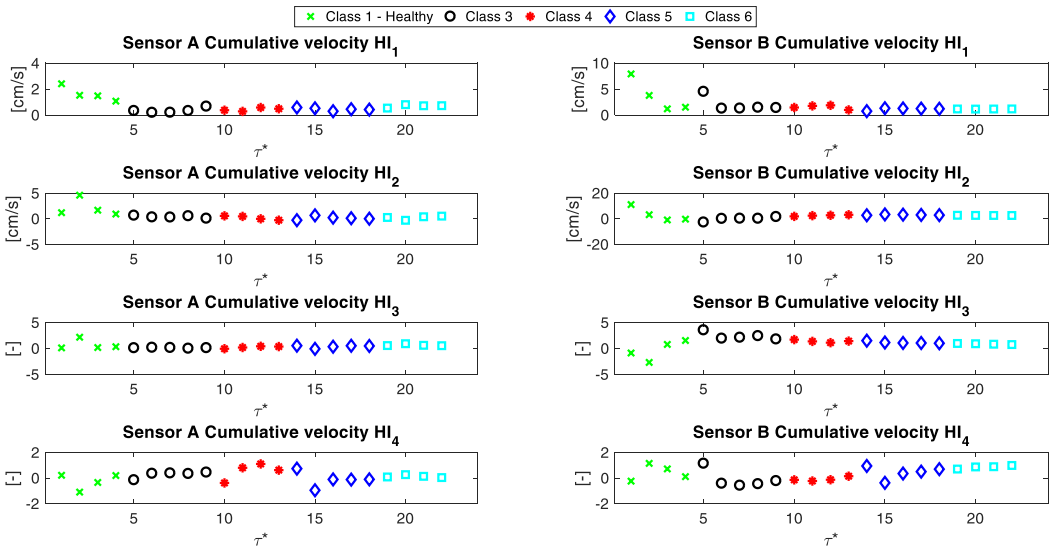

Figure D- 8. *HIs evolution of the extracted Cumulative velocity values*

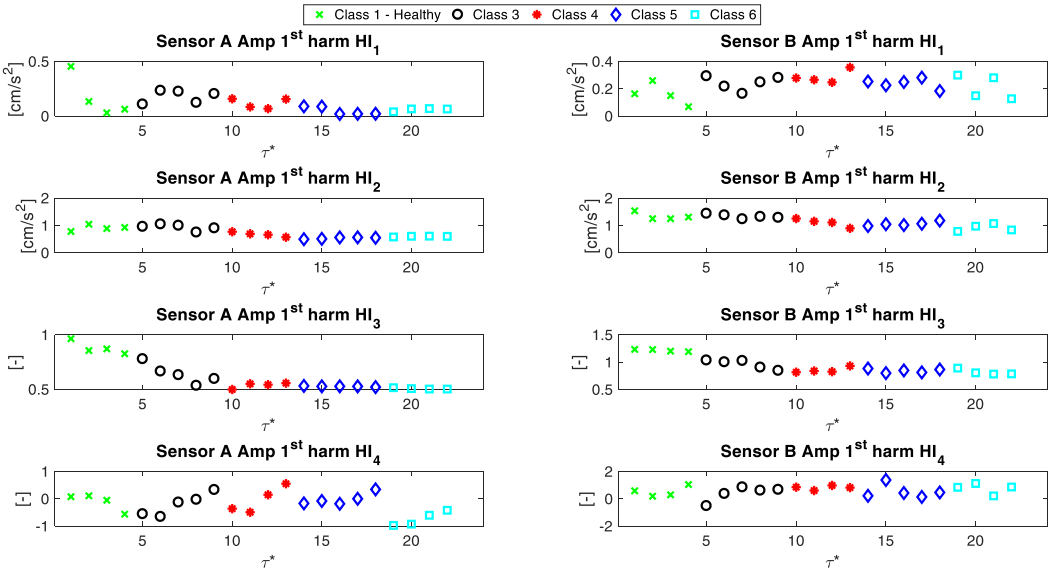

Figure D- 9. *HIs evolution of the extracted Amplitude of the first harmonic values*

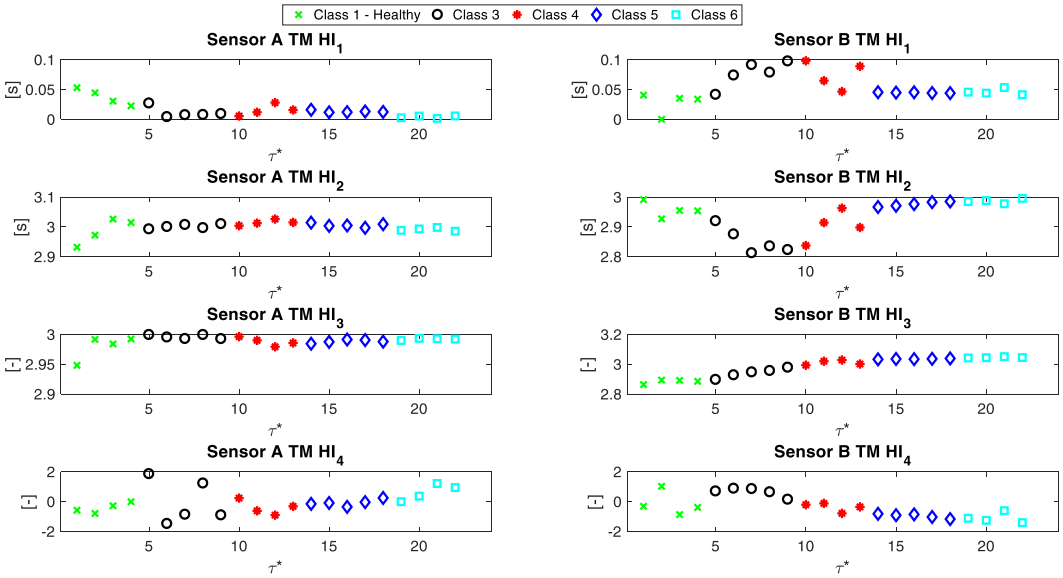

Figure D- 10. *HIs evolution of the extracted mean period of the bridge values*

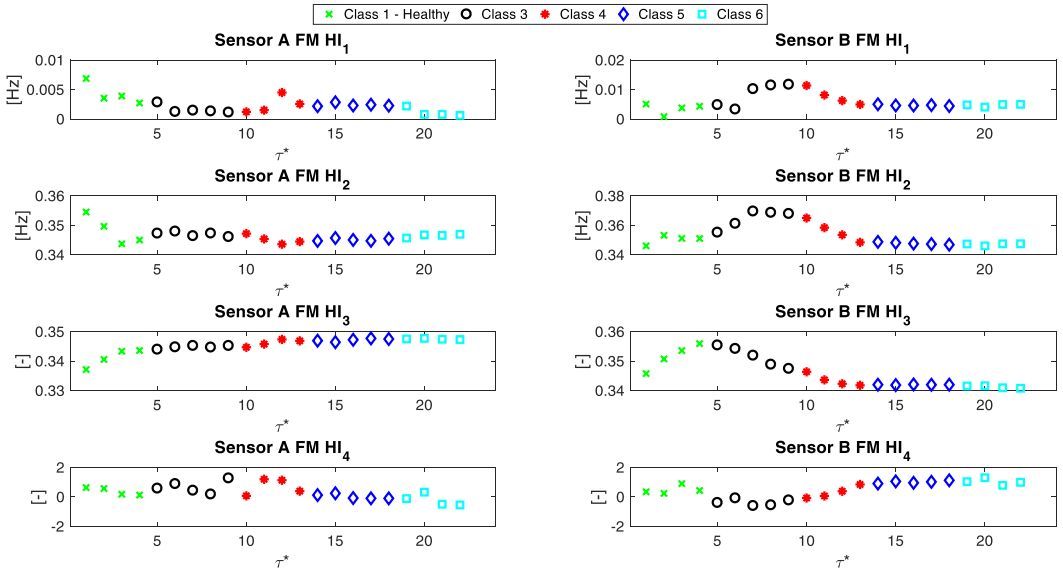

Figure D- 11. *HIs evolution of the extracted mean frequency of the bridge values*

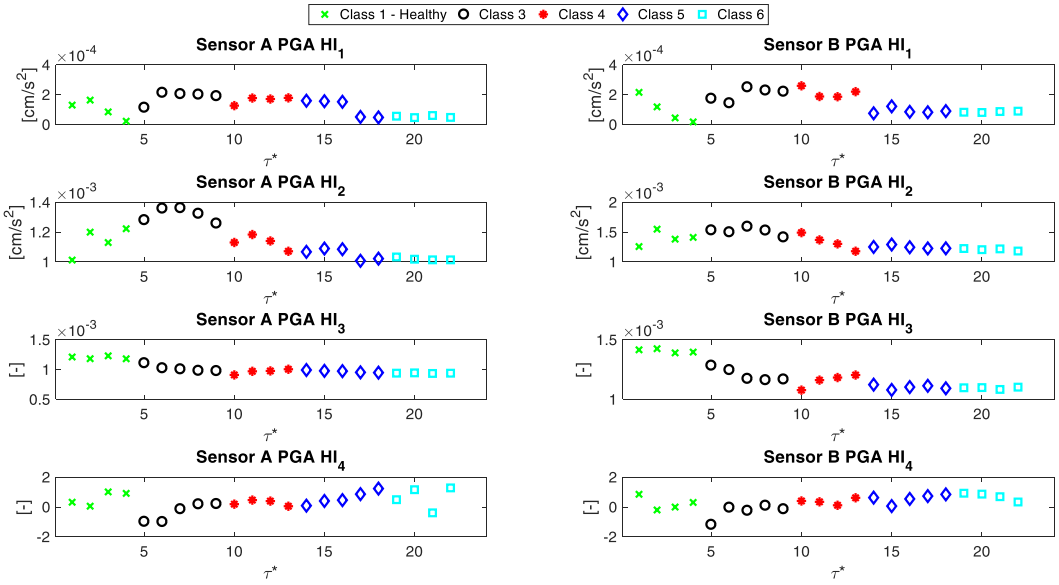

Figure D- 12. *HIs evolution of the extracted Peak Acceleration (PGA) values*

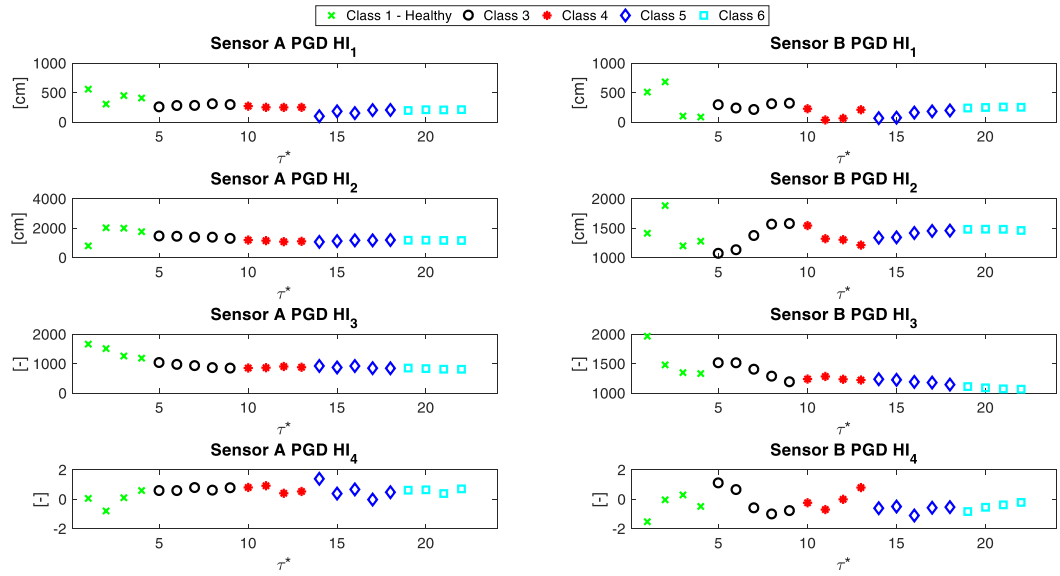

Figure D- 13. *HIs evolution of the extracted Peak Displacement (PGD) values*

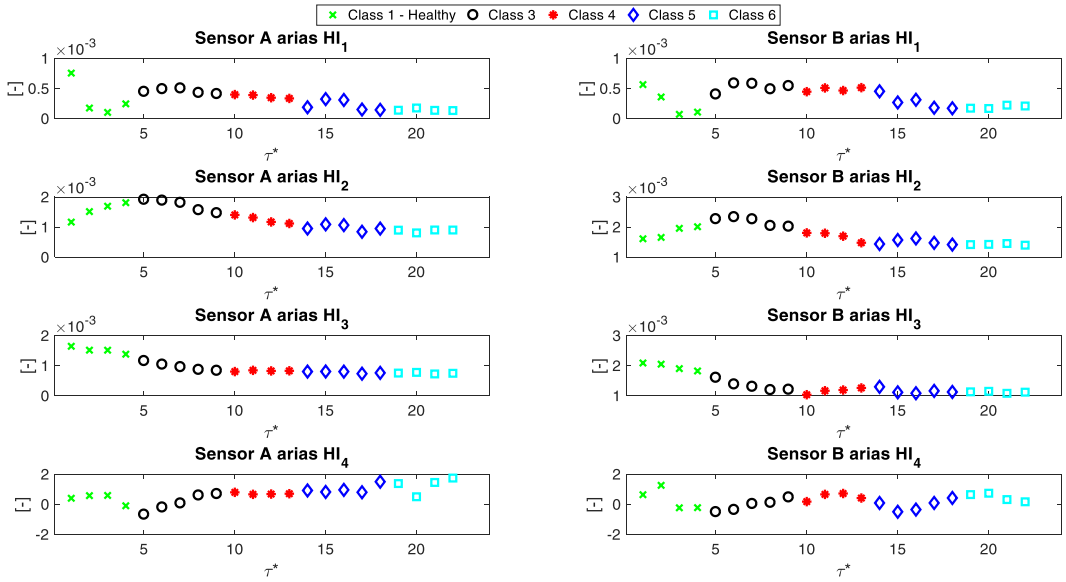

Figure D- 14. *HIs evolution of the extracted Arias values*

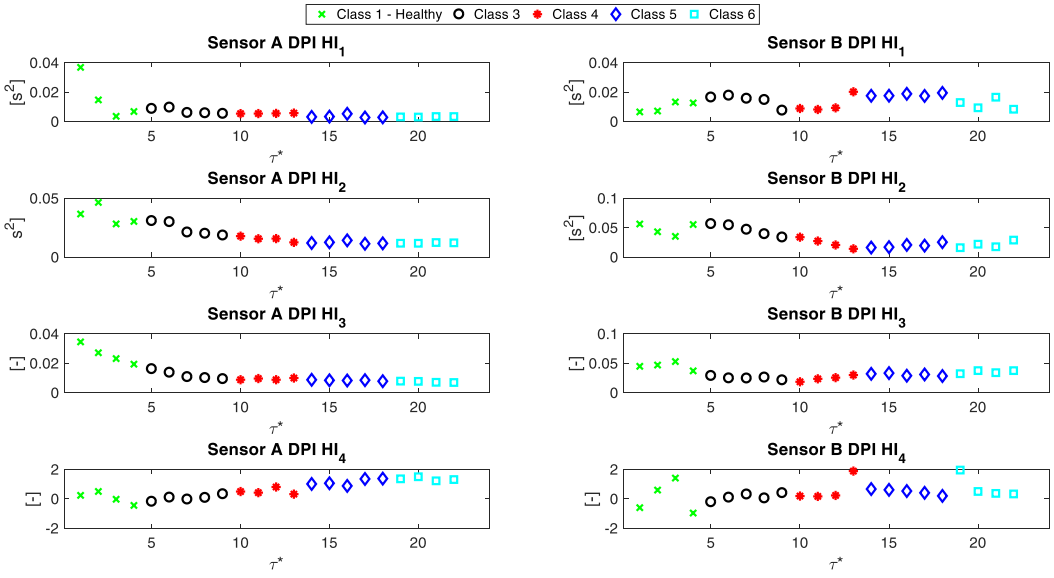

Figure D- 15. *HIs evolution of the extracted DPI values*

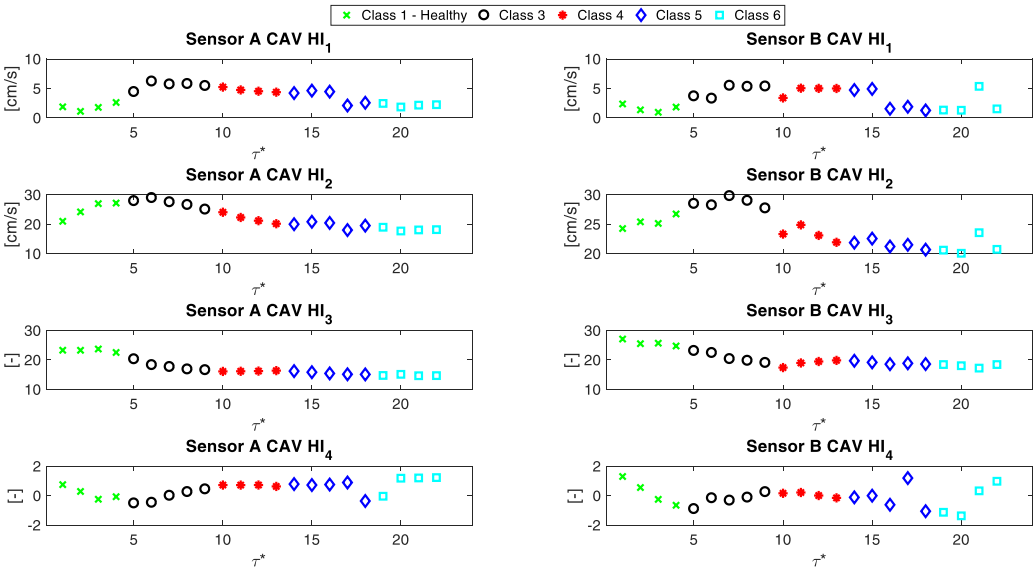

Figure D- 16. *HIs evolution of the extracted CAV values*